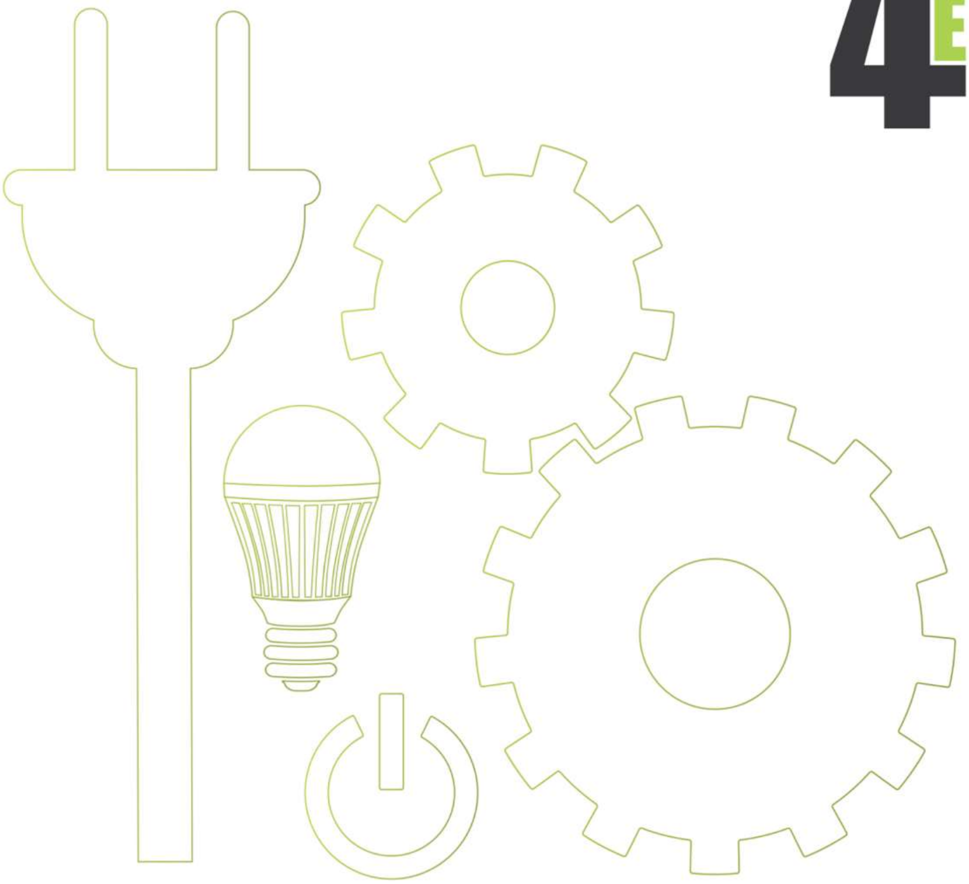

Solid State Lighting Annex: IC 2017 Interlaboratory Comparison

Final Report

Energy Efficient End-Use Equipment (4E)
International Energy Agency
SSL Annex Task 4

20 December 2021

IEA 4E Solid State Lighting Annex
Interlaboratory Comparison 2017 (IC 2017) Final Report

Authors:

Yoshi Ohno, SSL Annex IC 2017 Task Leader, National Institute of Standards and Technology, USA

Jean Gaudemer, SSL Annex IC 2017 Nucleus Laboratory Expert, Laboratoire national de métrologie et d'essais (LNE), France

Jun Seok Oh, SSL Annex IC 2017 Nucleus Laboratory Expert, Korea Institute of Lighting and ICT (KILT), Republic of Korea

Jimmy Dubard, SSL Annex IC 2017 Nucleus Laboratory Leader, Laboratoire national de métrologie et d'essais (LNE), France

Sangkyoo Jeon, SSL Annex IC 2017 Organizing Laboratory Leader, Korea Institute of Lighting and ICT (KILT), Republic of Korea

Michael Scholand, IEA 4E SSL Annex, Operating Agent Support, London, UK

The authors are grateful for the reviews by and support from all SSL Annex Experts and Management Committee members. The authors would like to express particular thanks to Steve Coyne and Carsten Dam-Hansen, SSL Annex Expert members, for their valuable comments and input for many improvements in this Final Report as well as Tony Bergen for his contributions. The authors also express their thanks to Professor Georges Zissis, SSL Annex Management Committee Chair, David Boughey, SSL Annex Management Committee Deputy Chair and Nils Borg, SSL Annex Operating Agent for their high-level guidance and support for this Interlaboratory Comparison.

About the IEA 4E Solid State Lighting (SSL) Annex

The SSL Annex was established in 2010 under the framework of the International Energy Agency's Energy Efficient End-use Equipment (4E) Implementing Agreement to provide advice to its member countries seeking to promote energy efficient lighting and to implement quality assurance programmes for SSL lighting. This international collaboration currently consists of the governments of Australia, Canada, Denmark, France, the Republic of Korea, Sweden and the United Kingdom. Information on the 4E SSL Annex is available from: https://www.iea-4e.org/ssl/

About the International Energy Agency's Technology Collaboration Programme on Energy Efficient End-Use Equipment (4E)

Fifteen countries from the Asia-Pacific, Europe and North America have joined together under the forum of 4E to share information and transfer experience in order to support good policy development in the field of energy efficient appliances and equipment. 4E focuses on appliances and equipment since this is one of the largest and most rapidly expanding areas of energy consumption. With the growth in global trade in these products, 4E members find that pooling expertise is not only an efficient use of available funds, but results in outcomes that are far more comprehensive and authoritative. Launched in 2008, in view of its achievements during the first and second five-year terms, the IEA endorsed 4E's application for a third term that will run to 2024. https://www.iea-4e.org/

Disclaimer

The authors have made their best endeavours to ensure the accuracy and reliability of the data presented herein, however neither they, the countries sponsoring the research, nor the IEA 4E Implementing Agreement make warranties as to the accuracy of data herein, nor accept any liability for any action taken or decision made based on the contents of this report. Furthermore, it should be noted that this report is issued as evidence for governments making policy decisions and does not necessarily reflect the views or policies of the governments who are part of the IEA 4E SSL Annex. This report does not mention the lamp brands or models associated with the measured data or analysis. Any products visible in the photographs are included strictly for clarity and ease of understanding and do not represent an endorsement by the IEA 4E, the IEA 4E SSL Annex, or any of the member governments.

Executive Summary

The International Energy Agency's Energy Efficient End-use Equipment (IEA 4E) Solid State Lighting Annex (SSL Annex) conducted an Interlaboratory Comparison 2017 (IC 2017) for measurement of SSL products using goniophotometers. This global interlaboratory comparison had 36 participating laboratories from 19 countries with a total of 42 goniophotometric instruments, the largest interlaboratory comparison of goniophotometers ever undertaken. This comparison was organized to investigate the level of agreement in measurements of SSL products by various types of goniophotometers including near-field type and source-rotating type, as well as mirror-type goniophotometers which are most commonly used.

IC 2017 was led by the National Institute of Standards and Technology (NIST) in the United States, and two reference laboratories having large mirror-type goniophotometers (called *Nucleus Laboratories* in IC 2017) that were assigned to carry out the measurement rounds. These two reference labs were the Korea Institute of Lighting and ICT (KILT) in the Republic of Korea, and Laboratoire national de métrologie et d'essais (LNE) in France. To establish equivalence of measurements between these two laboratories, a Nucleus Laboratory Comparison was conducted, using two sets of the comparison artefacts and measuring all the comparison quantities. The details and results of this comparison are available in IC 2017 Nucleus Laboratory Comparison Report (published on IEA 4E SSL Annex website).

IC 2017 was carried out as a star-type comparison between each participant and one of the Nucleus Laboratories. The Nucleus Laboratories prepared and measured the artefacts, shipped them to the participants, and measured them again upon their return. If reproducibility was poor, the measurement of a particular artefact with the participant was repeated. The measurements with participants were made in six rounds, two rounds by KILT and four rounds by LNE. These measurements, and any re-measurements, were conducted between January 2018 and November 2019.

IC 2017 compared measurements of 16 quantities, *i.e.*, eight general light source quantities (total luminous flux, luminous efficacy, RMS current, active power, power factor, chromaticity u', v', correlated colour temperature, and colour rendering index R_a) and eight goniophotometric quantities (centre beam intensity, beam angle, partial luminous flux (15° cone) of a beam lamp, three partial fluxes of a street lighting luminaire, and angular colour uniformity), as well as luminous intensity distribution.

The comparison artefacts were (1) narrow beam LED lamp with ≈ 12° beam angle; (2) 60 cm x 60 cm indoor planar LED luminaire, (3) 60 cm long linear batten LED luminaire including small upward light emission, and (4) street lighting LED luminaire having asymmetric intensity distributions, with a low power factor of ≈ 0.7.

IC 2017 used the international standard CIE S 025 (or equivalent European standard EN 13032-4) as the test method. This comparison was also designed in compliance with ISO/IEC 17043 so that it may serve as a proficiency test for SSL testing accreditation schemes around the world. Further details of the design of the comparison are available in IC 2017 Technical Protocol (published in IEA SSL Annex website).

Analyses were conducted to compare the results across the 42 laboratory instruments but also to compare results among different types of goniophotometers for each quantity and each artefact type to assess their equivalence. The first analysis presents comparisons among all 42 goniophotometers for each quantity and each artefact. The analysis of the results of general photometric and colorimetric quantities and electrical quantities found:

- Total Luminous Flux – Participants' results were mostly within ± 5 % from the reference value, which was an expected result.
- RMS Current – The results showed much larger variations than expected, with standard deviation of ≈ 3 % for the LED lamp, even though participants' reported measurement uncertainties were typically less than 1 % (expanded uncertainty, k=2). The variability depended very much on the artefact; the standard deviation of RMS current for the indoor planar luminaires was only 0.5 %.
- Colour Quantities – The results of chromaticity coordinates u', v' were in good agreement, mostly within ± 0.002 from the reference value, with a few outliers for each artefact. The results of CCT ranged from a standard deviation of 26 K for ART-1 (nominal CCT 2700 K) to 91 K for ART-2 (nominal CCT 5700 K), which were considered reasonable. Note that the participants were allowed to use an integrating sphere system equipped with a spectroradiometer (sphere-spectroradiometer) or a goniophotometer equipped with a spectroradiometer (gonio-spectroradiometer) for colour measurements.

There were larger variations than expected in the results for goniophotometric quantities (centre beam intensity, beam angle, partial luminous flux, colour uniformity) and some specific problems were observed. Some of the results indicated that significant variations in results occurred due to errors in interpreting the definitions of the quantity. For example, in 15° cone angle partial flux measurements, many participants were off by ≈ 30 %, which indicated that they mistakenly calculated flux for a 15° radius cone (corresponding to a 30° cone angle). For beam angle (≈ 12°), two participants reported a value that corresponds to the half angle (≈ 6°), possibly mistaking the beam angle as the radius. The house-side downward flux of the street lighting luminaire showed large variations up to ± 20 %, with standard deviation of ≈ 8 %, four times larger than that of street-side downward flux. This was likely due to a high sensitivity of alignment of the luminaire to this partial flux on house side, which was not considered in the uncertainty evaluation.

Luminous intensity distribution (LID) data for 0°, 90°, 180°, 270° C-planes were reported by all participants. The data, however, were often reported in an incorrect format. In many cases, the origin or the direction of the C angle rotation was incorrect (the CIE coordinate system was not followed). After correcting the problematic data, the participants' LID curves were compared, and generally found in reasonable agreement with those of the reference lab. However, there were large variations for the narrow beam lamp, as the participant's alignment of the lamp in some cases was significantly off, resulting in up to a 30 % difference in luminous intensity in the direction of the mechanical axis. There were also large variations observed in LID curves of the street lighting luminaire due to alignment variations.

In addition to the comparison across the 42 laboratory instruments, a second analysis was conducted comparing the three different types of goniophotometers: mirror type, near-field type, and source-rotating type. All 42 instruments' results were grouped into these three goniophotometer types and presented in graphs for each quantity and each artefact to allow for comparisons among them. For colour quantities, the results of sphere-spectroradiometers were separated, and compared with the results of gonio-spectroradiometers. After evaluating all the results, overall, no significant differences were observed between the three types, though the near-field goniophotometers showed slightly larger but still an acceptable level of deviation in the results for very narrow or structured intensity distributions. The source-rotating type goniophotometers (with operating position correction) did not show any issues, except that some of the instruments did not cover a sufficient angle range in the upward direction for the batten luminaire.

IC 2017 verified reasonable agreement overall among the participants' measurements of the important quantities such as total luminous flux, luminous efficacy, and chromaticity, while it showed unexpected larger variations for some electrical quantities, and revealed a number of specific problems in the measurements of goniophotometric quantities. These results indicate that more guidance is needed in CIE S 025 or other relevant standards for goniophotometric measurements of SSL products including the following:

- Reporting of LID results with correct C-angle rotation;
- How to calculate centre beam intensity and beam angle of a directional lamp;
- How to mount and accurately align a narrow-beam lamp to the goniophotometer;
- Practical uncertainty evaluation for goniophotometric quantities as well as other quantities;
- Development of acceptance criteria for near-field goniophotometers to demonstrate equivalence to a far-field goniophotometer; and
- Development of acceptance criteria for source-rotating type goniophotometers (with required correction for operating position).

This comparison also verified that the near-field goniophotometers and source-rotating type goniophotometers that participated in this IC had overall equivalent accuracies to (far-field) mirror-type goniophotometers for the types of light source used in this IC. It should be noted that this verification did not cover all types of products in the market nor all models of near-field goniophotometers available, thus further studies are encouraged. The results of IC 2017 presented in this Final Report may be useful for future improvements in metrology, test standards and measurement practice for solid state lighting.

Table of Contents

List of Tables

List of Figures

Acronyms, Abbreviations and Units

AC	alternating current
4E	Energy Efficient End-use Equipment
ART	artefact
°C	degrees Celsius
CCT	correlated colour temperature
cd	candela
CIE	Commission Internationale de l'Éclairage (International Commission on Illumination)
CIPM	Comité International des Poids et Mesures (International Committee for Weights and Measures)
CMC	Calibration and Measurement Capabilities
COFRAC	Comité Français d'Accréditation (French Accreditation Body)
COSD	Cooperation Organisation for Standards Development
CRI	colour rendering index
DC	direct current
DUT	device under test
EN	European Norm (European Standard)
EPA	Environmental Protection Agency (USA)
Hz	hertz
IC	Interlaboratory Comparison
IEA	International Energy Agency
IEC	International Electrotechnical Commission
IES	Illuminating Engineering Society
ISO	International Standards Organisation
ITR	Individual Test Report
K	kelvin
KATS	Korean Agency for Technology and Standards
KEA	Korea Energy Agency
KILT	Korea Institute of Lighting and ICT
KOLAS	Korea Laboratory Accreditation Scheme
LED	light emitting diode
LID	luminous intensity distribution
lm	lumen
LNE	Laboratoire national de métrologie et d'essais
min	minute
mm	millimetre
MR	multifaceted reflector
NIST	National Institute of Standards and Technology
nm	nanometre
RMS	root mean square
SDPA	Standard Deviation for Proficiency Assessment
SPD	spectral power distribution
SSL	solid state lighting
USA	United States of America
V	volt
W	watt

1 Introduction

Building on the experience of the successful Interlaboratory Comparison 2013 (IC 2013) where 110 labs from around the world were compared for measurements of various LED lamps [1], the International Energy Agency's Energy Efficient End-use Equipment (IEA 4E) Solid State Lighting Annex (SSL Annex) conducted an Interlaboratory Comparison 2017 (IC 2017) for measurement of LED luminaires using goniophotometers. The comparison used four different types of artefacts; three LED luminaires (a street lighting luminaire, a planar indoor luminaire, and a batten type indoor luminaire) and a narrow-beam LED lamp. IC 2017 compared measurements of 16 different measurement quantities (electrical, photometric, colorimetric, and goniophotometric quantities) including luminous intensity distributions, which are listed in the IC 2017 Technical Protocol [2]. IC 2017 was launched in June 2017 [3] with 36 participating laboratories from 19 countries with a total of 42 goniophotometric instruments from around the world.

IC 2017 was designed and carried out in compliance with ISO/IEC 17043 [4] to serve as proficiency testing for the participants. IC 2017 used CIE S 025 [5] (or equivalent EN 13032-4 [6]) as the test method so that the results of the individual participants could be used as proficiency test in laboratory testing accreditation for CIE S 025 or other regional test methods inclusive in CIE S 025 by accreditation programmes that recognise IC 2017. It was also intended that the results from the near-field goniophotometer measurements could be used for the requirement to demonstrate equivalence to a (far-field) mirror-type goniophotometer in CIE S 025.

IC 2017 accepted various types of goniophotometers covered in CIE S 025 including near-field type and source-rotating type as well as mirror-type goniophotometers, to investigate the level of agreement or variations in measurements between these different types of goniophotometers for different SSL products and for various measurement quantities as a technical study. See Annex 1 for descriptions of these three types of goniophotometer.

IC 2017 was led by the National Institute of Standards and Technology (NIST), USA, and its measurement rounds were carried out by two reference laboratories (called *Nucleus laboratories* in IC 2017): the Korea Institute of Lighting and ICT (KILT) in the Republic of Korea and the Laboratoire national de métrologie et d'essais (LNE) in France. To verify their measurement uncertainties and to bring equivalence of measurements by these two laboratories for the IC 2017 artefacts, comparisons between the Nucleus Laboratories were carried out using the comparison artefacts, the results of which are published in Nucleus Laboratory Comparison Report [7]. Based on the results of this comparison, the correction factors for equivalence of measurements by the two Nucleus laboratories were established and applied in the measurement rounds.

The measurements of all participants were carried out between January 2018 to November 2019, in six measurement rounds by the two Nucleus Laboratories. Upon completion of the analysis of results of each measurement round, Individual Test Reports (ITR) were issued to each participant in that round. This Final Report presents the results comparing measurements of all participants in anonymous manner, for each different artefact type, and for each of the measurement quantities, and discusses various problems observed and considerations made in the results.

2 Participants

There were 36 participating laboratories with a total of 42 instruments in IC 2017, as a few of the laboratories participated with two or three goniophotometers. Table 2-1 shows the list of participants, all of whom gave permission to be named in this report. Table 2-2 shows the list of instruments that the participants used in this comparison.

Table 2-1. List of IC 2017 Participants

Laboratory (Company/Institute)	Country
Steve Jenkins & Associates Pty Ltd.	Australia
Municipal Department 39, City of Vienna - Research Centre, Laboratory and Certification Services / Light Laboratory	Austria
XAL GmbH	Austria
Laboratorium voor Lichttechnologie, KU Leuven R&D	Belgium
Laborelec Engie Lab	Belgium
SCHREDER - RTECH	Belgium
DEKRA Testing and Certification (Shanghai) Ltd.	China
EVERFINE Test and Calibration Technology Co., Ltd, Hangzhou	China
Intertek Testing Services Shanghai	China
Intertek Testing Services (Hangzhou) Limited	China
Lidl Hong Kong Limited	China
Test Laboratory of LEDVANCE Lighting Ltd.	China
TÜV SÜD Certification and Testing (China) Co., Ltd. Shanghai Branch	China
Zhejiang SENSING Optronics Co., Ltd.	China
DTU Fotonik	Denmark
SSL Resource Oy	Finland
LED Engineering Development	France
Instrument Systems GmbH	Germany
LMT Lichtmesstechnik GmbH Berlin	Germany
NORKA GmbH & Co. KG	Germany
OSRAM GmbH	Germany
Photometrik GmbH	Germany
Technische Universität Ilmenau	Germany
TÜV SÜD Product Service GmbH	Germany
Bajaj Electricals Limited Laboratory	India
OSRAM S.p.A.	Italy
Philips Lighting Test Centre Europe	Netherlands
Russian Lighting Research Institute named after S.I. Vavilov (VNISI)	Russia
Eskom Holdings SOC Ltd., Demand Management Department	South Africa

Laboratory (Company/Institute)	Country
PHILIPS INDAL, S.L.	Spain
Swedish Energy Agency, Testlab	Sweden
RISE Research Institutes of Sweden AB	Sweden
Regent Lighting	Switzerland
Lighting Industry Association	United Kingdom
Thorn Lighting Ltd	United Kingdom
UL Verification Services Inc.	United States

Table 2-2. List of Goniophotometers used by the participants (alphabetical order) [1]

Goniophotometer Type	Goniophotometer Model	Count	Total
Mirror Type	EVERFINE GO-R5000	6	19
	GMS2000 SENSING INSTRUMENT	1	
	GMS3000 SENSING INSTRUMENT	1	
	Custom-made	1	
	LMT GO-DS 2000	6	
	LMT GO-DS 1600	2	
	Oxytech T4	1	
	UL/LSI 6440T	1	
Near-field Type	Custom-made	2	12
	TechnoTeam RiGO 801 (size varies)	10	
Source-rotating Type	Gerh. Döbele (modified)	1	10
	Custom-made	1	
	Instrument Systems LGS1000	2	
	LMT GO-V 1900	2	
	LMT GO-R 3060	1	
	PSI model ASG-3.0, C/gamma geometry	1	
	SSL Resource Oy, SSL C-1R.1600.2A	1	
	Viso Systems / LabSpion	1	
Other Type	Custom-made (detector rotates, source fixed)	1	1

Annex 1 of this report provides descriptions of the three types of goniophotometers used in IC 2017.

[1] The company and product names are listed for technical information to assist in understanding the results presented in this report. They do not represent endorsement of any particular models of goniophotometer of any manufacturer, by the National Institute of Standards and Technology, by the IEA 4E SSL Annex or any of its member governments.

3 Protocol of IC 2017

The detailed protocol of IC 2017 was published in IC 2017 Technical Protocol [2]. This section provides a summary of the protocol.

3.1 Comparison Artefacts

Table 3-1 shows the set of four artefacts, designated ART-1, ART-2, ART-3 and ART-4, that were used in IC 2017. One set of these artefacts (one each of ART-1, 2, 3, 4) was sent to each participant in two rigid shipping containers. All the artefacts were seasoned and tested for stability, and measured by a Nucleus Laboratory, before sending to participants.

The comparison artefacts selected were typical indoor and outdoor luminaires plus a narrow-beam directional lamp. These four artefacts were selected in order to test many different aspects of goniophotometric measurements:

- ART-1 is a typical MR-16 narrow beam LED lamp (beam angle of ≈12°) chosen especially to compare measurements of beam angle, centre beam intensity, and partial luminous flux;
- ART-2 is a typical indoor planar LED luminaire with a broad (near-Lambertian) intensity distribution;
- ART-3 is another indoor LED luminaire with small upward light emission chosen to test capability for measurement for upward angles; and
- ART-4 is a typical street lighting LED luminaire having significantly asymmetric intensity distributions in the horizontal plane. And to further test the participants, a model with fairly low power factor (≈ 0.7) was chosen.

Table 3-1. Specifications of the Comparison Artefacts

Designation Type	Picture (actual)	Size	Rated voltage, Power, CCT	Characteristics
ART-1: Narrow-beam lamp		MR-16 50 mmϕ x 45 mm	12 V DC 7.5 W 2700 K	Narrow beam (≈12° beam angle)
ART-2: Planar luminaire		615 mm x 615 mm x 15 mm	220 V AC, 60 Hz 40 W 5700 K	Broad (near Lambertian) distribution
ART-3: Batten luminaire		625 mm x 56 mm x 85 mm diffuse cover	220 V AC, 60 Hz 20 W 4000 K	Broad distribution with small upward emission
ART-4: Street lighting luminaire		500 mm x 251 mm x 105 mm 5.5 kg	220 V AC, 60 Hz 30 W* 4000 K	Asymmetric beam emission pattern; low power factor

*A 20 W version of ART-4 was inadvertently sent to two labs and their results were officially used, as all characteristics other than power were identical to the 30 W version.

Figure 3-1 shows photographs of the light-emitting areas of ART-1 narrow-beam lamp and ART-4 street lighting luminaire. ART-1 produces very directional high luminance from the reflector and lens, and ART-4 produces very high luminance spots from direct emissions of the LED packages. Due to these characteristics, both of these artefacts were considered potentially challenging for near-field goniophotometers.

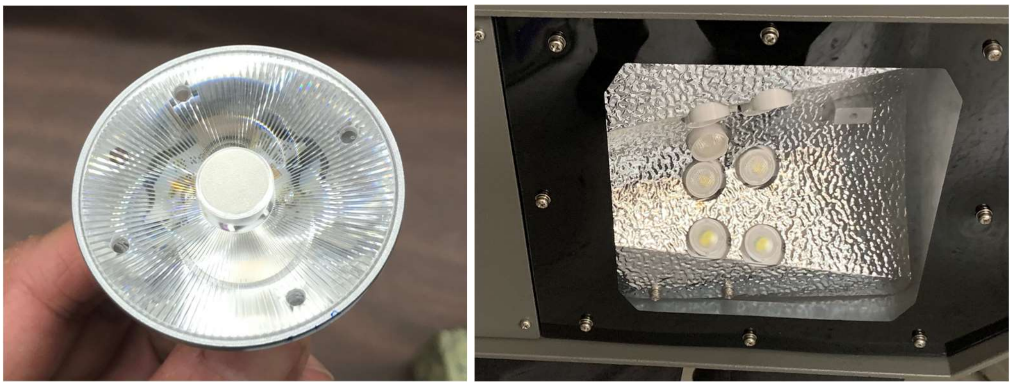

Figure 3-1. Light-emitting areas of ART-1 lamp (left) and ART-4 street lighting luminaire (right)

3.2 Measurement Quantities

The measurement quantities used in IC 2017 are listed in Table 3-2 and Table 3-3. The quantities in Table 3-2 are the same general light source quantities used in IC 2013. The reported results for these quantities were analysed in such a way that these could be used for laboratory performance assessment. The quantities in Table 3-3 are goniophotometric quantities and the main purpose of these measurements was for technical study. While we requested all participants to measure and report results of all the quantities in Table 3-2 and Table 3-3, if any participants had difficulty, it was acceptable for them not to report one or more quantities. In Table 3-3, the artefacts and quantities marked with an "X" are the ones participants were asked to measure and report.

Table 3-2. General quantities (for all Artefacts)

No.	Quantity	unit
1	Total luminous flux	lm
2	Luminous efficacy	lm/W
3	Active power (DC power for ART-1)	W
4	RMS current	A
5	Power factor	1
6	Chromaticity coordinate (u', v') – spatially averaged	1
7	Correlated colour temperature (CCT) – spatially averaged	K
8	Colour rendering index (CRI) R_a – spatially averaged	1

Table 3-3. Goniophotometric quantities to be reported, only those marked "X" were requested

No.	Quantity	Artefact Identifier			
		ART-1	ART-2	ART-3	ART-4
9	Luminous intensity distribution (cd), value at (0,0)	X	X	X	X
	C angle (horizontal)	2 planes only (0° – 180°, 90° – 270°)**			
	Vertical angle range and interval	1° step for 0° to 90°	5° step for 0° to 90°	5° step for 0° to 180°	1° step for 0° to 90°, 10° step for 90° to 180°
10	Partial luminous flux (lm) for cone angle 15°	X			
11	Street-side downward flux (lm) (Forward light*)				X
12	House-side downward flux (lm) (Back light*)				X
13	Upward flux (Uplight*) (lm)				X
14	Beam angle (°) (average of 2 planes)	X			
15	Central beam intensity (cd)	X			
16	Angular spatial colour uniformity $\Delta_{u'v'}$	X		X	

* These quantities (for street lighting luminaire) are defined in IES TM-15 [8].
** These C angle planes are only for reporting luminous intensity distributions. To measure total luminous flux and partial luminous flux, goniophotometer must be scanned with C angle intervals much smaller than 90°.

For the details of some of these goniophotometric quantities, references to the sections in CIE S 025 [5] below were provided to participants.

- Partial luminous flux: section 3.33
- Centre beam intensity: section 6.6 (including NOTE in this section)
- Beam angle: section 3.17 and section 6.6. Report the average beam angle from the two C planes (0° – 180°, 90° – 270°)
- Angular colour uniformity: section 7.1.4

Street light partial flux (three partial fluxes), defined in IES TM-15-11 [8], is illustrated in Figure 3-2. For the street lighting luminaire (ART-4), even if the luminaire structure may indicate that there is no upward flux, participants were asked to measure the luminous intensity distributions from γ=0° to 180° range and report measured data and calculate upward flux.

This is to test laboratories' capability to measure very low-level light emission in uplight region when required, e.g., for TM-15 BUG rating.

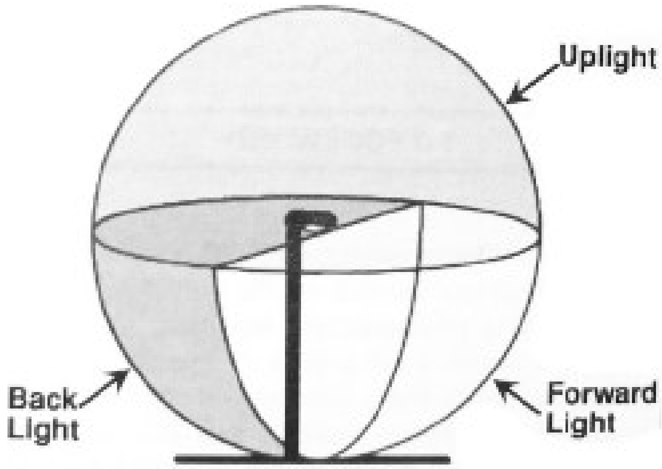

Figure 3-2. The three primary solid angles of the Luminaire Classification System (LCS) defined in IES TM-15

3.3 Test Method

The current international standard for testing solid state lighting products, CIE S 025 [5] (or equivalent European standard EN 13032-4 [6]), was used to perform measurements by the participants and the Nucleus Laboratories. The participants were asked to report any deviations from the requirements for the instruments and procedures in CIE S 025. In addition, some guidance specific to the artefacts, e.g., mounting and alignment of the artefact to a goniophotometer, was given in the IC 2017 Technical Protocol [2].

3.4 Measurement Instruments Accepted

All types of goniophotometers covered in CIE S 025 were eligible to participate in IC 2017, including:

1) Various mirror type goniophotometers with photometer head or spectroradiometer (gonio-spectroradiometer);
2) Near-field goniophotometers, including those with additional illuminance head for flux integration. In CIE S 025, a near-field goniophotometer is accepted if it is demonstrated to have equivalent accuracy with a conventional mirror-type (far-field) goniophotometer, which IC 2017 intended to provide, so near-field goniophotometers were accepted in IC 2017 without validation; and
3) Source-rotating type goniophotometers which rotate the light source around two axes without a mirror. These instruments were also accepted if the effects of changing a light source's operating position were corrected as required in CIE S 025.

All of the goniophotometers were required to use the CIE (C, γ) coordinate system as defined in CIE 121 [9].

In combination with the goniophotometers, participants were allowed to use sphere-spectroradiometers for colour measurements, as this is common practice in testing laboratories.

See Annex 1 for a detailed description of these three types of goniophotometer.

3.5 Nucleus Laboratories

To handle the measurement comparison with a large number of participants around the world, two Nucleus Laboratories were designated in IC 2017. Participants were assigned to work with one of these Nucleus Laboratories, taking into account the region and their available capacity. The two Nucleus laboratories were: Korea Institute of Lighting and ICT (KILT), Republic of Korea, and Laboratoire national de métrologie et d'essais (LNE), France.

KILT is the Korean Industrial Standards certification body and has been accredited for ISO/IEC 17025 by Korea Laboratory Accreditation Scheme (KOLAS) for optical radiation measurements. KILT has also been accredited as the Korean Industrial Standards (KS) testing laboratory by the Korean Agency for Technology and Standards (KATS) and is an accredited high efficiency certification programme testing lab by the Korea Energy Agency (KEA) for photometry. KILT has developed the safety and photometric performance requirements for KS as a Cooperation Organisation for Standards Development (COSD), and KILT also provides testing services for the Energy Star programme as a US Environmental Protection Agency (EPA) recognised lab.

LNE is the national metrology institute for France, maintaining photometric and radiometric units (such as lumen, candela, watt) and disseminates standards for luminous flux, luminous intensity, spectral irradiance, etc. Their calibration and measurement capabilities (CMC) for many photometric and radiometric quantities are certified and published by International Committee for Weights and Measures (CIPM) under the framework of CIPM Mutual Recognition Arrangement (MRA) (CIPM 1999). LNE is accredited for ISO/IEC 17025 by COFRAC (French Accreditation Body) on a wide variety of calibration services in photometry and radiometry. LNE also provides testing services for LED lighting products compliant with CIE S 025 and is accredited for ISO/IEC 17025 by Comité Français d'Accréditation (COFRAC) for optical radiation measurements.

KILT also served as the organising laboratory for IC 2017, responsible for receiving purchased artefacts, seasoning and testing them, and shipping them to the other Nucleus laboratory, LNE. In addition, KILT served as the pilot laboratory for the Nucleus laboratory comparison, preparing the two sets of artefacts used for that comparison, conducting measurements before shipping them to LNE, and then after the lamps were returned from LNE, they evaluated the reproducibility and results.

See section 4 of this report for information on the measurement facilities used at the Nucleus Laboratories. See section 5 for information on the comparison between the two Nucleus Laboratories as well as the IC 2017 Nucleus Laboratory Comparison Report [7].

3.6 Structure of IC 2017

IC 2017 was conducted as a star-type comparison between each participant laboratory and one of the Nucleus Laboratories. Each set of four artefacts was first measured by the Nucleus Laboratory ('Before' measurement) and then sent to the participant for their measurements. When the participant completed measurements and submitted their results, they returned the artefact set to the Nucleus Laboratory, which performed a repeat of the measurements of the artefacts ('After' measurement).

The reproducibility was checked on the pre-determined criteria as set in the IC 2017 technical protocol [2]. If the difference between the two measurements (Before - After) by the Nucleus Laboratory, for total luminous flux, active power, or chromaticity *u', v'*, exceeded 0.8 x SDPA[2] (see section 6.4), the results were rejected and a replacement artefact of the same type was sent to the participant and the comparison measurements were repeated.

The measurement campaign was initially scheduled in three rounds by KILT and LNE and the participants were assigned to one of these measurement rounds. However, the schedule had to change, and actual measurement rounds were carried out in four rounds as shown in Table 3-4 plus additional rounds for re-measurements. KILT measurement rounds had to stop after Round 2 due to an unexpected problem with the KILT goniophotometer. KILT Round 3 participants were moved to LNE Round 4, which was originally not scheduled. The problem of the KILT goniophotometer affected only ART-1 artefact measurements, thus these results were rejected and all ART-1 lamps in Rounds 1 and 2 were re-measured by the participants and KILT, after the KILT goniophotometer was repaired.

[2] SDPA is the Standard Deviation for Proficiency Assessment

Table 3-4. Measurement Rounds of IC 2017

Measurement Rounds	KILT participants	LNE participants	Period
Round 1 (KILT, LNE)	5	7	Jan – April 2018
Round 2 (KILT, LNE)	4	9	April – July 2018
Re-measurements of ART-1	9	-	Oct 2018 – Mar 2019
Re-measurements of ART-2	-	2	Jun - Oct 2018
Round 3 (LNE)	-	11	Aug 2018 – Oct 2019
Re-measurements of ART-1	-	3	Nov 2019
Round 4 (LNE)	-	6	Dec 2018 – Mar 2019
Re-measurements of ART-1	-	2	April – Aug 2019
Re-measurements of artefacts other than ART-1	2 (ART-2) 1 (ART-4)		Feb – July 2018

4 Measurement Instruments Used by the Nucleus Laboratories

Both KILT and LNE maintain a mirror-rotating type (far-field) goniophotometer with a photometer head plus a spectroradiometer (gonio-spectroradiometer) and also an integrating sphere system (2 m diameter) with a spectroradiometer (sphere-spectroradiometer). For IC 2017, both laboratories used the goniophotometer with a photometer head for luminous flux and luminous intensity distribution (which allows fast scanning), and a sphere-spectroradiometer for colour quantities (spatially averaged), and gonio-spectroradiometer for colour uniformity. The photometric distances for luminous intensity distribution are 12 m (KILT) and 25 m (LNE).

LNE applied a spectral mismatch correction to each device under test (DUT) with its spectral power distribution (SPD) measured using a sphere-spectroradiometer system. KILT uses a photometer head with f_1' = 1.2 % (meeting CIE S 025 requirement) and thus no spectral mismatch correction was applied at KILT.

In the IC 2017 Technical Protocol, colour quantities can be measured either by (1) using gonio-spectroradiometer and calculating spatially averaged values or (2) using a sphere-spectroradiometer. This same option was offered to the Nucleus laboratories, and they decided which instruments they used. Both KILT and LNE chose to use their sphere-spectroradiometer for colour quantities, however angular colour uniformity was measured with a gonio-spectroradiometer (i.e., a goniophotometer with a spectroradiometer).

4.1 Instruments Used by KILT

The specifications of instruments used by KILT are listed in Table 4-1 and Table 4-2, and a photo of their goniophotometer is shown in Figure 4-1. The construction of KILT's goniophotometer is such that the mirror rotates vertically around the DUT which is mounted at the centre of rotation of the mirror. This system is illustrated as "Design 1" in Annex 1 Figure A1-2. The DUT is at a fixed position and rotates horizontally around its mechanical axis. The mirror rotates over 180° covering a half vertical plane, thus the DUT rotates 360° horizontally with rotation axis toward direction of gravity. The measurement is taken in on-the-fly mode for the photometer head. Measurement with a spectroradiometer is taken in a stop-and-go mode.

Table 4-1. Information of the Goniophotometer used by KILT

Aspect / Equipment	Characteristic / Value
Goniophotometer Manufacturer/Model	PSI / LG-2.0 Mirror Goniophotometer
Type of Goniophotometer	Light source is at rotation centre, and mirror rotates around the light source
Operating position of DUT	Fixed (rotation axis of light source is in the direction of gravity
Photometric distance for photometer head	12 m
Photometric distance for spectroradiometer	12 m
Photometer head f_1' (including mirror)	1.23 %
Spectroradiometer (for colour uniformity only)	LG-2.0 Spectroradiometer
γ angle scanning range	0° to 180°
Traceability of luminous intensity and luminous flux (goniophotometer)	Total spectral radiant flux standards traceable to NIST (Everfine Certificate No. C201410200505, No. C201410200506) (for IC 2017)
Traceability of gonio-spectroradiometer mode (colour uniformity only)	Total spectral radiant flux standards traceable to NIST (for IC 2017)
AC power supply used	EXTECH 6920
AC power meter used	Yokogawa WT210
Voltage measurement	At the DUT and 4-wire connection to instruments
Length of cable between DUT and power supply/power meter	7 m

Figure 4-1. A photo of the goniophotometer at KILT

Table 4-2. Information of the Sphere-Spectroradiometer system used by KILT

Aspect / Equipment	Characteristic / Value
Diameter of integrating sphere	2 m
Spectroradiometer	Array-spectroradiometer (Everfine Model HASS/2000)
Wavelength range	350 nm to 830 nm
Bandwidth of spectroradiometer	2.0 nm
Wavelength interval	1.0 nm
Traceability	Total spectral radiant flux standard lamps traceable to NIST (Everfine Certificate No. C201410200505, No. C201410200506)
AC power supply used	Everfine DPS2010_V100
AC power meter used	Everfine PF2010
Voltage measurement	At the DUT and 4-wire connection to instruments
Length of cable between sphere and power supply/power meter	3 m

The uncertainties of measurements by KILT on all quantities for each comparison artefact are shown in section 5.1, Table 5-1.

4.2 Instruments Used by LNE

The specifications of instruments used by LNE are listed in Table 4-3 and Table 4-4, and a photo of their goniophotometer is shown in Figure 4-2.

Table 4-3. Information of Goniophotometer used by LNE

Aspect / Equipment	Characteristic / Value
Goniophotometer Manufacturer/Model	Built by LNE
Type of Goniophotometer	Light source is at rotation centre, and mirror rotates around the light source
Operating position of DUT	Fixed (rotation axis of light source is in the direction of gravity
Photometric distance for photometer head	25 m
Photometric distance for spectroradiometer	6 m
Photometer head f_1' (including mirror)	4.9 % (spectral mismatch correction applied)
Spectroradiometer (for colour uniformity only)	Array-spectroradiometer (QE Pro QEP01419)
γ angle scanning range	0° to 160°
Traceability of luminous intensity and luminous flux (goniophotometer)	Total luminous flux scale realized by LNE (BIPM Key Comparison Database, Appendix C [3])
Traceability of goniospectroradiometer mode	Spectral irradiance scale realized by LNE (BIPM Key Comparison Database, Appendix C [3])
AC power supply used	ELGAR 1251
AC power meter used	Yokogawa WT210
Voltage measurement	At the DUT and 4-wire connection to instruments
Length of cable between goniophotometer and power supply/power meter	10 m

The construction of LNE's goniophotometer is such that the DUT is mounted at the end of a rotating arm, and rotates vertically around the mirror in the centre, keeping its burning position constant with respect to gravity. This system is illustrated as "Design 2" in Annex 1 Figure A1-2. The mirror rotates around itself with rotation of DUT so that its optical axis to the detector is a fixed line. The DUT's operating position is kept constant while it rotates around the mirror, and DUT itself also rotates horizontally around its mechanical axis. The vertical movement (rotation) of the DUT is 360° so that DUT's horizontal rotation is 0° to 180°. The measurement is taken in on-the-fly mode for both the photometer head and the spectroradiometer. The dead angle (160° to 180° in γ angle) affected only ART-3 results, which were corrected for the LID curves and total luminous flux but the correction in total luminous flux were insignificant. Also, in the measurement of the halogen standard lamps for total spectral radiant flux, this dead angle was shadowed by the base of the lamp so there were no effects.

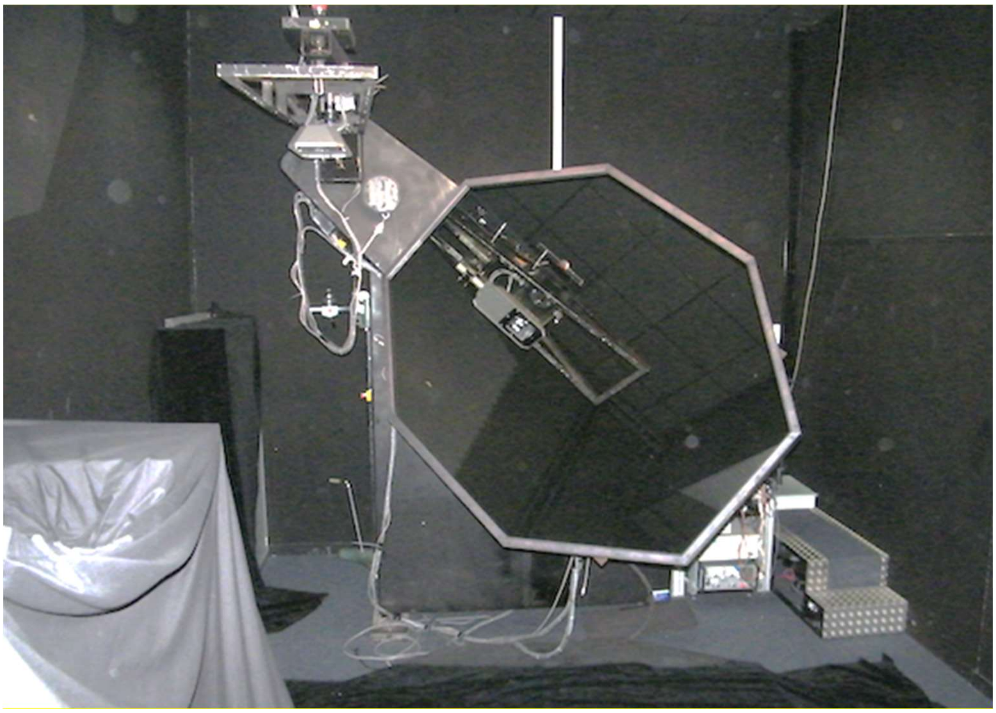

Figure 4-2. A photo of the goniophotometer at LNE, with ART-4 sample mounted

Table 4-4. Information of the Sphere-Spectroradiometer system used by LNE

Aspect / Equipment	Characteristic / Value
Diameter of integrating sphere	2 m
Spectroradiometer	Array-spectroradiometer (QE Pro QEP01419)
Wavelength range	350 nm to 1100 nm
Bandwidth of spectroradiometer	1.5 nm
Wavelength interval	0.8 nm
Traceability	Total spectral radiant flux scale realized by LNE
AC power supply used	ELGAR CW801
AC power meter used	Yokogawa WT210
Voltage measurement	At the DUT and 4-wire connection to instruments
Length of cable between sphere and power supply/power meter	10 m

The uncertainties of measurements by LNE for all quantities for each comparison artefact are shown in section 5.1, Table 5-2.

5 Nucleus Laboratory Comparison

Prior to the measurement rounds of IC 2017, to establish the equivalence between the two Nucleus Laboratories, measurements for two sets of the four artefacts for all quantities by KILT and LNE were compared. The details of the comparison and results are available in IC 2017 Nucleus Laboratory Comparison Report [7]. In this section, a summary of the report is presented.

5.1 Uncertainties of Measurements by Nucleus Labs

The uncertainties of measurements of the comparison artefacts by KILT and LNE were first evaluated and determined by each laboratory. The results are shown in Table 5-1 and Table 5-2.

Table 5-1. Uncertainties of Measurements by KILT (expanded uncertainty, *k*=2)

No.	Quantity	unit	ART-1	ART-2	ART-3	ART-4
Operating conditions						
	Ambient temperature	°C	0.7	0.7	0.7	0.7
	Supply voltage	%	0.13	0.22	0.22	0.22
General quantities						
1	RMS current (DC current for ART-1)	%	1.0	1.0	1.0	1.0
2	Active power	%	1.0	1.3	2.5	1.1
3	Power factor	1	-	0.01	0.01	0.01
4	Total luminous flux	%	2.0	1.5	1.5	1.5
5	Luminous efficacy	%	2.2	2.0	2.9	1.9
6	Chromaticity coordinate u'	1	0.0008	0.0008	0.0008	0.0012
	Chromaticity coordinate v'	1	0.0012	0.0012	0.0012	0.0016
7	Correlated colour temperature (K)	K	20	60	35	45
8	Colour Rendering Index (CRI) R_a	1	0.4	0.4	0.4	0.4
Goniophotometer quantities						
9	Luminous intensity distribution (cd) at (0,0)	%	3.0	3.0	3.0	3.0
10	Partial luminous flux (15° cone angle)	%	4.0	-	-	-
11	Street light partial flux					
	Street-side downward flux	%	-	-	-	3.0
	House-side downward flux	%	-	-	-	3.0
	Upward flux	lm	-	-	-	2.0
12	Centre beam intensity	%	3	-	-	-
13	Beam angle	°	0.3	-	-	-
14	Angular spatial colour uniformity $\Delta_{u'v'}$	1	0.0006	-	0.0007	-

Table 5-2. Uncertainties of Measurements by LNE (expanded uncertainty, *k*=2)

No.	Quantity	unit	ART-1	ART-2	ART-3	ART-4
Operating conditions						
	Ambient temperature	°C	0.7	0.7	0.7	0.7
	Supply voltage	%	0.04	0.09	0.18	0.05
General quantities						
1	RMS current (DC current for ART-1)	%	1.00	1.00	1.00	1.00
2	Active power	%	0.70	0.50	0.69	0.51
3	Power factor	1	-	0.01	0.01	0.01
4	Total luminous flux	%	1.7	1.3	1.3	1.3
5	Luminous efficacy	%	1.8	1.4	1.5	1.4
6	Chromaticity coordinate *u*'	1	0.0007	0.0007	0.0007	0.0010
	Chromaticity coordinate *v*'	1	0.0010	0.0010	0.0010	0.0015
7	Correlated colour temperature (K)	K	15	45	25	35
8	Colour Rendering Index (CRI) R_a	1	0.3	0.3	0.3	0.3
Goniophotometer quantities						
9	Luminous intensity distribution (cd) at (0,0)	%	2.5	2.5	2.5	2.5
10	Partial luminous flux (15° cone angle)	%	3	-	-	-
11	Street light partial flux					
	Street-side downward flux	%	-	-	-	1.8
	House-side downward flux	%	-	-	-	1.8
	Upward flux	lm	-	-	-	1.0
12	Centre beam intensity	%	2.5	-	-	-
13	Beam angle	°	0.15	-	-	-
14	Angular spatial colour uniformity $\Delta_{u'v'}$	1	0.0005	-	0.0005	-

5.2 Determining Assigned Values

Each uncertainty value in Table 5-1 (KILT) and Table 5-2 (LNE) was converted to standard uncertainty, denoted u_1, u_2, respectively, and these were combined with the artefact stability uncertainty u_{stab} by:

$$u_{1,\mathrm{s}} = \sqrt{u_1^2 + u_{\mathrm{stab}}^2} \text{ and } u_{2,\mathrm{s}} = \sqrt{u_2^2 + u_{\mathrm{stab}}^2} \tag{1}$$

where:

$$u_{\mathrm{stab}} = \frac{\Delta_{\mathrm{stab}}}{2\sqrt{3}} \tag{2}$$

Δ_{stab} is the difference between the two measurements at the pilot laboratory (KILT) of this comparison, for each quantity, each artefact, and is taken as a rectangular distribution to calculate the standard uncertainty u_{stab}.

The weighted mean ($\bar{x}$) of the results of KILT (x_1) and LNE (x_2) for each artefact, each set and for each quantity, were calculated based on the combined uncertainties above, $u_{1,s}$ and $u_{2,s}$ of each lab:

$$\bar{x} = x_1 \cdot w_1 + x_2 \cdot w_2$$
$$\text{where } w_1 = \left[u_{1,s}^{-2} / \left(u_{1,s}^{-2} + u_{2,s}^{-2} \right) \right] \text{ and } w_2 = \left[u_{2,s}^{-2} / \left(u_{1,s}^{-2} + u_{2,s}^{-2} \right) \right] \quad (3)$$

The final assigned values were calculated from the weighted mean of the results from the two artefact sets.

5.3 Correction Factors for Assigned Values

Since the differences in results between KILT and LNE could be significant in some cases due to some unknown systematic errors, as described in IC 2017 Technical Protocol [2], it was decided to determine correction factors for each Nucleus Laboratory for each quantity, each artefact, based on the differences between the results of KILT and LNE, and to apply them in all comparison measurement results to force the two laboratories' results to be equal (in principle).

The correction factors for each quantity and each artefact were calculated from the weighted mean of the results of KILT and LNE as shown in Section 5.2 and given as the average of those for artefact Set 1 and artefact Set 2.

For quantities that use relative uncertainties (e.g., luminous flux), the correction factors c_1 for KILT, and c_2 for LNE, for each quantity x in each artefact set, are calculated using the following formulae:

$$c_1 = \frac{\bar{x}}{x_1}, \; c_2 = \frac{\bar{x}}{x_2} \quad (4)$$

For quantities that use absolute uncertainties (e.g., chromaticity coordinates u', v'), the correction factors d_1 for KILT, and d_2 for LNE, for each quantity x in each artefact set, were calculated using the following formulae:

$$d_1 = \bar{x} - x_1, \; d_2 = \bar{x} - x_2 \quad (5)$$

The values of c_1, c_2, or d_1, d_2 for each quantity from the measurements of two artefact sets, #1 and #2, were averaged.

The resulting correction factors are given in Table 5-3 (for KILT) and Table 5-4 (for LNE). Note that the correction factors are given as relative ratio values (denoted c_1 or c_2 in factor column) for luminous flux, luminous efficacy, RMS current, active power, partial fluxes, centre beam intensity, and given as absolute difference values (denoted d_1 or d_2 in factor column) for all other quantities.

Table 5-3. Correction factors for KILT measurements to set Assigned Values

Quantity	factor	ART-1	ART-2	ART-3	ART-4
RMS current (DC for ART-1)	c_1	1.011	1.000	1.006	0.999
Active power	c_1	1.013	0.999	0.990	0.999
Power factor	d_1	-	0.000	-0.009	0.001
Total luminous flux	c_1	1.006	1.014	1.005	1.004
Luminous efficacy	c_1	0.994	1.017	1.013	1.005
Chromaticity coordinate *u*'	d_1	0.0001	0.0000	0.0003	-0.0003
Chromaticity coordinate *v*'	d_1	0.0001	0.0005	-0.0002	0.0013
Correlated colour temperature (K)	d_1	-4	-23	-8	-24
Colour Rendering Index (CRI) R_a	d_1	-0.1	-0.2	0.1	-0.2
Luminous intensity distributions					
Partial luminous flux (15° cone angle)	c_1	1.032	-	-	-
Street light partial flux					
Street-side downward flux	c_1	-	-	-	1.014
House-side downward flux	c_1	-	-	-	0.993
Upward flux	d_1	-	-	-	*
Centre beam intensity	c_1	1.024	-	-	-
Beam angle (°)	d_1	0.2	-	-	-
Angular colour uniformity $\Delta_{u'v'}$	d_1	0.0001	-	0.0003	-

* No correction was made for upward flux.

Table 5-4. Correction factors for LNE measurements to set Assigned Values

Quantity	factor	ART-1	ART-2	ART-3	ART-4
RMS current (DC for ART-1)	c_2	0.989	1.000	0.994	1.001
Active power	c_2	0.993	1.000	1.001	1.000
Power factor	d_2	-	0.000	0.009	-0.001
Total luminous flux	c_2	0.996	0.989	0.996	0.997
Luminous efficacy	c_2	1.004	0.991	0.997	0.997
Chromaticity coordinate *u*'	d_2	-0.0001	0.0000	-0.0002	0.0002
Chromaticity coordinate *v*'	d_2	-0.0001	-0.0004	0.0002	-0.0012
Correlated colour temperature (K)	d_2	2	15	4	14
Colour Rendering Index (CRI) R_a	d_2	0.05	0.16	-0.09	0.14
Goniophotometric quantities					
Partial luminous flux (15° cone angle)	c_2	0.981	-	-	-
Street light partial flux					
Street-side downward flux	c_2	-	-	-	0.991
House-side downward flux	c_2	-	-	-	1.005
Upward flux	d_2	-	-	-	*
Centre beam intensity	c_2	0.989	-	-	-
Beam angle (unit: degree)	d_2	-0.05	-	-	-
Angular colour uniformity $\Delta_{u'v'}$	d_2	-0.0001	-	-0.0002	-

* No correction was made for upward flux.

5.4 Uncertainties of the Assigned Values

The uncertainties of the weighted mean values (Assigned Values) were calculated for each quantity x for each set by:

$$u(\bar{x}) = \left[1/\left(u_{1,s}^{-2} + u_{2,s}^{-2}\right)\right]^{\frac{1}{2}} \tag{6}$$

The uncertainties of the resulting Assigned Values in measurement rounds of Nucleus Lab 1, $u(X_{N1})$, for each quantity, each artefact, were calculated by:

$$u(X_{N1}) \approx \left[u^2(\bar{x}) + u_A^2(x_1) + u_A^2(X_1)\right]^{\frac{1}{2}} \tag{7}$$

where $u(\bar{x})$ is from equation (6), $u_A(x_1)$ is a Type A component of the uncertainty in x_1 (Nucleus Lab comparison result), and $u_A(X_1)$ is a Type A component of the uncertainty in X_1 (IC 2017 measurement round result of Nucleus Lab 1). $u_A(x_1)$ was determined based on repeated measurements by the Nucleus Lab. $u_A(X_1)$ was estimated from $u_A(x_1)$ and long-term reproducibility of measurements by the Nucleus lab. The uncertainty of the Assigned Values from Nucleus Lab 2, $u(X_{N2})$, is calculated similarly. The details of the calculations and results are in Ref. [7]. The expanded uncertainties of the Assigned Values in the measurement rounds are listed in Table 5-5.

Table 5-5. Expanded uncertainties (*k*=2) of the Assigned Values

Quantity	KILT				LNE			
	ART-1	ART-2	ART-3	ART-4	ART-1	ART-2	ART-3	ART-4
RMS current (%)	0.90	0.74	1.8*	0.75	0.77	0.74	1.8*	0.75
Active power (%)	0.77	0.54	2.3*	0.59	0.65	0.48	2.3	0.56
Power factor	-	0.007	0.018*	0.007	-	0.007	0.018*	0.007
Total luminous flux (%)	1.5	1.2	1.2	1.1	1.4	1.1	1.1	1.1
Luminous efficacy (%)	1.8	1.3	2.5*	1.3	1.6	1.3	2.5	1.3
Chromaticity coordinate *u'*	0.0007	0.0014	0.0007	0.0009	0.0007	0.0008	0.0007	0.0009
Chromaticity coordinate *v'*	0.0009	0.0010	0.0009	0.0012	0.0009	0.0012	0.0009	0.0012
Correlated colour temperature (K)	13	95	26	31	13	68	25	31
Colour Rendering Index (CRI) R_a	0.33	0.37	0.35	0.34	0.43	0.37	0.34	0.34
Goniophotometric quantities								
Partial luminous flux (15° cone angle) (%)	4.5	-	-	-	2.0	-	-	-
Street-side downward flux (%)	-	-	-	1.7	-	-	-	1.5
House-side downward flux (%)	-	-	-	1.9	-	-	-	1.7
Upward flux (lm)	-	-	-	2.2	-	-	-	2.2
Centre beam intensity (%)	2.1	-	-	-	2.1	-	-	-
Beam Angle (°)	0.65	-	-	-	0.27	-	-	-
Angular spatial colour uniformity	0.0008	-	-	-	0.0008	-	-	-

* Nucleus laboratories identified additional sources of uncertainty for ART-3 and these uncertainty values have been increased from the values reported in Ref. [7].

6 Data Analysis

6.1 Correction of Nucleus Lab Measurement for Equivalence

All results of the Nucleus Laboratories were first corrected to apply correction factors for equivalence using equations (4) and (5) and the data in Table 5-3 and Table 5-4 as described in Section 5.3. In addition, the measurement results of total luminous flux and luminous efficacy were corrected to ambient temperature of exactly 25 °C, though the temperatures during their measurements were within ± 1 °C from 25 °C in most cases, using the sensitivity coefficients measured for each artefact in a thermal chamber.

6.2 Reference Value of the Comparison

The assigned values determined by either of the Nucleus laboratories after applying corrections described in 6.1 were used as the *reference values* of the comparison for each measurement quantity for each artefact type in the measurement round. In the data analysis of the comparison, the laboratory that gave reference values (which is one of Nucleus laboratories) is called *reference laboratory*.

6.3 Differences Between the Participant's Result and the Reference Value

The data analyses were conducted by determining the (relative) difference between the measured result of a participant and that by the reference laboratory. Relative differences, in percentage (%), are calculated for all photometric and electrical quantities (except power factor), and absolute differences are calculated for all colour quantities and power factor.

6.4 z' Score

The *z'* score for the results of participants in the measurement rounds are calculated by:

$$z' = \frac{x - X}{\sqrt{\hat{\sigma}^2 + u_X^2 + u_{\mathrm{drift}}^2}} \tag{8}$$

where x is the participant's result and X is the Assigned Value. $\hat{\sigma}$ is the SDPA value (Standard Deviation for Proficiency Assessment) which, in this IC test, is considered to be the generic standard uncertainty of participants' measurements. The u_X is the standard uncertainty of the Assigned Value (equating to half of the expanded uncertainty values in Table 5-5), and u_{drift} was calculated, as prescribed in the IC 2017 Technical Protocol [2], by:

$$u_{\mathrm{drift}} = \frac{0.8 \cdot \hat{\sigma}}{2\sqrt{3}} \tag{9}$$

In IC 2017, z' scores (and E_n numbers) are reported only for the eight quantities that were compared in IC 2013 (the quantities in Table 3-2). The SDPA values for these eight quantities in IC 2017 were determined from the robust standard deviations (for all artefacts) of the goniophotometer participants' data in IC 2013 [1] as shown in Table 6-1. The robust standard deviation values of CCT are adjusted for the CCTs of each artefact in IC 2017.

Table 6-1. SDPA Values for IC 2017

Quantity	ART-1	ART-2	ART-3	ART-4
RMS current (%)	1.8	1.8	1.8	1.8
Active power (%)	0.93	0.93	0.93	0.93
Power factor	-	0.013	0.013	0.013
Total luminous flux (%)	2.5	2.5	2.5	2.5
Luminous efficacy (%)	2.7	2.7	2.7	2.7
Chromaticity coordinate u'	0.0016	0.0016	0.0016	0.0016
Chromaticity coordinate v'	0.0017	0.0017	0.0017	0.0017
Correlated colour temperature (K)	20	104	40	56
Colour Rendering Index (CRI) R_a	0.5	0.5	0.5	0.5

6.5 E_n Number

E_n numbers (defined in ISO/IEC 17043 [1]) are calculated, if the uncertainties of measurements are reported by the participant, according to:

$$E_{\mathrm{n}} = \frac{x - X}{\sqrt{U_{\mathrm{lab}}^2 + U_{\mathrm{ref}}^2}} \tag{10}$$

or if these uncertainties are given in relative uncertainties, then E_n is calculated by

$$E_{\mathrm{n}} = \frac{(x - X)/X}{\sqrt{U_{\mathrm{lab,rel}}^2 + U_{\mathrm{ref,rel}}^2}} \tag{11}$$

where:

x: value measured by the participant
X: assigned value (average of the Reference Laboratory measurements, before and after measurements)
U_{lab}, $U_{\mathrm{lab,rel}}$: (relative) expanded uncertainty (k=2) of a participant's result
U_{ref}, $U_{\mathrm{ref,rel}}$: (relative) expanded uncertainty (k=2) of the assigned value, and are calculated by

$$u_{\mathrm{ref}} = \sqrt{\left(\frac{u_1 + u_2}{2}\right)^2 + \frac{(X_1 - X_2)^2}{\left(2\sqrt{3}\right)^2}} \tag{12}$$

or

$$u_{\mathrm{ref,rel}} = \sqrt{\left(\frac{u_{1,\mathrm{rel}} + u_{2,\mathrm{rel}}}{2}\right)^2 + \left(\frac{(X_1 - X_2)/X_1}{2\sqrt{3}}\right)^2} \tag{13}$$

and

$$U_{\mathrm{ref}} = 2\ u_{\mathrm{ref}} \tag{14}$$

or

$$U_{\mathrm{ref,rel}} = 2\ u_{\mathrm{ref,rel}} \tag{15}$$

where X_1 and X_2 are measured values by the reference laboratory, before and after the participant's measurement, and u_1 and u_2 are their standard uncertainties.

The equation assumes that the uncertainties of the two measurements (u_1 and u_2) are fully correlated. The second term in the square root in equation (12) or equation (13) is the standard uncertainty associated with the drift of the artefacts as measured by the reference laboratory (taken as a rectangular distribution).

The concept of the E_n number is to test whether the claimed measurement uncertainties of a laboratory are valid. Generally, the value of $|E_n| \le 1$ is considered to be satisfactory, $|E_n| > 1.0$ is considered to be unsatisfactory; that is, the difference in the quantities measured by the participant laboratory and the reference laboratory is greater than the expanded uncertainty of the comparison.

7 Results of Comparison

Results of measurements by all participants, in comparison with the reference laboratory (one of Nucleus Laboratories), are presented. The results from individual goniophotometers at the participant laboratories are shown anonymously by using "lab codes" which start with the letter G (for goniophotometer) and are followed by two numbers (ranging from 01 to 99). These lab codes were randomly assigned to each goniophotometer when the laboratory registered for IC 2017. Section 7.1 presents the average absolute results for each artefact and each measurement quantity for all participants measured by the reference laboratories. Section 7.2 presents the analysis comparing the results of all 42 instruments against the two reference laboratories for each measured quantity of each artefact type. Section 7.3 presents the same set of data in Section 7.2 but grouped into three different types of goniophotometers – mirror type, near-field type, and source-rotating type – to compare the results of the different types and evaluate the equivalence between them.

7.1 Average Results of Reference Laboratories for Each Artefact Type

To provide some indicative information on the absolute values of the measured quantities of each comparison artefact type, the average values of all the artefacts of each type measured by the reference laboratories during the course of this comparison are shown in Table 7-1 and their standard deviations in Table 7-2. The standard deviation values in Table 7-2 include individual variations of these products as well as reproducibility of measurements by the reference labs. Approximately 20 sets of artefacts were used in the measurement rounds conducted by KILT and LNE. No absolute values measured by each participant or each reference lab are presented in this report.

Table 7-1. Average results of the reference laboratories' measurements of each artefact type

Measurement quantity	Unit	ART-1	ART-2	ART-3	ART-4
Total luminous flux	lm	403.8	4628	2169	2047
RMS current (DC current for ART-1)	A	0.6272	0.1794	0.0981	0.1995
Active power (DC power for ART-1)	W	7.58	38.70	19.58	29.63
Luminous efficacy	lm/W	53.6	120.0	111.0	69.2
Power factor	1	-	0.980	0.918	0.675
Chromaticity coordinate u'	1	0.2615	0.2056	0.2234	0.2203
Chromaticity coordinate v'	1	0.5290	0.4798	0.5008	0.4898
Correlated colour temperature	K	2714	5487	4082	4444
Colour rendering index (CRI) R_a	1	96.7	83.6	84.2	77.6
Luminous intensity distribution (0,0)	cd	6154	1605	600	498
Partial luminous flux (15° cone)	lm	211	-	-	-
Centre beam intensity	cd	6174	-	-	-
Beam angle	°	12.07	-	-	-
Street-side downward flux	lm	-	-	-	1626
House-side downward flux	lm	-	-	-	419
Upward flux	lm	-	-	-	2.16
Angular spatial colour uniformity $\Delta_{u'v'}$	1	0.0024	-	0.0032	-

Table 7-2. Standard deviations of the values in Table 7-1 (due to products variations and measurement variations)

Measurement quantity	Unit	ART-1	ART-2	ART-3	ART-4
Total luminous flux	%	4.1	2.4	0.9	1.0
RMS current (DC current for ART-1)	%	3.0	0.9	1.1	0.7
Active power (DC power for ART-1)	%	3.0	0.9	1.1	0.9
Luminous efficacy	%	5.6	2.7	0.8	0.9
Power factor	1	-	0.002	0.009	0.007
Chromaticity coordinate u'	1	0.0011	0.0005	0.0003	0.0007
Chromaticity coordinate v'	1	0.0010	0.0010	0.0005	0.0035
Correlated colour temperature	K	21	60	19	101
Colour rendering index (CRI) R_a	1	0.5	0.4	0.2	1.6
Luminous intensity distribution (0,0)	%	4.5	2.5	2.3	4.7
Partial luminous flux (15° cone)	%	4.5	-	-	-
Centre beam intensity	%	4.3	-	-	-
Beam angle	°	0.23	-	-	-
Street-side downward flux	%	-	-	-	1.0
House-side downward flux	%	-	-	-	3.0
Upward flux	lm	-	-	-	0.14
Angular spatial colour uniformity $\Delta_{u'v'}$	1	0.0007	-	0.0005	-

7.2 Differences in Measurement Results Between Participants and Reference Laboratory

In this section, the (relative) differences of results between the participant laboratories (Lab) and the reference laboratory (Ref), calculated by (Lab - Ref) or (Lab - Ref)/Ref, for all quantities for all participants, and for all artefact types, are presented in graphical formats. Relative differences are used for total luminous flux, luminous efficacy, active power, RMS current, partial fluxes, luminous intensity at (0,0), and centre beam intensity. Absolute differences are used for power factor, all colour quantities, colour uniformity, and beam angle. Uplight flux is not shown as differences from the reference laboratory but as a ratio of participant's uplight flux value divided by their total luminous flux.

For each quantity, the first graph shows the results for all artefacts together, including any extreme results (e.g., Figure 7-1), which gives an overall picture of the results for the quantity. It is followed by a graph comparing standard deviations of results for the four artefact types (e.g., Figure 7-2). The dashed lines (blue) in the graph show the values of SDPA (shown in Table 6-1) for the quantity. The SDPA values were predetermined as expected standard deviations in participants' results, thus if the standard deviation of a result is close to or inside the SDPA lines, the variation in the result is considered reasonable.

Next four graphs show the results for each artefact (ART-1, ART-2, ART-3, ART-4) with participants' reported uncertainties (e.g., Figure 7-3 to Figure 7-6). There are fewer graphs for goniophotometric quantities (centre beam intensity, beam angle, etc.), as they were measured for only one artefact (ART-1 or ART-4). Colour uniformity was measured for two artefacts (ART-1, ART-3). In some cases, some participant labs did not report results of particular quantities, in which case no points for those labs are plotted in the graphs.

In these graphs, the horizontal axis shows Lab codes of participants, which were randomly assigned when they were registered. The error bars in the figures show the expanded uncertainties (k=2) of measurement reported by the participants and are shown only when the uncertainties were reported. Note that when a data point does not have an error bar, it means, in most cases, uncertainty was not reported, but in some cases, the reported uncertainty value could be so small that bar is hidden behind the data point.

The dashed lines (black) in the figures show the range of 2 x SDPA. Multiplying by two makes it a probability for a 95 % confidence interval. It was expected that the results would lie mostly within this range. The dotted lines (green) in each figure show the range of the expanded uncertainty (k=2) of the reference value from Table 5-5. When evaluating participants' reported uncertainties, the error bar of each point is expected to overlap with this range (green dotted lines) if the reported uncertainty is appropriate. However, this is only a statistical consideration; overlap does not assure that the reported uncertainty is accurate.

In these graphs, there may be some outliers whose points are out of the scale presented, in which case they are indicated by a red arrow and their values shown in red text at the upper or lower edge of the graph (e.g., in Figure 7-3). The full scale of each graph was determined for each case based on the distribution of data points but were typically four to six times of ± SDPA. These outliers were excluded in the calculation of the standard deviations, as these extreme results were likely caused by some mistakes by the participant and considered not representing statistical variations of the population. Note that the exclusion of outliers was only to calculate standard deviations to evaluate the variations in results among different artefacts, and it did not affect the results of the participants with respect to the reference values.

7.2.1 Total Luminous Flux

The overall result of total luminous flux is shown in Figure 7-1. Most labs were within the SDPA x 2 range except for a few labs which were outside, with only one outlier in all results, and the result is considered reasonable overall. Figure 7-2 shows that the standard deviations for all artefacts (one outlier excluded) were close to or less than the SDPA value and the variations in results were also considered reasonable.

In Figure 7-2, ART-1 shows the largest variations, which is possibly due to combined effects of its very narrow beam intensity distribution and the angle setting accuracies of the goniophotometers among the participants.

Figure 7-3 to Figure 7-6 show the results for each artefact with the reported uncertainties (shown by error bars) of the participants. The uncertainty values of the labs seem to be reasonable overall for all the artefacts.

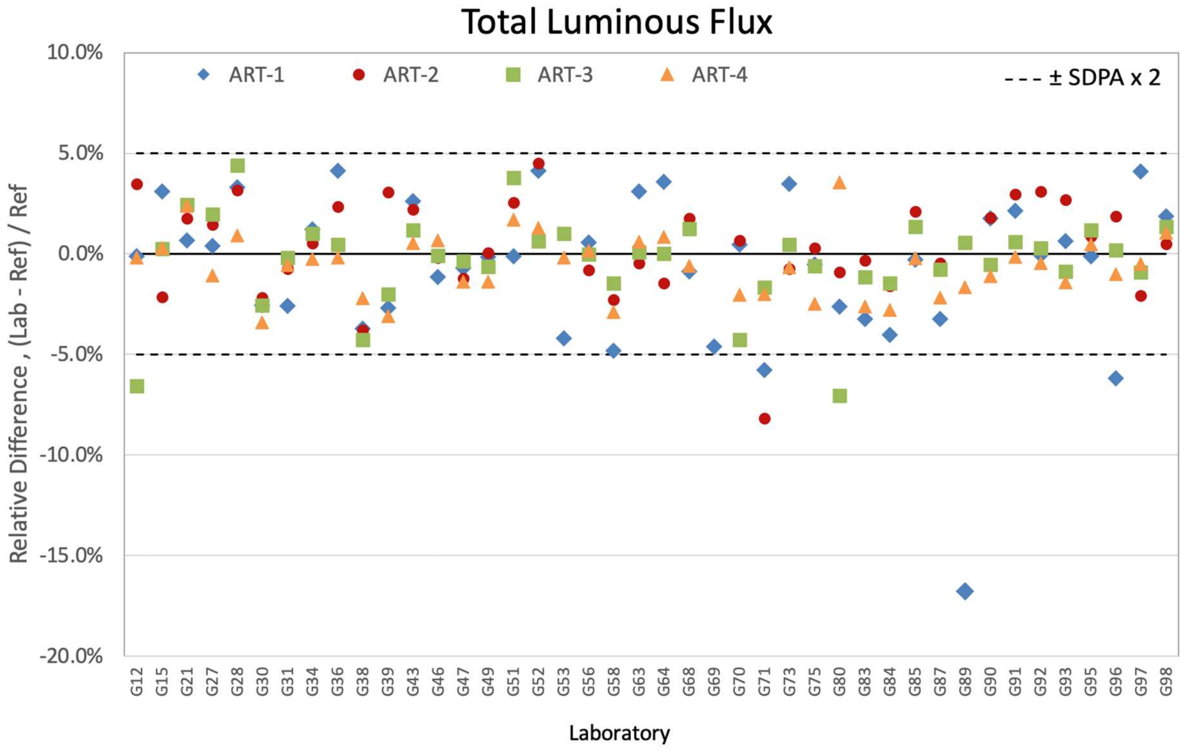

Figure 7-1. Relative differences of total luminous flux for all artefacts

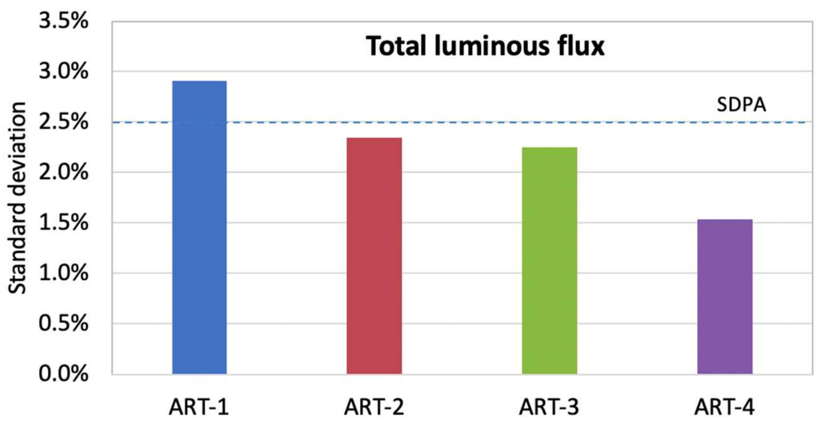

Figure 7-2. Relative standard deviations of total luminous flux results

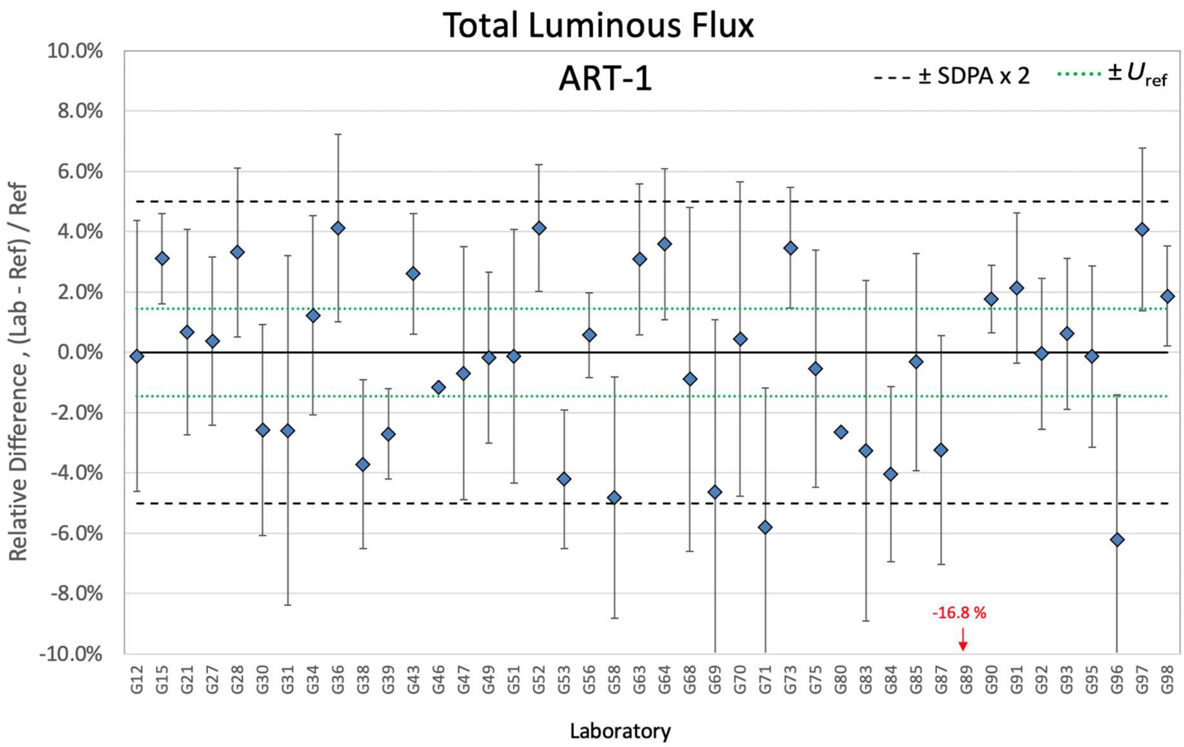

Figure 7-3. Relative differences of total luminous flux for ART-1

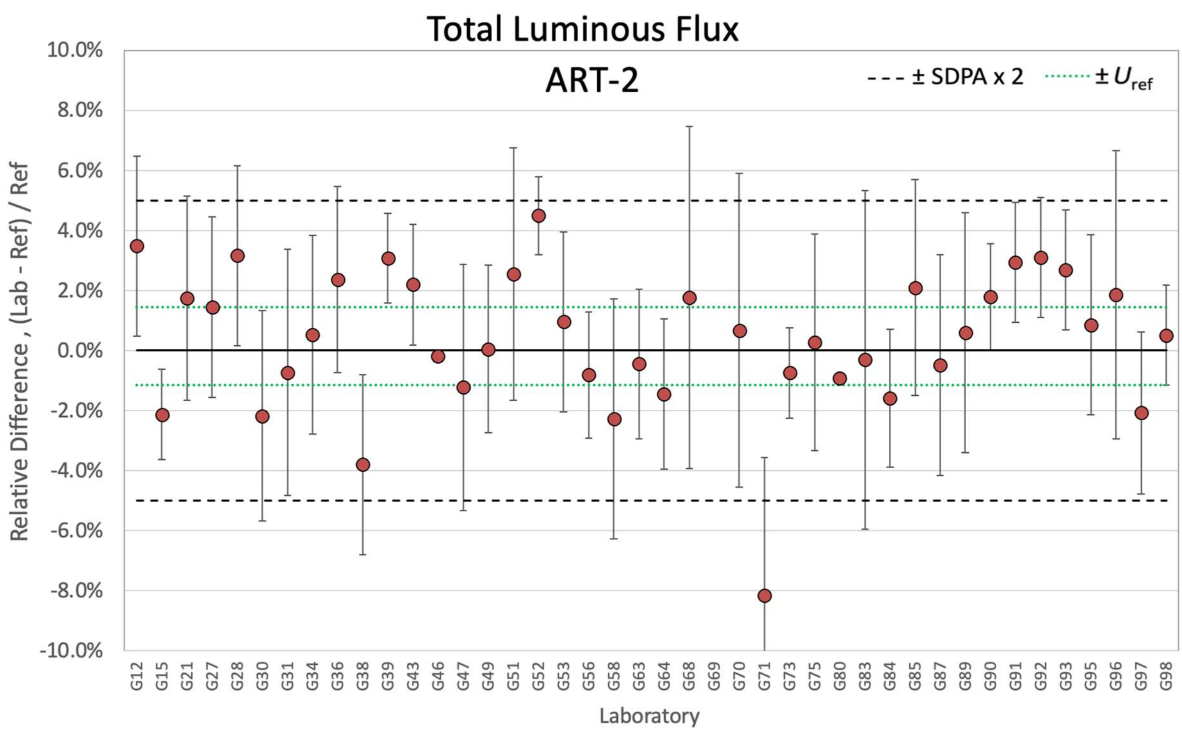

Figure 7-4. Relative differences of total luminous flux for ART-2

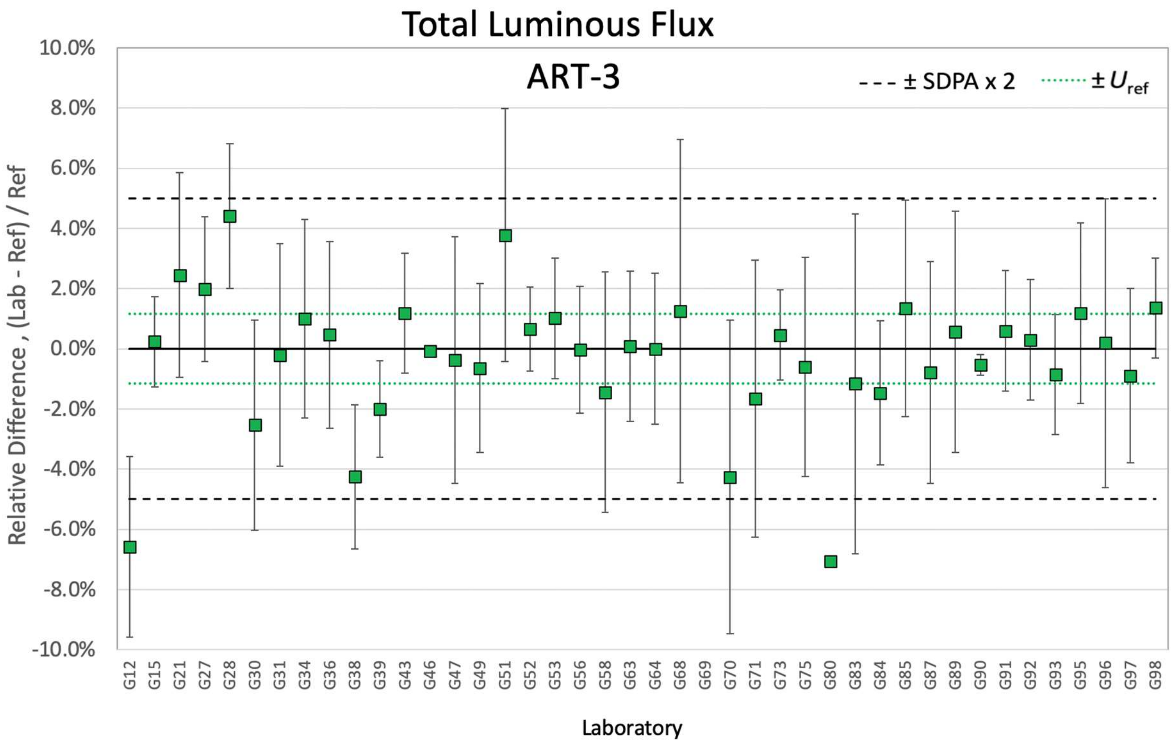

Figure 7-5. Relative differences of total luminous flux for ART-3

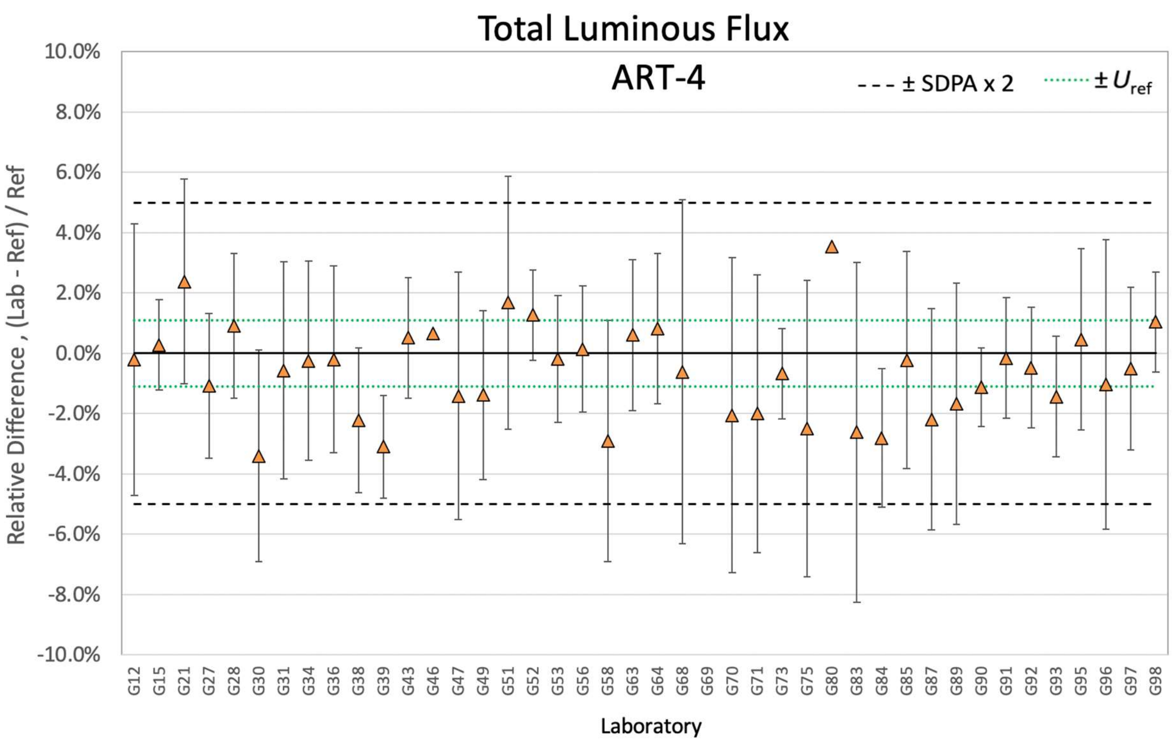

Figure 7-6. Relative differences of total luminous flux for ART-4

7.2.2 Active Power

The overall result of active power is shown in Figure 7-7. Note that the values for ART-1 are DC power. The variations are mostly within SDPA x 2, except ART-1, which showed significantly large variations. The standard deviations of results (only one outlier point excluded) for each artefact are shown in Figure 7-8, which clearly shows a large variation in the result of ART-1, while other artefacts show reasonable variations.

The reason for large variation in ART-1 may be related to the low voltage of this lamp (12V DC) with relatively higher current and small connection pins of MR-16 for electrical connection. Varied voltage drops at the connection pins and socket may be causing such large variations in the voltage supplied to the lamp. However, further investigation determined that the total luminous flux of ART-1 lamps was not sensitive to changes in supply voltage or current, possibly due to some kind of constant power control within the lamp, as no such large variation is observed for ART-1 in total luminous flux result (Figure 7-2), though it is slightly higher than others. It is considered that the (DC) power of ART-1 measured at the socket may be different from the power consumed by the lamp due to the voltage drop at the socket.

Figure 7-9 to Figure 7-12 show the results for each artefact with the reported uncertainties of the participants. The results for artefacts other than ART-1 appear very good. The uncertainty values of the labs seem to be reasonable except those for ART-1. Especially ART-2 showed excellent agreement with small variations. These results indicate that variation in measurement depends much on the electronics design of each artefact.

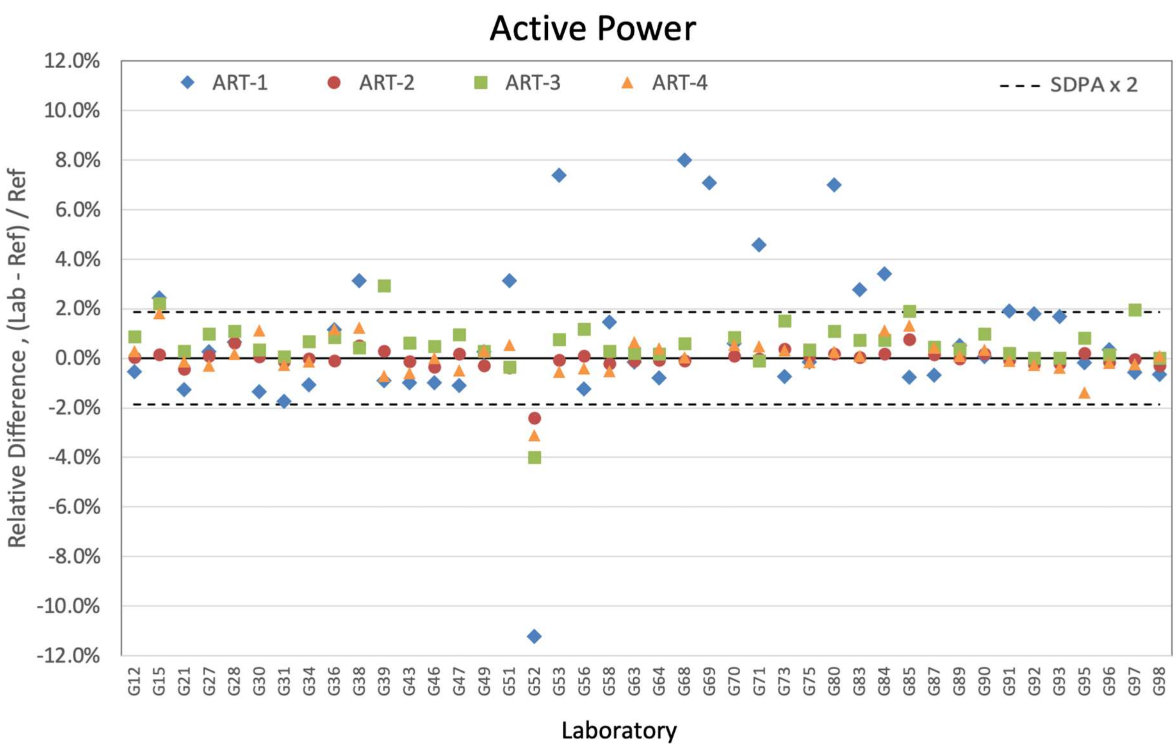

Figure 7-7. Relative differences of active power for all artefacts

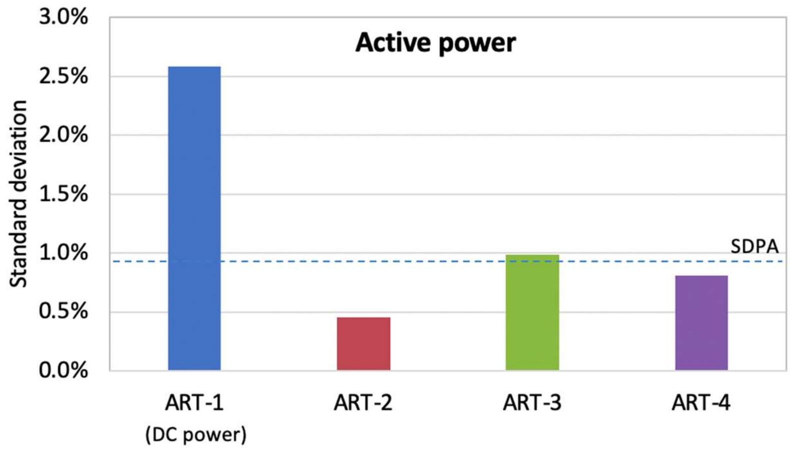

Figure 7-8. Relative standard deviations of active power results

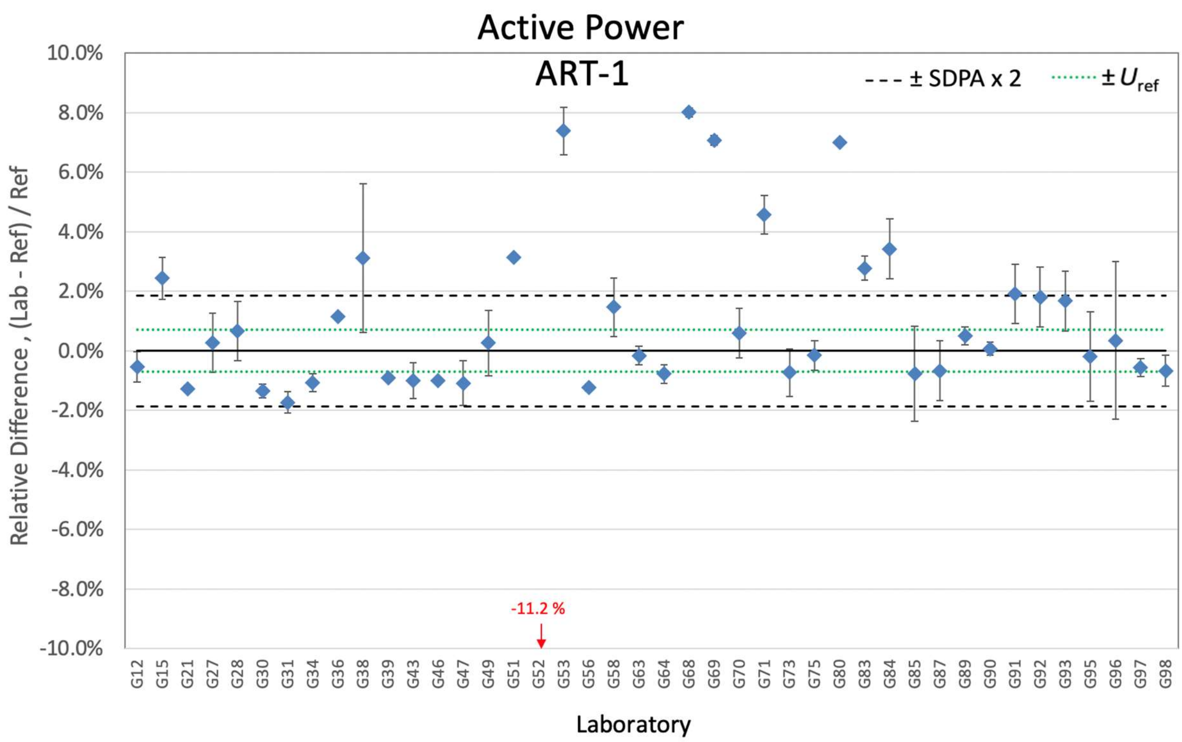

Figure 7-9. Relative differences of active power for ART-1

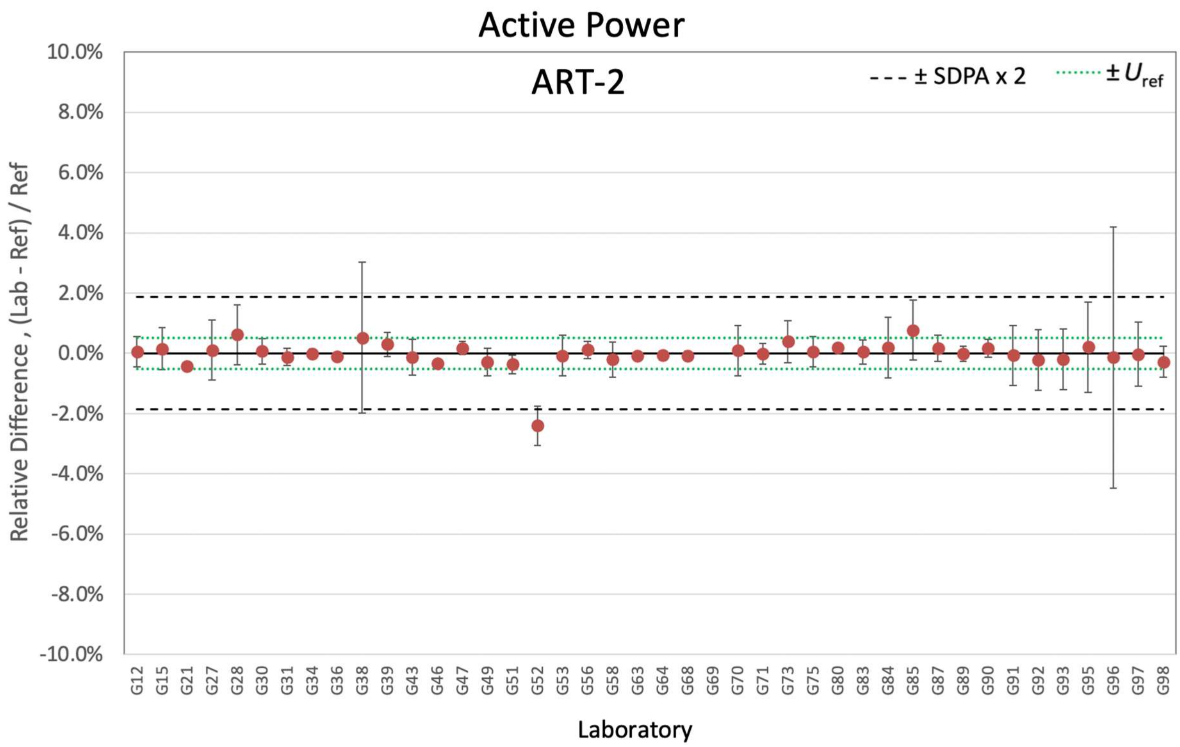

Figure 7-10. Relative differences of active power for ART-2

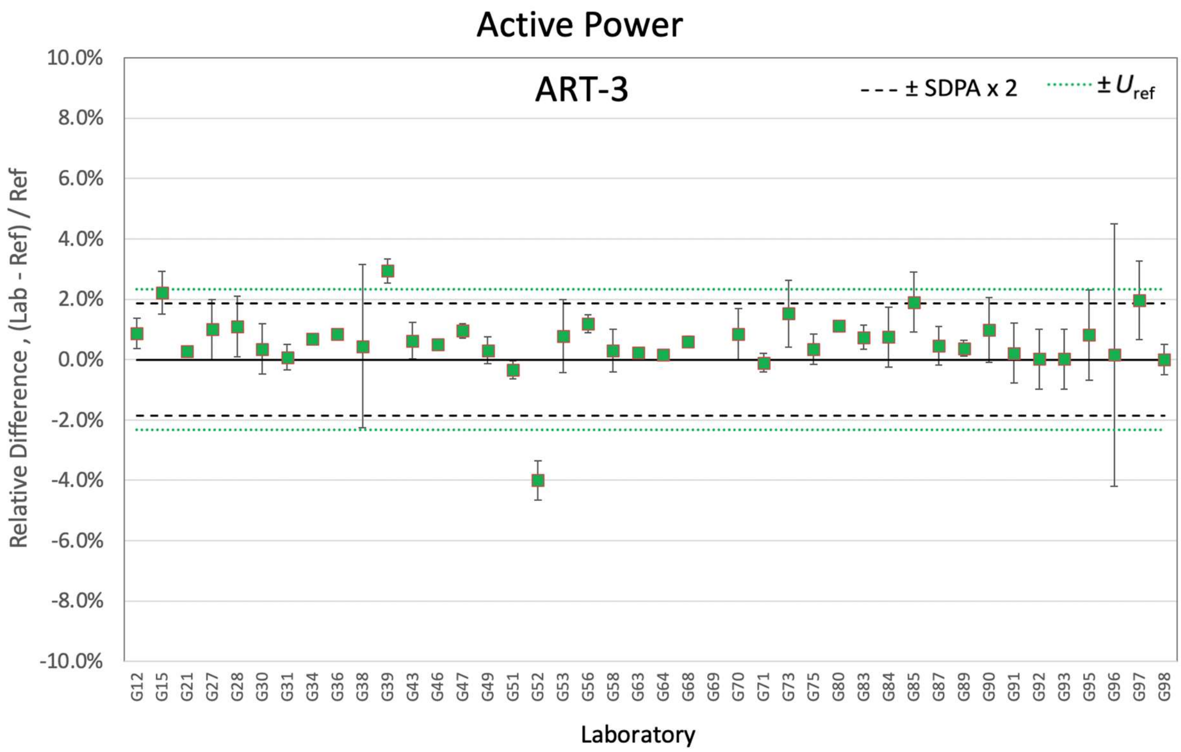

Figure 7-11. Relative differences of active power for ART-3

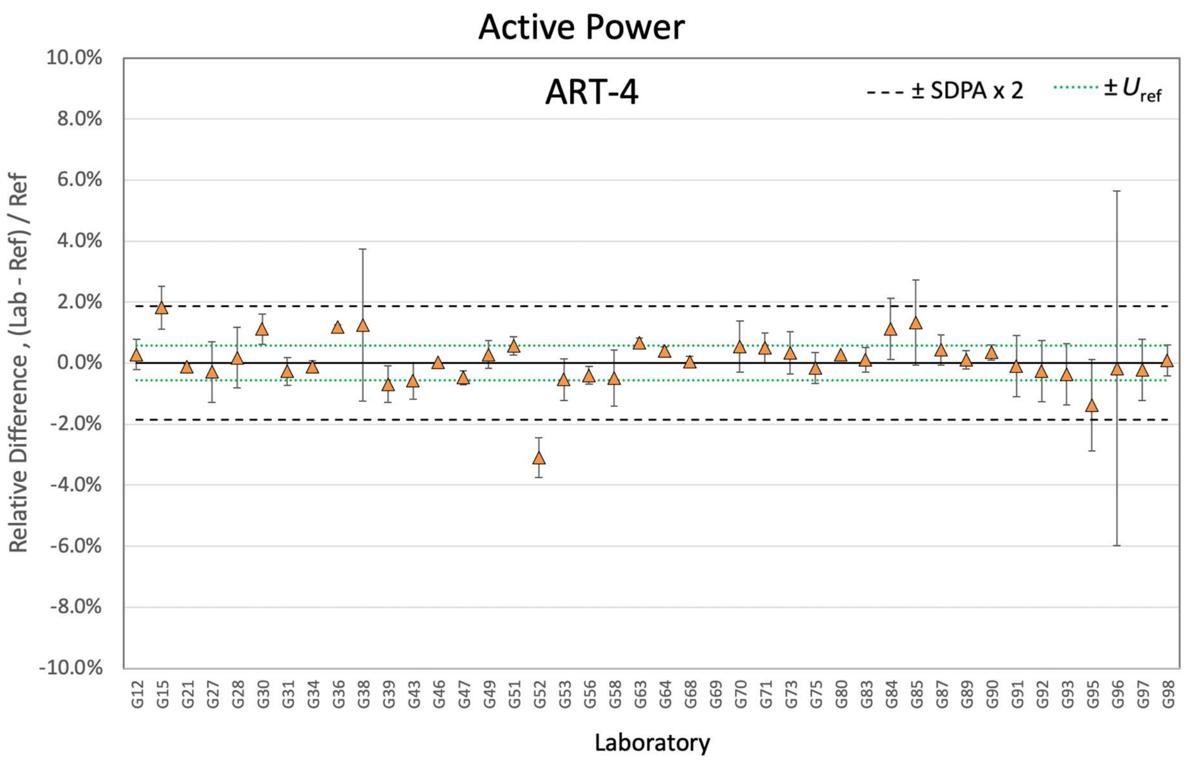

Figure 7-12. Relative differences of active power for ART-4

7.2.3 RMS current

The overall result of RMS current is shown in Figure 7-13. The standard deviations of results (three outliers excluded) for each artefact are shown in Figure 7-14. Note that the values for ART-1 are DC current. The results are similar to active power because the artefacts were operated on rated supply voltage. The variations for artefacts other than ART-1 and ART-3, compared to the range of SDPA x 2, appear to be reasonable. The variation for ART-2 is much smaller than others, the reason for which must be related to the electronic driver design of the product, but no detail is available.

Figure 7-15 to Figure 7-18 show the results for each artefact with the reported uncertainties of the participants. It appears that the uncertainties are underestimated in many cases except for ART-2.

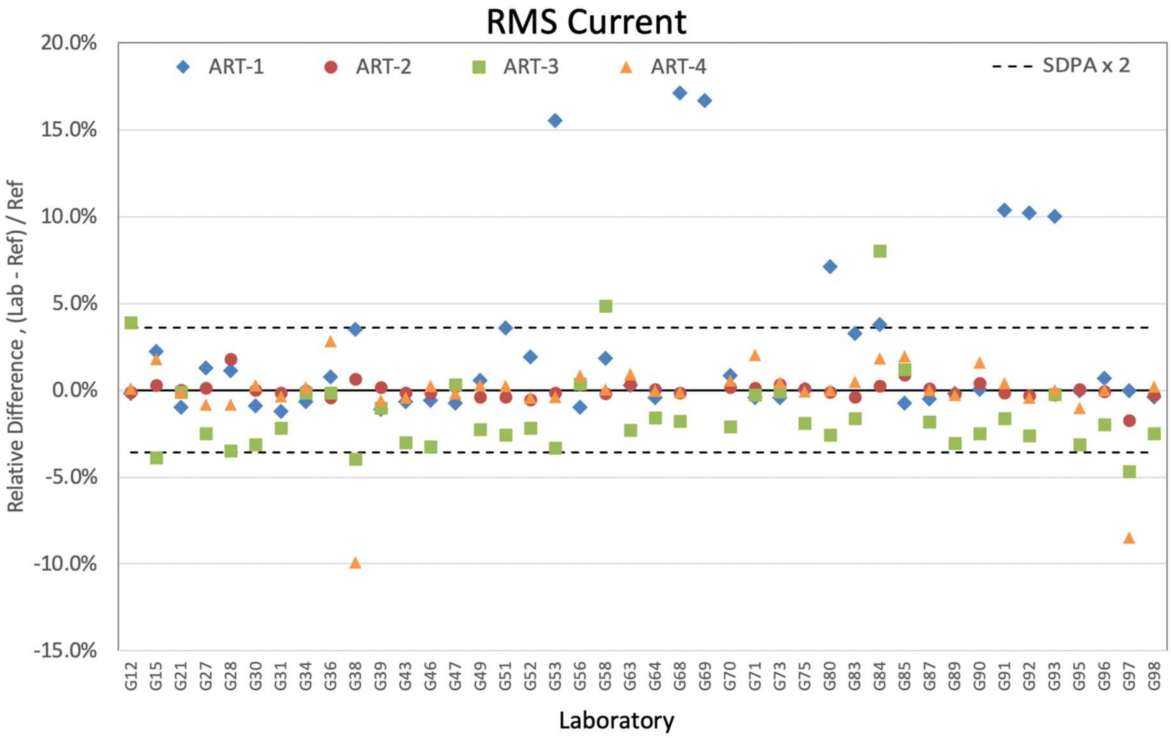

Figure 7-13. Relative differences of RMS current for all artefacts

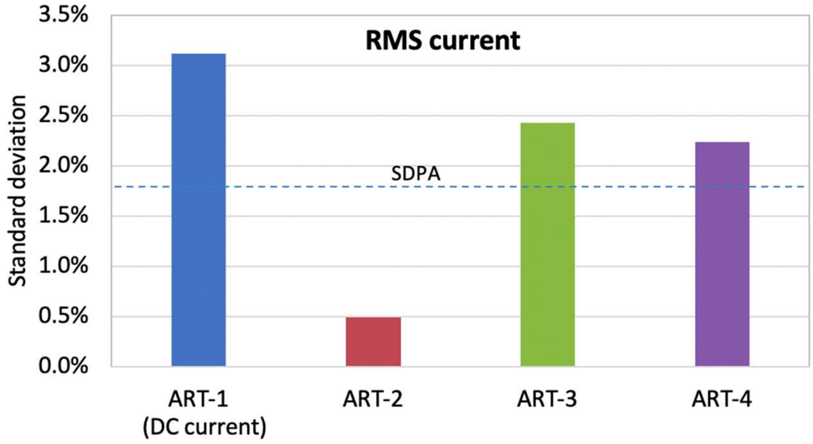

Figure 7-14. Relative standard deviations of RMS current results

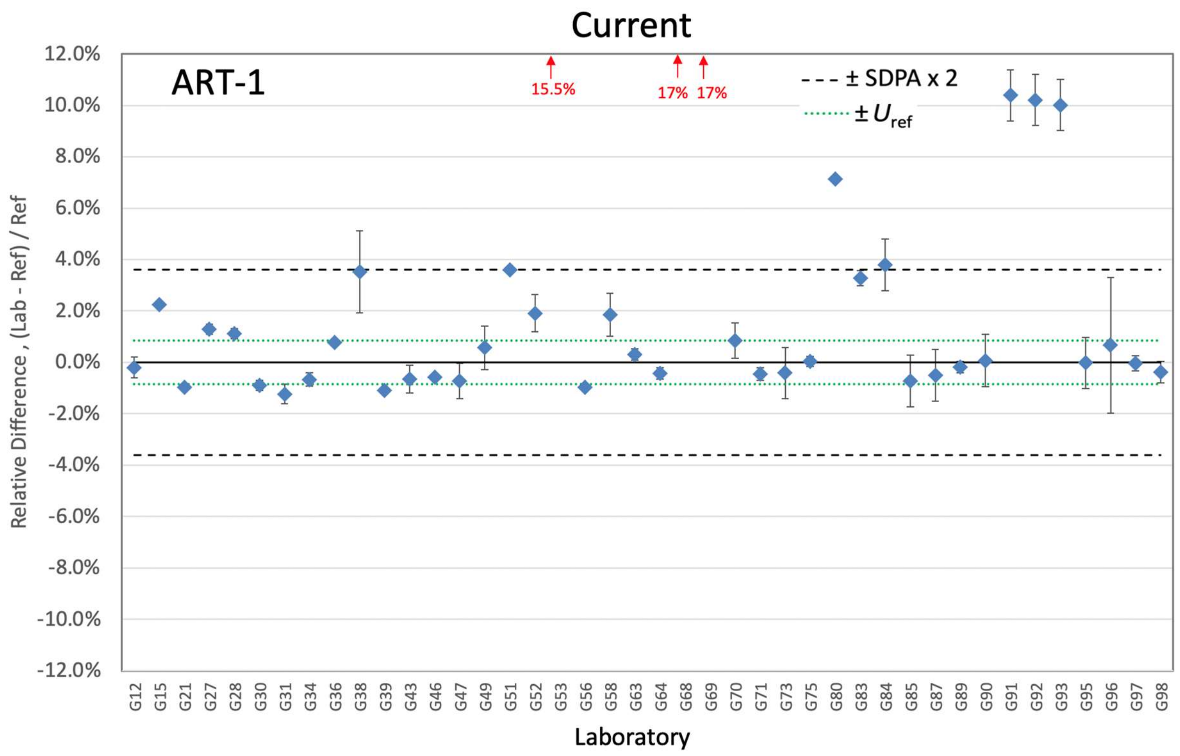

Figure 7-15. Relative differences of RMS current for ART-1

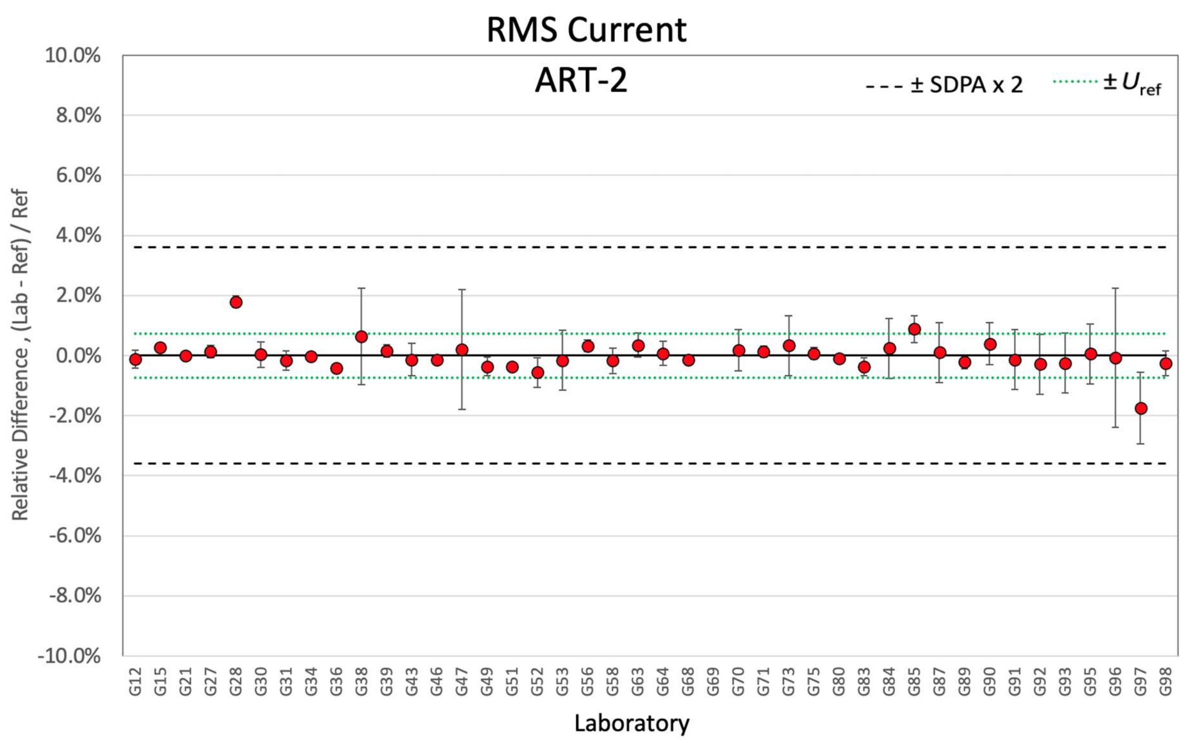

Figure 7-16. Relative differences of RMS current for ART-2

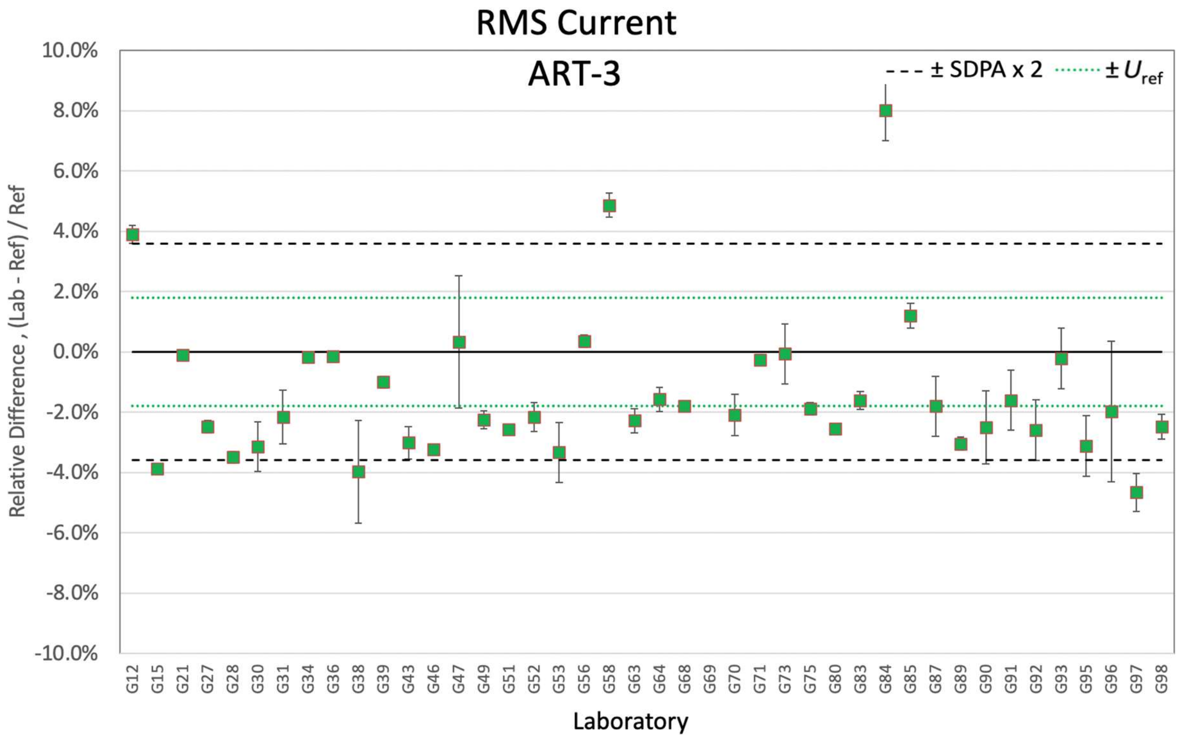

Figure 7-17. Relative differences of RMS current for ART-3

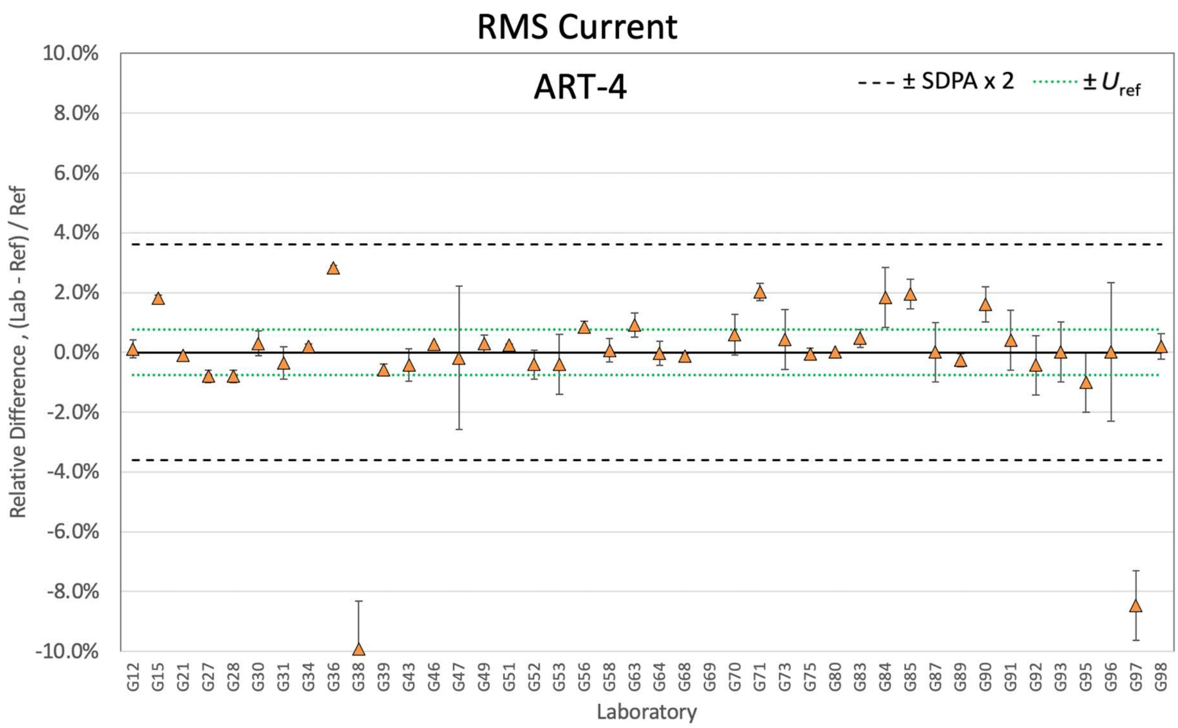

Figure 7-18. Relative differences of RMS current for ART-4

7.2.4 Luminous efficacy

The overall result of luminous efficacy is shown in Figure 7-19. The standard deviations of results (outliers excluded) for each artefact are shown in Figure 7-20. The results are similar to total luminous flux, except that the variation of ART-1 is larger, which is reflected by its large variation in active power results.

Figure 7-21 to Figure 7-24 show the results for each artefact with the reported uncertainties of the participants. It appears that the reported uncertainties were overall reasonable.

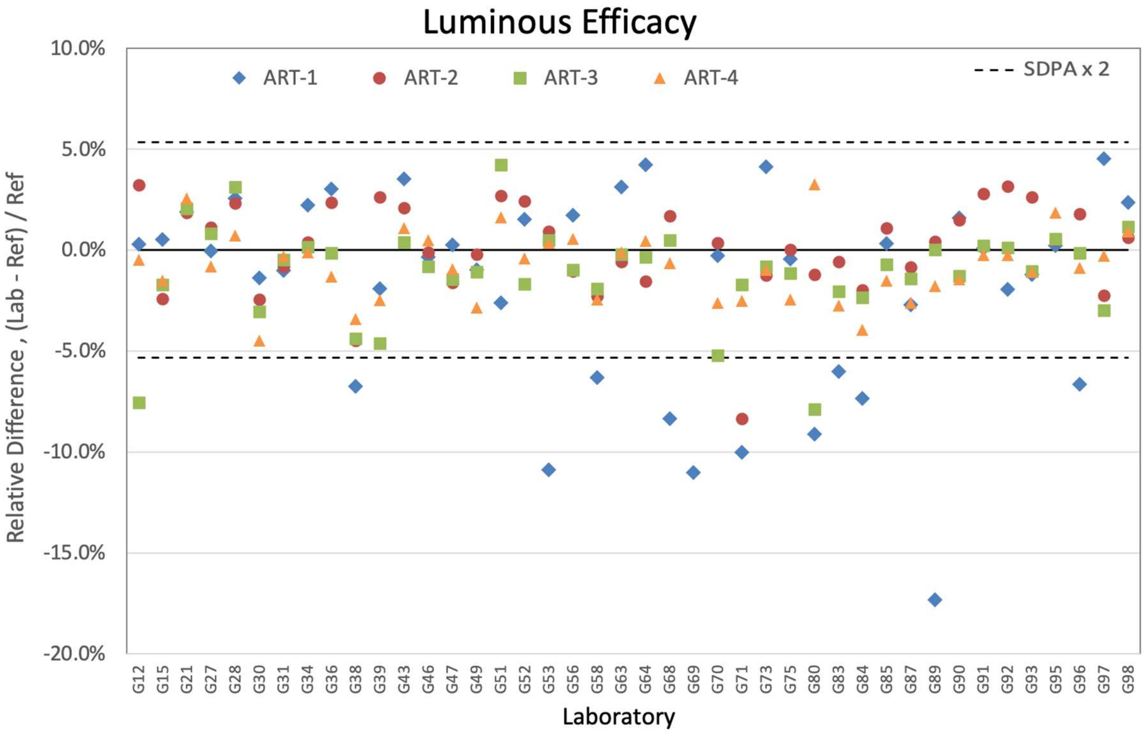

Figure 7-19. Relative differences of luminous efficacy for all artefacts

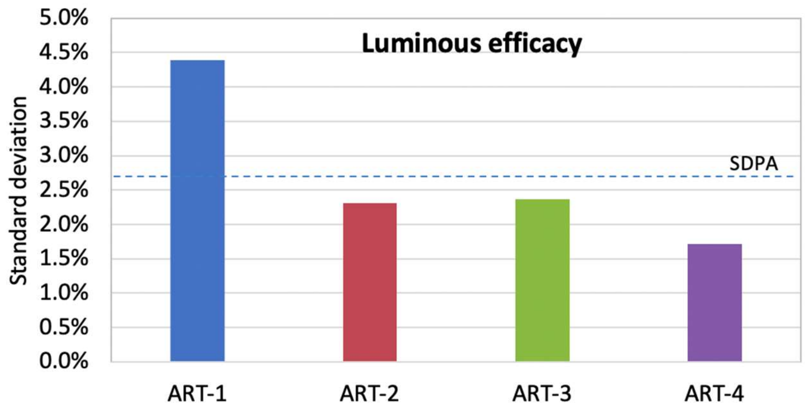

Figure 7-20. Relative standard deviations of luminous efficacy results

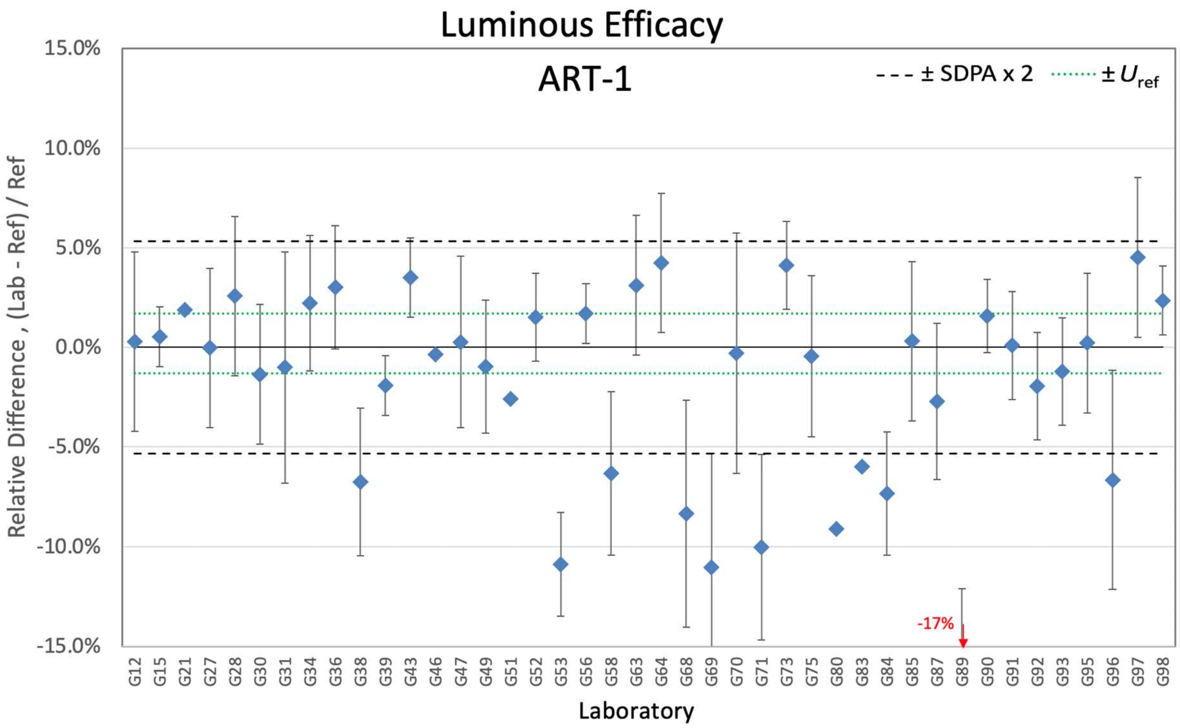

Figure 7-21. Relative differences of luminous efficacy for ART-1

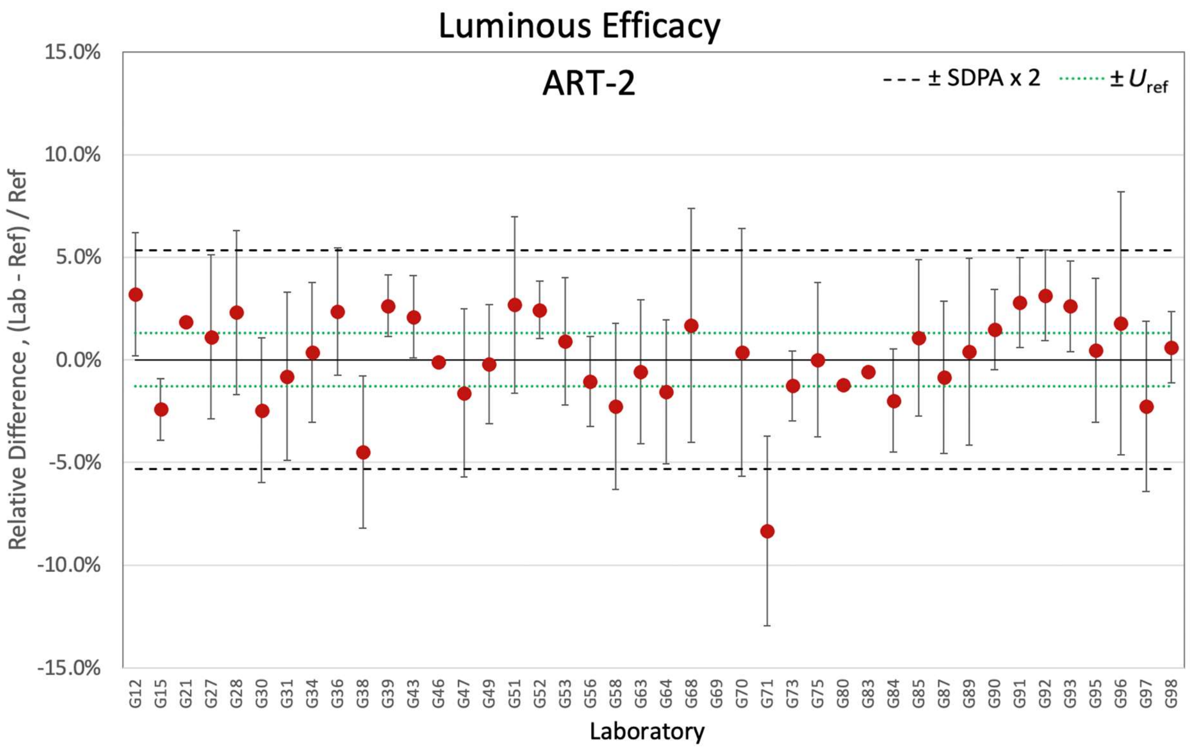

Figure 7-22. Relative differences of luminous efficacy for ART-2

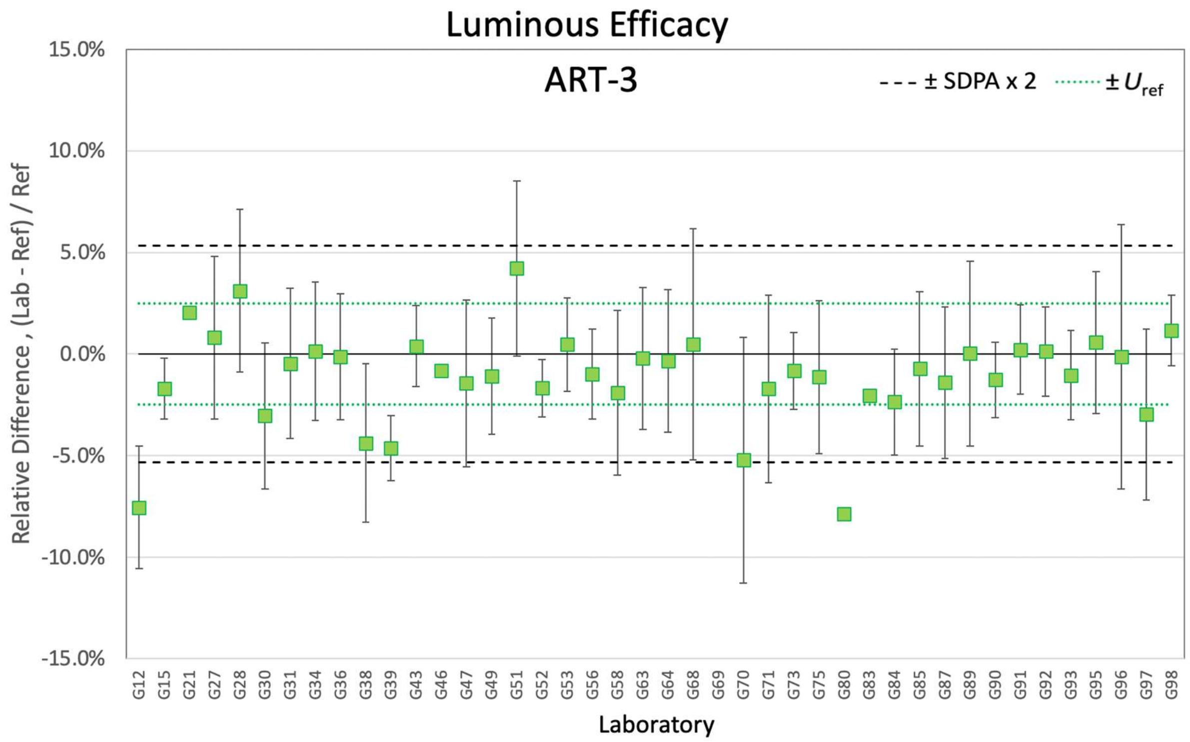

Figure 7-23. Relative differences of luminous efficacy for ART-3

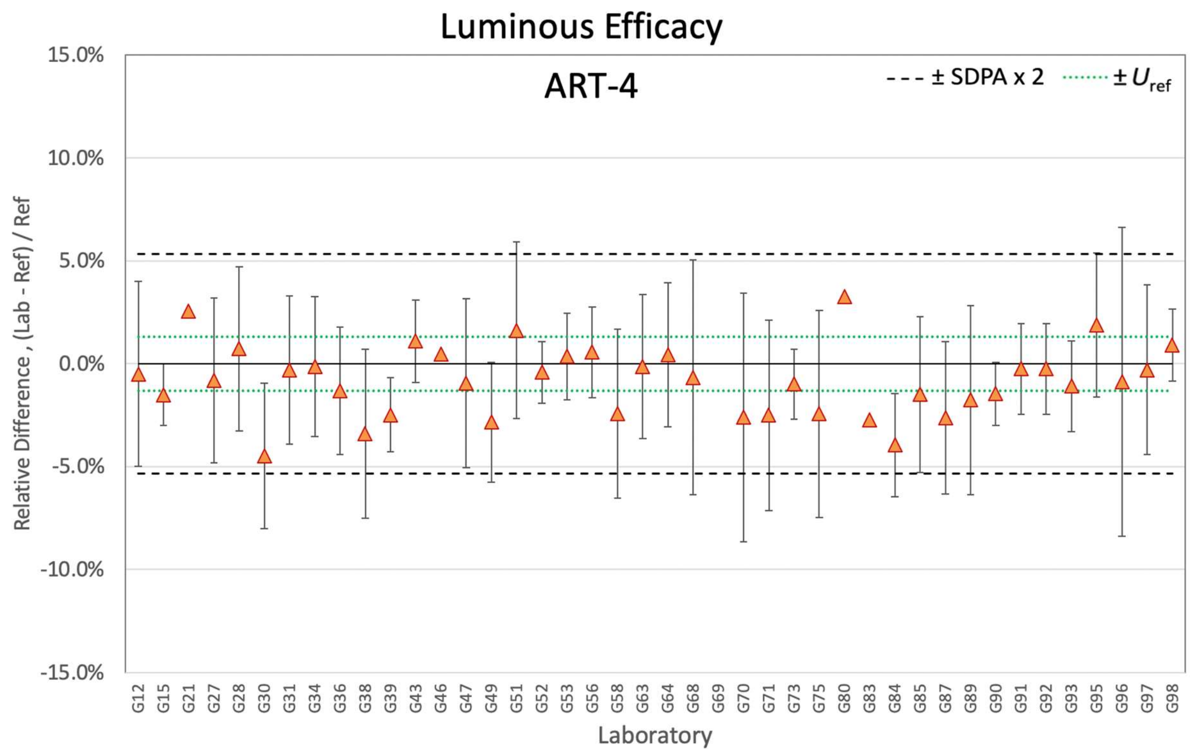

Figure 7-24. Relative differences of luminous efficacy for ART-4

7.2.5 Power Factor

The overall result of power factor is shown in Figure 7-25. The standard deviations of results (five outliers excluded) for each artefact are shown in Figure 7-26. ART-1 is not included in these figures because this lamp was operated on DC power and power factor is not applicable. The results show extremely large variations in ART-3 results (which is consistent with the RMS current results), while other artefacts show reasonable variations. The power factor values of the artefacts are approximately 0.98, 0.94, 0.68 for ART-2, ART-3, ART-4, respectively. There were large differences for ART-3 in Nucleus Lab Comparison also, while measured value reproduced well, and for this reason, a higher value of uncertainty for the reference value was given for ART-3 (Table 5-5). It is considered that this artefact's electronics has some unknown characteristics (e.g., some very high frequency components in current, though not identified) that are sensitive to the power supplies and electrical conditions used.

Figure 7-27 to Figure 7-29 show the results for each artefact (except ART-1) with the reported uncertainties of the participants. It shows a large range of uncertainty values reported by participants. Points with no error bar means the uncertainty was not submitted.

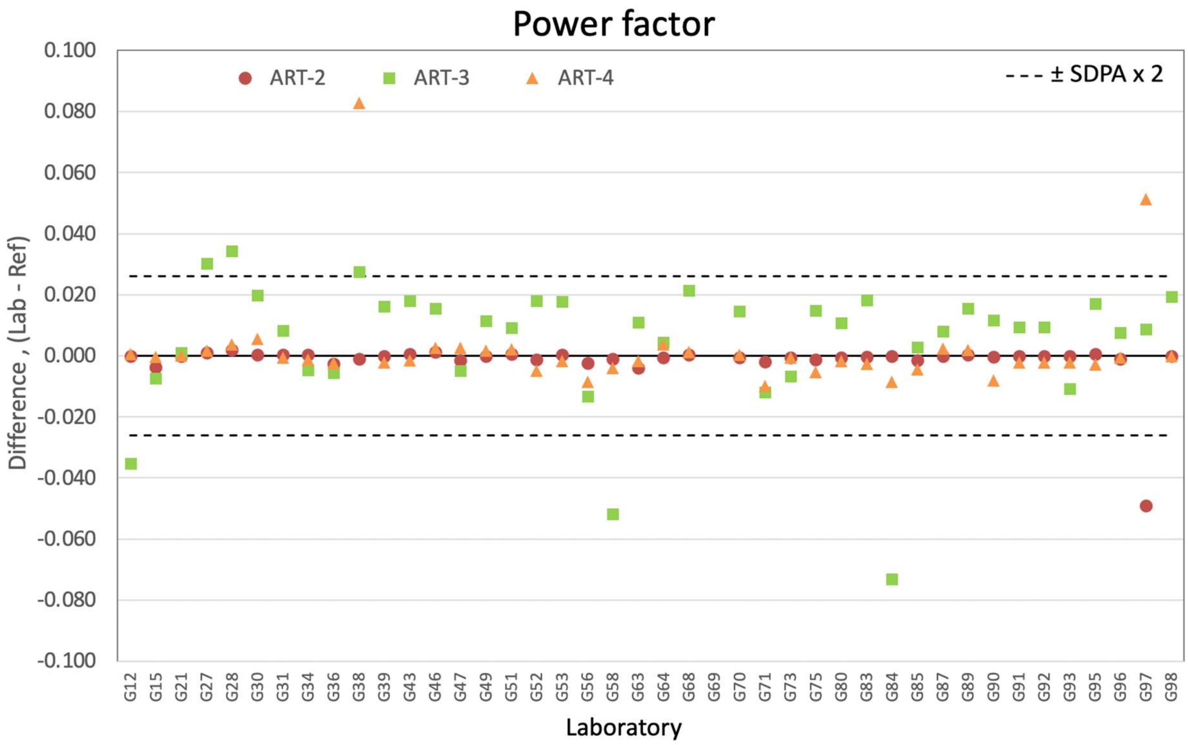

Figure 7-25. Differences of power factor for all artefacts

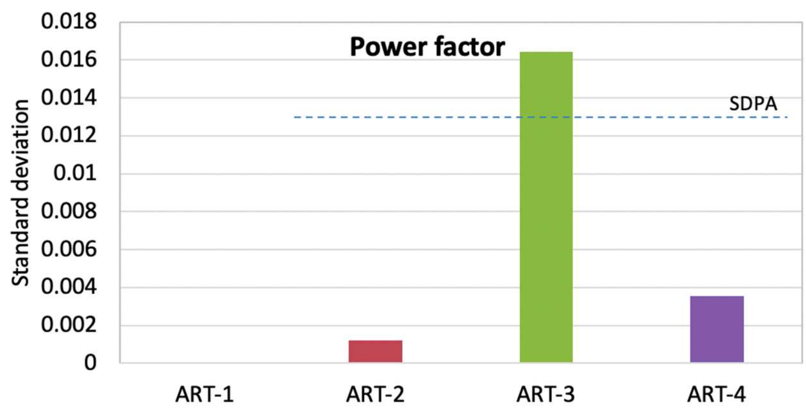

Figure 7-26. Standard deviations of power factor results

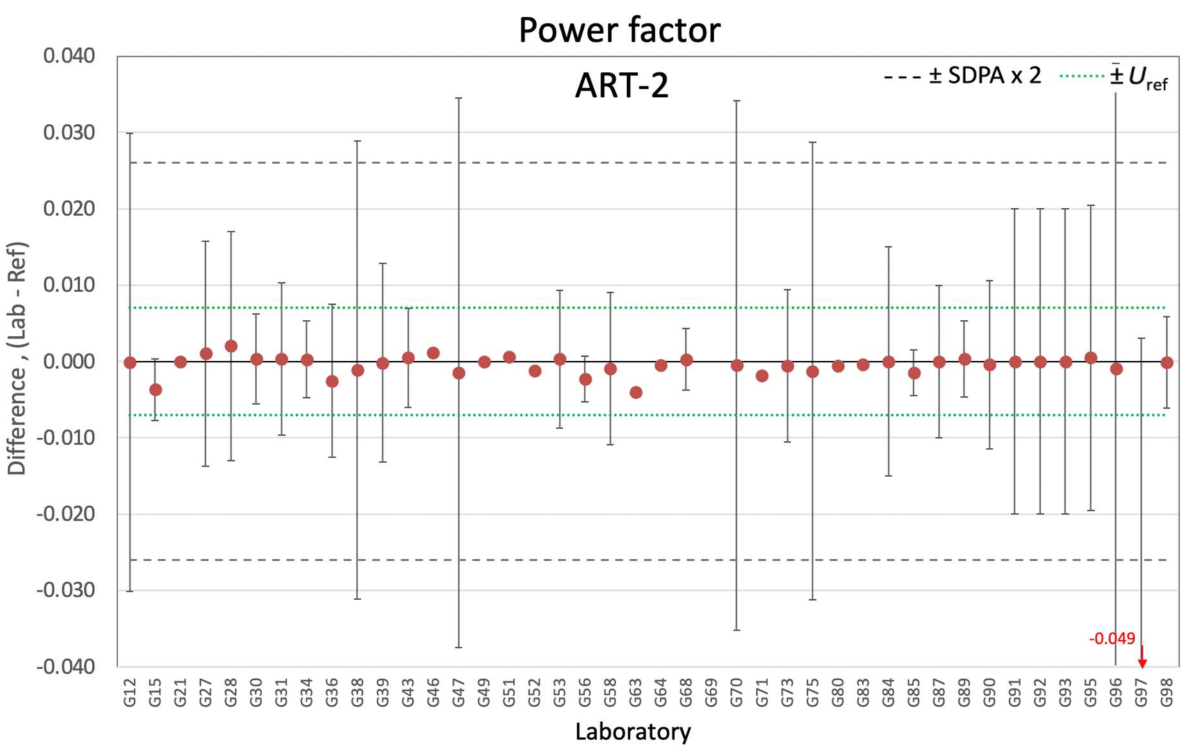

Figure 7-27. Differences of power factor for ART-2

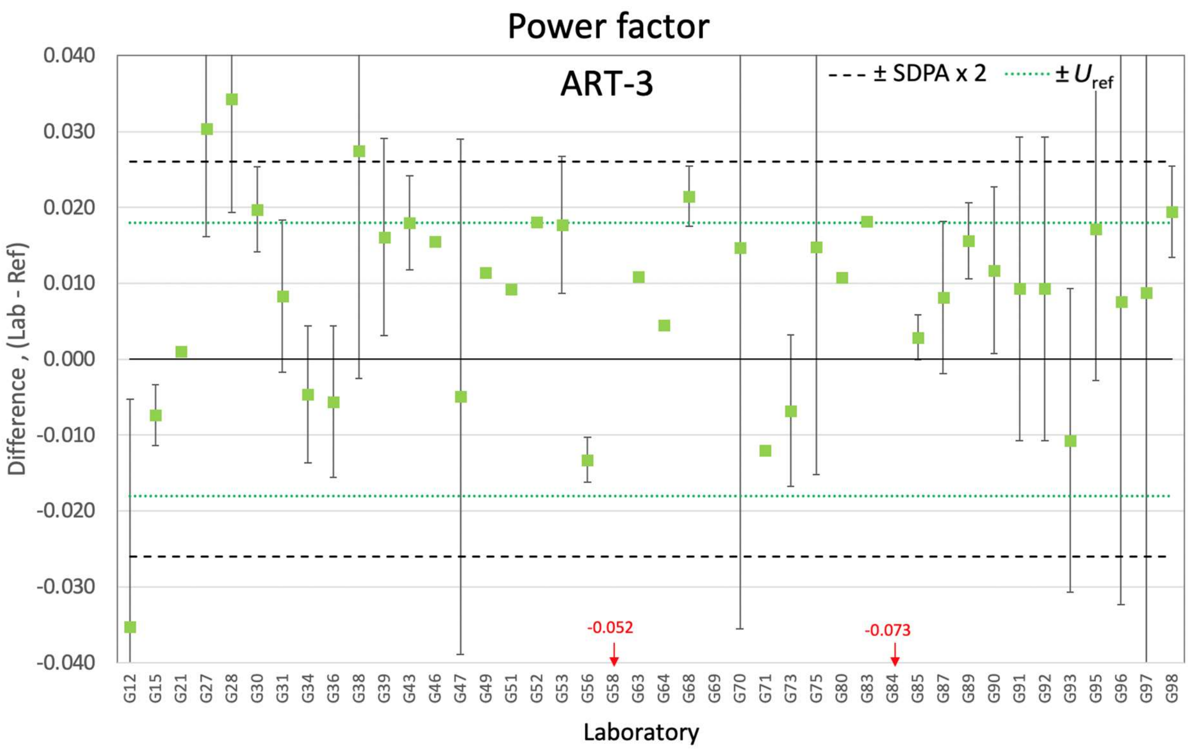

Figure 7-28. Differences of power factor for ART-3

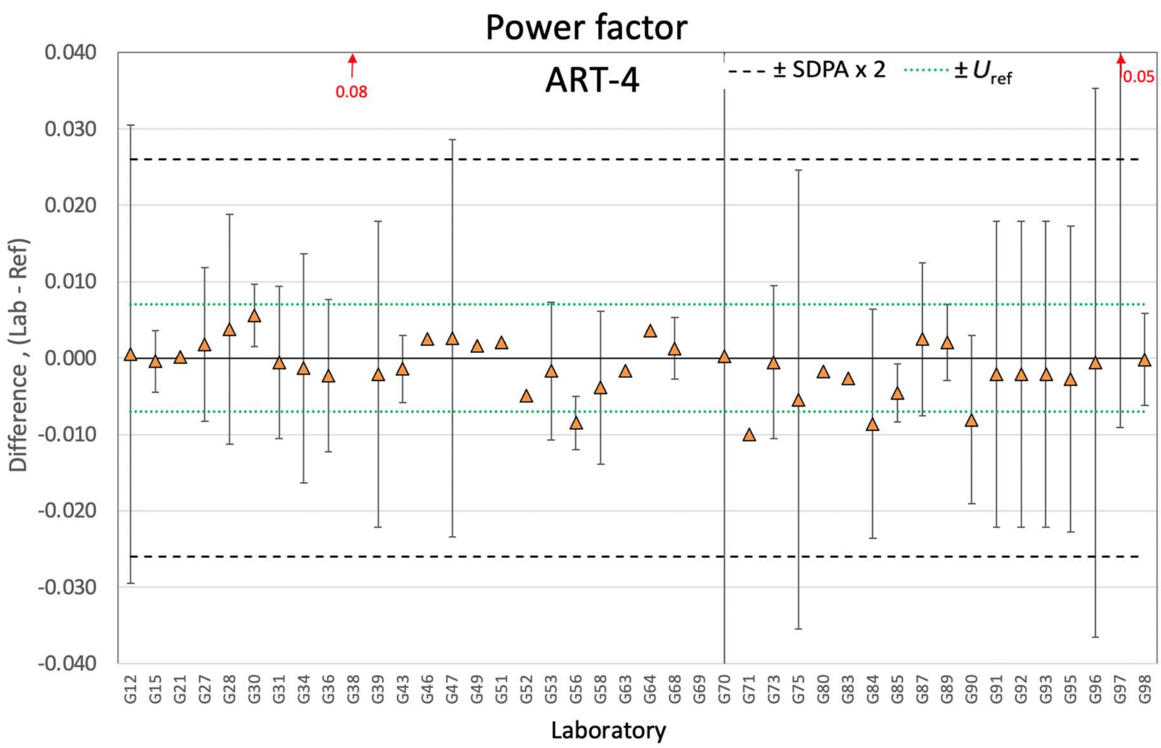

Figure 7-29. Differences of power factor for ART-4

7.2.6 Chromaticity *u'*, *v'*

The overall results of chromaticity *u'* and *v'* are shown in Figure 7-30 and Figure 7-31, which show good agreement, with most of the results within ± 0.002 and well within ± 2 x SDPA, except a few outliers in *v'*.

Figure 7-32 shows the standard deviations of results (no outliers for *u'*, two outliers for *v'* excluded) for each artefact, showing variations less than the SDPA line for all artefacts and no notable differences between artefact types.

Figure 7-33 to Figure 7-36 show the results of *u'* for each artefact with the reported uncertainties of the participants, and for *v'* in Figure 7-37 to Figure 7-40. The reported uncertainties appear to be reasonable in most cases, and it appears that several labs overestimated their uncertainties.

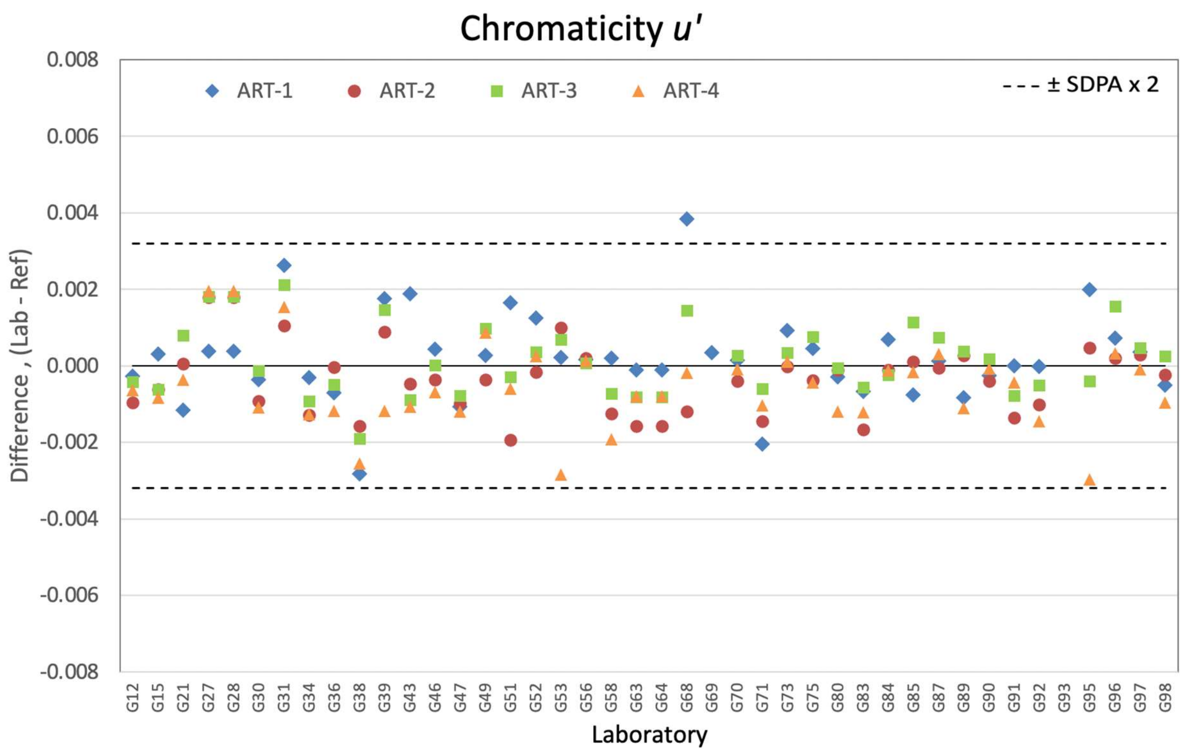

Figure 7-30. Differences of chromaticity *u'* for all artefacts

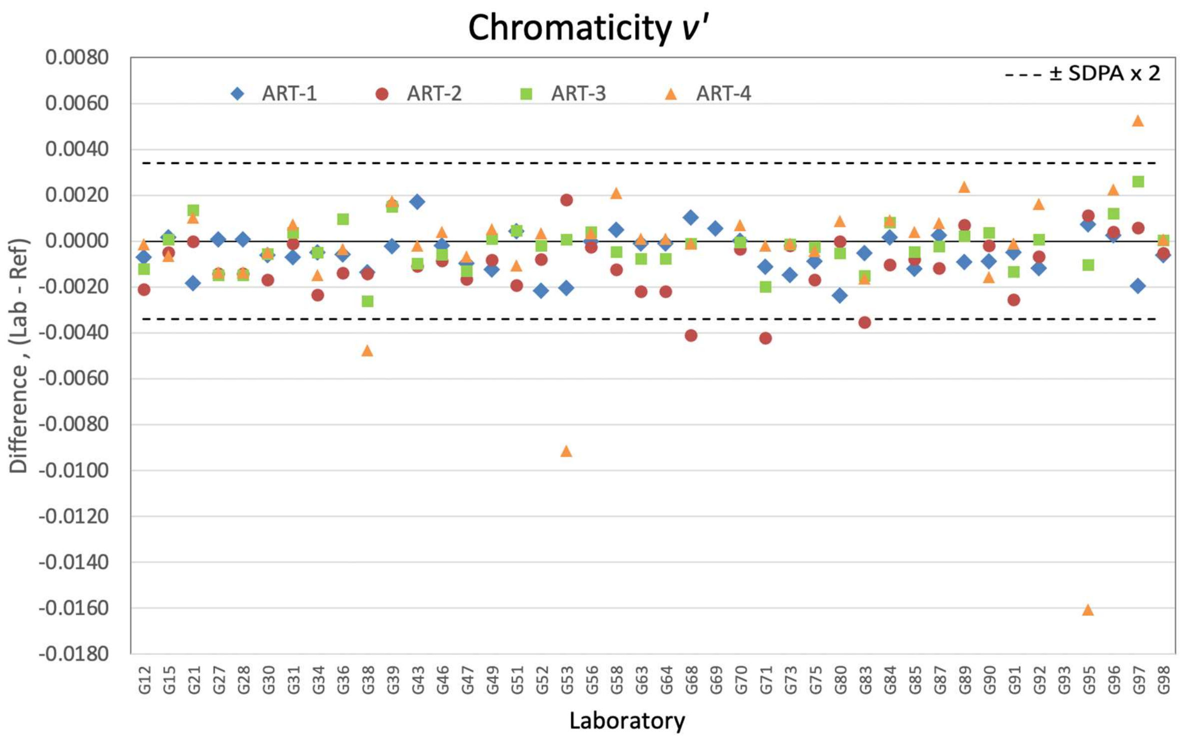

Figure 7-31. Differences of chromaticity *v*′ for all artefacts

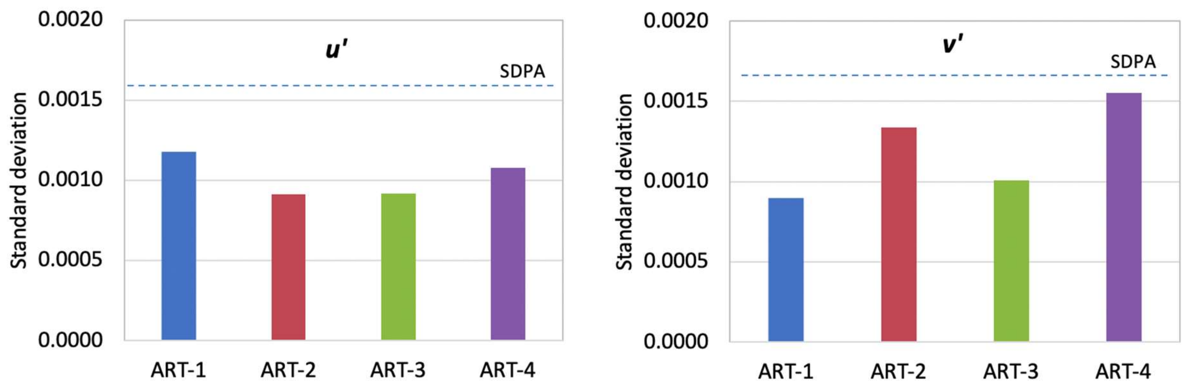

Figure 7-32. Standard deviations of chromaticity *u*′, *v*′ results

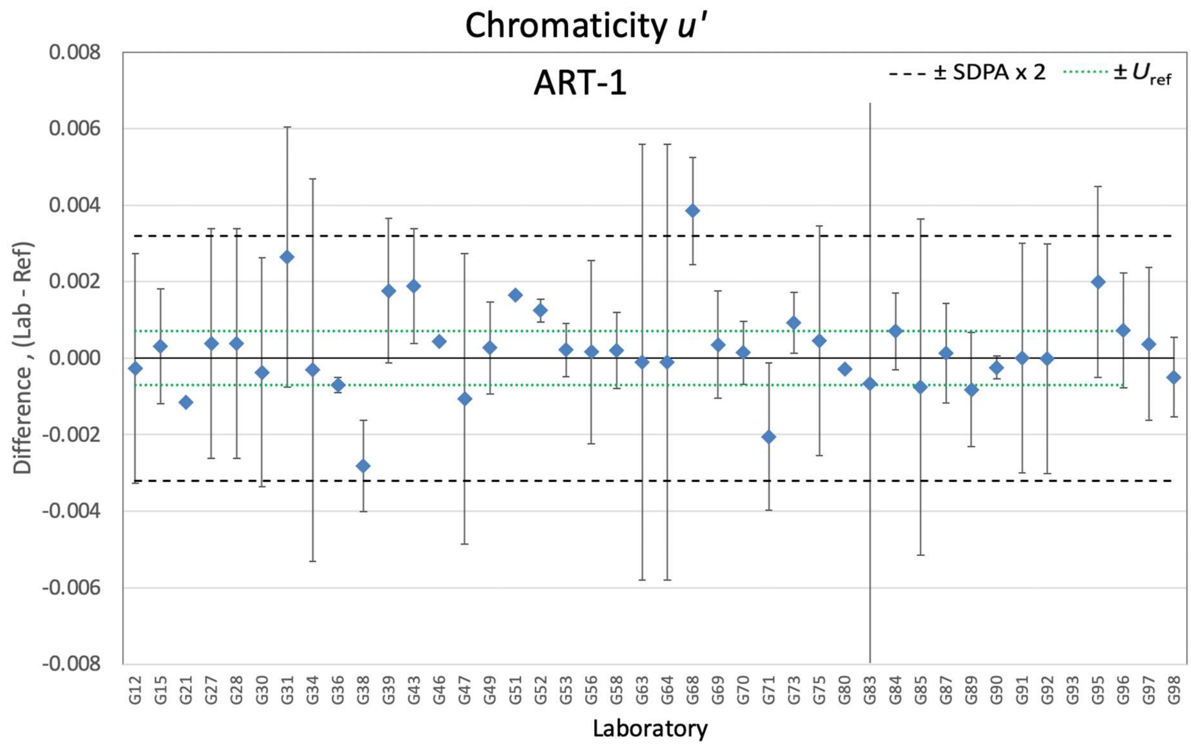

Figure 7-33. Differences of chromaticity *u′* for ART-1

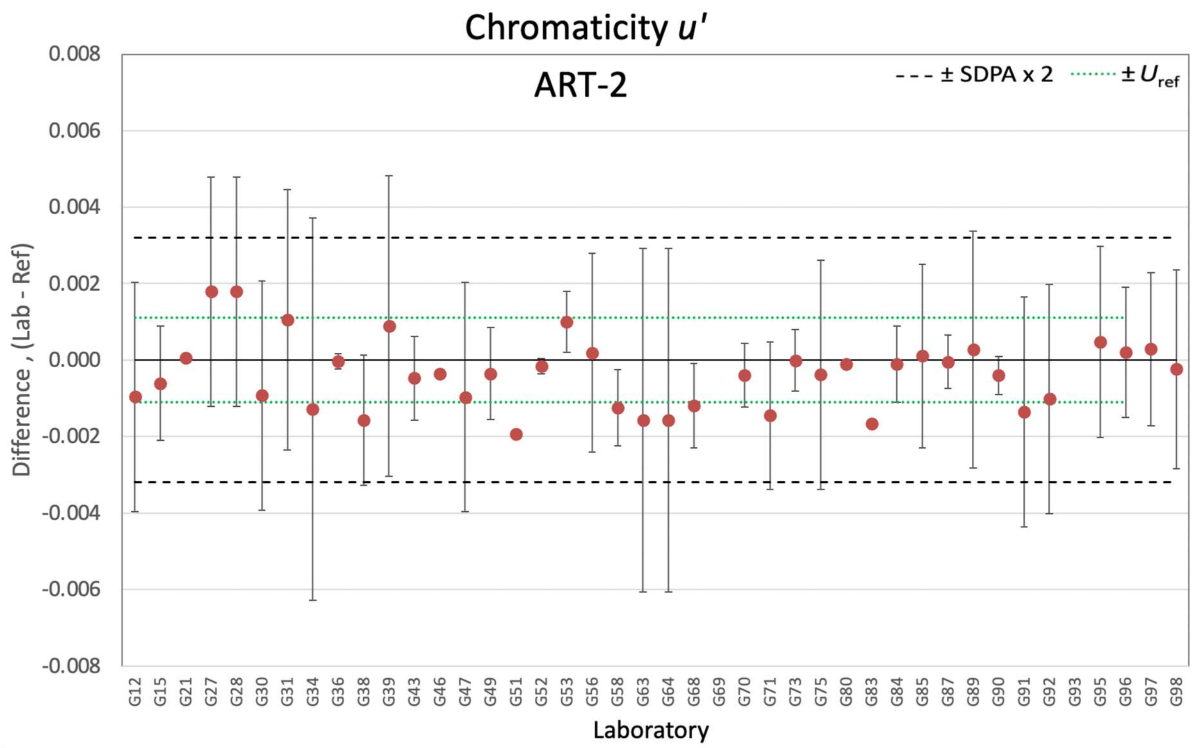

Figure 7-34. Differences of chromaticity *u′* for ART-2

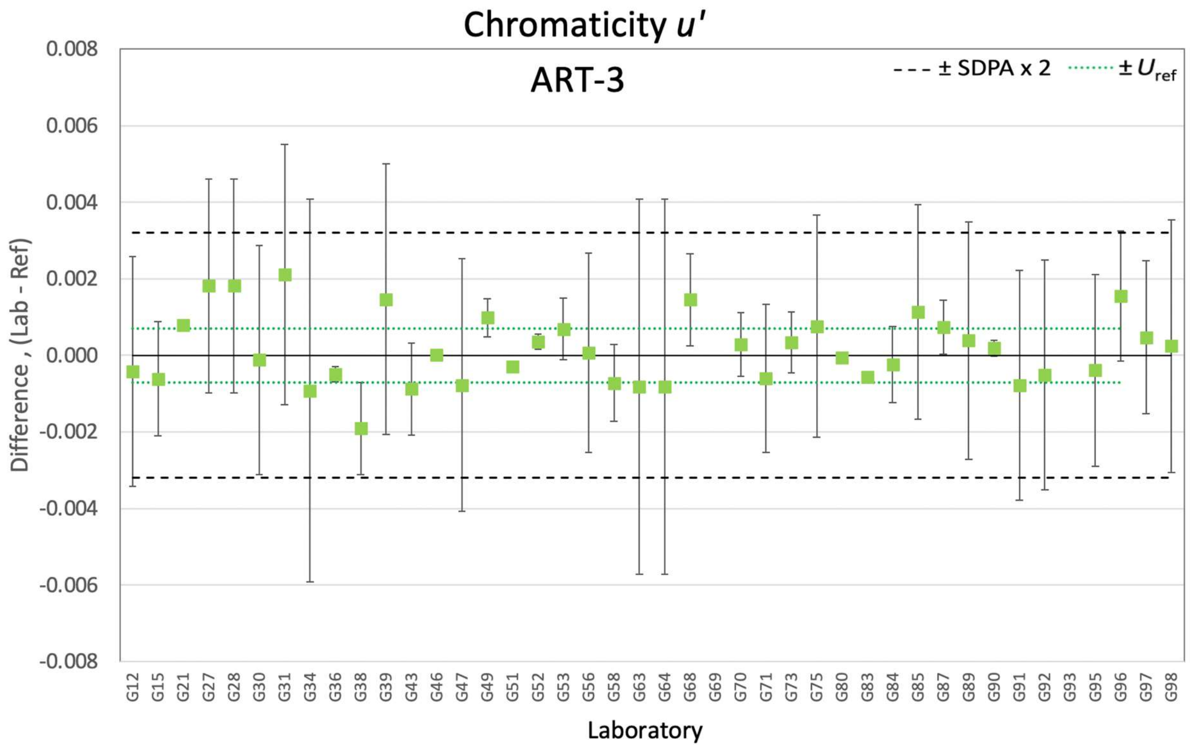

Figure 7-35. Differences of chromaticity *u′* for ART-3

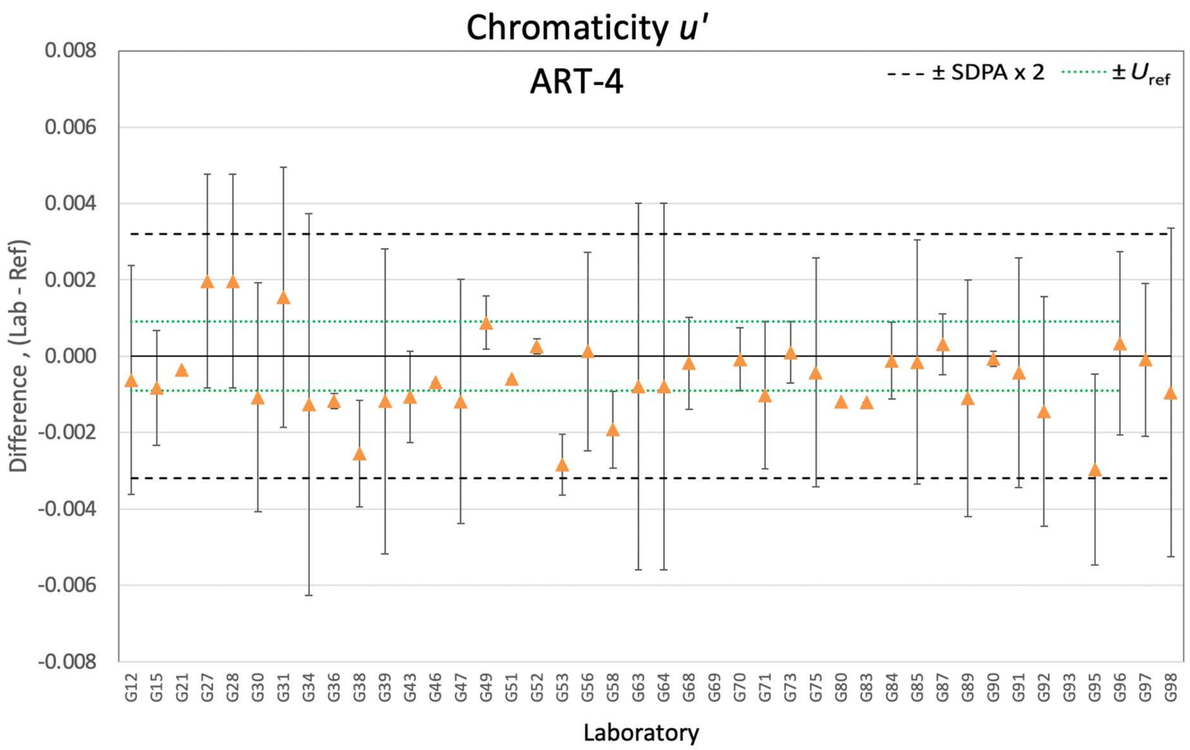

Figure 7-36. Differences of chromaticity *u′* for ART-4

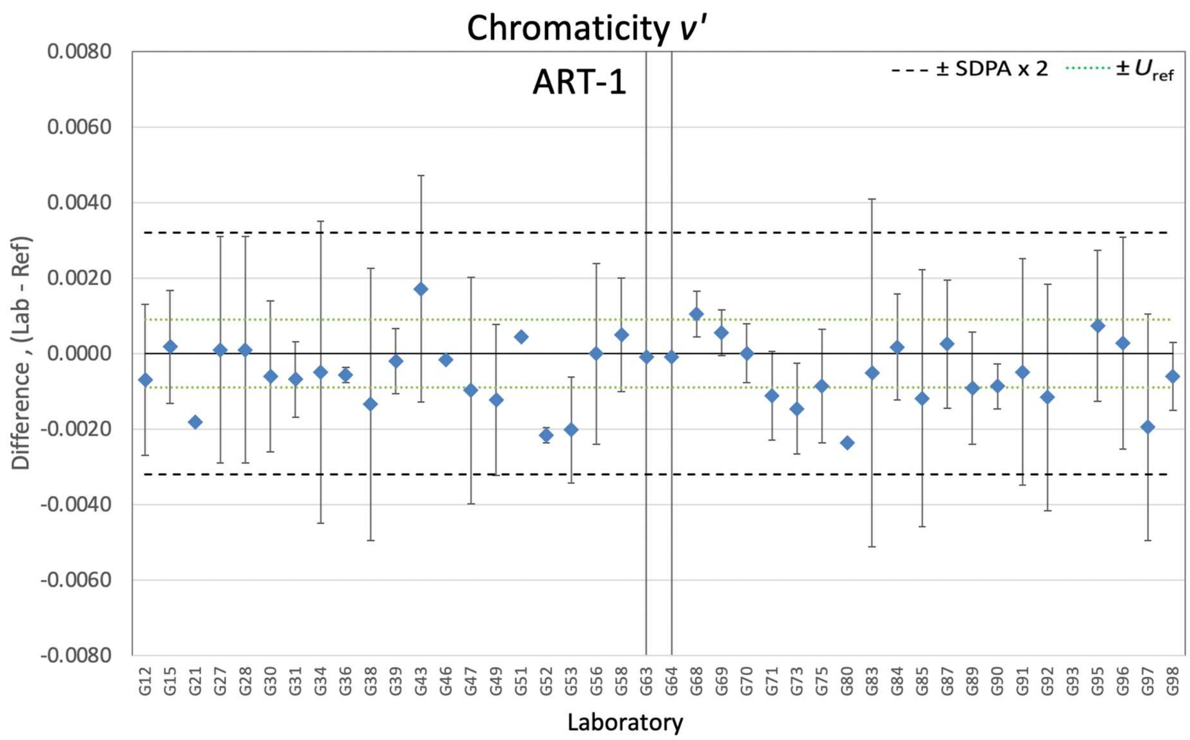

Figure 7-37. Differences of chromaticity *v'* for ART-1

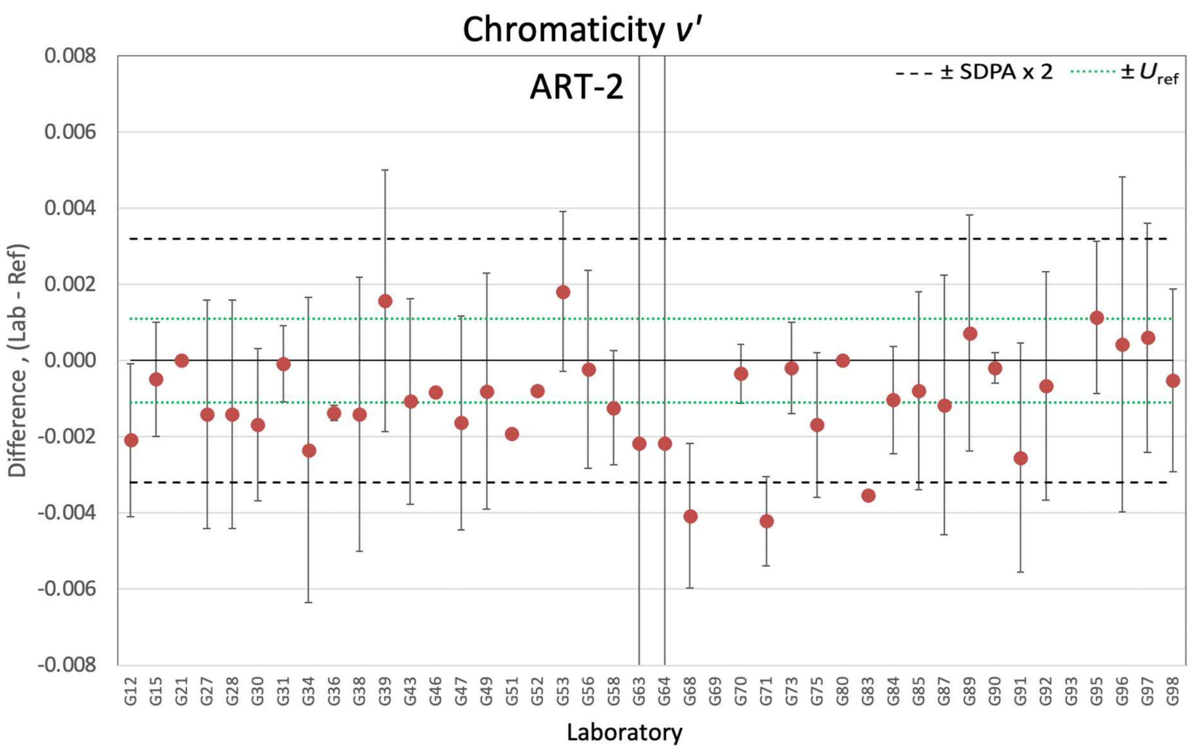

Figure 7-38. Differences of chromaticity *v'* for ART-2

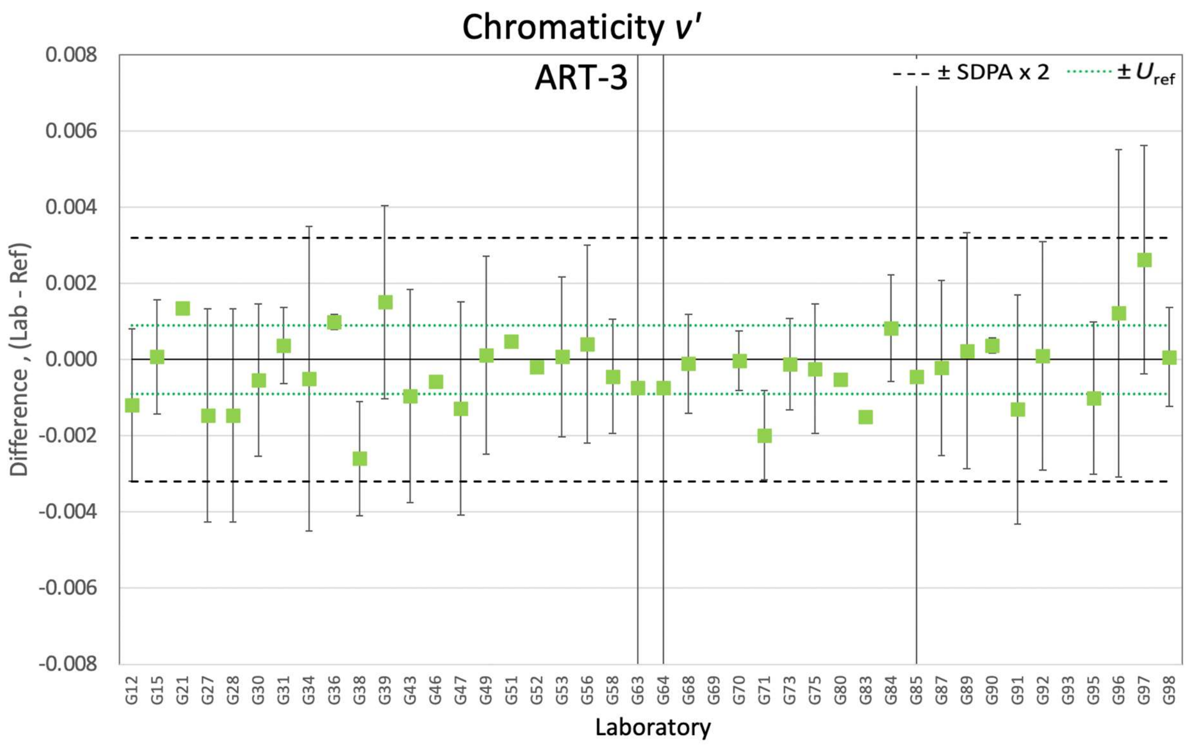

Figure 7-39. Differences of chromaticity *v′* for ART-3

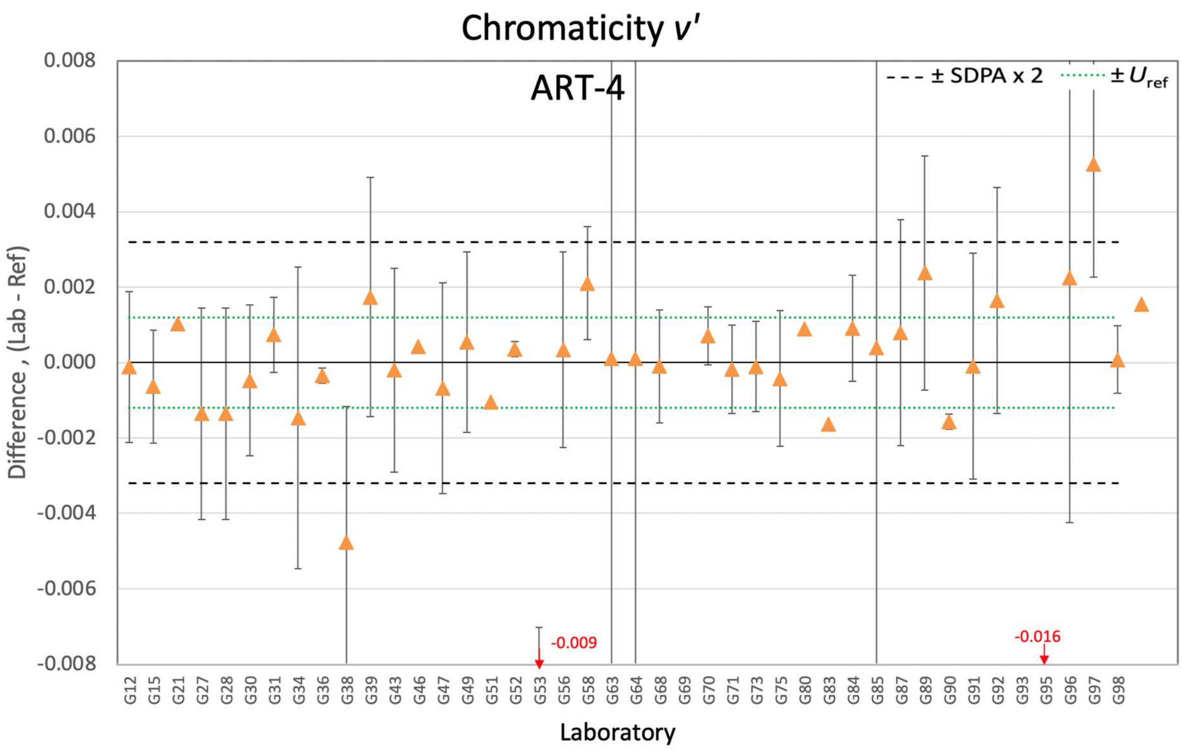

Figure 7-40. Differences of chromaticity *v′* for ART-4

7.2.7 Correlated Colour Temperature (CCT)

The overall results of CCT are shown in Figure 7-41. The standard deviations of results (two outlier points excluded) for each artefact are shown in Figure 7-42. However, the results cannot be simply compared between different artefacts because the artefacts had different CCTs and the CCT scale is non-linear. The typical measured CCTs of the artefacts were around 2700 K, 5500 K, 4100 K, and 4400 K, for ART-1, ART-2, ART-3, and ART-4, respectively. Figure 7-42 shows different levels of SDPA values for the different artefacts. Figure 7-43 to Figure 7-46 show the results for each artefact with their SDPA lines. These graphs show generally good agreement of all results (except a few outliers), and the participants' uncertainties also appear reasonable in most cases.

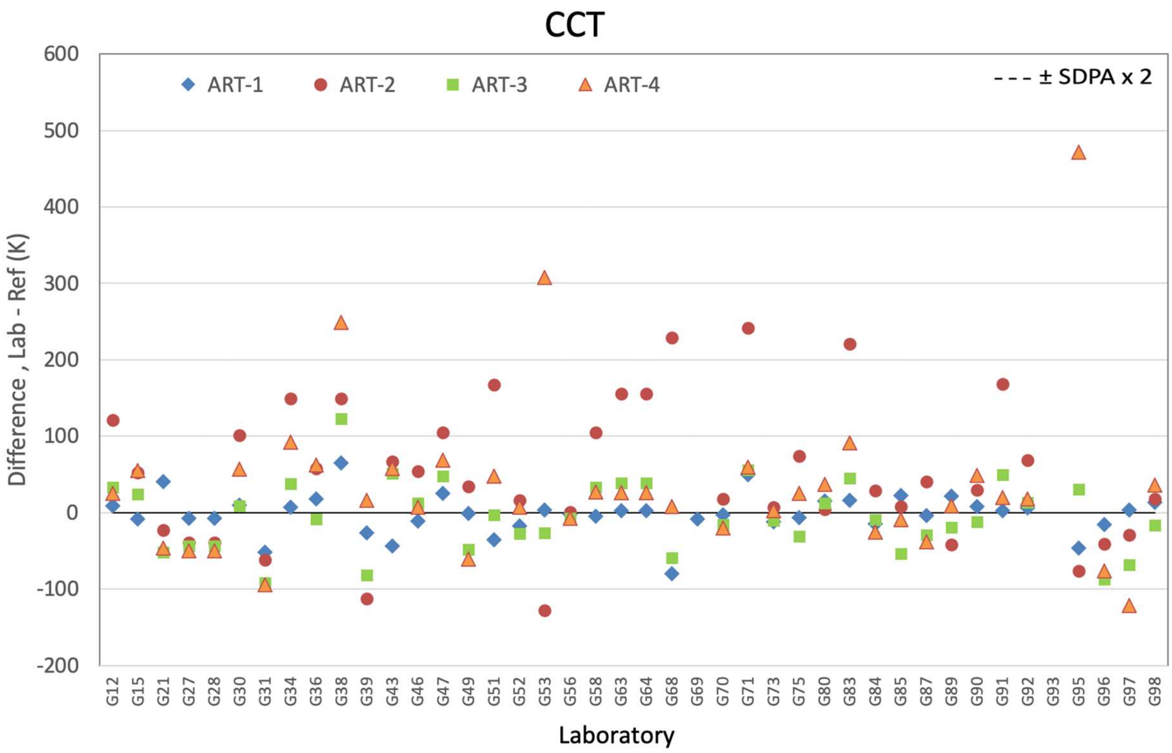

Figure 7-41. Differences of CCT for all artefacts

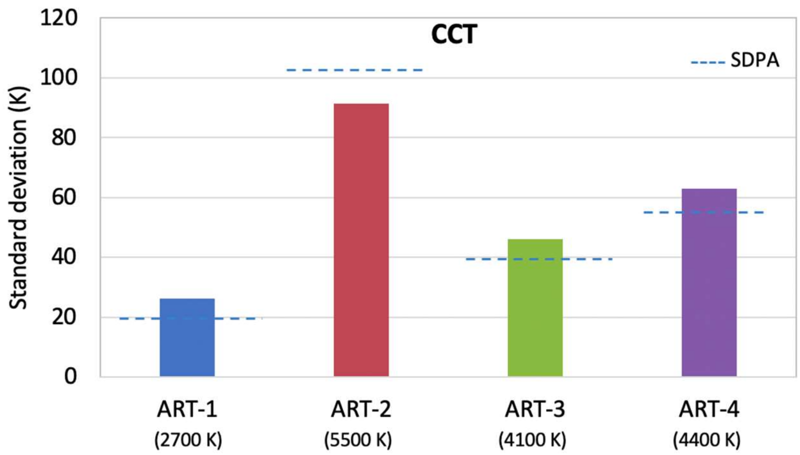

Figure 7-42. Standard deviations of CCT results

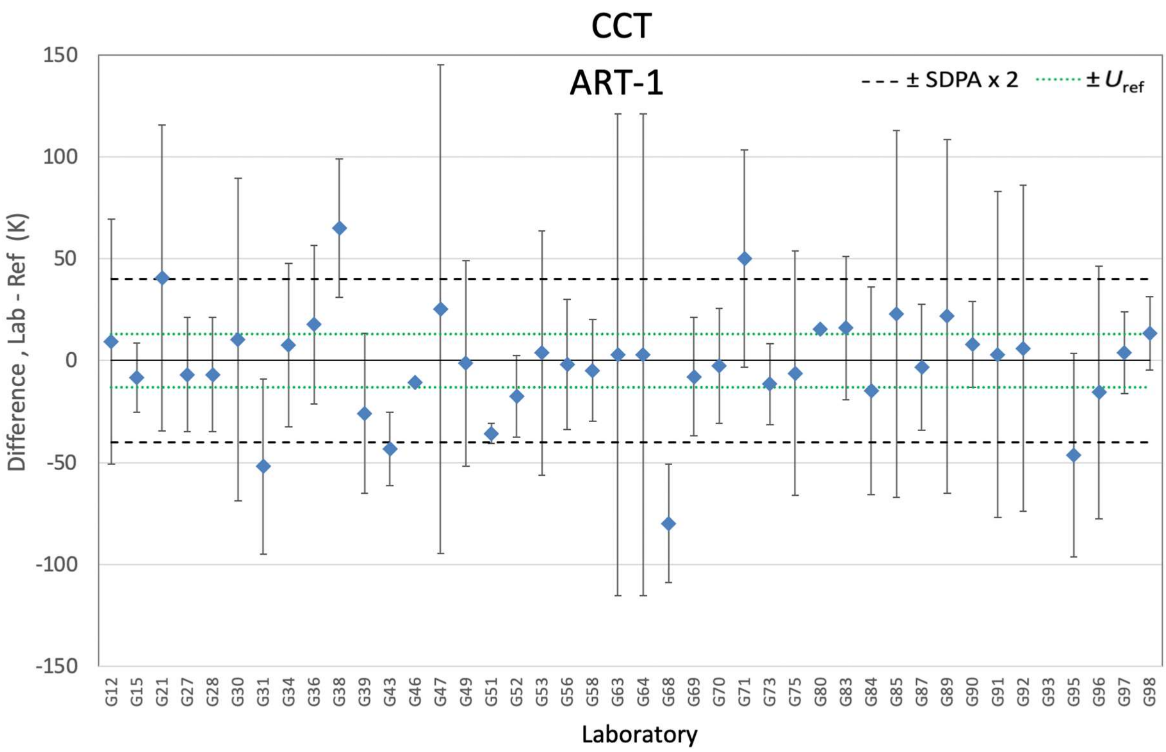

Figure 7-43. Differences of CCT for ART-1 (2700 K)

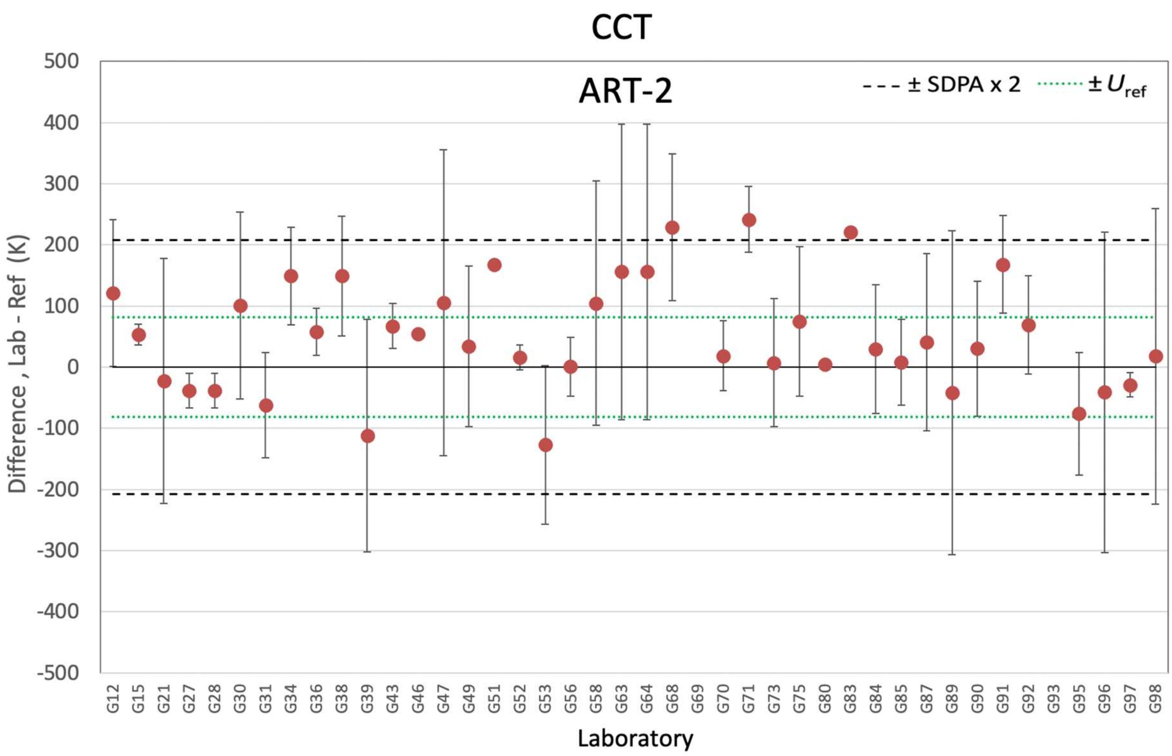

Figure 7-44. Differences of CCT for ART-2 (5500 K)

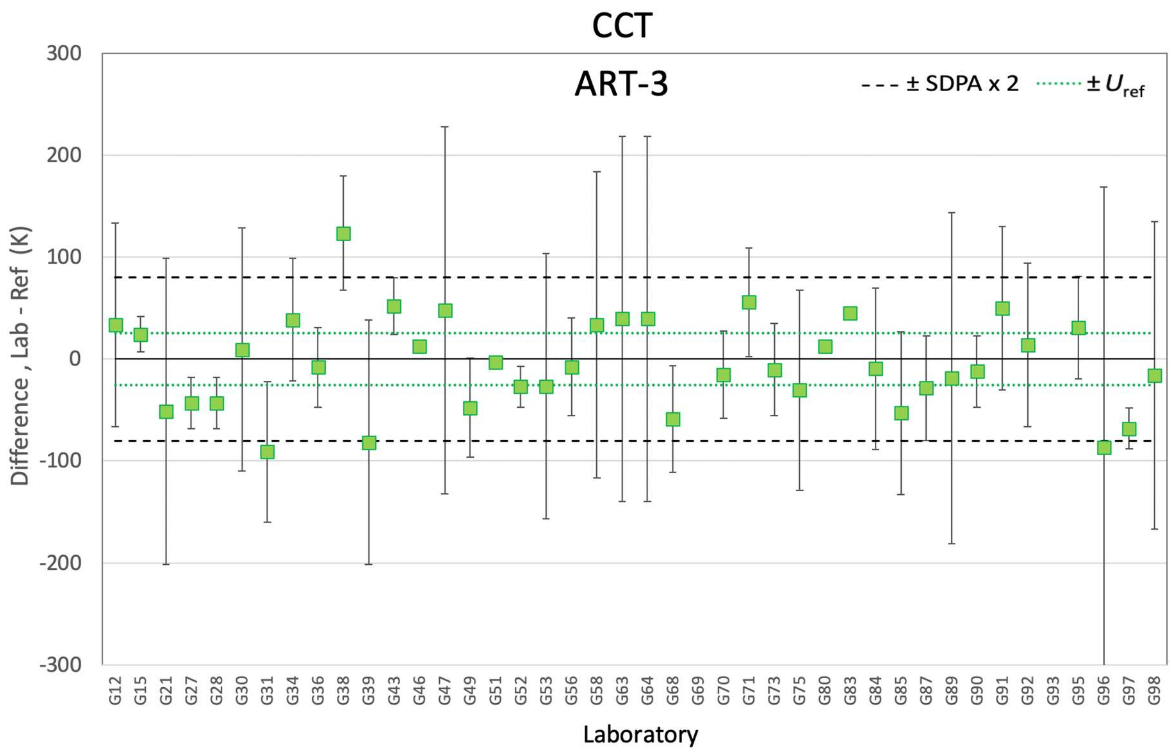

Figure 7-45. Differences of CCT for ART-3 (4100 K)

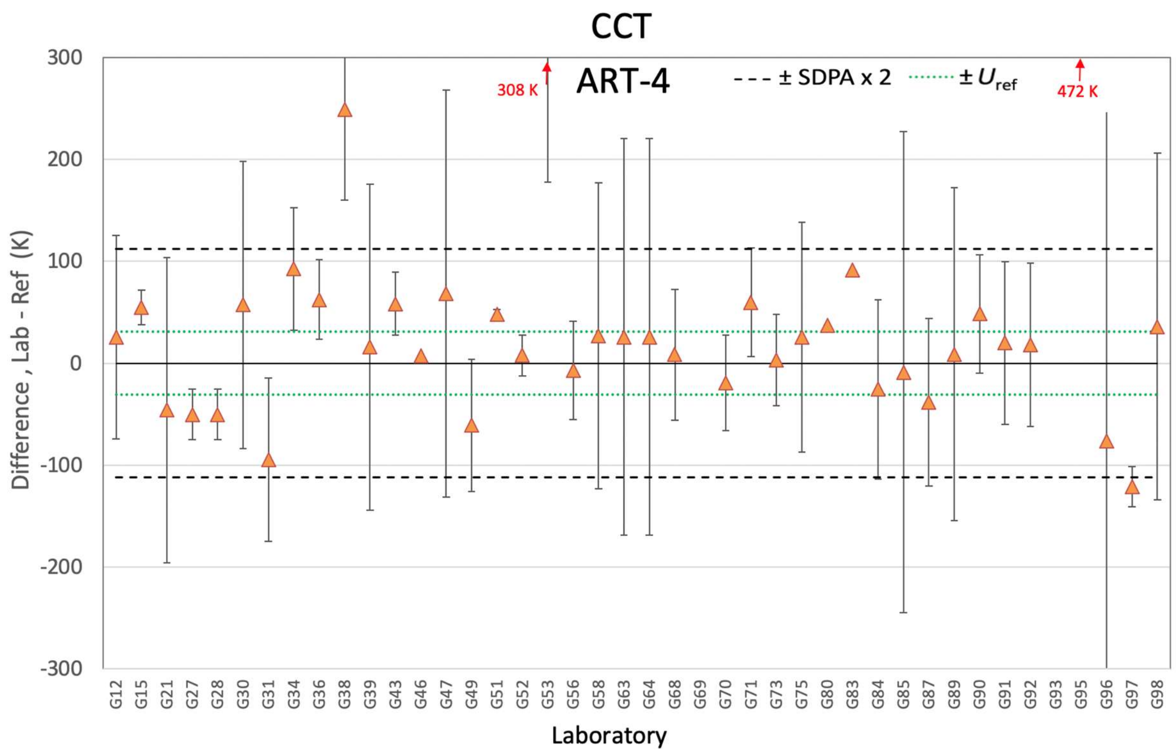

Figure 7-46. Differences of CCT for ART-4 (4400 K)

7.2.8 Colour Rendering Index (CRI Ra)

The overall result of CRI R_a is shown in Figure 7-47. The standard deviations of results (two outlier points excluded) for each artefact are shown in Figure 7-48. The measured CRI R_a values were around 97, 84, 84, and 78, for ART-1, ART-2, ART-3, and ART-4, respectively. The variation in ART-1 was smaller because its R_a value is closer to 100. Otherwise, no significant differences are noted among different artefacts.

Figure 7-49 to Figure 7-52 show the results for each artefact with the reported uncertainties of the participants. Comparing with the SDPA x 2 range, the results appear in reasonable agreement, except a few outliers in ART-4. It is noted that the reported uncertainties are generally much larger than the agreement of results, meaning that many labs over-estimated the uncertainties. Their uncertainties can be re-evaluated based on these results.

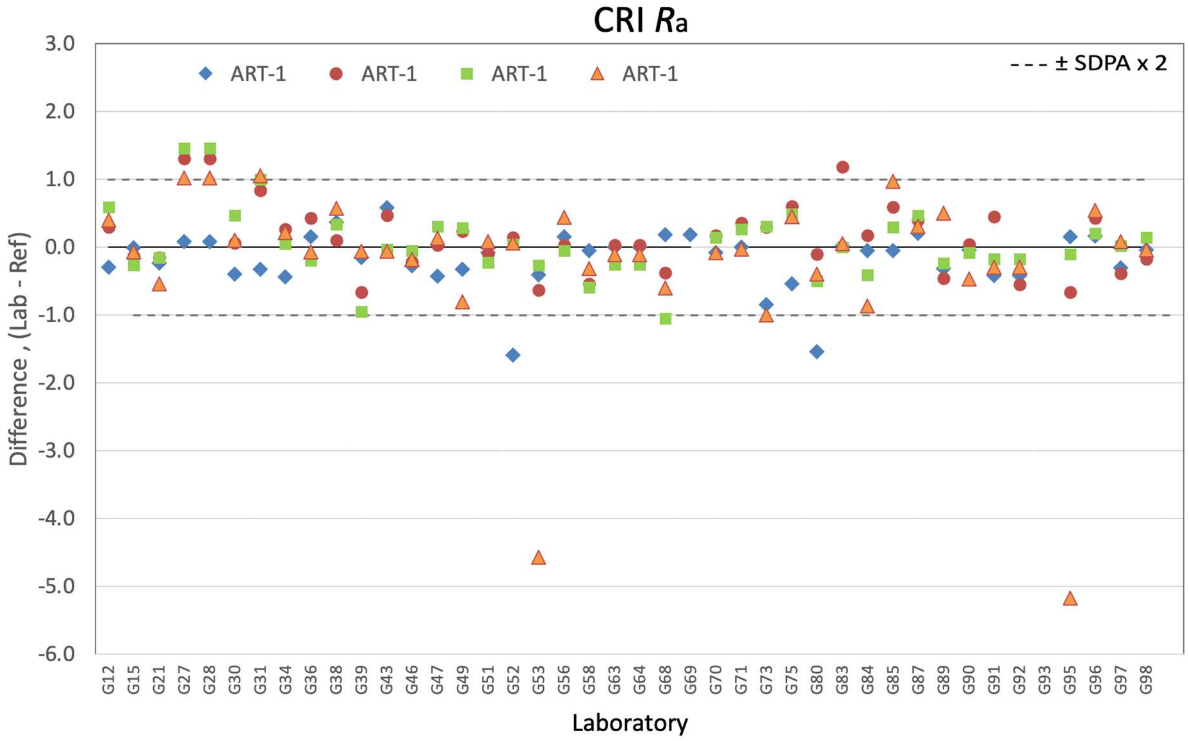

Figure 7-47. Differences of CRI R_a for all artefacts

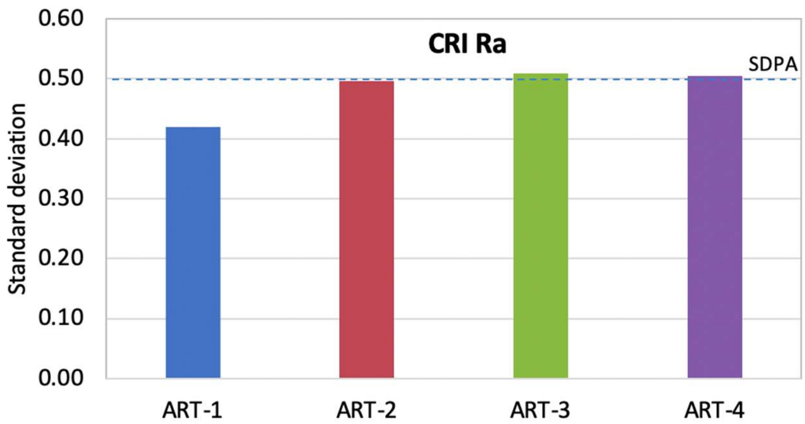

Figure 7-48. Standard deviations of CRI R_a results

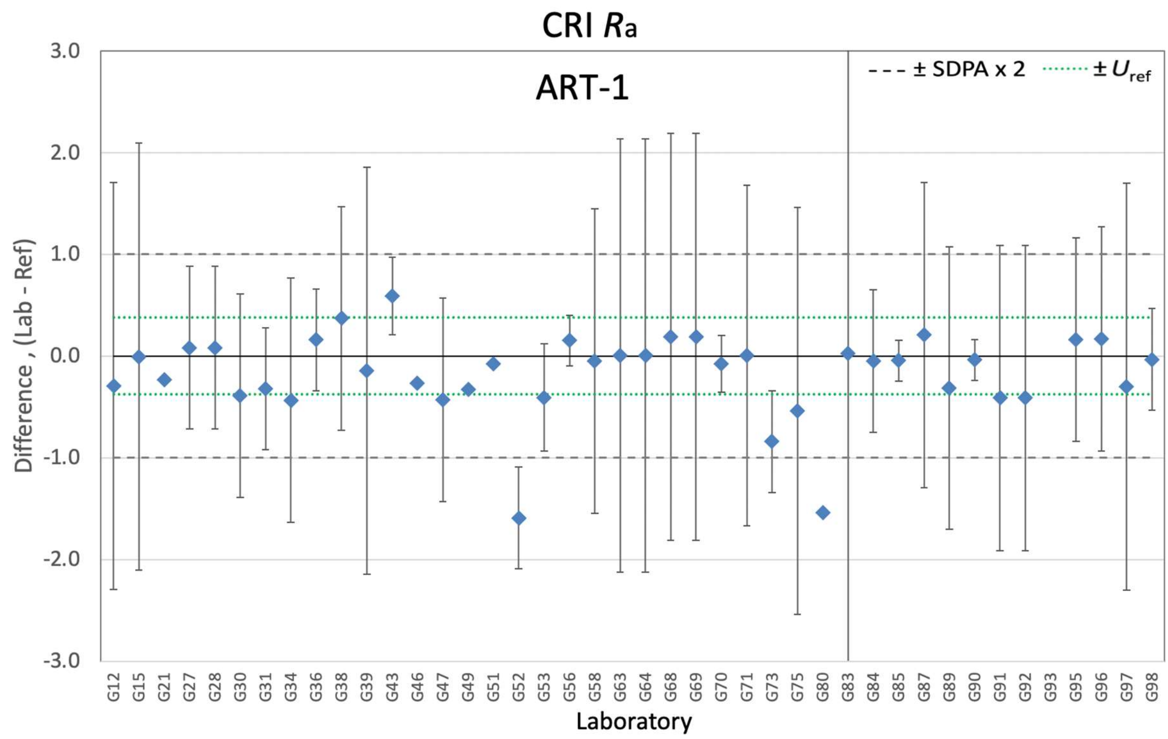

Figure 7-49. Differences of CRI R_a for ART-1

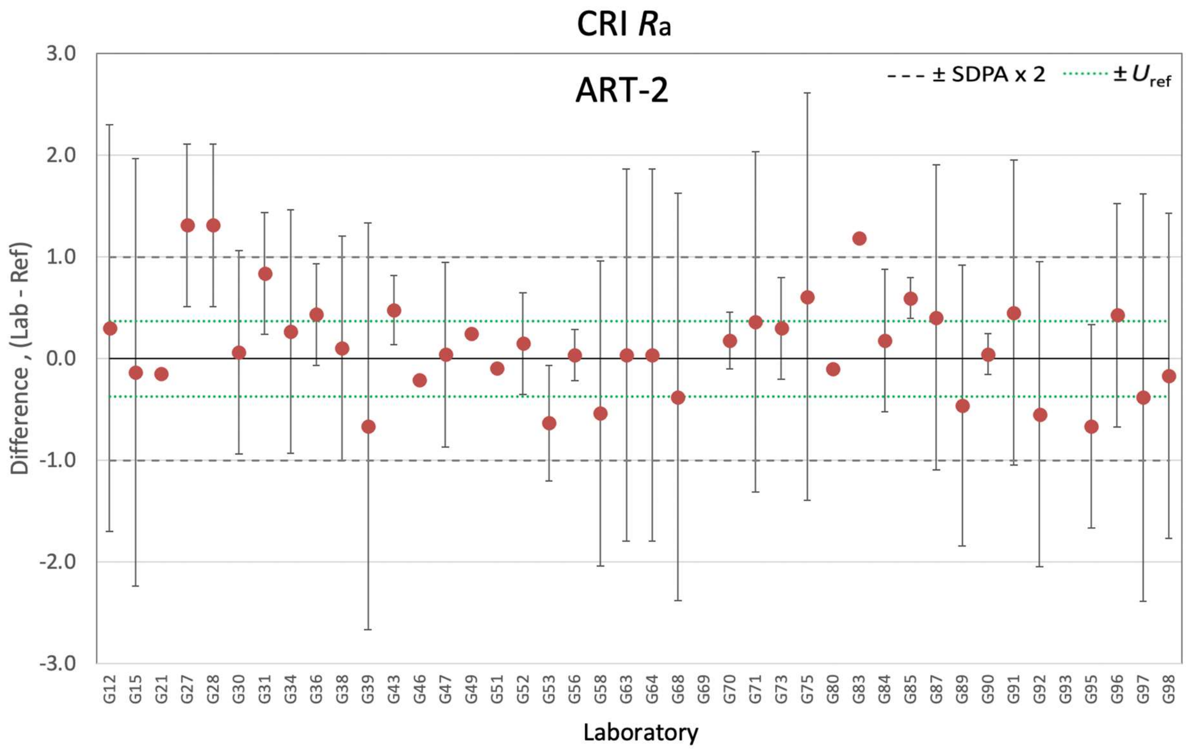

Figure 7-50. Differences of CRI R_a for ART-2

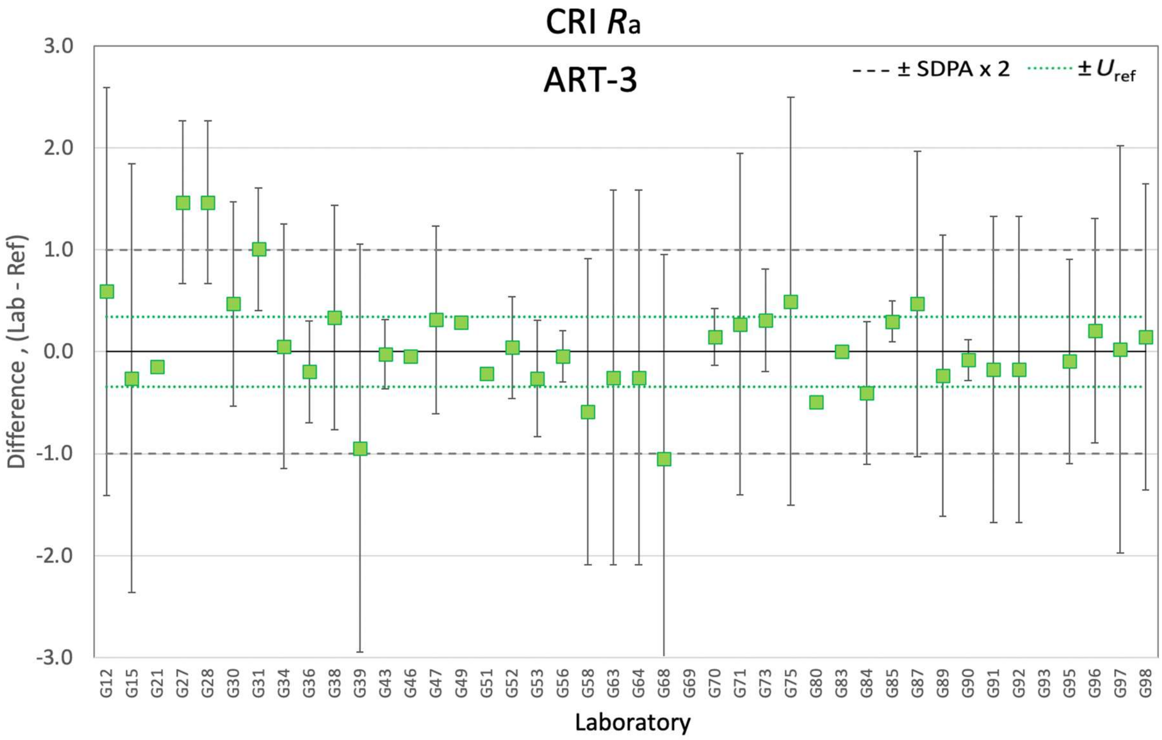

Figure 7-51. Differences of CRI R_a for ART-3

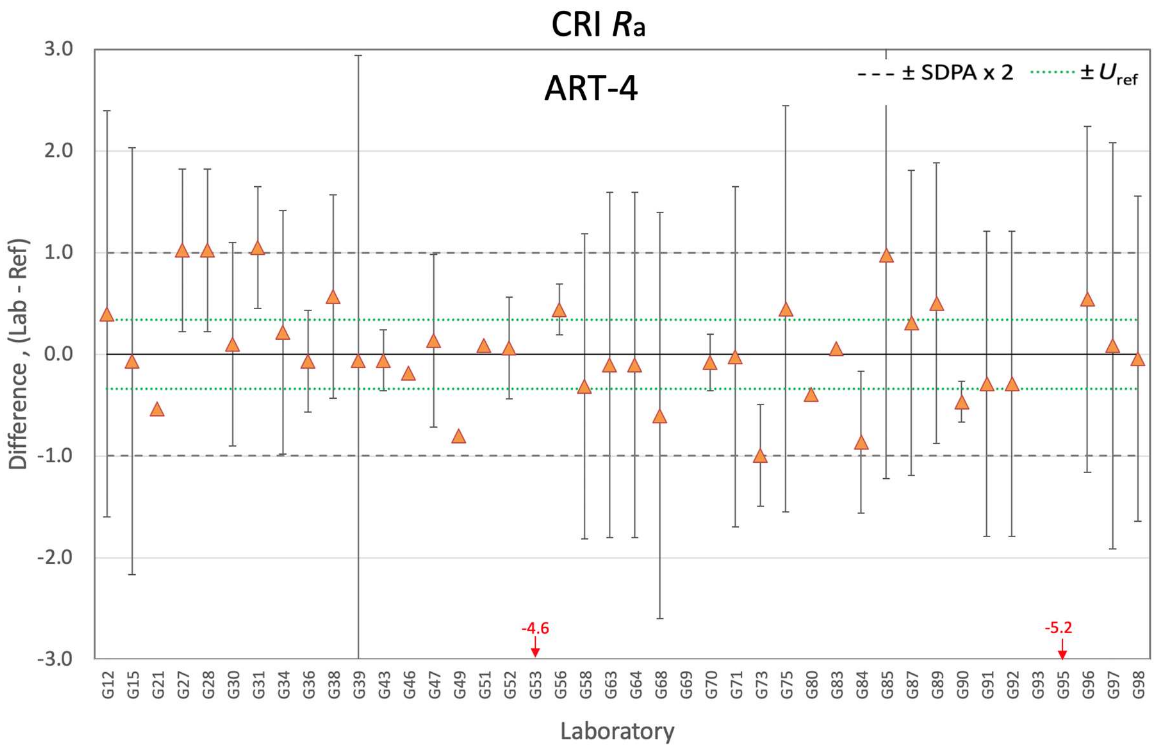

Figure 7-52. Differences of CRI R_a for ART-4

7.2.9 Luminous intensity at (0,0)

In this section, the results of luminous intensity in the direction of the mechanical axis (C, γ) = (0,0) are reported. Note that SDPA values were not determined for this quantity (and all other goniophotometric quantities presented in section 7.2.10), thus, in the graphs, two times the standard deviations of the results of all the points (all artefacts measured) are shown by dashed lines (blue) instead of SDPA x 2. In the standard deviation graphs, a dashed line for one standard deviation (σ) is shown instead of SDPA.

Luminous intensity at (0,0) was included as a part of comparison of luminous intensity distributions. Participants reported the results of (C, γ) = (0,0) of each artefact from their luminous intensity distribution data measured. The overall result is shown in Figure 7-53. The standard deviations of results (four outlier points excluded) are shown in Figure 7-54. The results for each artefact are shown in Figure 7-55 to Figure 7-58. The ART-3 results show very good agreement with only one outlier point. This verifies good agreement of the luminous intensity scale of the participants' goniophotometers.

Figure 7-54 shows a large variation in ART-1 and Figure 7-55 shows many negative points. This may be attributable to the alignment of the lamp that, since the optical axes of ART-1 lamps are well aligned to their mechanical axes, alignment deviations from the mechanical axis always result in negative errors. It is considered that lamp alignment to the goniophotometer by the participants probably had larger deviations on the average than that by the reference laboratory. Figure 7-54 also shows a larger variation of ART-4 results, which is considered due to a sharp slope of luminous intensity in the direction at (0,0). See Figure 7-69 for an illustration of this slope for ART-4.

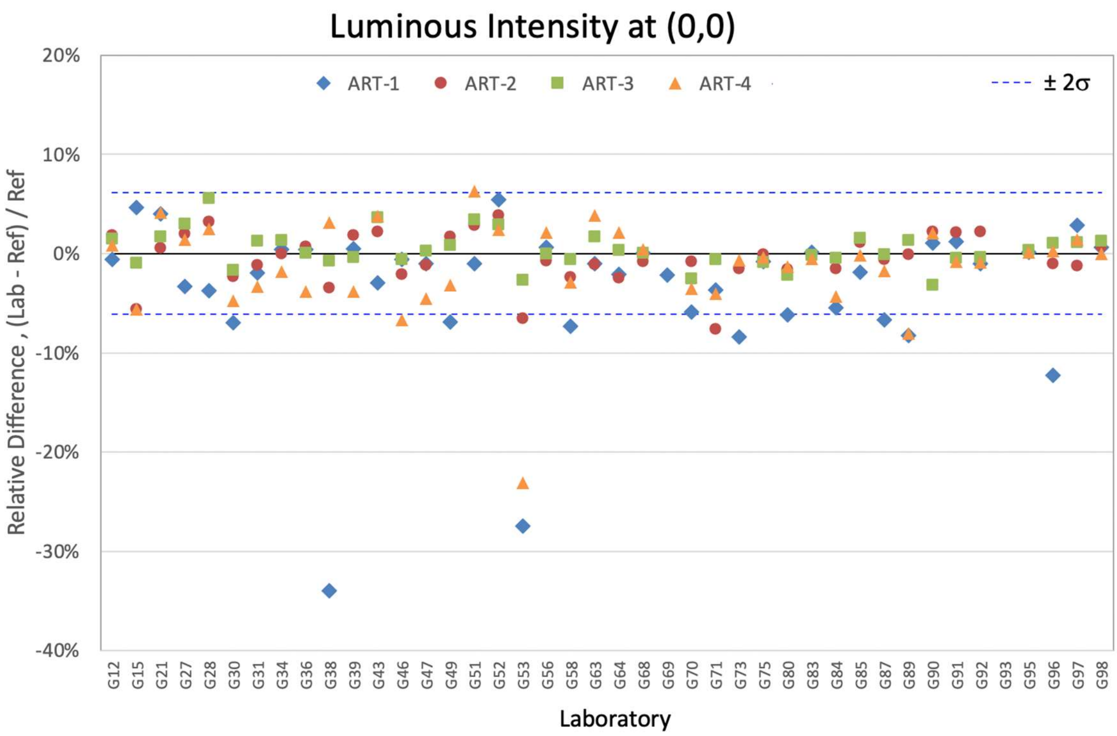

Figure 7-53. Relative differences of luminous intensity at (0,0) for all artefacts

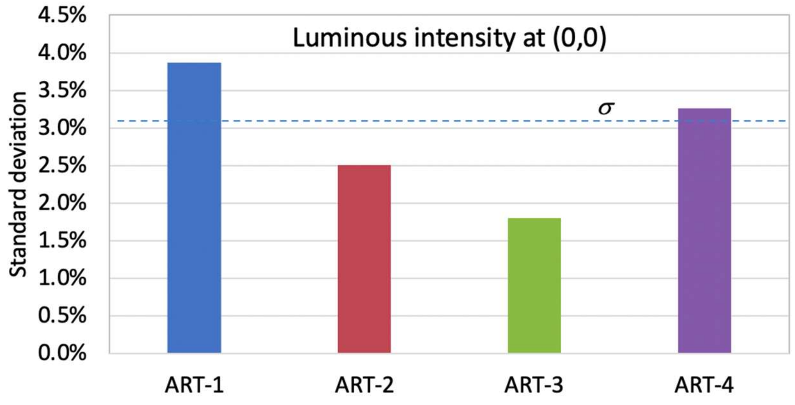

Figure 7-54. Standard deviations of luminous intensity at (0,0) results

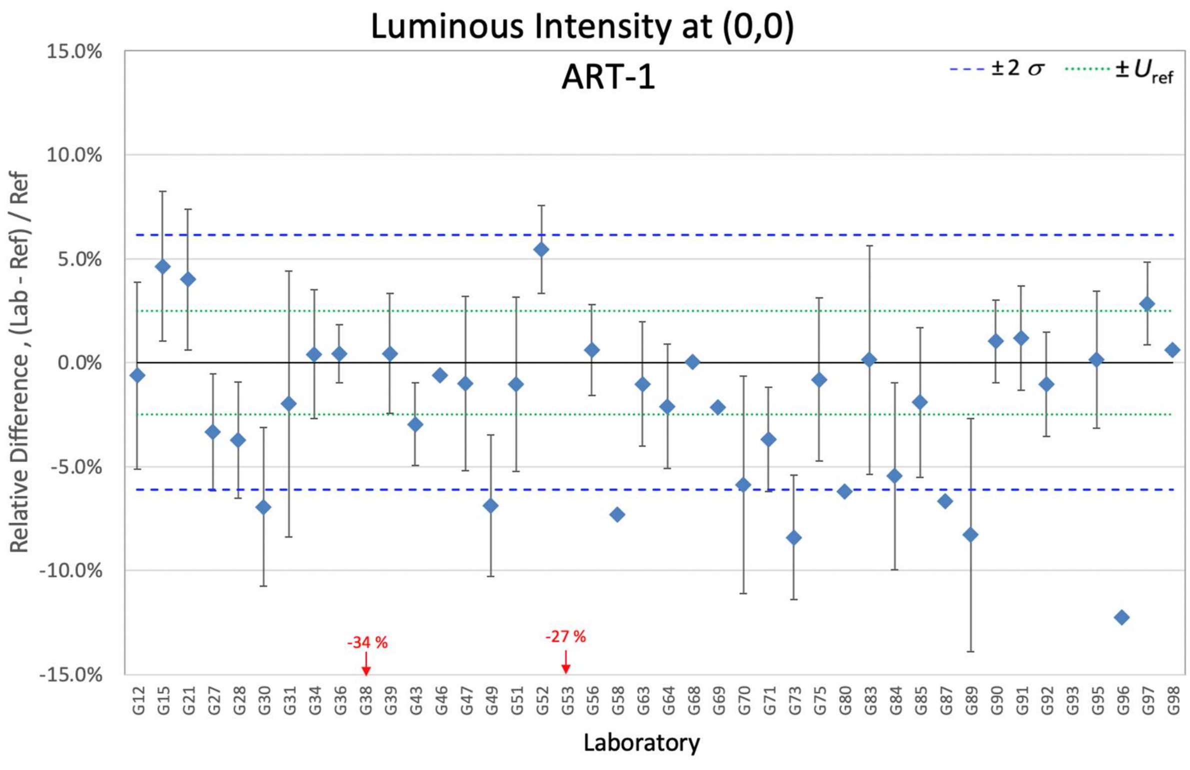

Figure 7-55. Relative differences of luminous intensity at (0,0) for ART-1

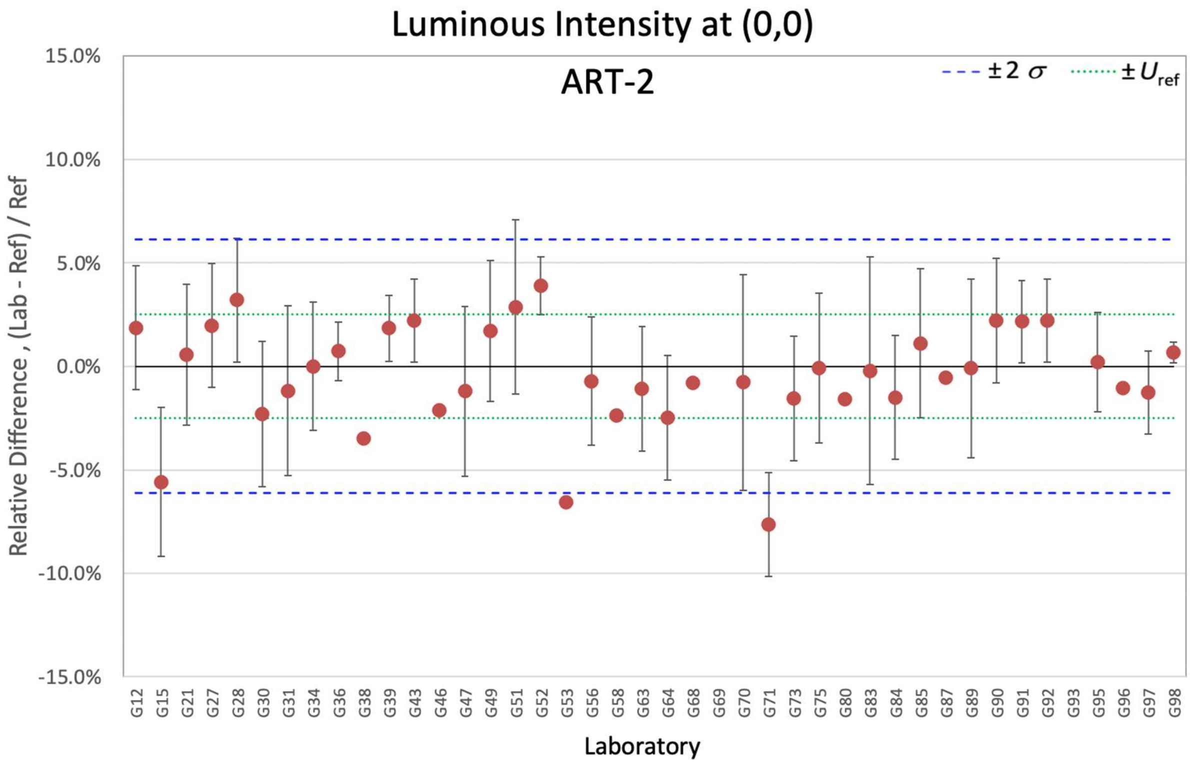

Figure 7-56. Relative differences of luminous intensity at (0,0) for ART-2

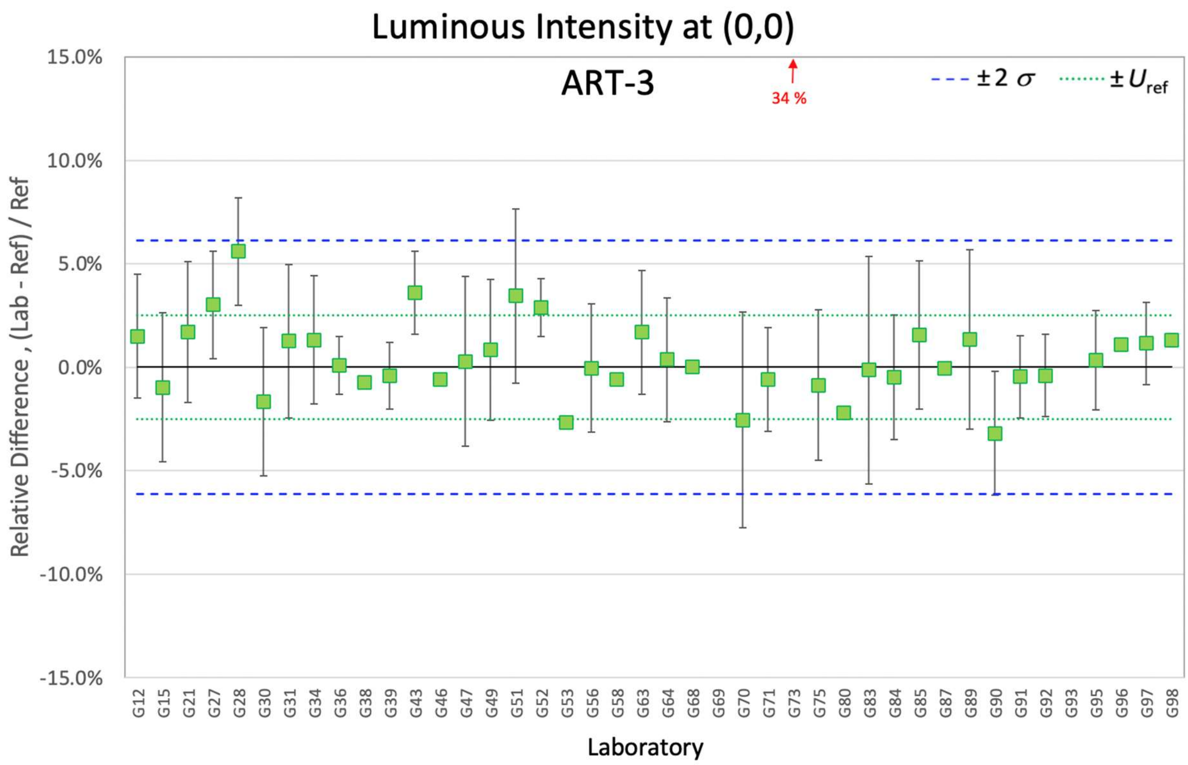

Figure 7-57. Relative differences of luminous intensity at (0,0) for ART-3

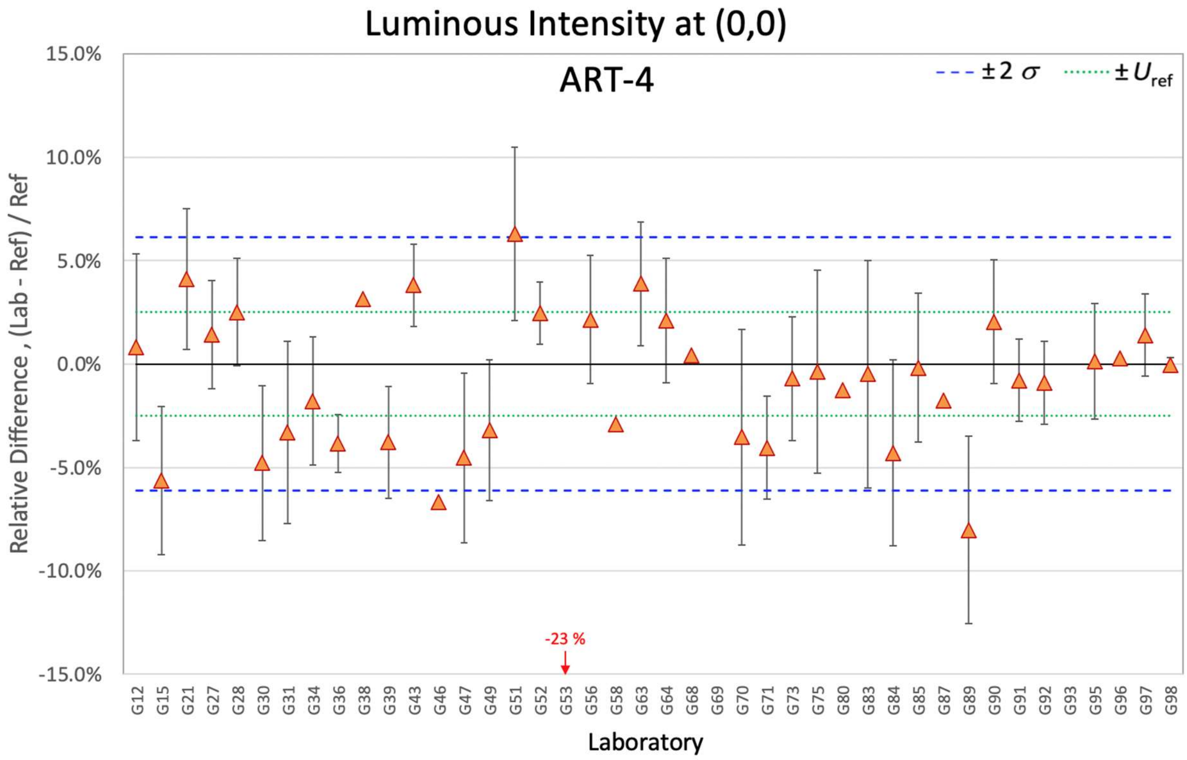

Figure 7-58. Relative differences of luminous intensity at (0,0) for ART-4

7.2.10 Other goniophotometric quantities

In this section, the results of the following quantities are reported in graphical form:

- Centre beam intensity (ART-1)
- Partial luminous flux (15° cone angle) (ART-1)
- Beam angle (ART-1)
- Street-side downward flux (ART-4)
- House-side downward flux (ART-4)
- Uplight flux (ART-4)
- Colour uniformity (ART-1, ART-3)

The standard deviations of centre beam intensity, partial luminous flux (15° cone), street-side downward flux, house-side downward flux, and colour uniformity, are shown in Figure 7-67.

Figure 7-59 shows the result of centre beam intensity (ART-1). This result was expected to be better than that of luminous intensity at (0,0) because it is calculated for the optical axis of the beam, whereby any effects of alignment differences should be mostly removed. However, the standard deviations are very similar to those of luminous intensity at (0,0), suggesting that many participants did not correctly calculate the centre beam intensity as per IEC 61341:2010 (referenced in CIE S 025). See additional analysis in section 7.2.11 (a).

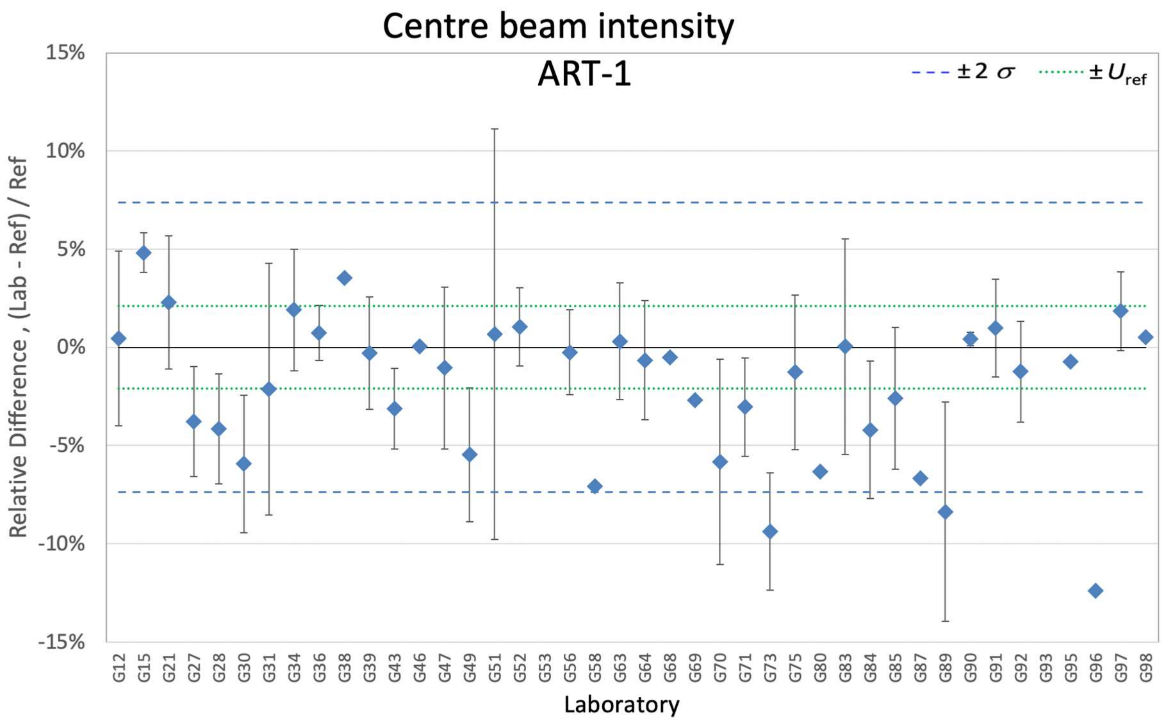

Figure 7-59. Relative differences of centre beam intensity for ART-1

Figure 7-60 shows the result of partial luminous flux (15° cone angle) for ART-1, showing very large variations (standard deviation of 17 % excluding one outlier). We found that there were two groups of results and many participants' results deviated from the expected values by approximately 30 %. We consider that these participants misunderstood the meaning of cone angle, interpreting the 15° as a radius rather than a diameter, and thereby calculating partial flux for a 30° cone angle. A calculation for 30° angle flux verifies approximately a 30 % increase in flux. Excluding these points, the standard deviation of other results would be 3.8 %, a reasonable agreement similar to luminous flux of ART-1 (2.9 %).

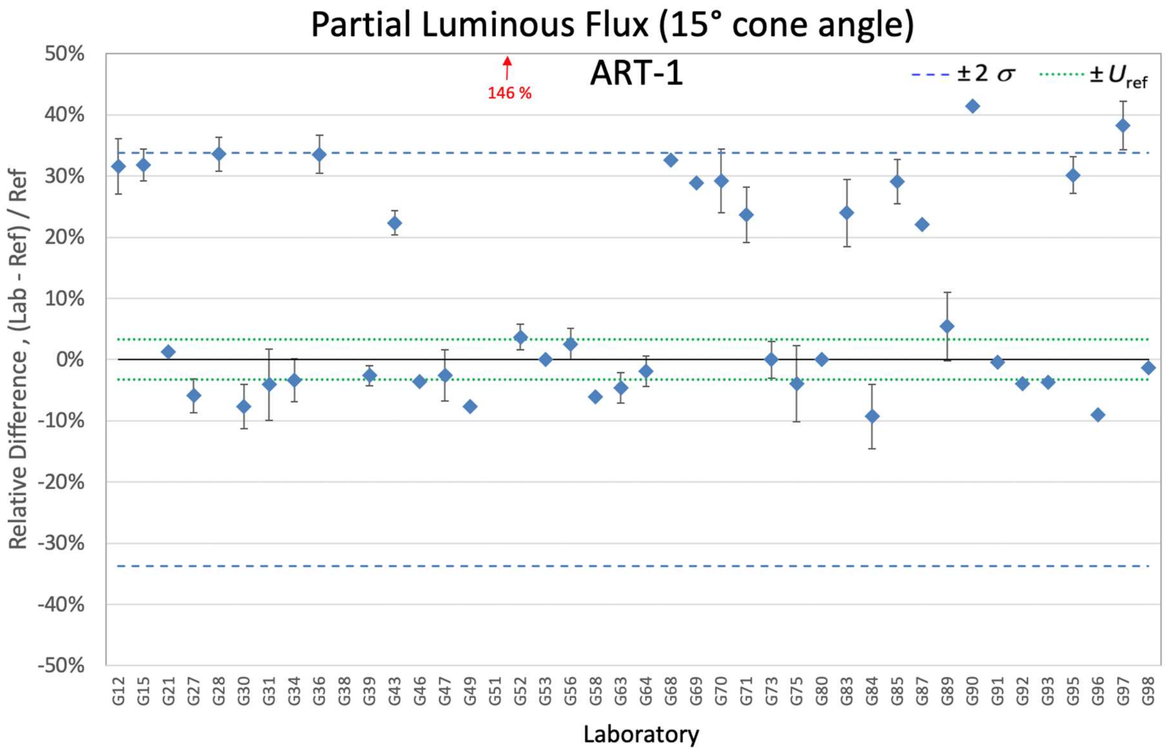

Figure 7-60. Relative differences of partial luminous flux for ART-1

Figure 7-61 shows the result of beam angle of ART-1. After excluding three outliers, the results are within 0.5° with standard deviation 0.44°, which appear reasonable compared to the uncertainty of the reference value. Among the three outliers, two participants reported about half of the correct beam angle (≈12°), with possible misunderstanding of the definition of beam angle. Some participants reported very large uncertainties while their results were good. They are encouraged to re-evaluate their uncertainties. Also, about 1/3 of the participants did not report uncertainties, which indicates that they were unable to do this. Guidance is needed on how to calculate uncertainties of measured beam angle.

The sources of uncertainty in beam angle measurement are discussed in section 7.4.7. There is another consideration. While beam angle of a plane is clearly defined in CIE S 025 (sections 3.17 and 6.6), there is no guidance on how to determine beam angle of a lamp (e.g., how many C planes should be averaged). Due to this, the technical protocol of IC 2017 specified to calculate beam angle from two C planes for simplicity. However, there was a possibility that the peak of luminous intensity distribution may have been missed in these two C planes if the ART-1 lamp was not accurately aligned. In those situations, the maximum intensity is determined to be lower, which could have contributed to variation in the beam angle result.

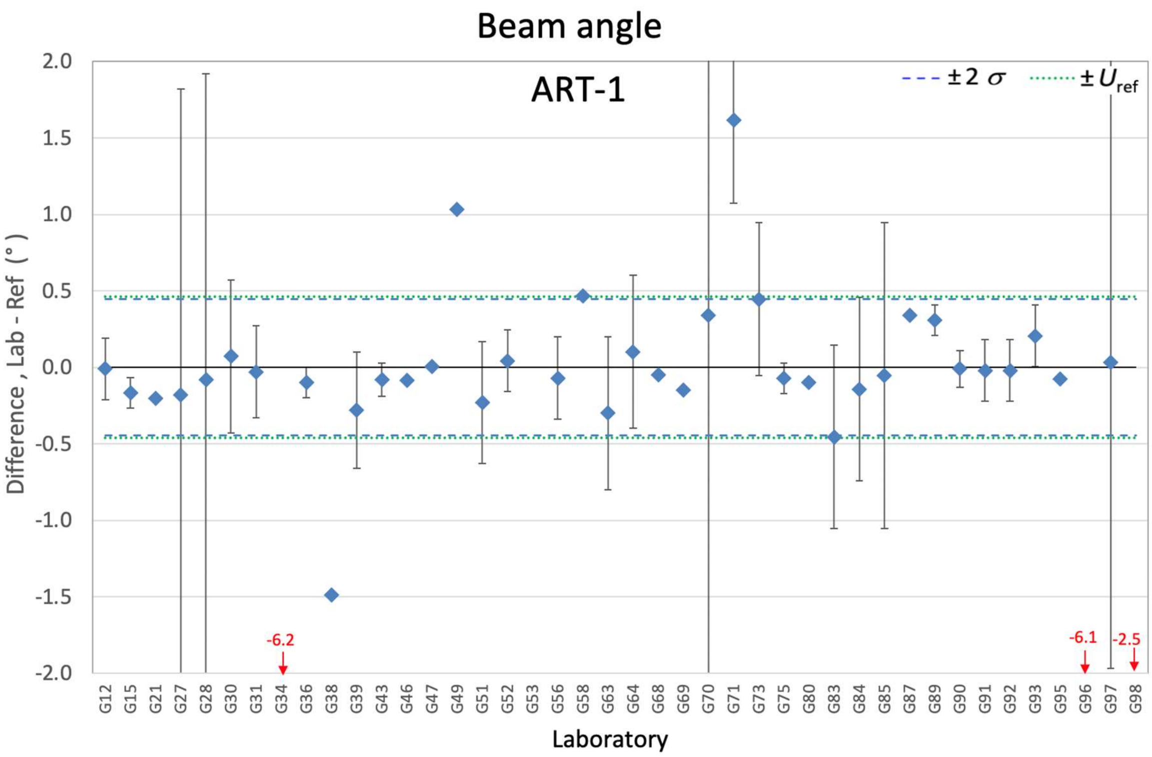

Figure 7-61. Differences of beam angle for ART-1

Figure 7-62 and Figure 7-63 show the results of Street-side downward flux and House-side downward flux of ART-4. These are the partial fluxes for street lighting luminaires specified in IES TM-15-11 [8]. The result of Street-side downward flux shows good agreement (standard deviation 2.0 % excluding the three outliers). On the other hand, the variations in House-side downward flux were much larger up to 20 % (standard deviation 8.3 % excluding the two outliers), about four times larger variations than Street-side downward flux, as also shown in **Figure 7-67**. This is considered due to the sharp slope of the intensity distribution of ART-4 on the House-side. See 7.2.11 (b), Figure 7-69 for additional analysis.

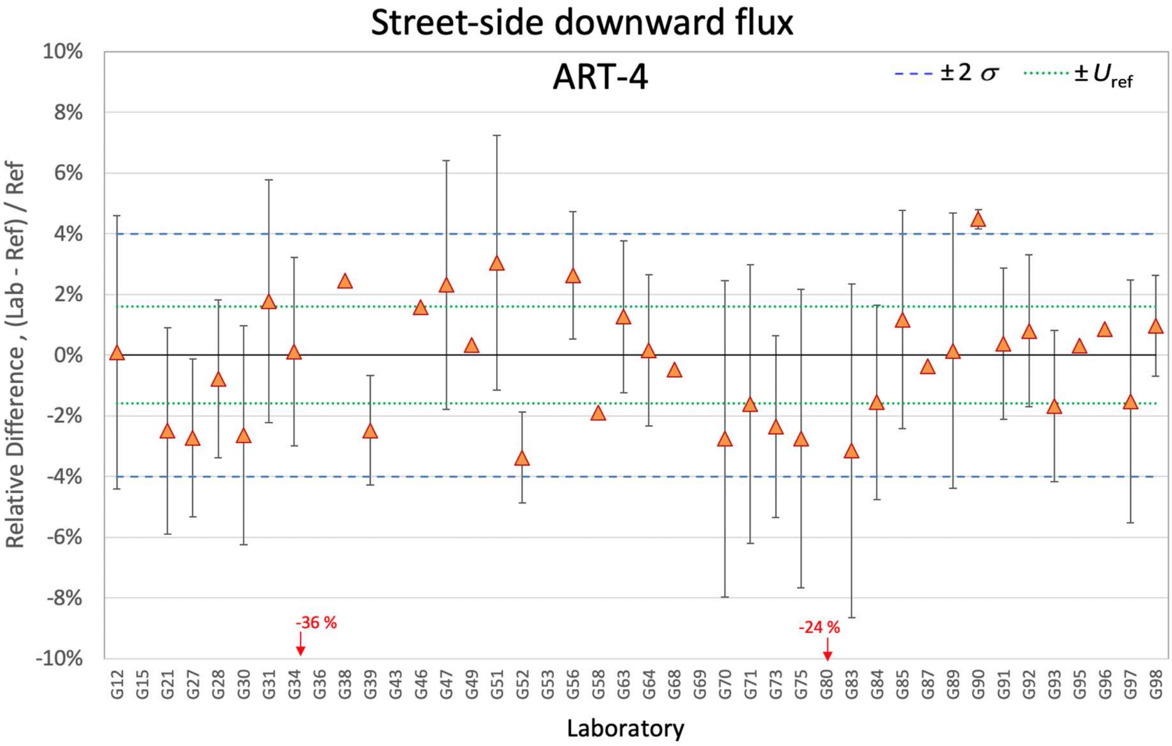

Figure 7-62. Relative differences of Street-side downward flux for ART-4

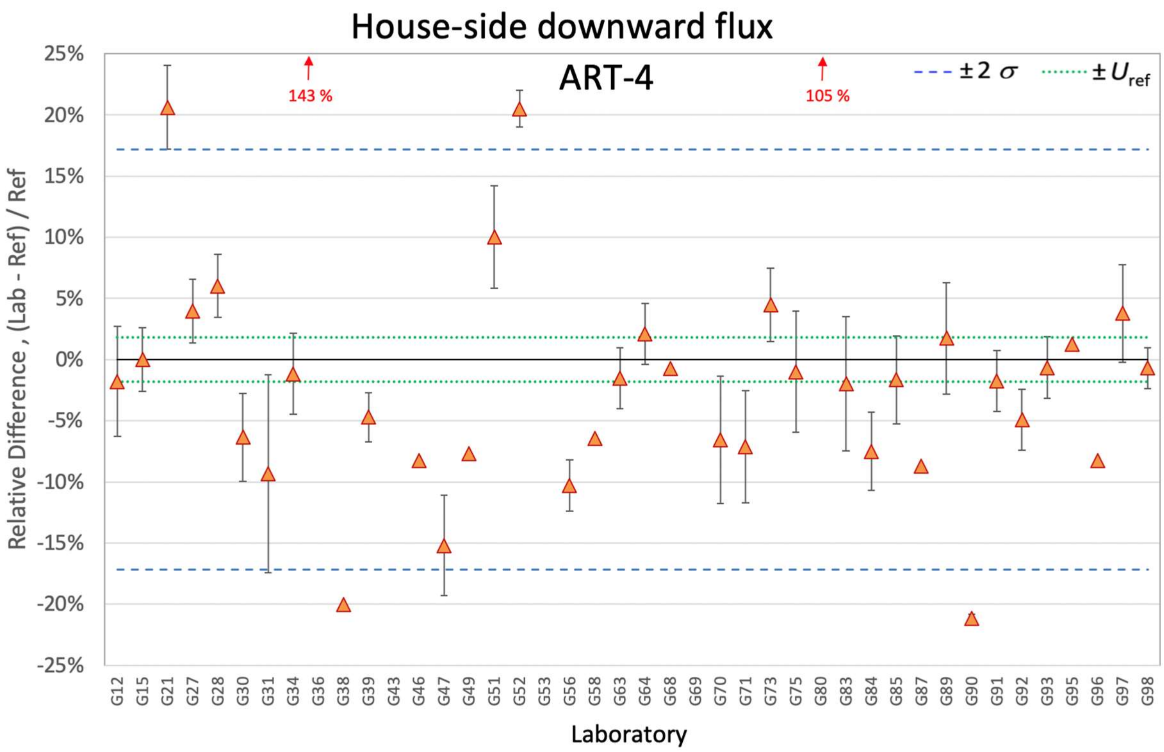

Figure 7-63. Relative differences of House-side downward flux for ART-4

Figure 7-64 shows the results of uplight flux, which is defined in IES TM-15-11 [8] (see Fig. 3-1). ART-4, by its design, does not have any upward emission, but the participants were asked to measure ART-4 luminaire in upward directions to determine uplight flux. Thus, this was not a comparison with the reference laboratory but to test what low level of uplight the labs could measure. The results in Figure 7-64 are presented as a ratio of reported uplight flux to its total luminous flux. The results of the reference laboratories are shown at the right end of the graph. Many labs show good results (less than 0.2 %), while a few labs showed nearly 1 %, which must be stray light of the goniophotometer. Note that several laboratories reported "0 lm" and plotted as 0 % in the graph, but it is not clear whether these zero values were rounded from real measurements or given from other determination (not following the protocol).

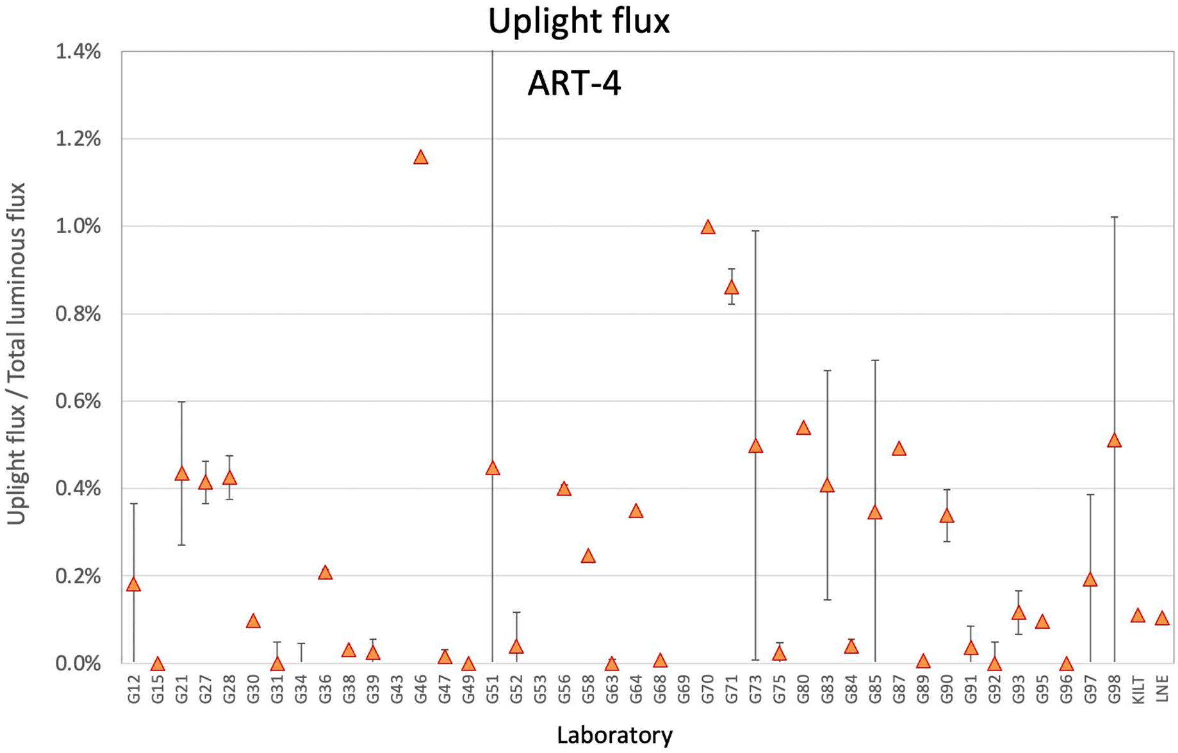

Figure 7-64. Uplight flux relative to total luminous flux for ART-4

Figure 7-65 and Figure 7-66 show the results of colour uniformity. This quantity is defined in CIE S 025 [5]. Participants were asked to measure this quantity for ART-1 and ART-3. The actual colour uniformity values as measured by the reference laboratories were 0.0015 to 0.0025 for ART 1 and 0.0025 to 0.0035 for ART 3 depending on individual lamps or luminaires. The standard deviations of all results (excluding two outliers) were 0.0009 for ART-1 and 0.0012 for ART-3, which are about the same level as the results of *u*', and *v*' (Figure 7-32). Much better results were expected because colour uniformity is determined from relative colour measurements. It is calculated as maximum deviations in chromaticity (in nearly full solid angle where light is emitted), which tend to come from the point at low intensity level, and it is considered that the signal level for some gonio-spectroradiometers at a long photometric distance could have been insufficient. Many participants did not report uncertainties, and a few labs reported very large uncertainties. Some guidance is needed on how to evaluate the uncertainty of colour uniformity, and improvements are needed to reduce the large variations in this measurement.

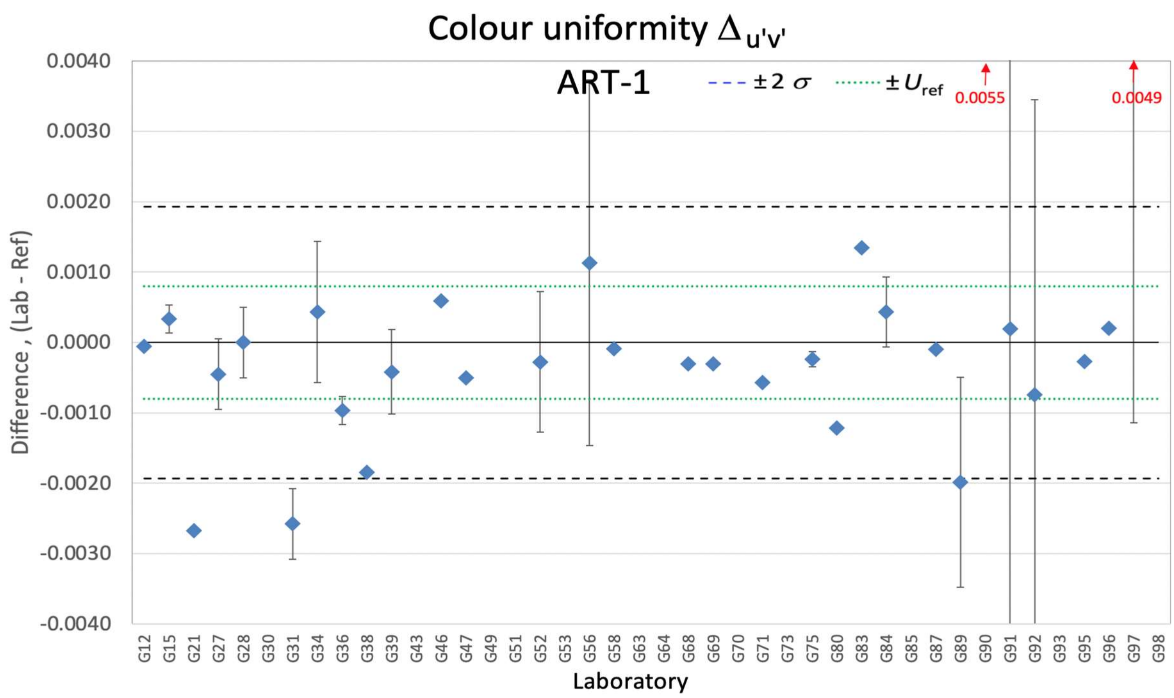

Figure 7-65. Differences of colour uniformity for ART-1

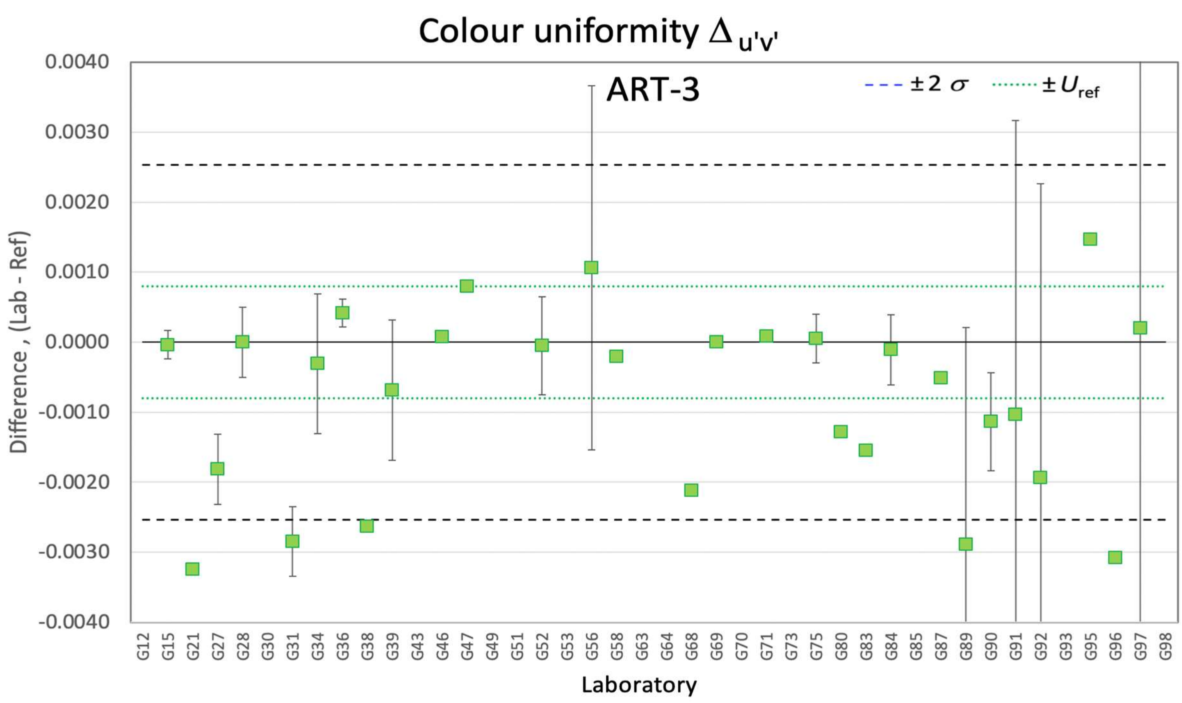

Figure 7-66. Differences of colour uniformity for ART-3

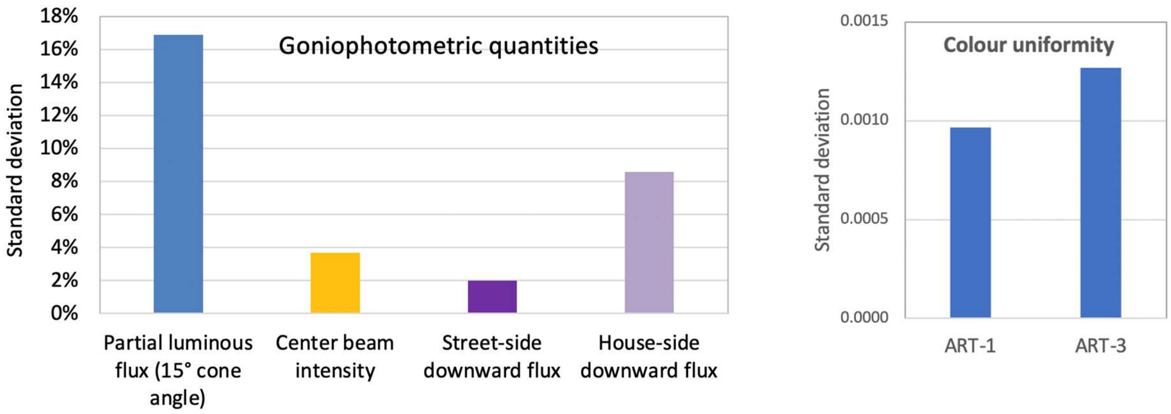

Figure 7-67 Standard deviations of four goniophotometric quantities and colour uniformity

7.2.11 Additional analyses

(a) Analysis on centre beam intensity

Figure 7-68 shows the ratios of luminous intensity at (0,0) to centre beam intensity (CBI) measured by each participant laboratory and the reference laboratory. Since the beam profile of ART-1 has a mono peak and mostly axial symmetry distributions, centre beam intensity values for ART-1 must be nearly equal to the maximum intensity of the beam, while I(0,0) may not be measured at the peak of the beam. Therefore, in most instances, the I(0,0) value must be close to, but slightly lower than, the CBI value. The ratios shown in Figure 7-68 demonstrate this. However, the ratio values of 21 participant labs are exactly 1.000 as observed in this graph, indicating that they reported exactly the same value as I(0,0) for CBI, meaning that half of the participants did not calculate this quantity. This indicates a lack of guidance on calculating this quantity. One laboratory reported I(0,0) higher than CBI, which must be an obvious error.

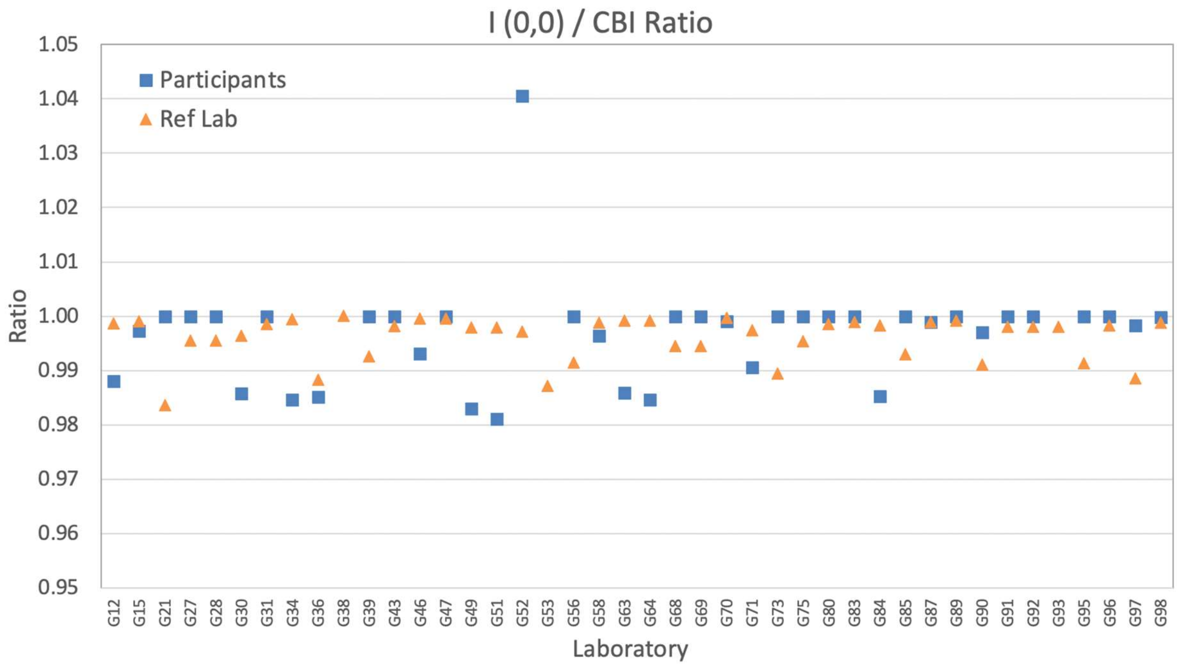

Figure 7-68. The ratios of luminous intensity at (0,0) to centre beam intensity (CBI) measured by each participant laboratory and reference laboratory.

(b) Analysis on House-side downward flux

Figure 7-69 shows an example of the C=0° – 180° plane of ART-4 luminous intensity distribution. It shows that the luminous intensity sharply decreases from γ=0° to the house side. Due to this sharp slope of the intensity distribution in the direction perpendicular to the roadway, this quantity is extremely sensitive to the angle alignment of the luminaire, and this is the reason for the very large variation of the results for this quantity. The measurement uncertainty should be evaluated taking into account this effect.

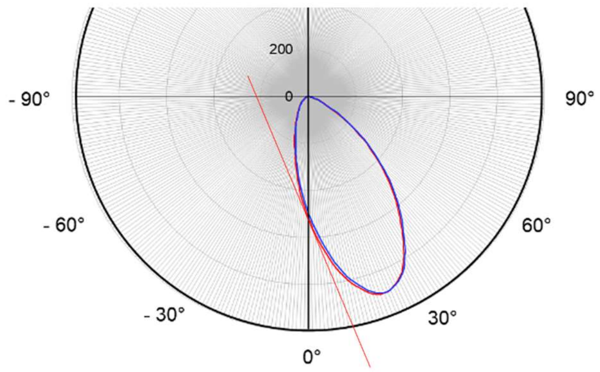

Figure 7-69. Luminous intensity distribution of ART-4 in the plane perpendicular to road direction

7.3 Differences in measurement results sorted by goniophotometer types

The results presented in this section are the same set of data presented in 7.2 but the results are sorted and grouped by goniophotometer types – mirror type, near-field type, and source-rotating type. This allows comparisons of results between and among different types of goniophotometer.

There was a goniophotometer that uses a rotating detector which rotates around a fixed luminaire. This goniophotometer is included in the near-field type group, as this design is similar to a cosine-corrected photometer head rotating around the fixed light source at fairly close distance to measure total luminous flux in near field goniophotometers. No results for goniophotometric quantities were reported for this goniophotometer.

7.3.1 presents the graphs for general photometric quantities and electrical quantities, 7.3.2 presents the graphs for colour quantities, and 7.3.3 presents the graphs for goniophotometric quantities. The analyses and discussions on all the results presented in these subsections are provided in section 7.4.

7.3.1 General photometric and electrical quantities

This section presents the graphs for the results of general photometric quantities and electrical quantities (item 1 to 5 in Table 3-1) sorted by the type of goniophotometer.

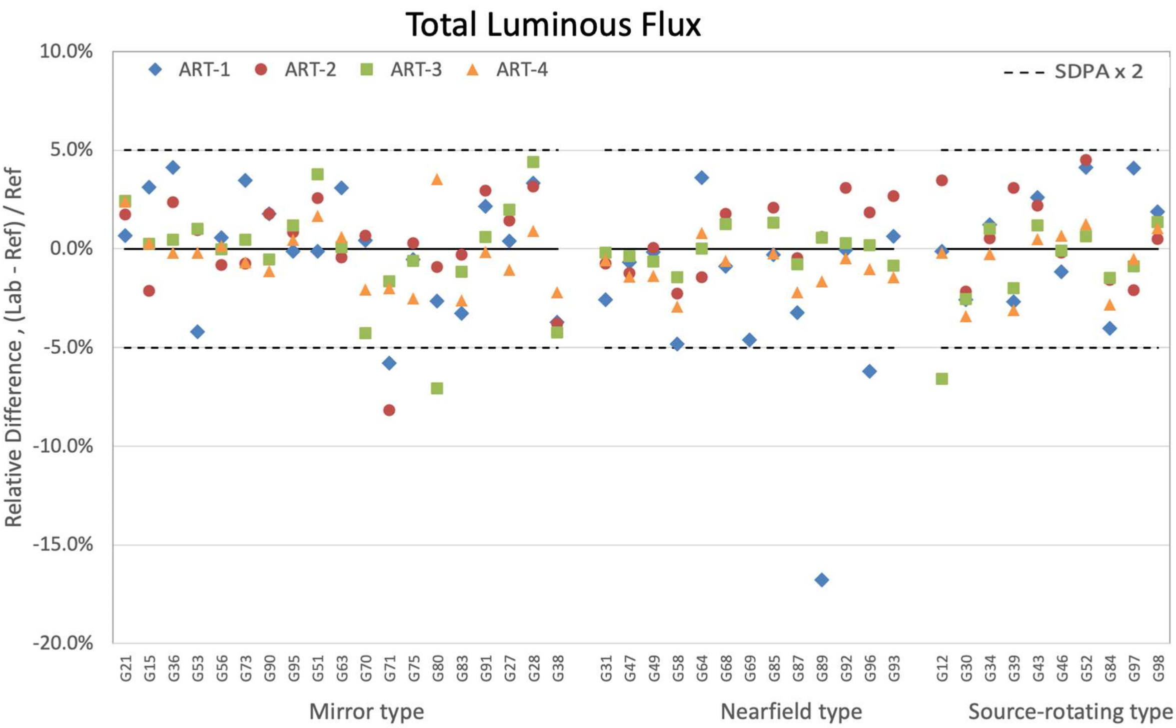

Figure 7-70. Relative differences of total luminous flux for all artefacts sorted by goniophotometer type

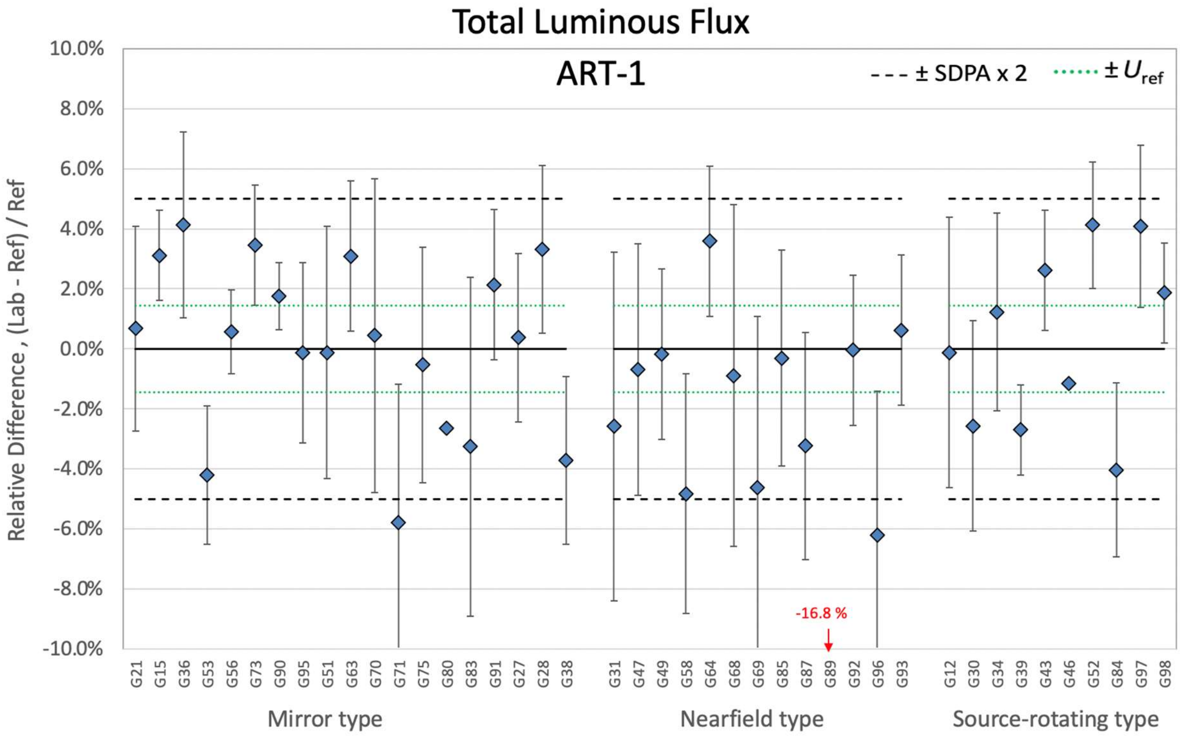

Figure 7-71. Relative differences of total luminous flux for ART-1 by goniophotometer type

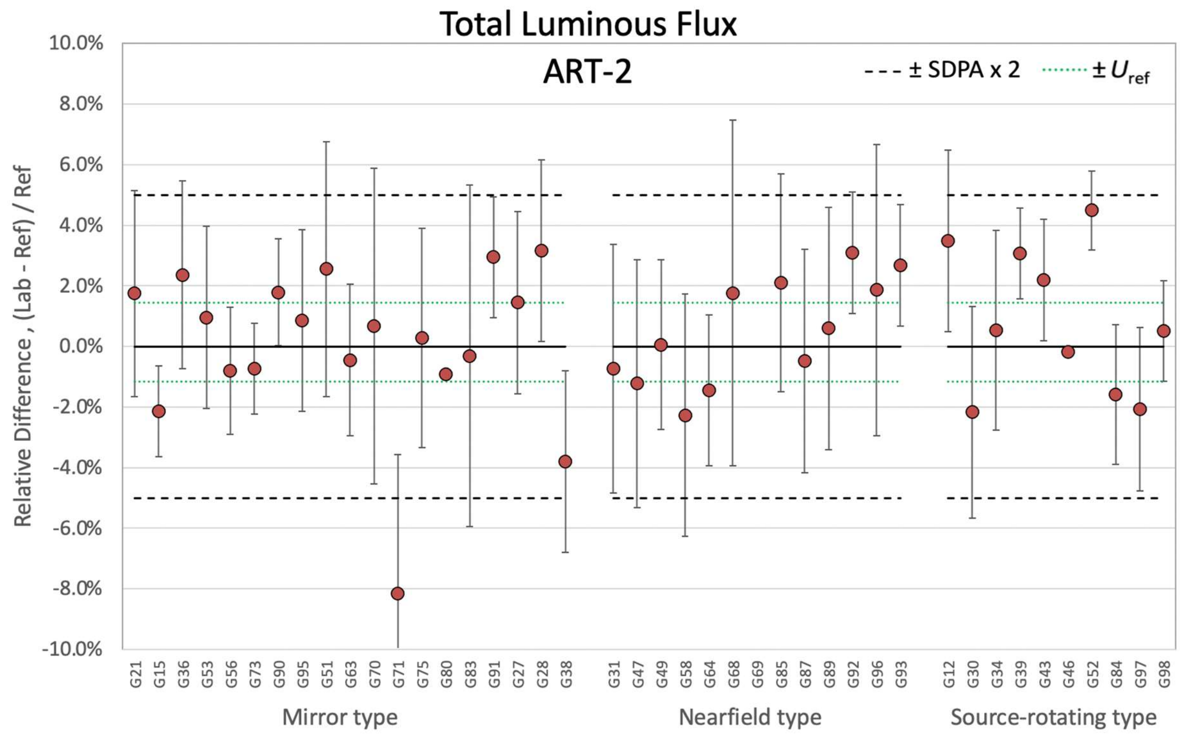

Figure 7-72. Relative differences of total luminous flux for ART-2 by goniophotometer type

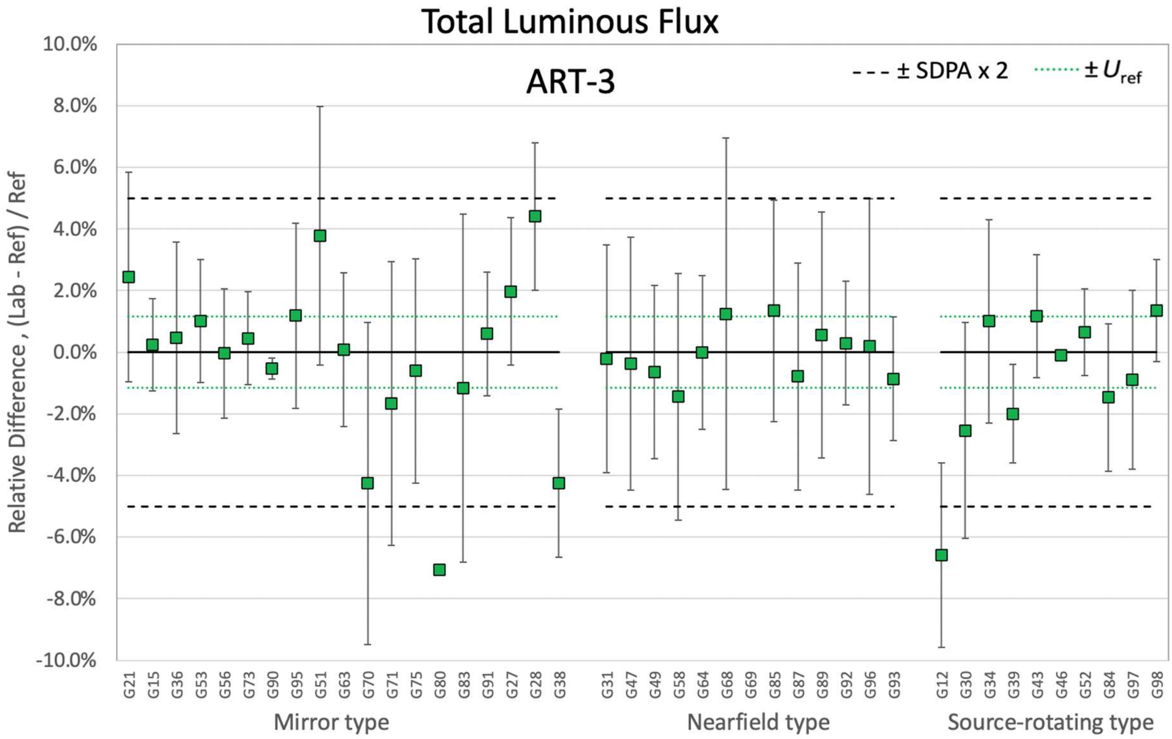

Figure 7-73. Relative differences of total luminous flux for ART-3 by goniophotometer type

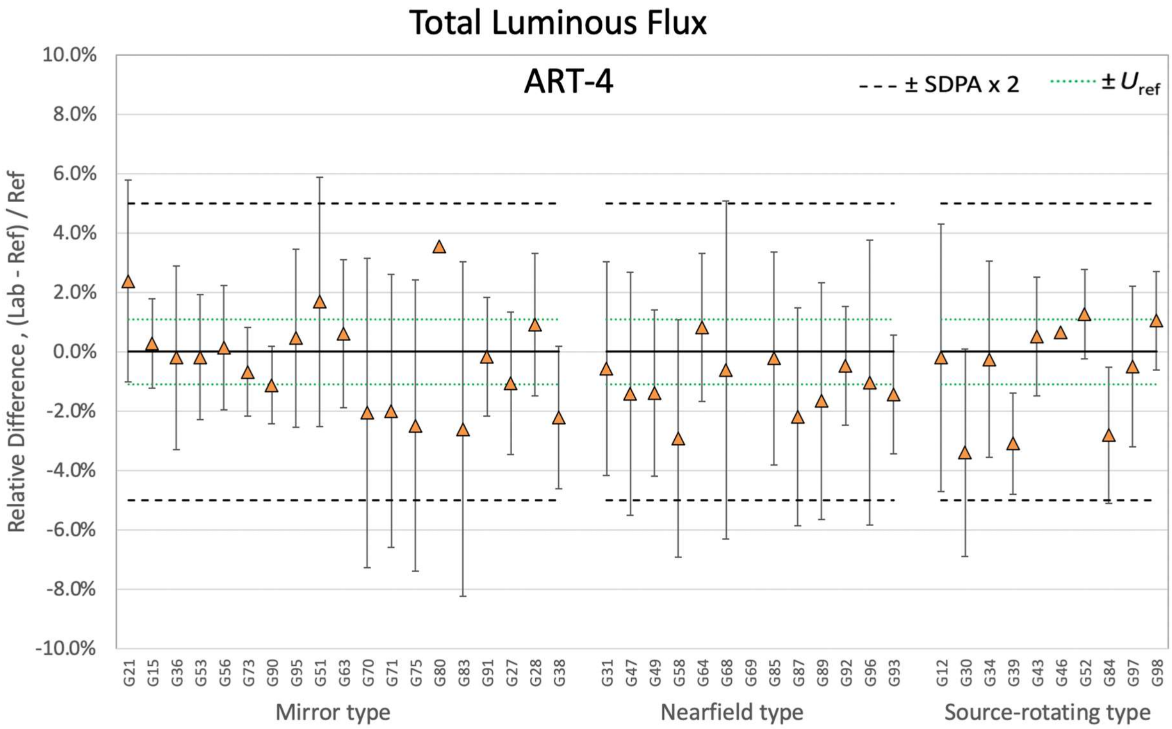

Figure 7-74. Relative differences of total luminous flux for ART-4 by goniophotometer type

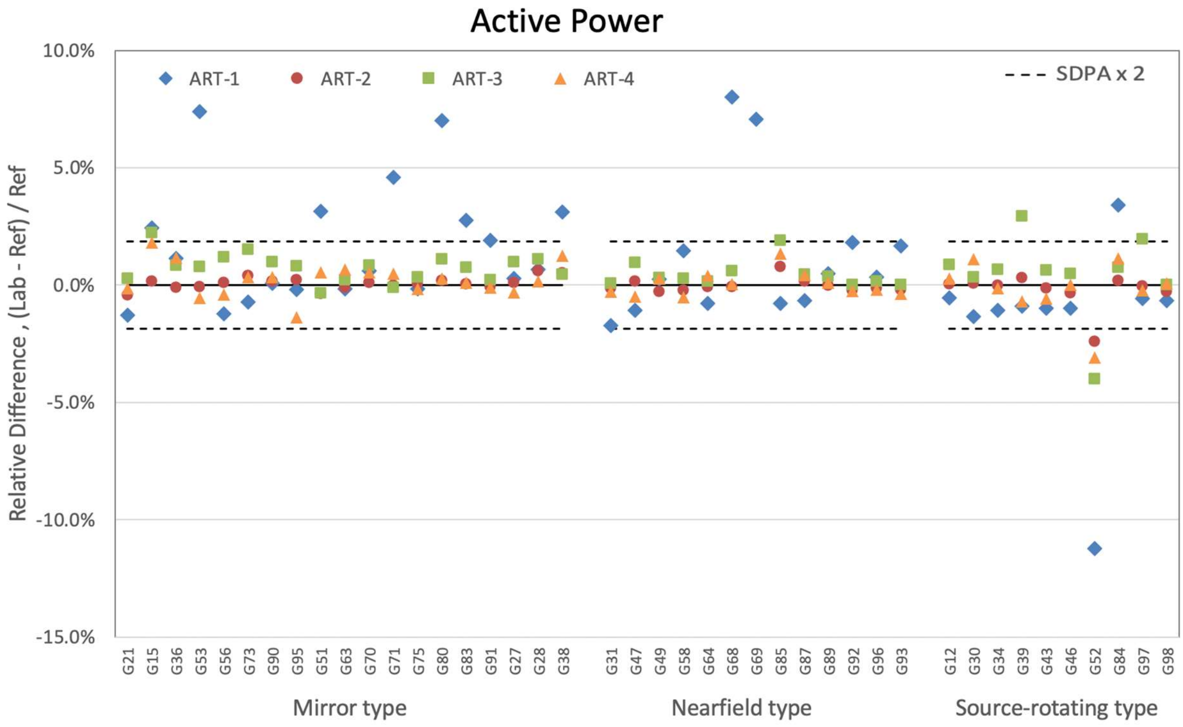

Figure 7-75. Relative differences of active power for all artefacts by goniophotometer type

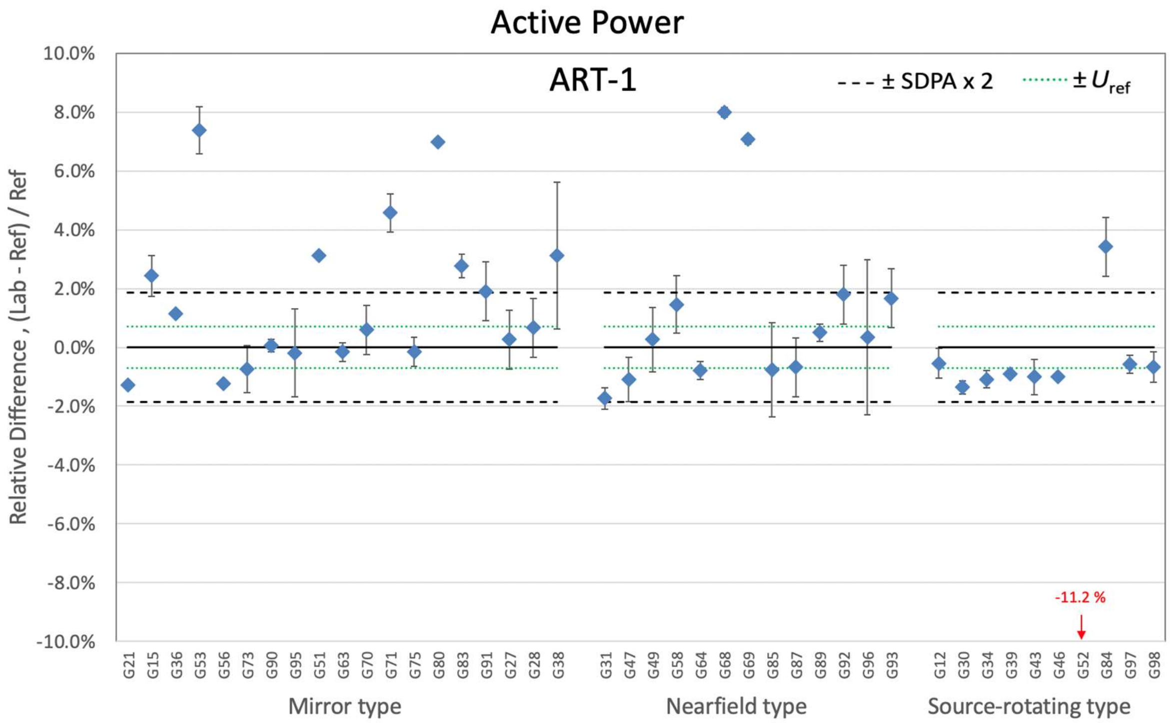

Figure 7-76. Relative differences of active power for ART-1 by goniophotometer type

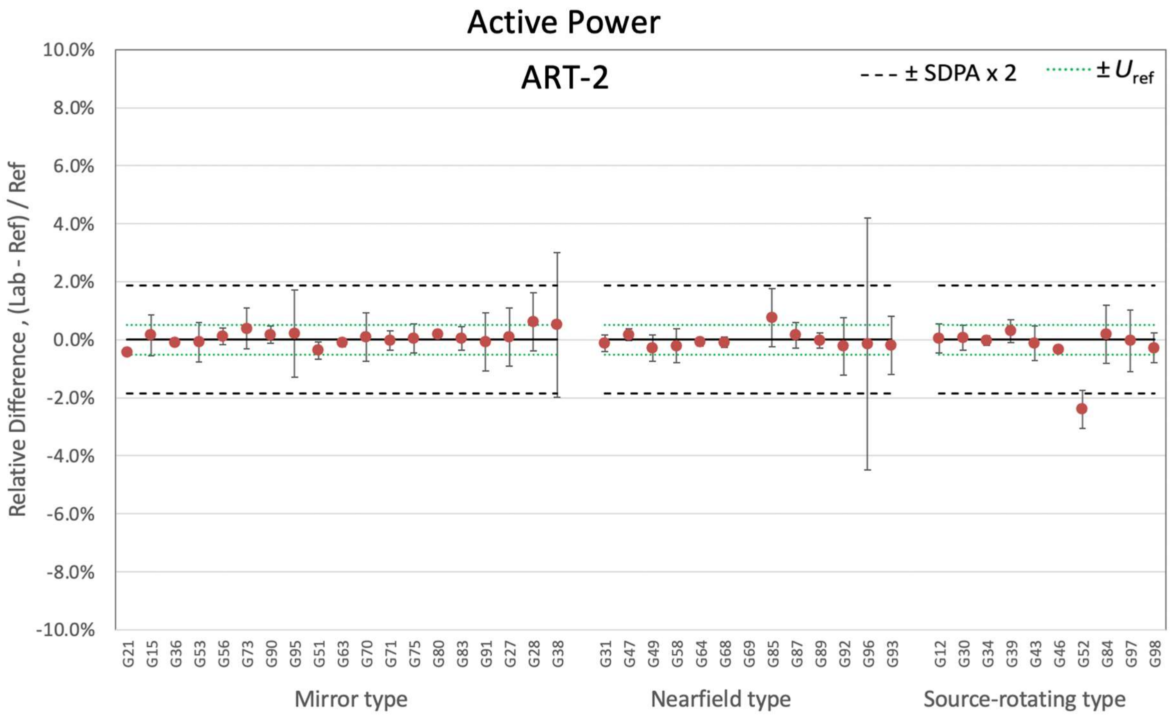

Figure 7-77. Relative differences of active power for ART-2 by goniophotometer type

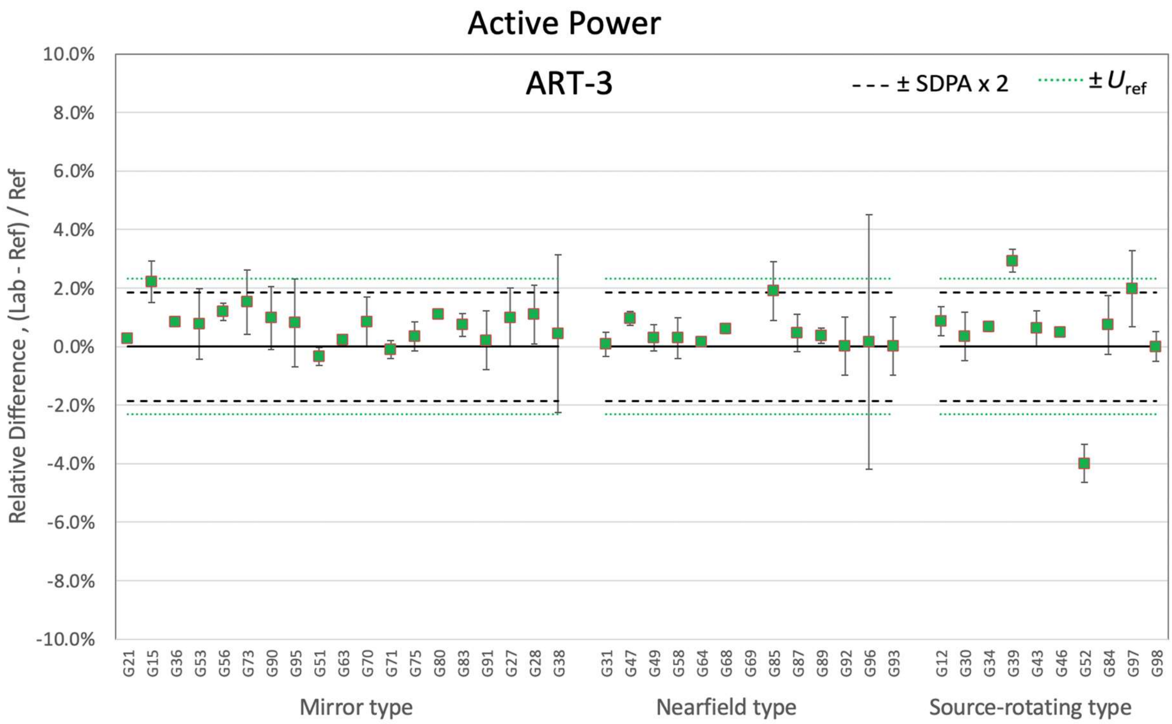

Figure 7-78. Relative differences of active power for ART-3 by goniophotometer type

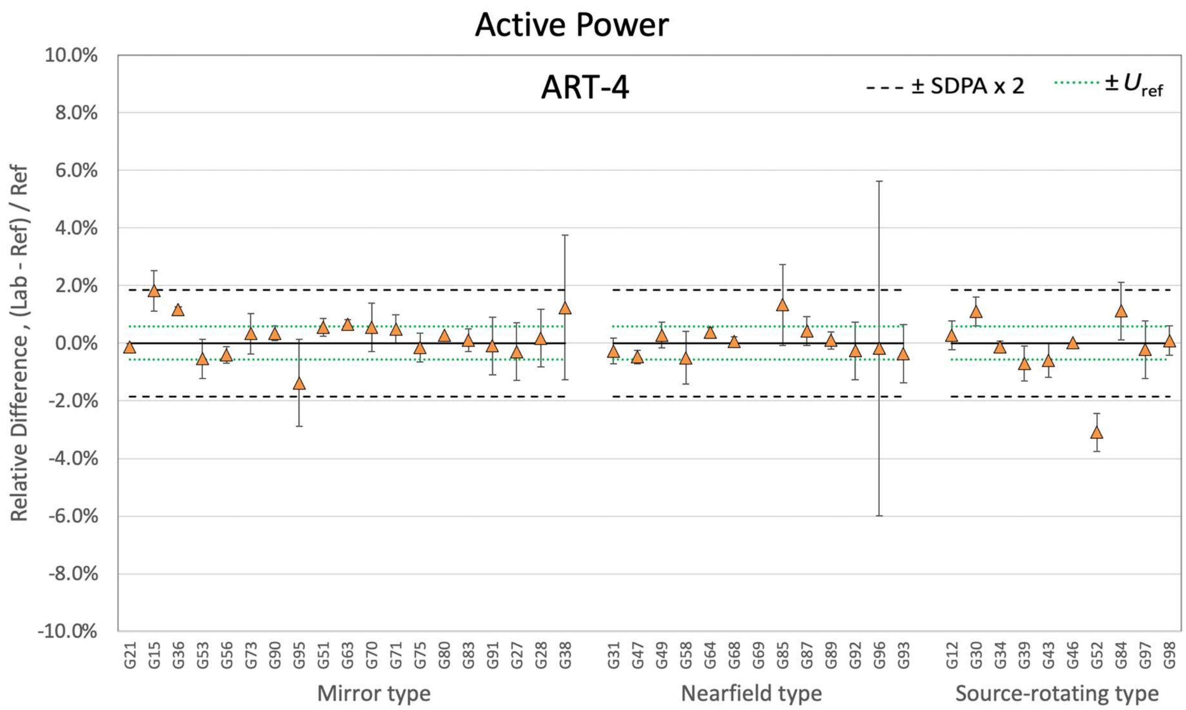

Figure 7-79. Relative differences of active power for ART-4 by goniophotometer type

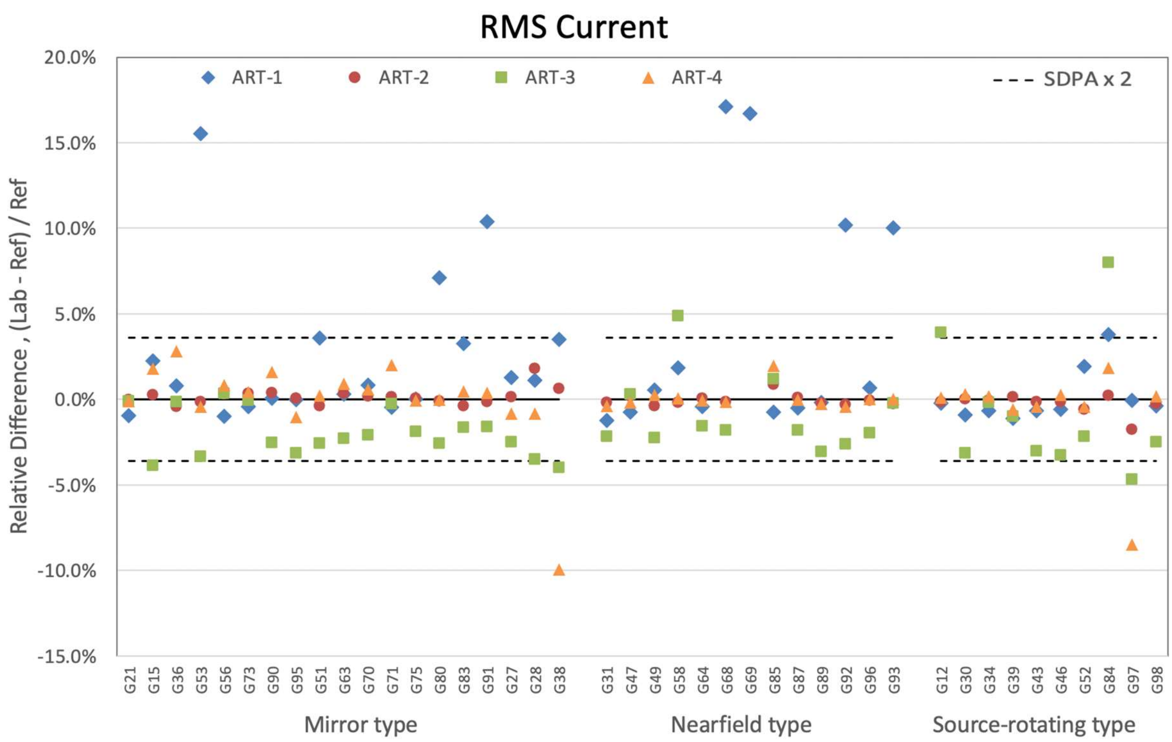

Figure 7-80. Relative differences of RMS current for all artefacts by goniophotometer type

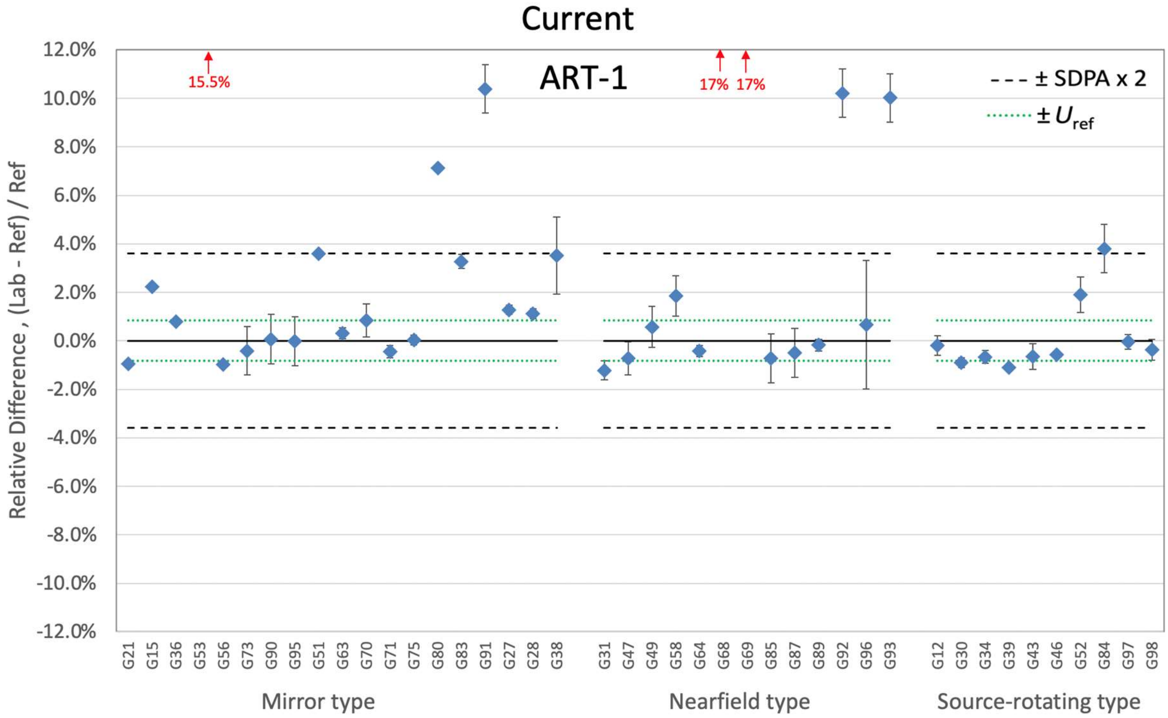

Figure 7-81. Relative differences of RMS current for ART-1 by goniophotometer type

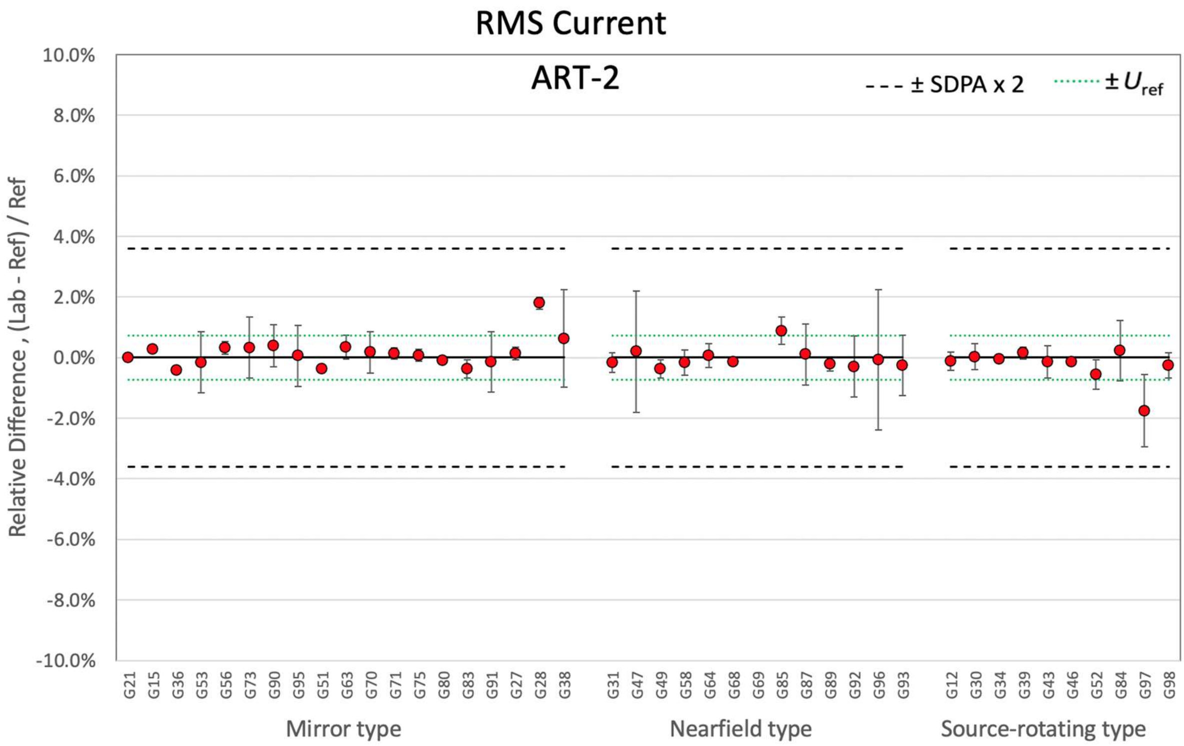

Figure 7-82. Relative differences of RMS current for ART-2 by goniophotometer type

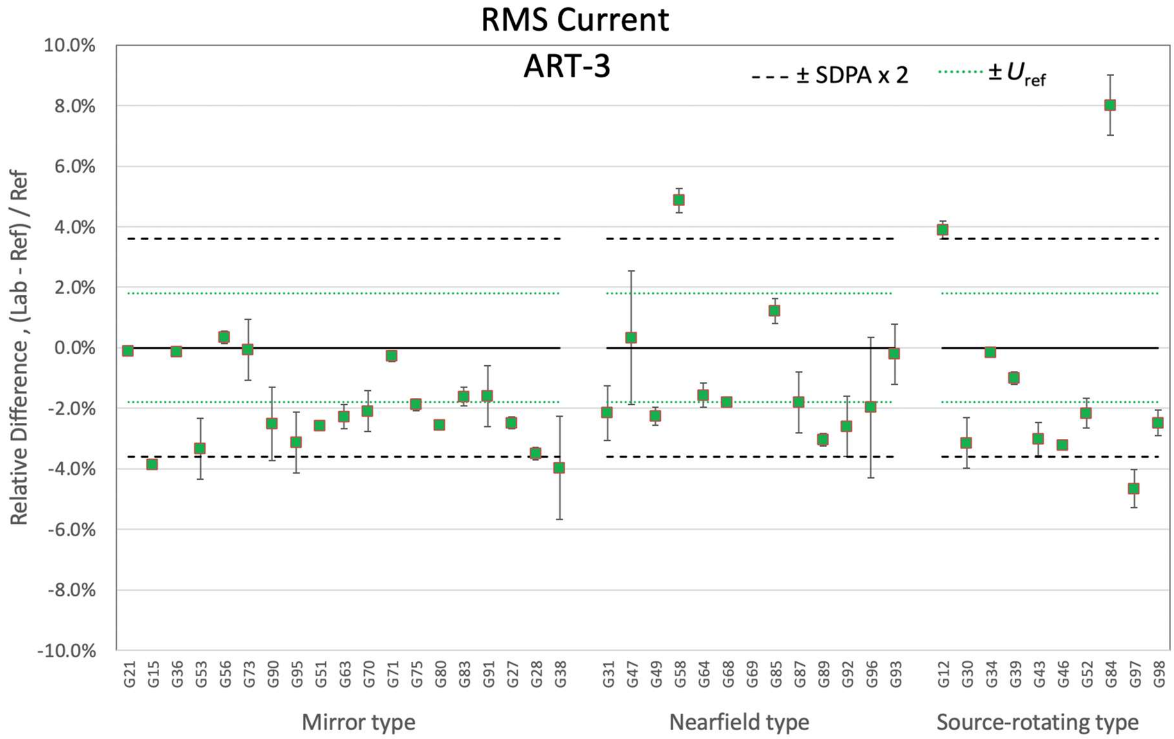

Figure 7-83. Relative differences of RMS current for ART-3 by goniophotometer type

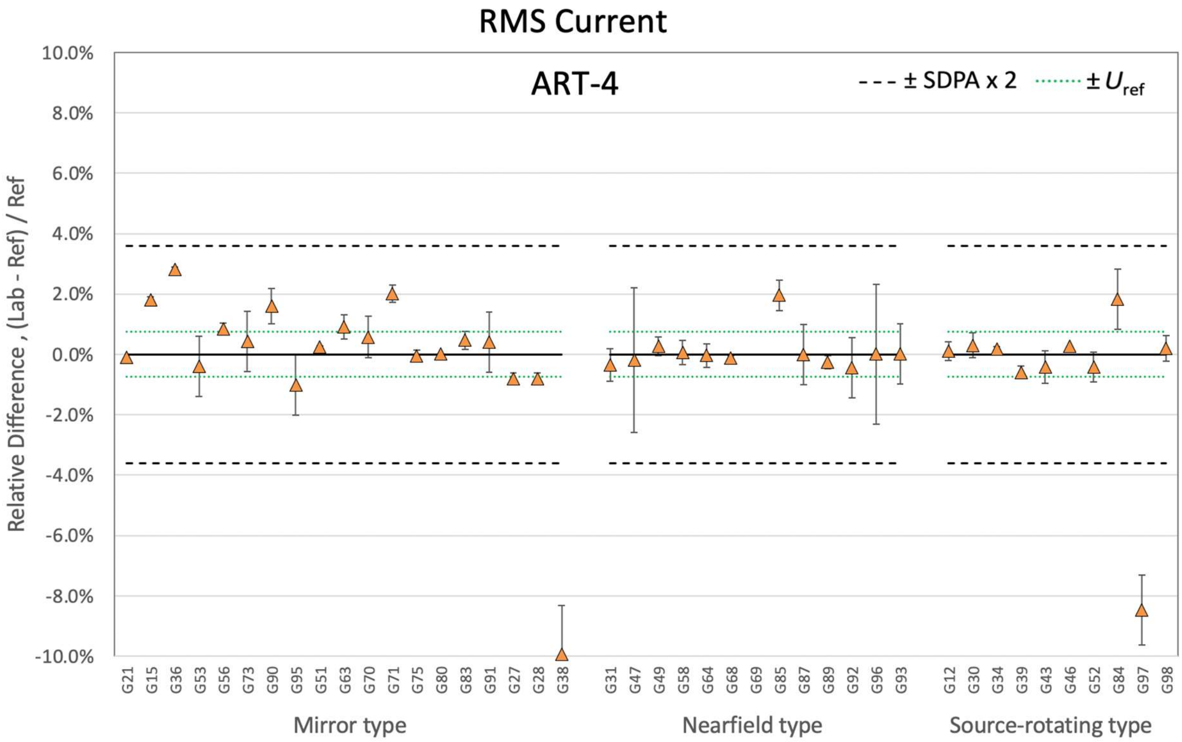

Figure 7-84. Relative differences of RMS current for ART-4 by goniophotometer type

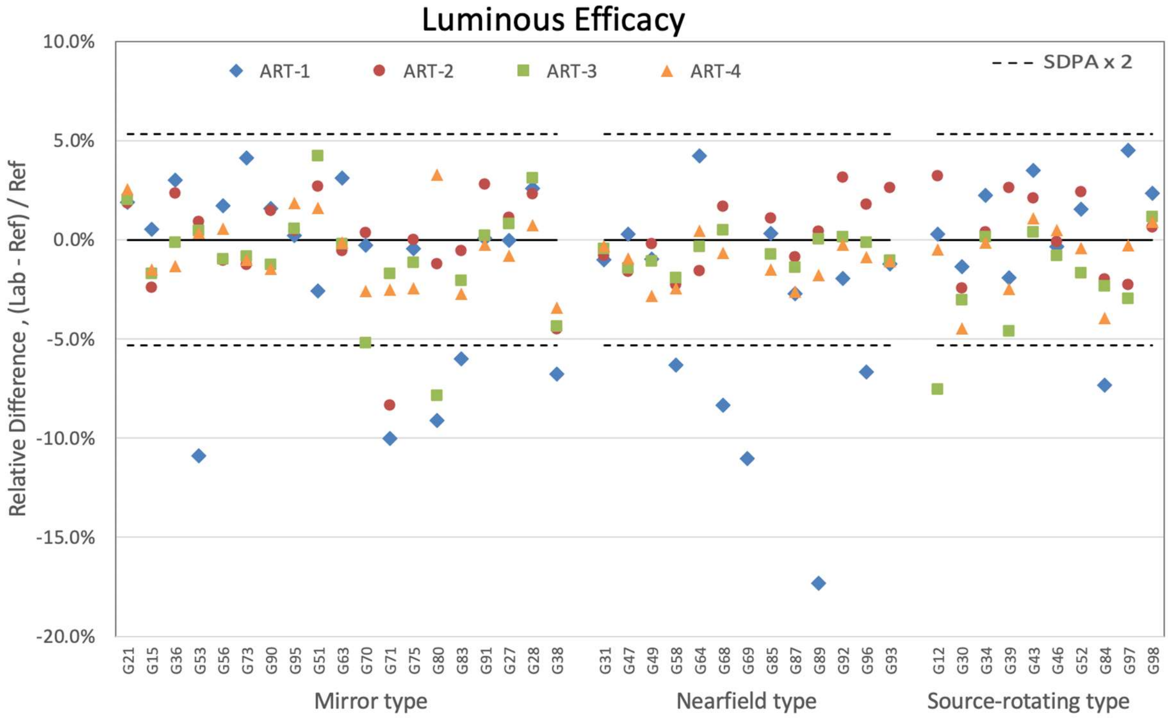

Figure 7-85. Relative differences of luminous efficacy for all artefacts by goniophotometer type

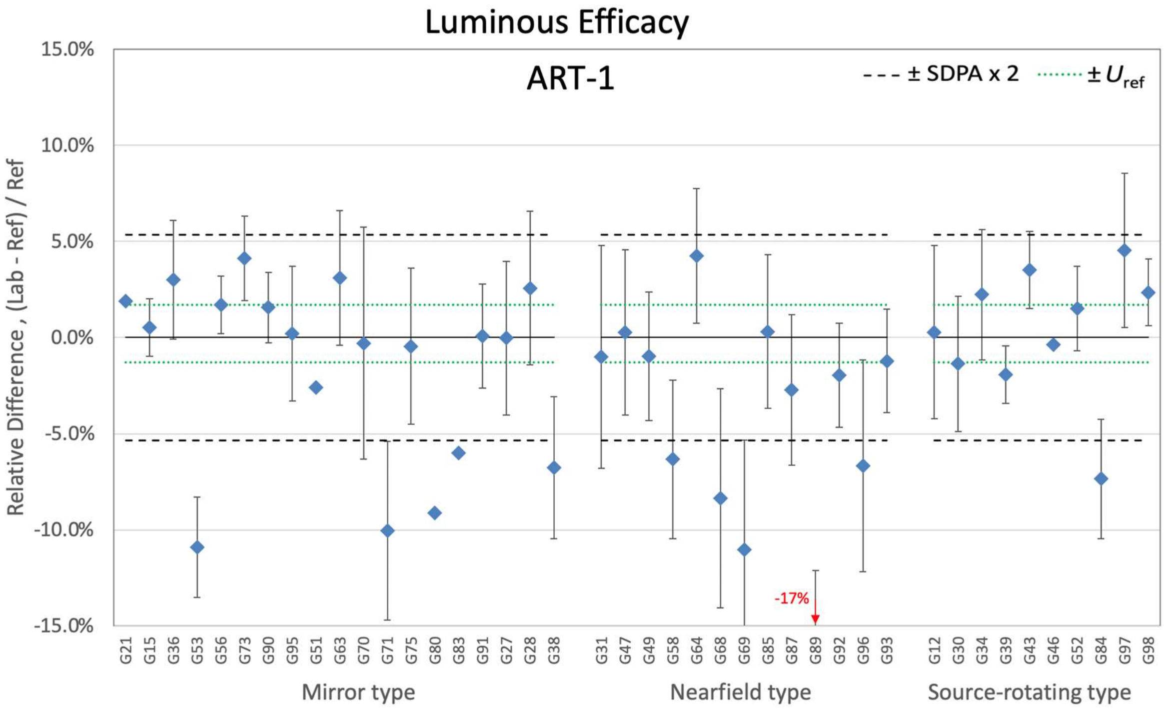

Figure 7-86. Relative differences of luminous efficacy for ART-1 by goniophotometer type

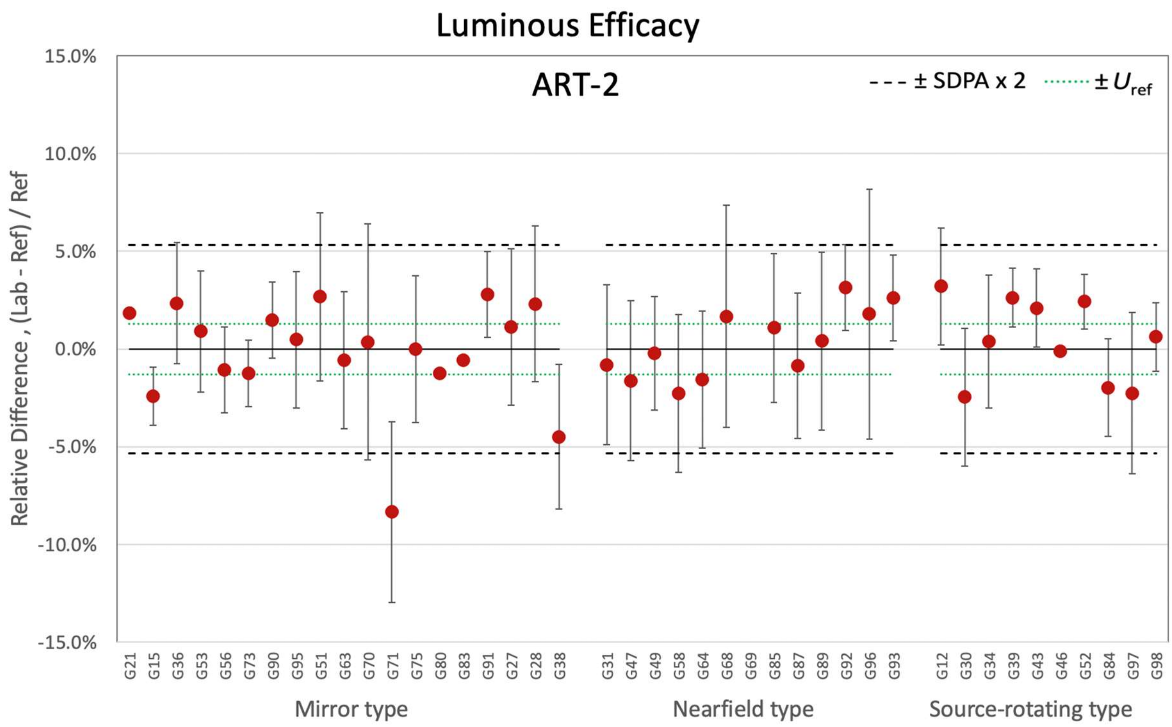

Figure 7-87. Relative differences of luminous efficacy for ART-2 by goniophotometer type

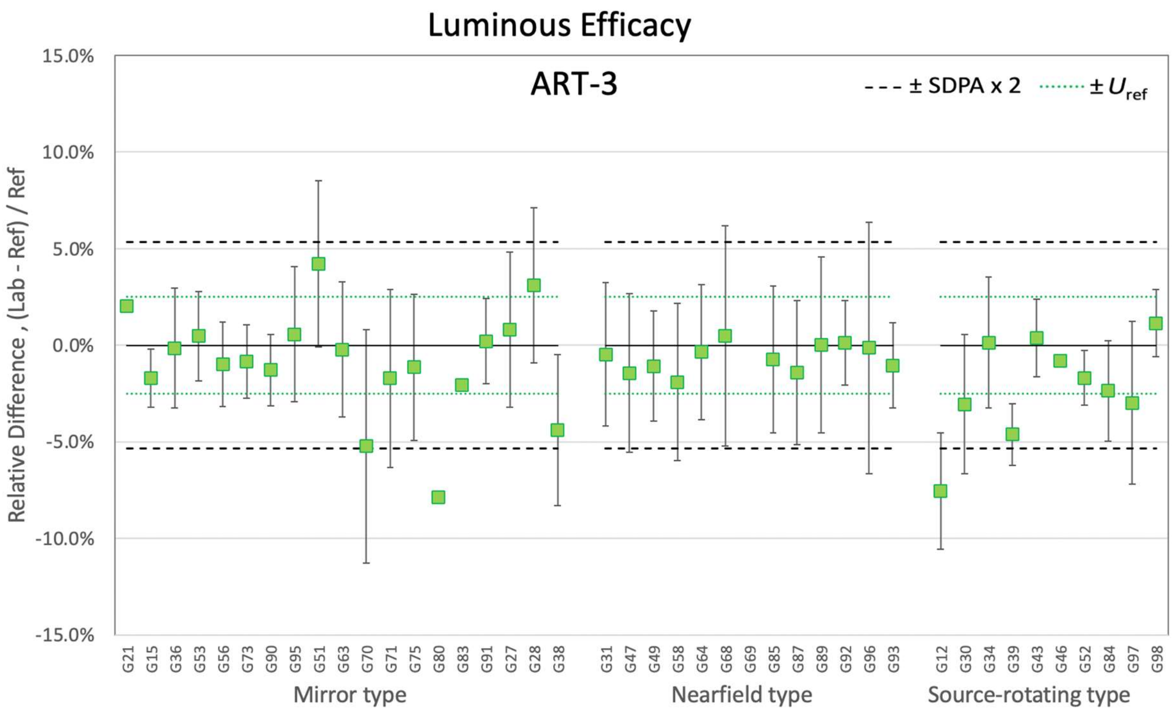

Figure 7-88. Relative differences of luminous efficacy for ART-3 by goniophotometer type

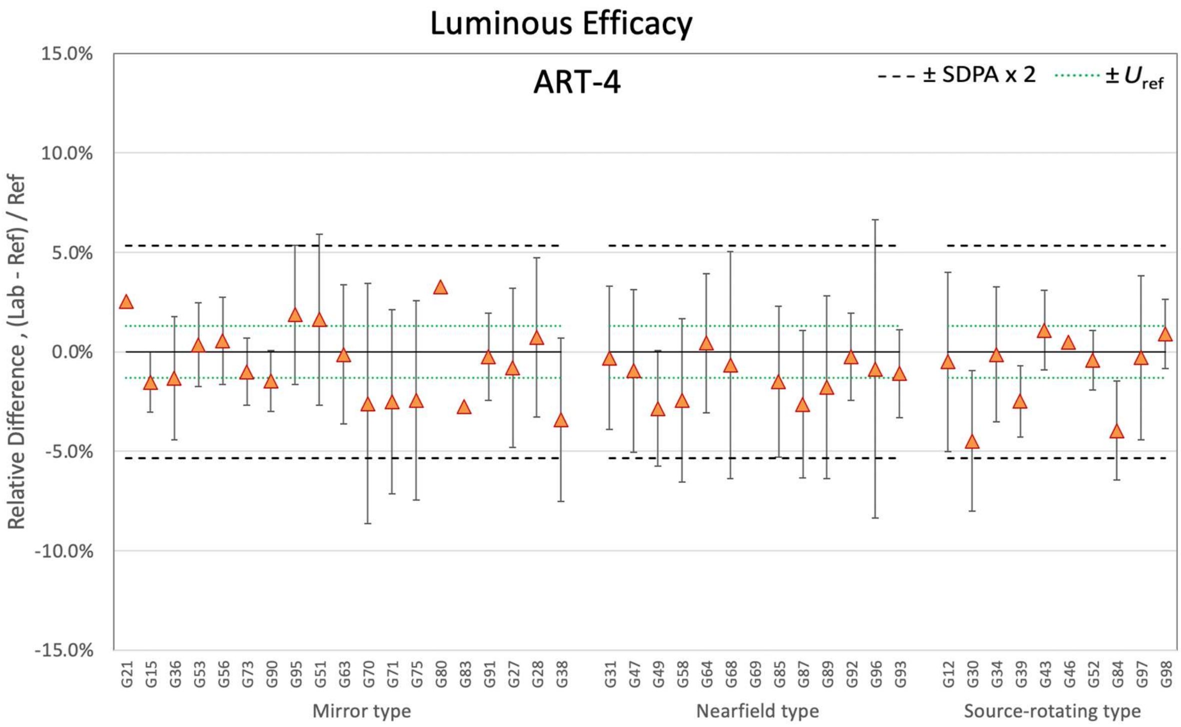

Figure 7-89. Relative differences of luminous efficacy for ART-4 by goniophotometer type

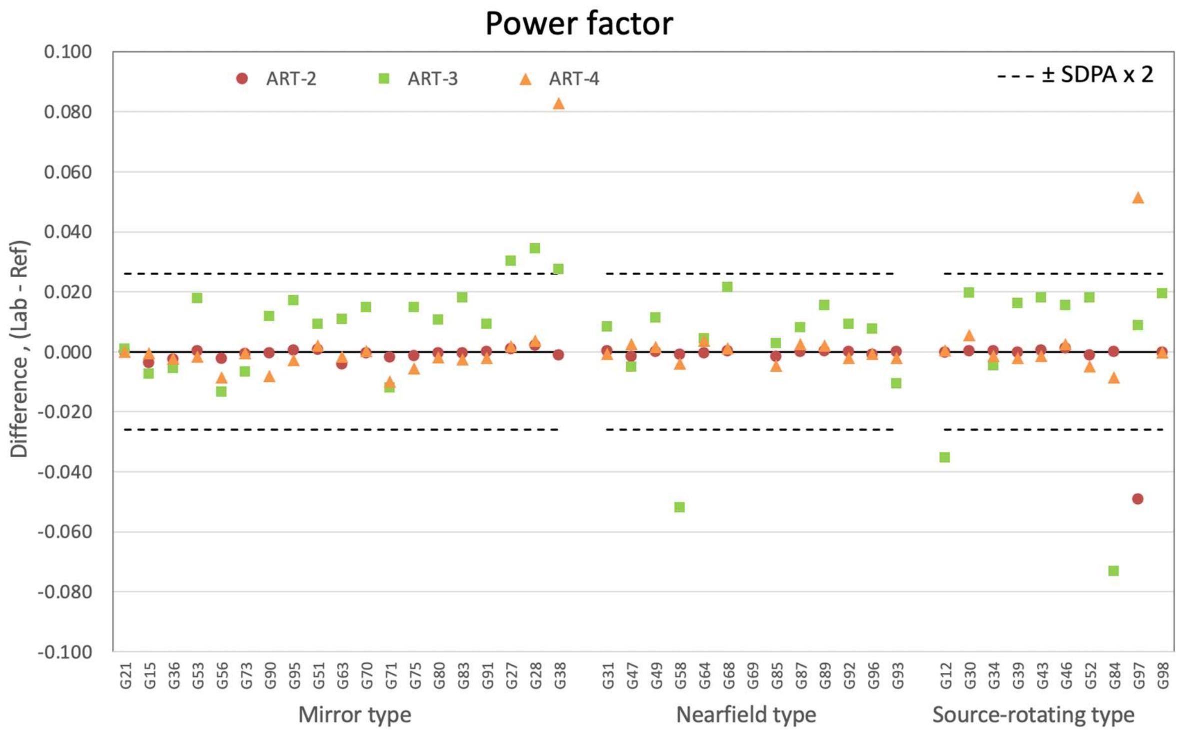

Figure 7-90. Differences of power factor for all artefacts by goniophotometer type (ART-1 was DC, not included)

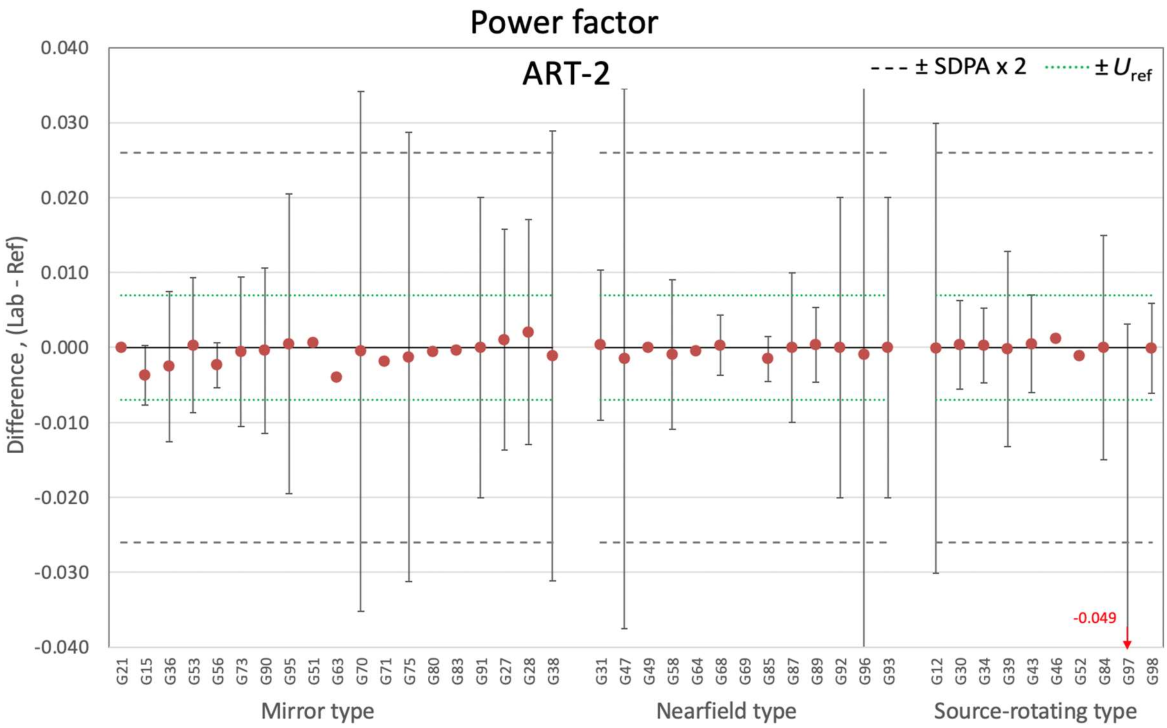

Figure 7-91. Differences of power factor for ART-2 by goniophotometer type

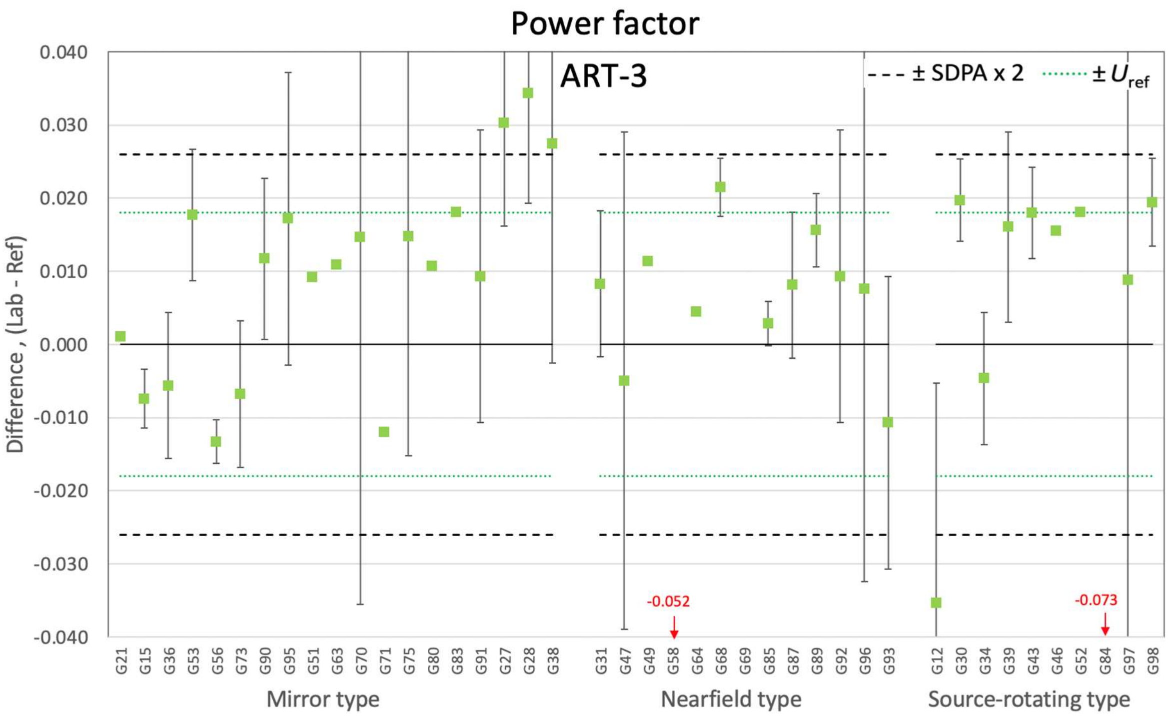

Figure 7-92. Differences of power factor for ART-3 by goniophotometer type

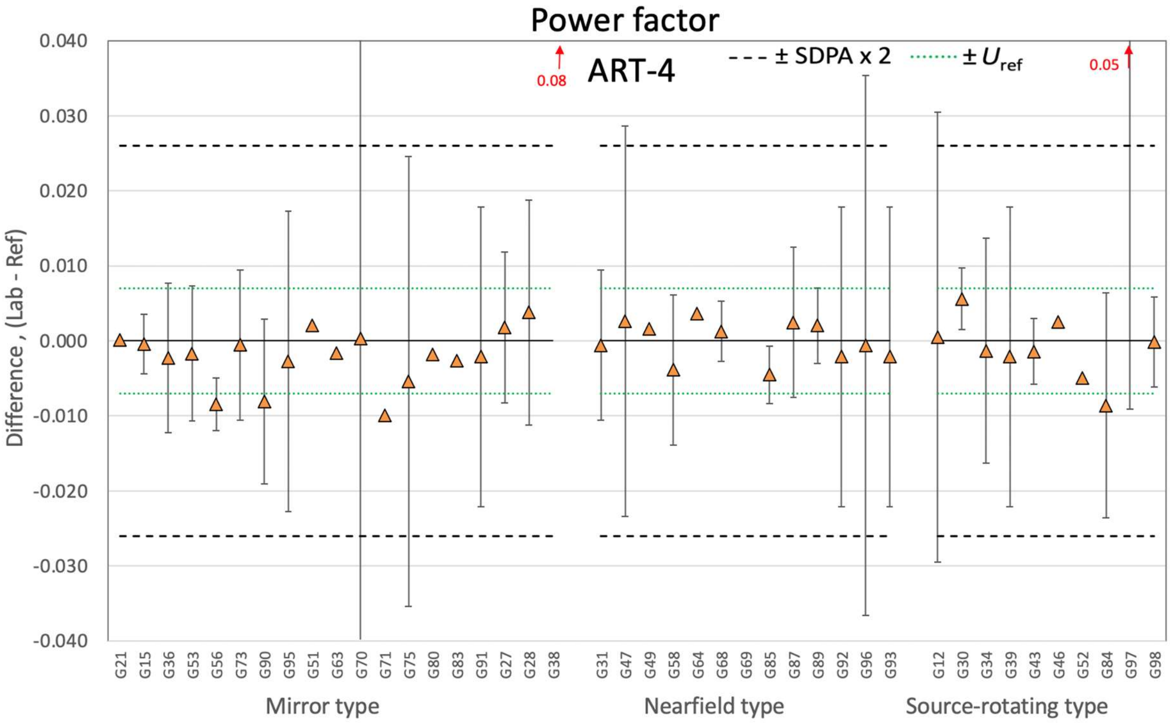

Figure 7-93. Differences of power factor for ART-4 by goniophotometer type

7.3.2 Colour quantities

The colour quantities were measured by either a gonio-spectroradiometer or a sphere-spectroradiometer, therefore, the data were further sorted so that those labs who used sphere spectroradiometers to measure colour quantities were separated into another group. This allows comparison of data between goniophotometer systems (gonio-spectroradiometers) and sphere systems (sphere-spectroradiometers).

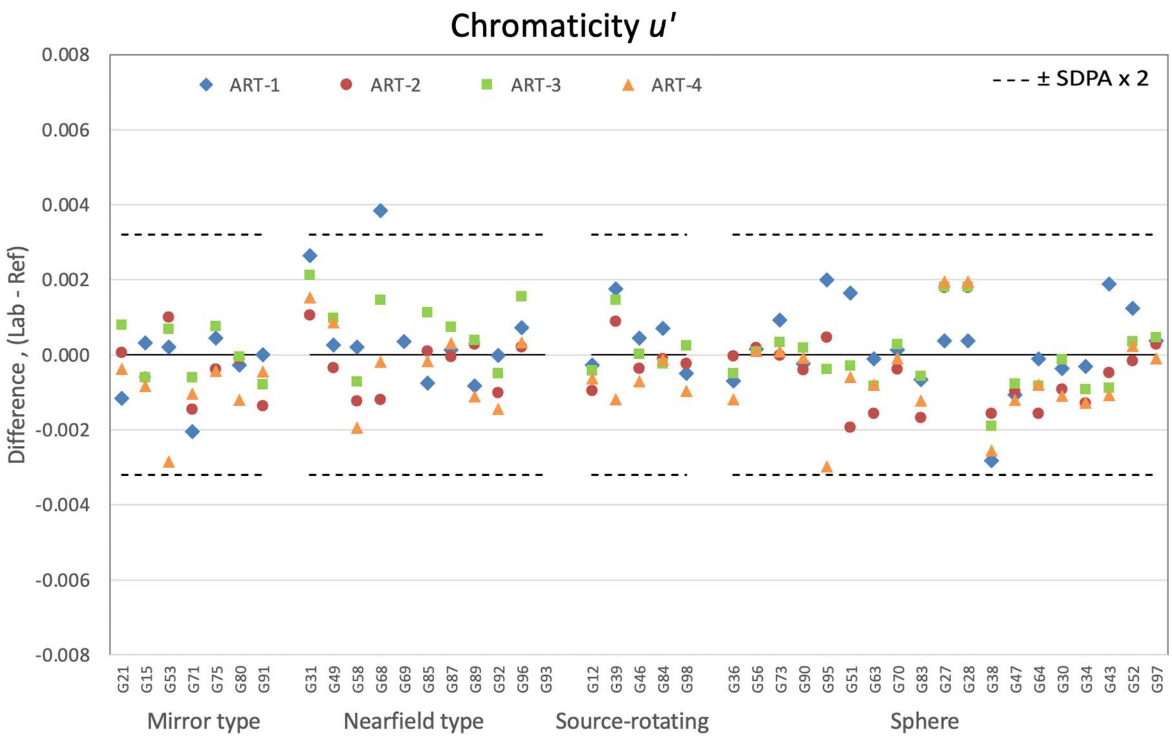

Figure 7-94. Differences of chromaticity *u*' for all artefacts by goniophotometer type and sphere

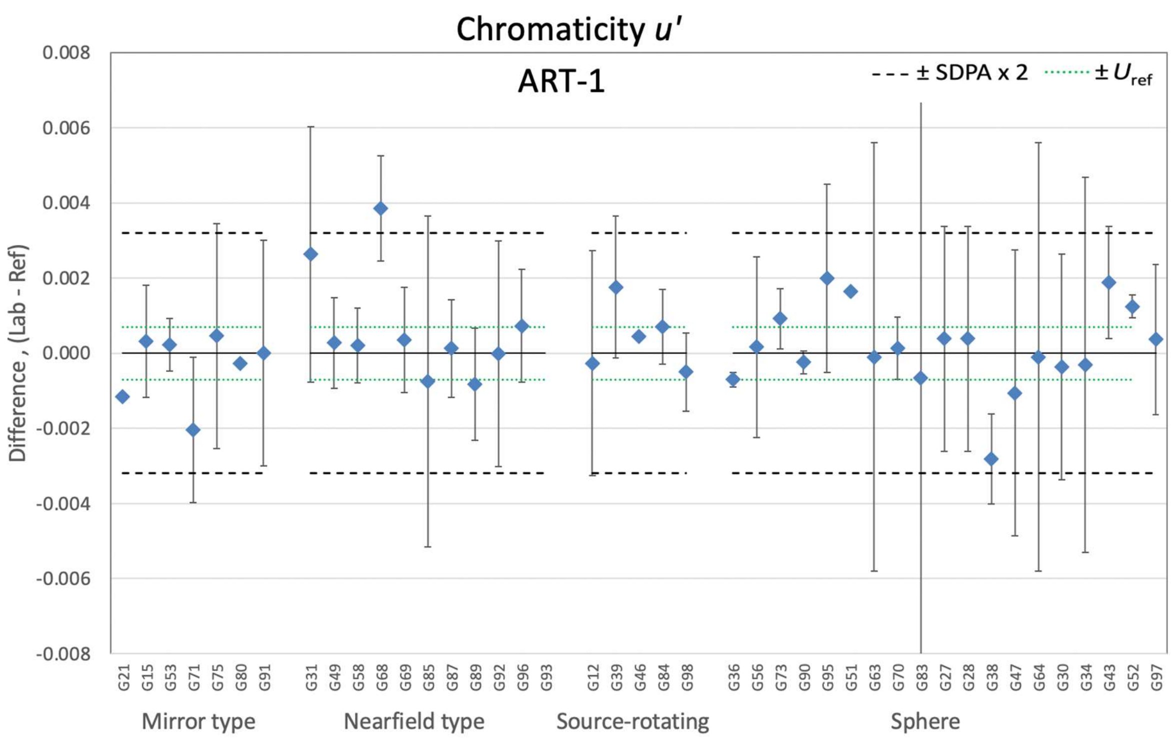

Figure 7-95. Differences of chromaticity *u*' for ART-1 by goniophotometer type and sphere

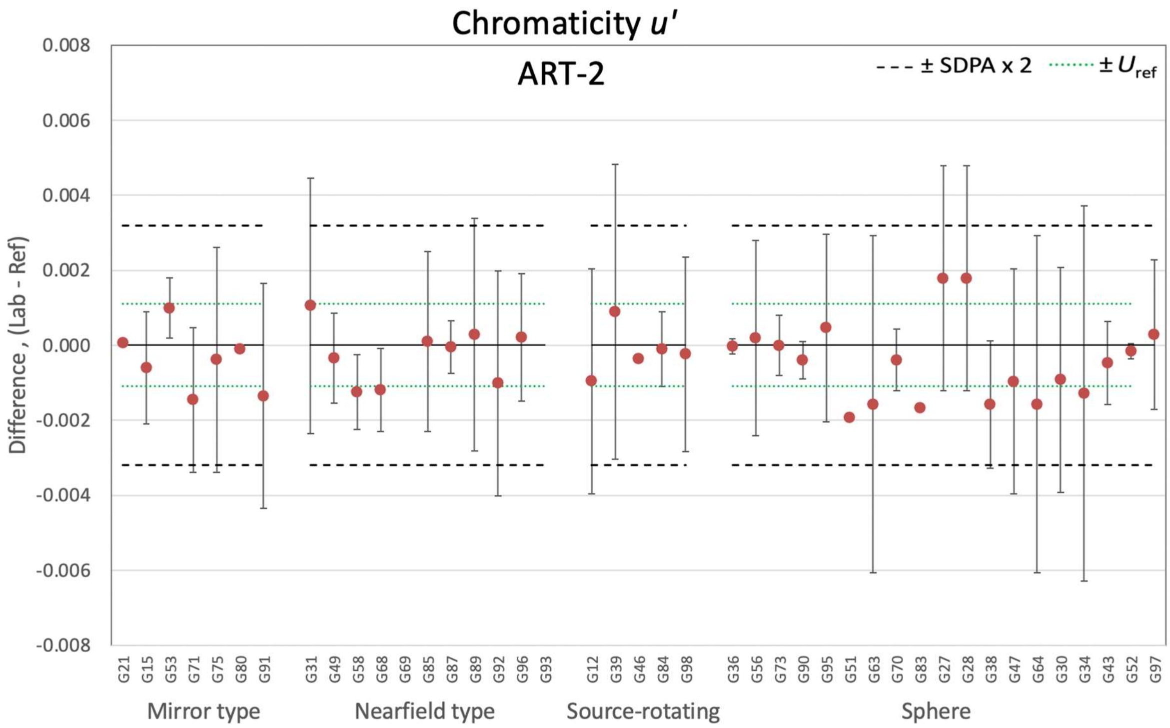

Figure 7-96. Differences of chromaticity u' for ART-2 by goniophotometer type and sphere

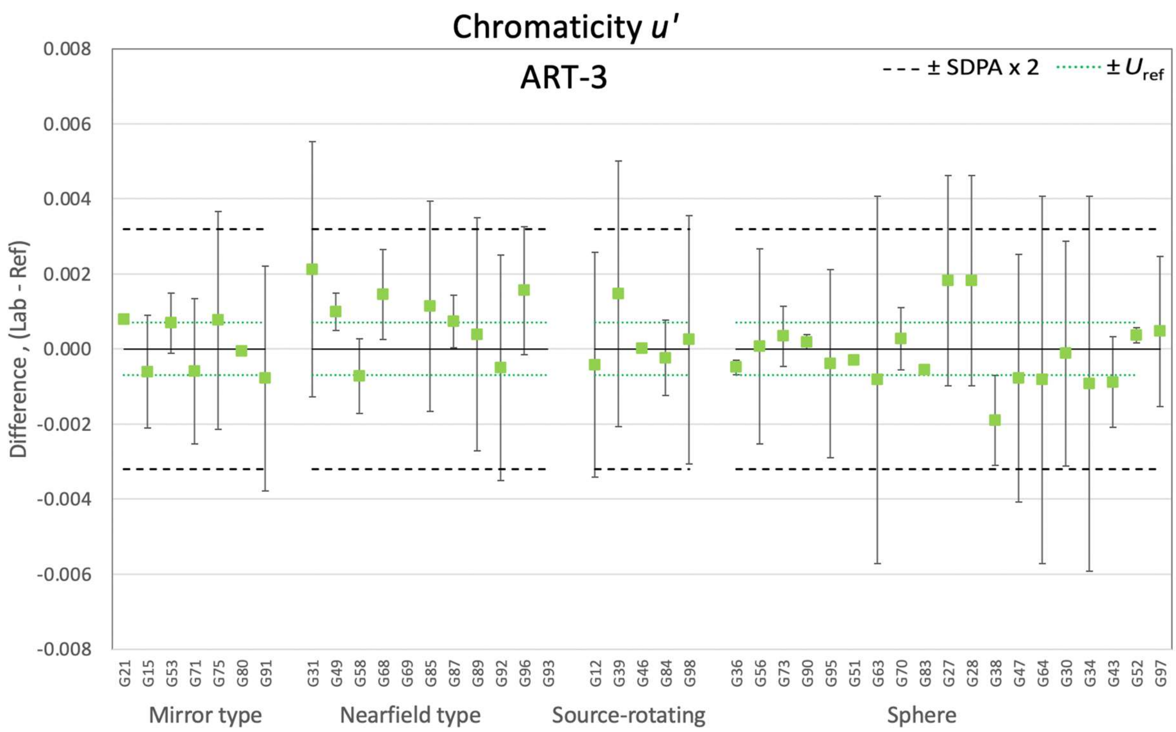

Figure 7-97. Differences of chromaticity *u'* for ART-3 by goniophotometer type and sphere

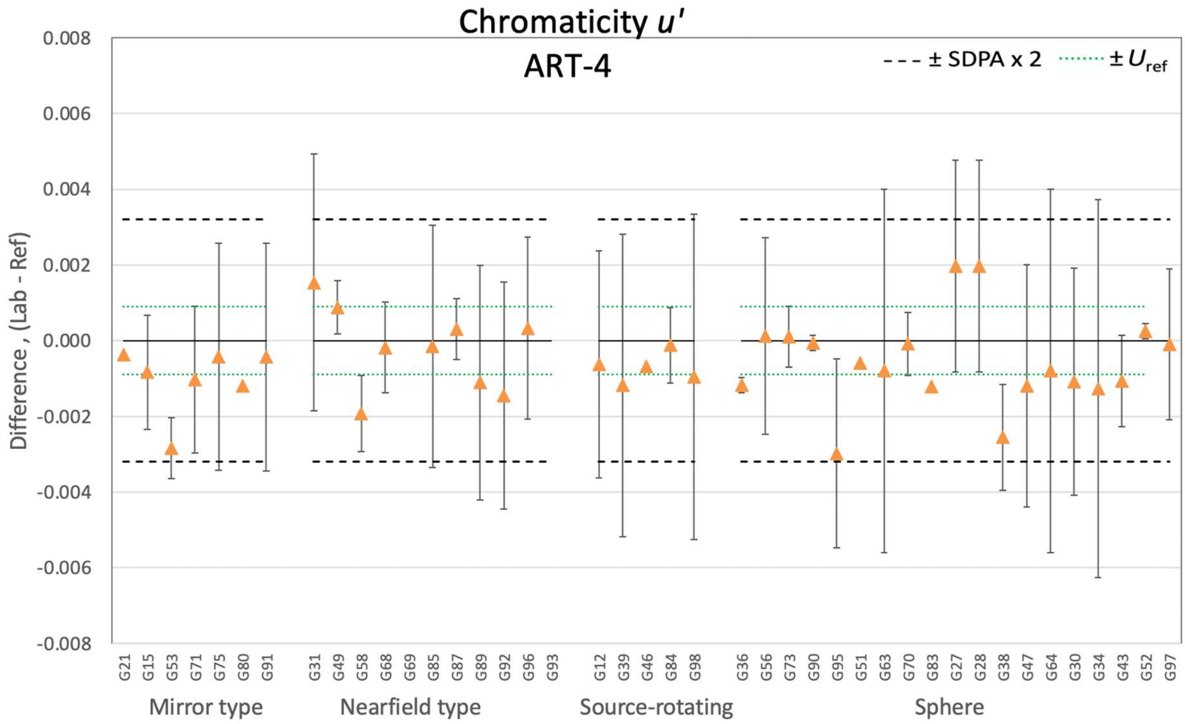

Figure 7-98. Differences of chromaticity *u*' for ART-4 by goniophotometer type and sphere

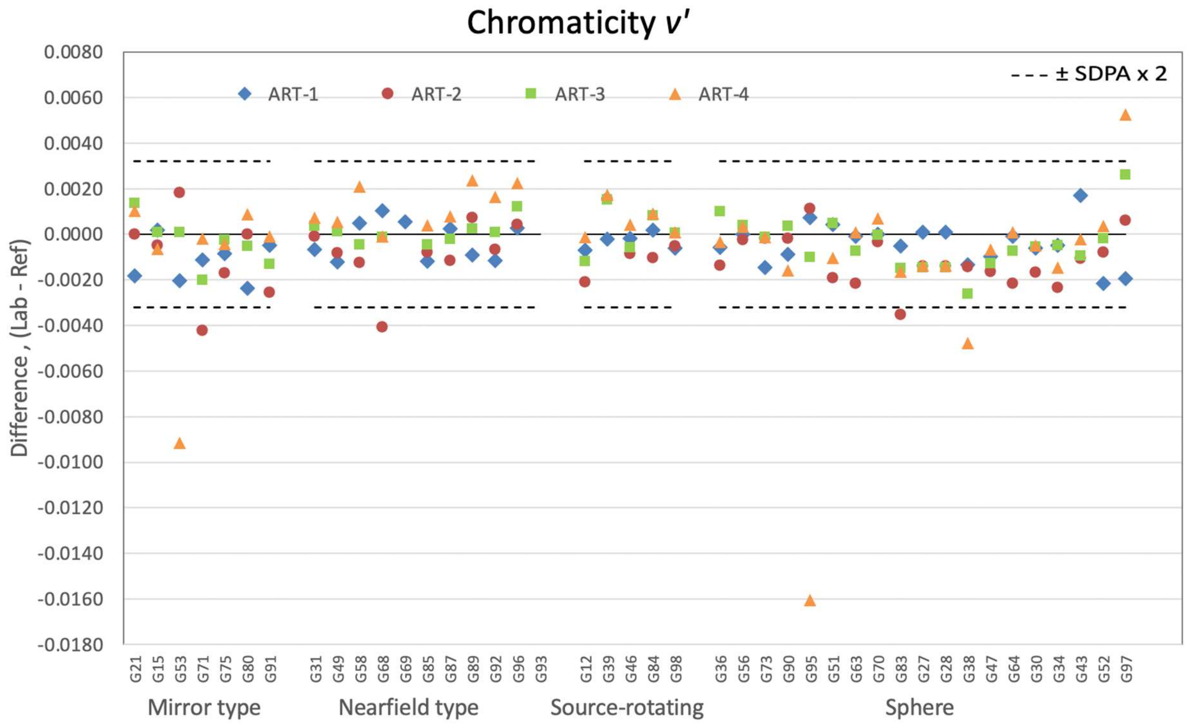

Figure 7-99. Differences of chromaticity v' for all artefacts by goniophotometer type and sphere

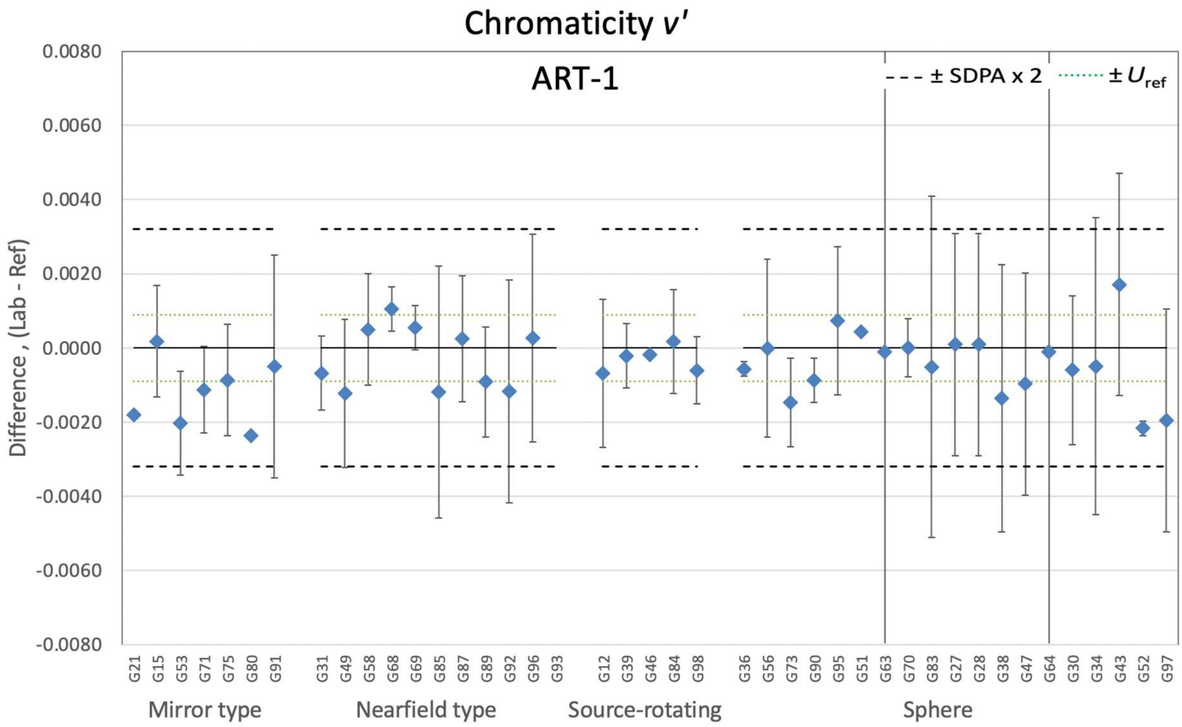

Figure 7-100. Differences of chromaticity v′ for ART-1 by goniophotometer type and sphere

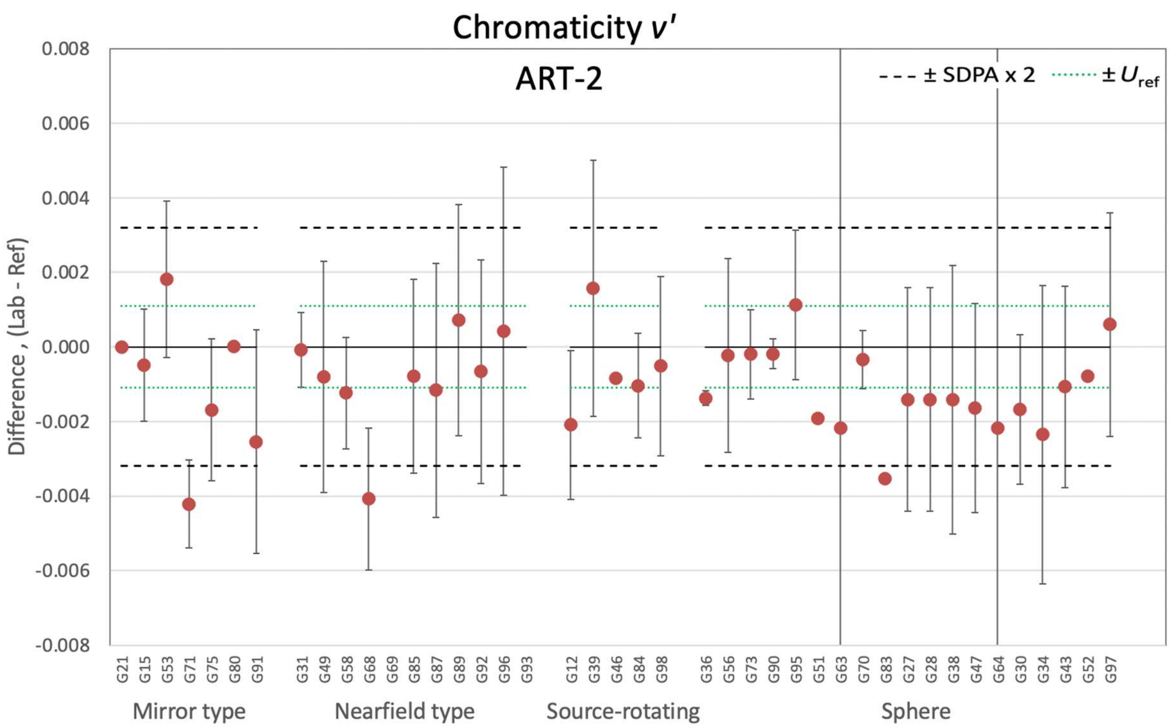

Figure 7-101. Differences of chromaticity v′ for ART-2 by goniophotometer type and sphere

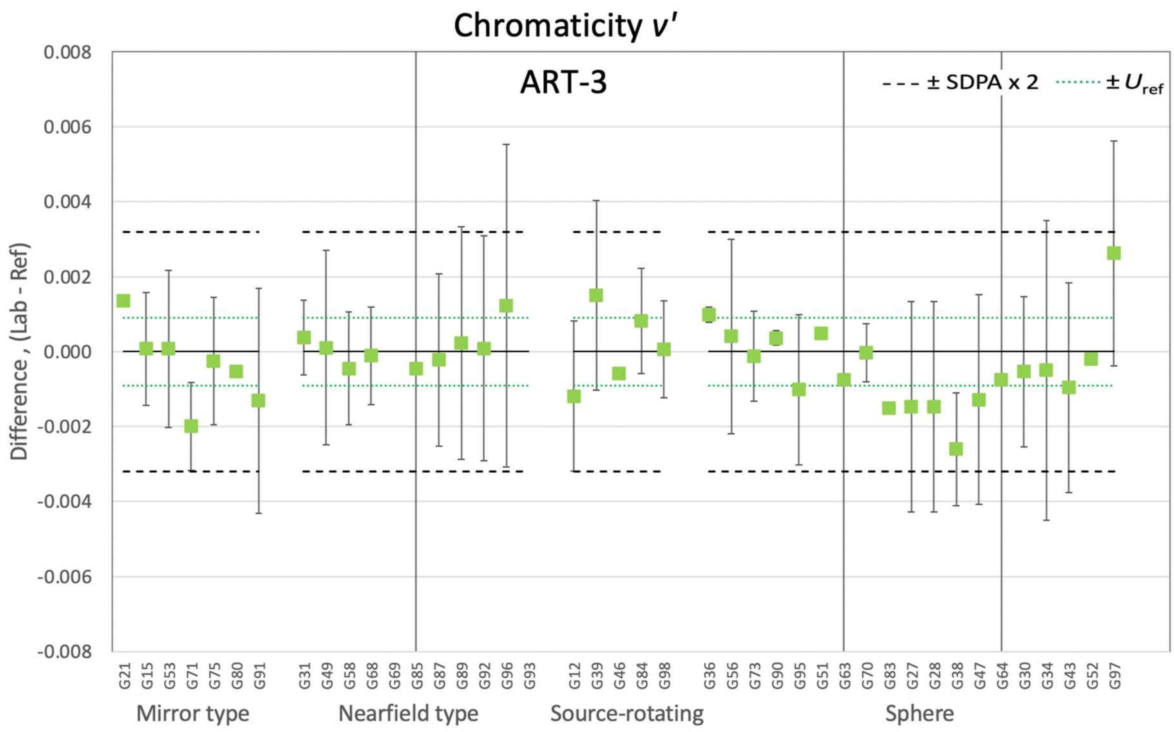

Figure 7-102. Differences of chromaticity v′ for ART-3 by goniophotometer type and sphere

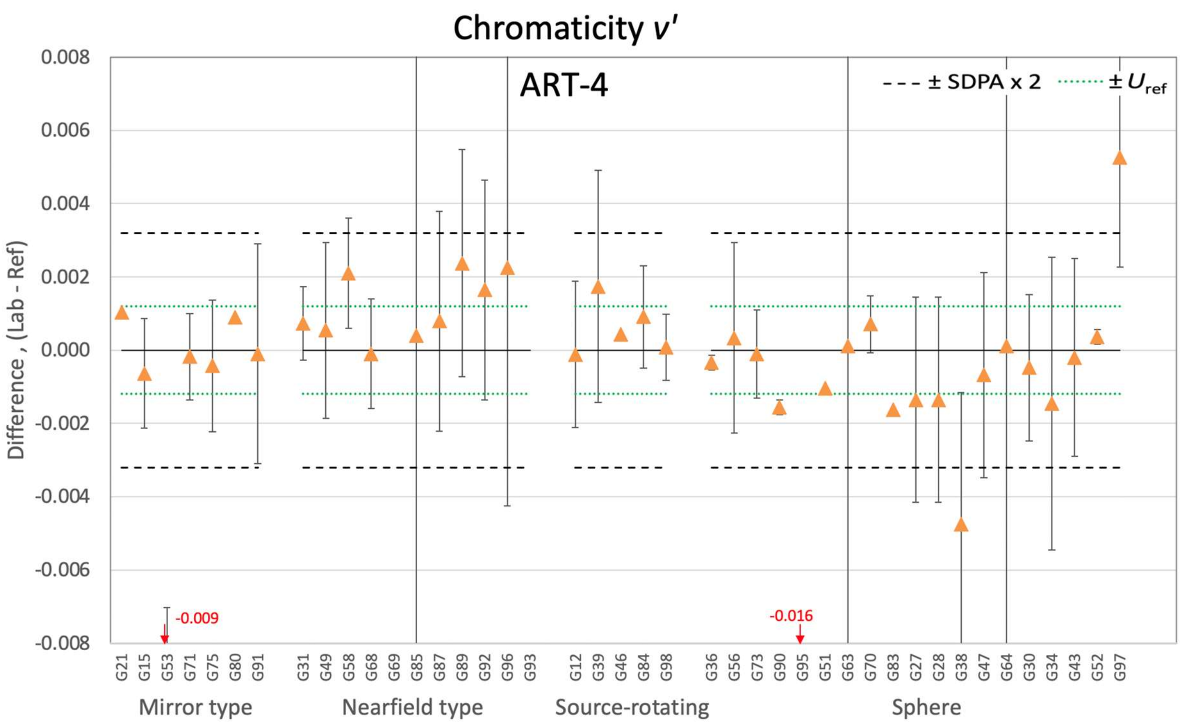

Figure 7-103. Differences of chromaticity v′ for ART-4 by goniophotometer type and sphere

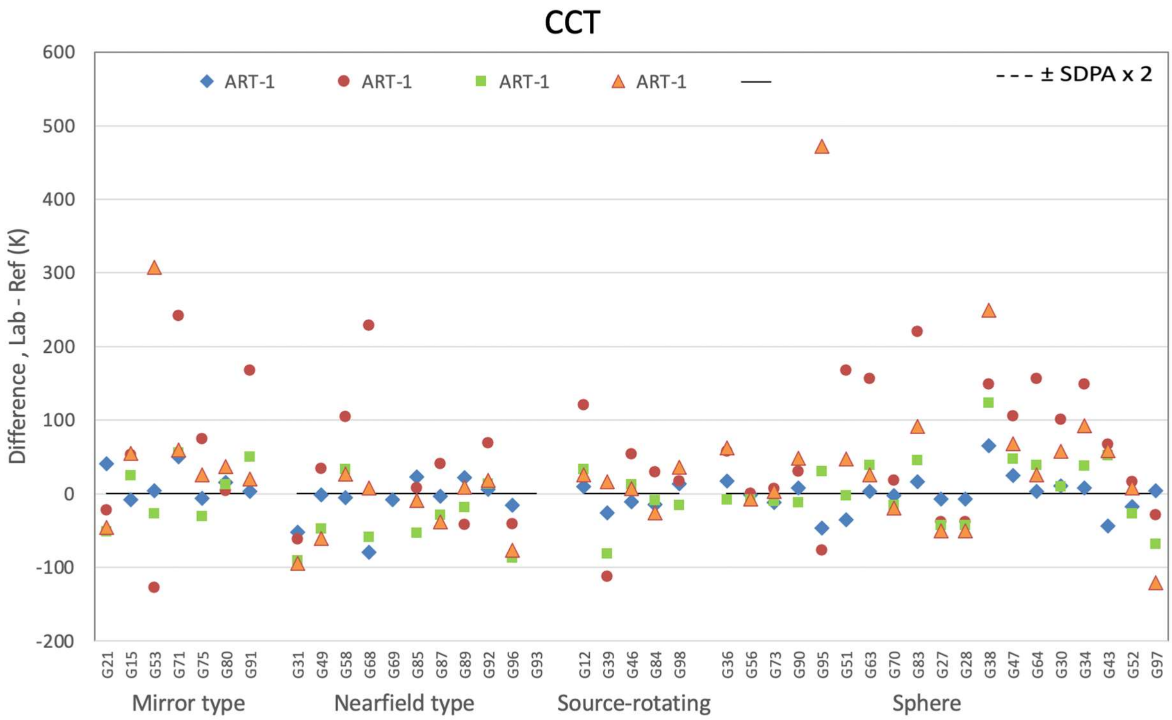

Figure 7-104. Differences of CCT for all artefacts by goniophotometer type and sphere

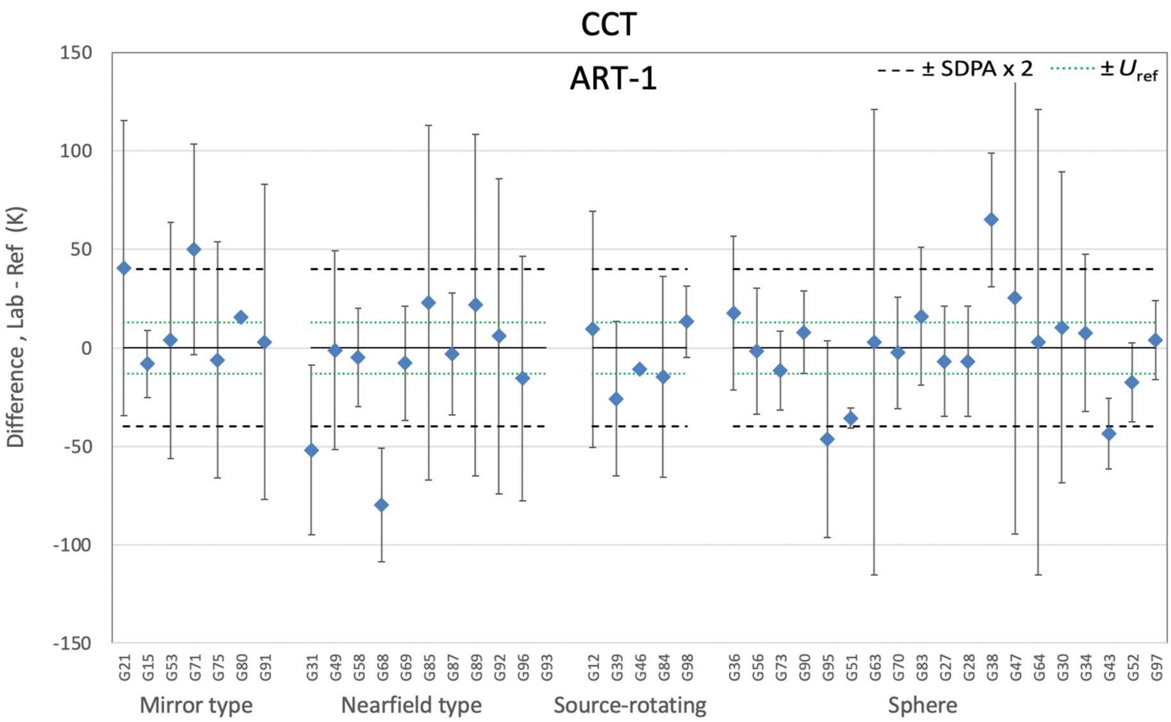

Figure 7-105. Differences of CCT for ART-1 by goniophotometer type and sphere

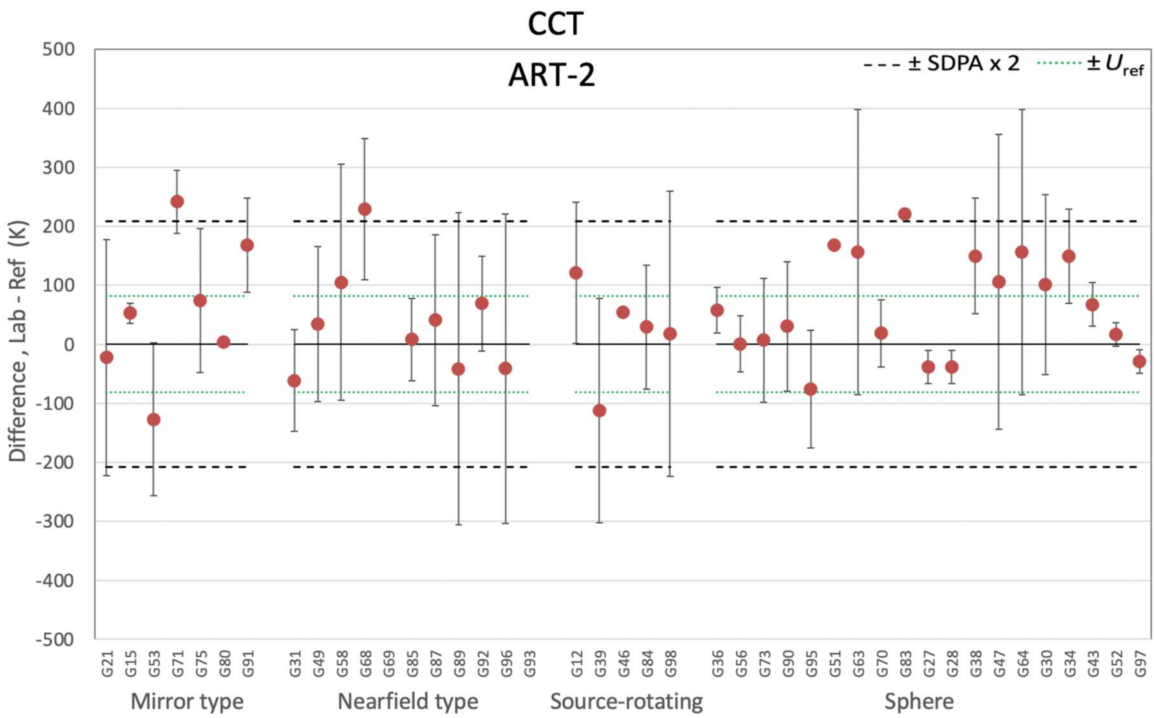

Figure 7-106. Differences of CCT for ART-2 by goniophotometer type and sphere

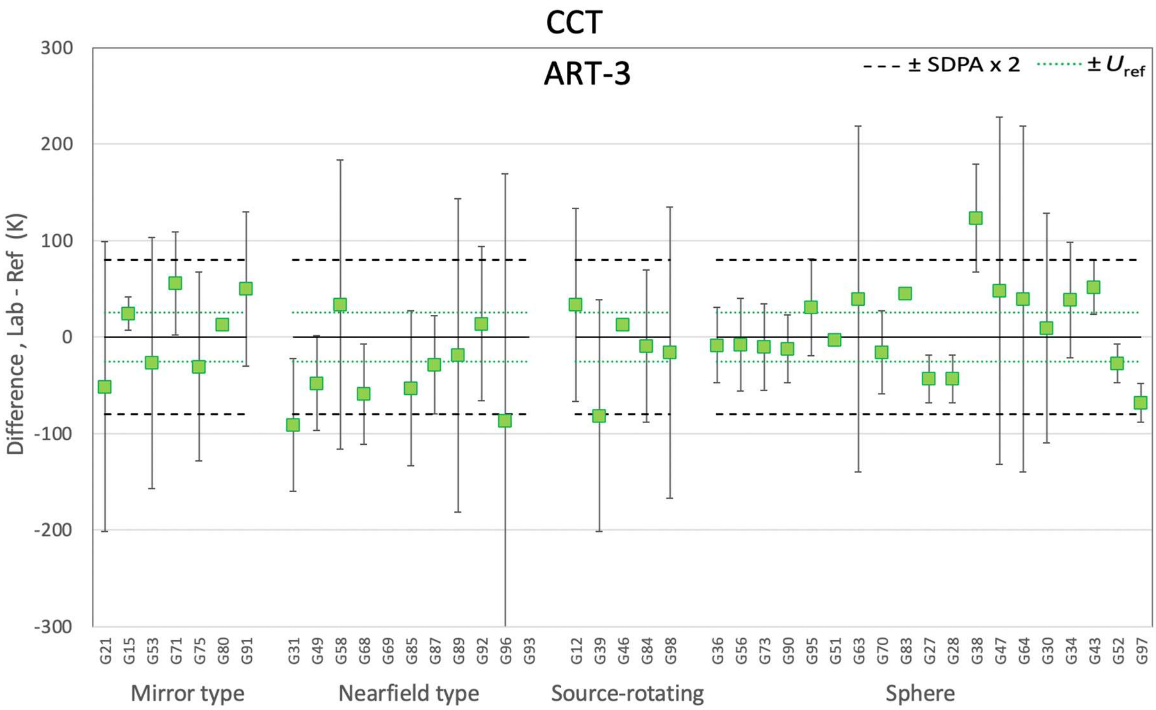

Figure 7-107. Differences of CCT for ART-3 by goniophotometer type and sphere

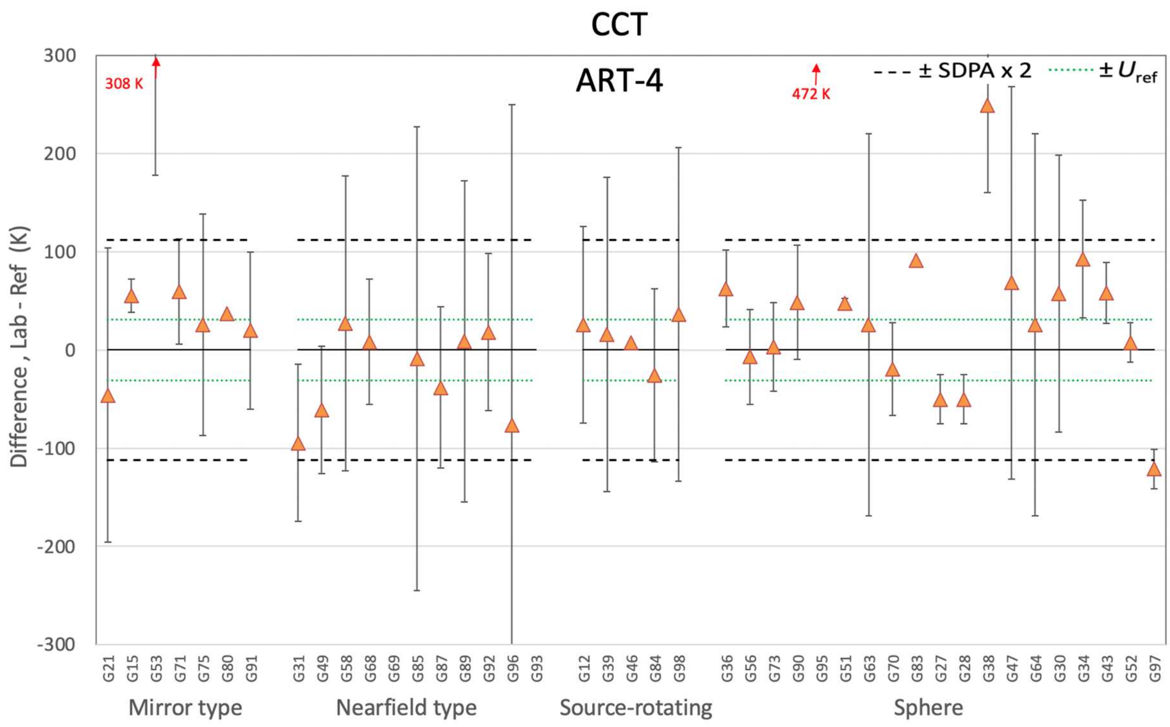

Figure 7-108. Differences of CCT for ART-4 by goniophotometer type and sphere

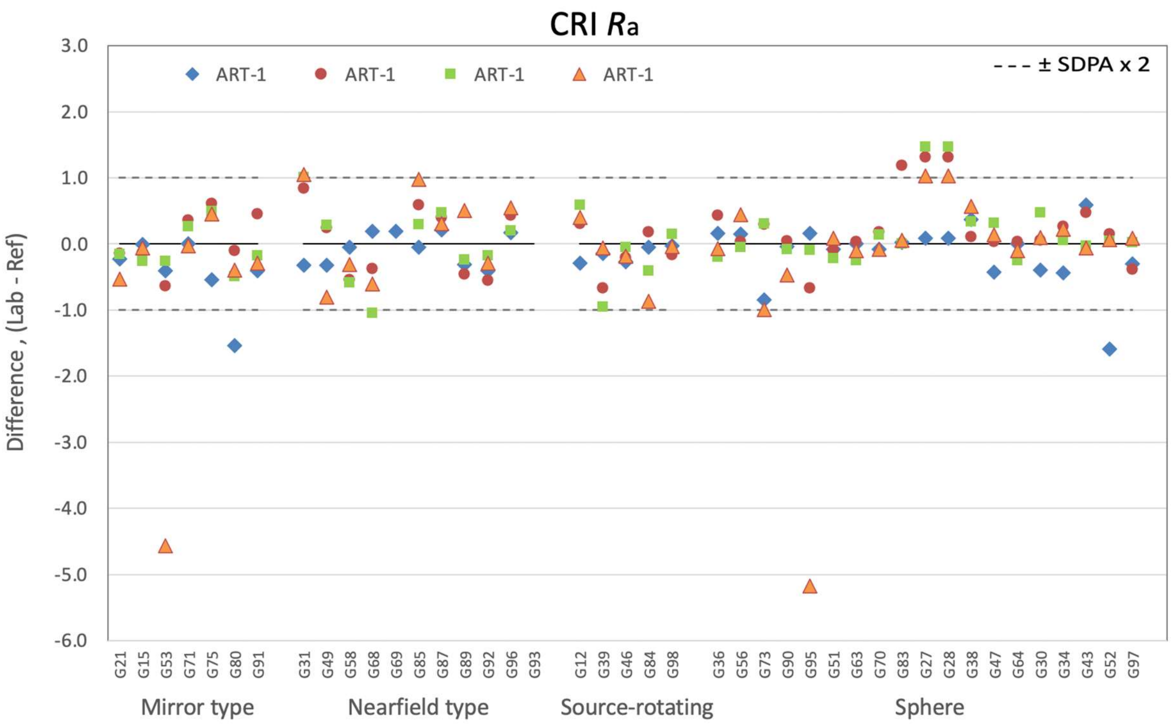

Figure 7-109. Differences of CRI R_a for all artefacts by goniophotometer type and sphere

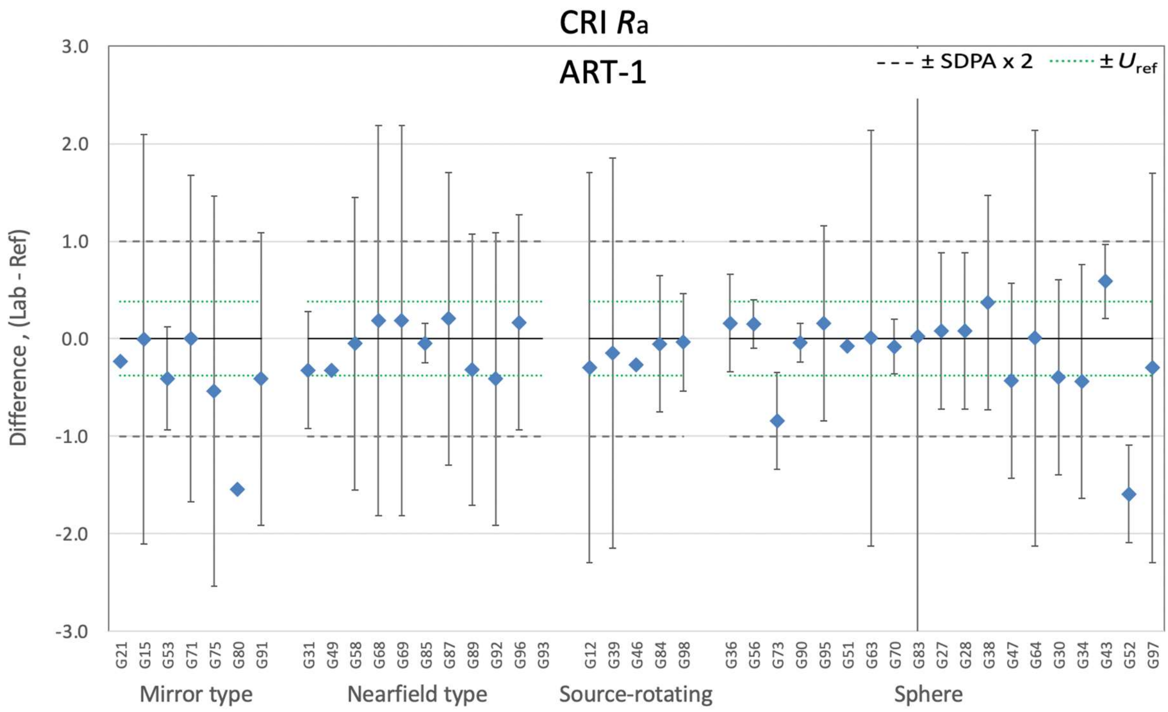

Figure 7-110. Differences of CRI R_a for ART-1 by goniophotometer type and sphere

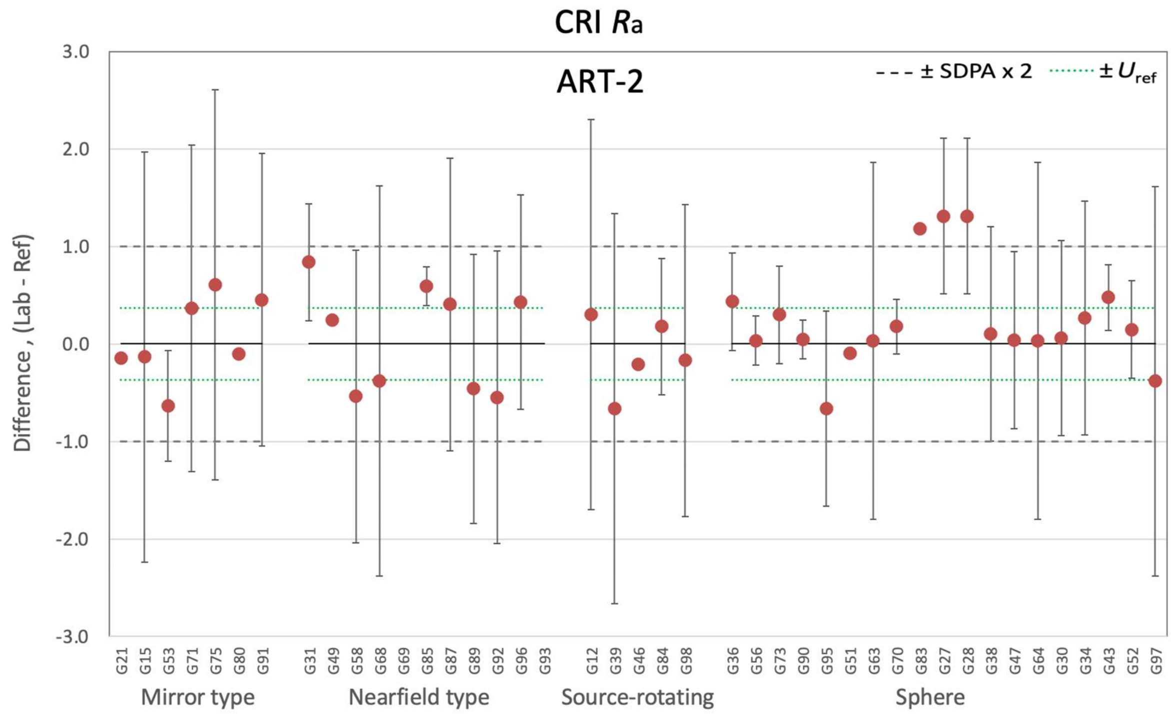

Figure 7-111. Differences of CRI R_a for ART-2 by goniophotometer type and sphere

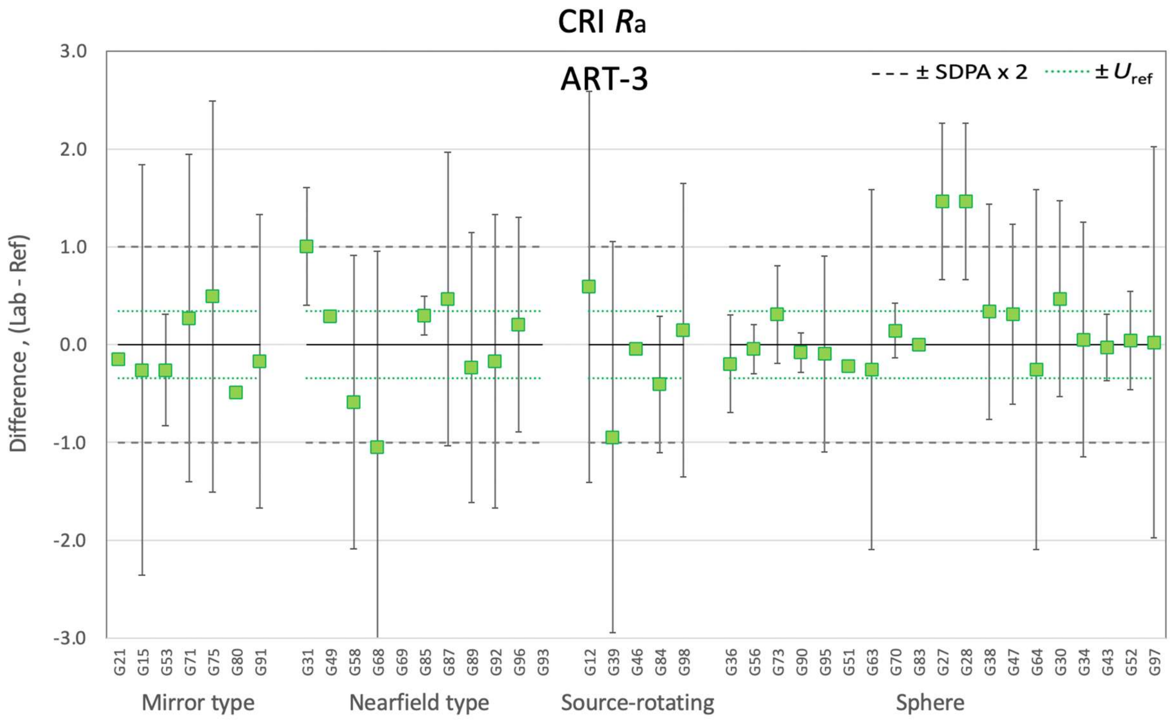

Figure 7-112. Differences of CRI R_a for ART-3 by goniophotometer type and sphere

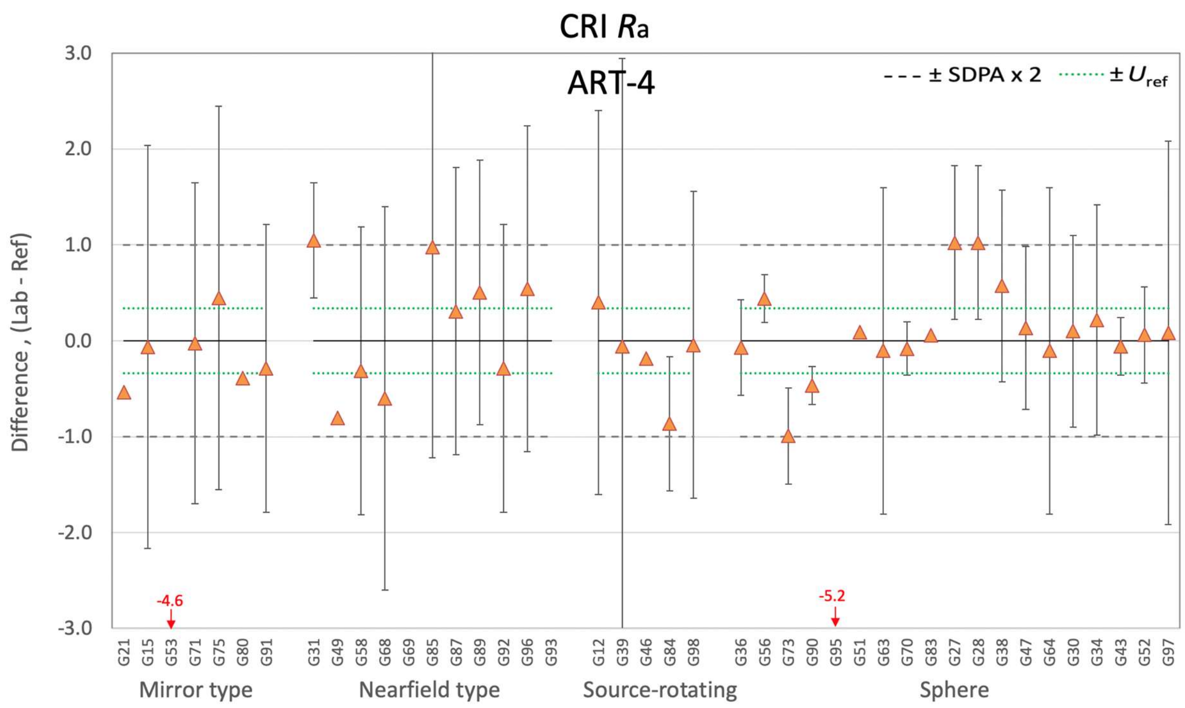

Figure 7-113. Differences of CRI R_a for ART-4 by goniophotometer type and sphere

7.3.3 Goniophotometric quantities

This section presents the graphs for the results of goniophotometric quantities (Table 3-2) sorted by the types of goniophotometer. The results of luminous intensity distributions are presented separately in section 7.5.

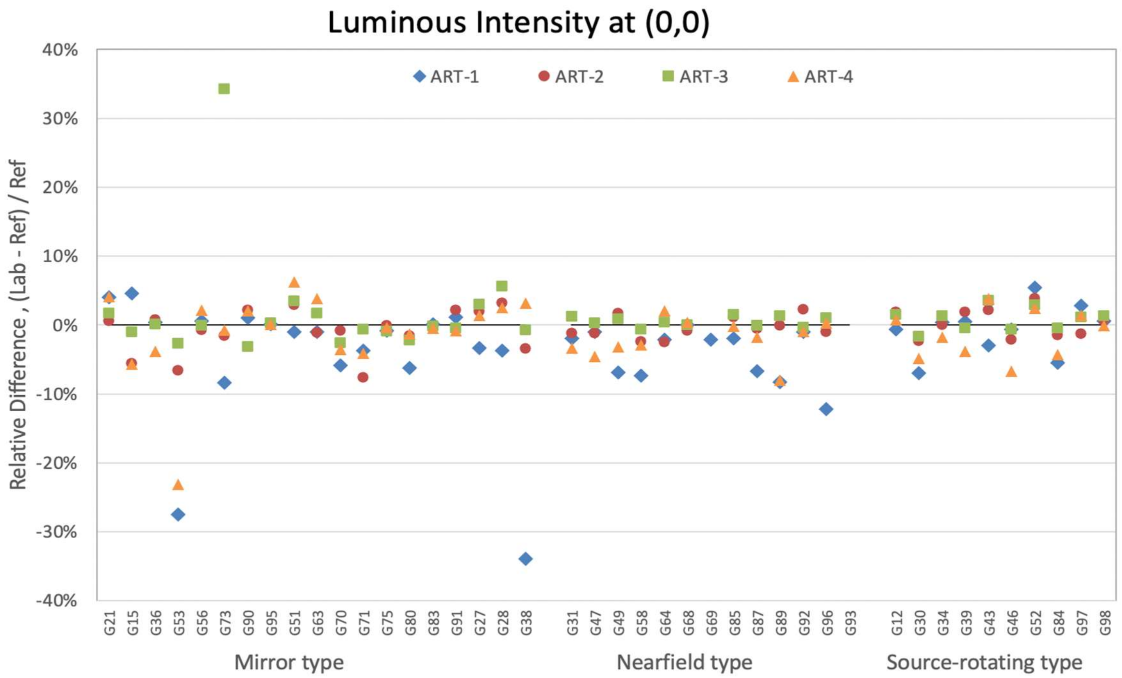

Figure 7-114. Relative differences of luminous intensity at (0,0) for all artefacts by goniophotometer type

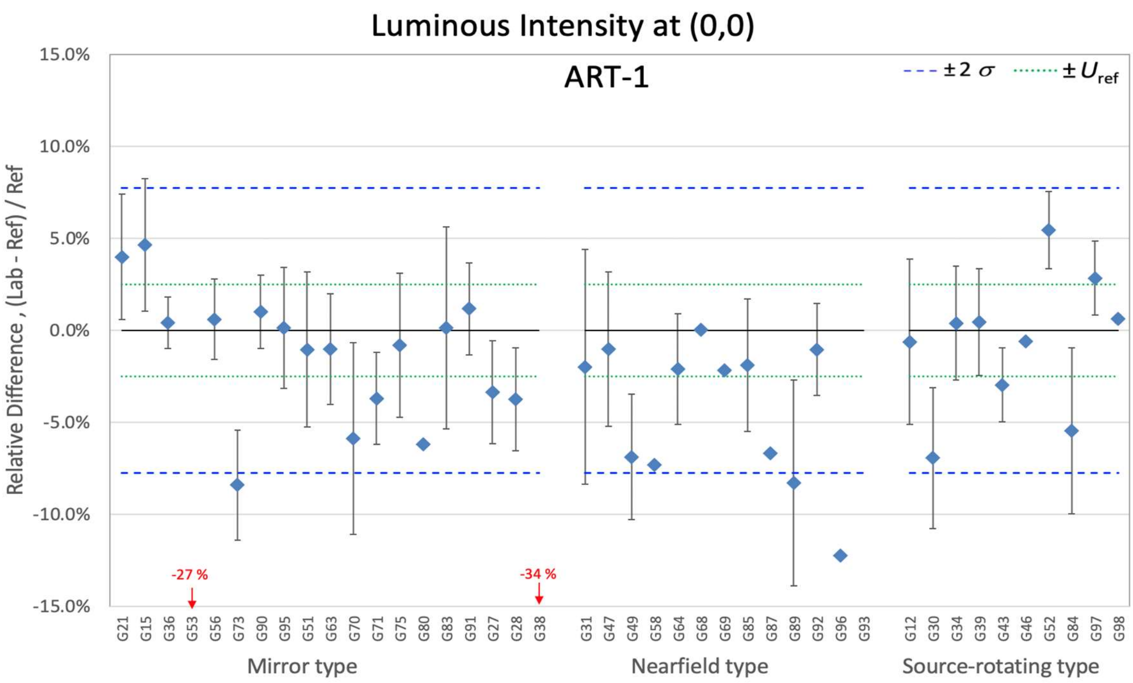

Figure 7-115. Relative differences of luminous intensity at (0,0) for ART-1 by goniophotometer type

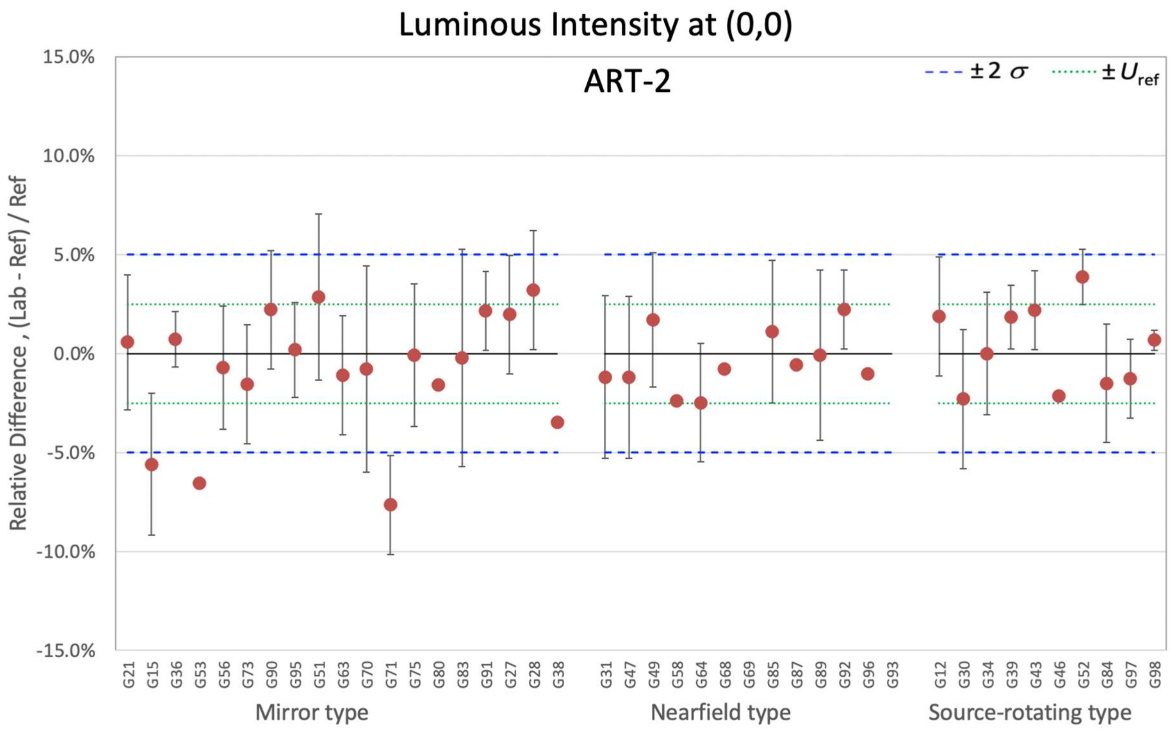

Figure 7-116. Relative differences of luminous intensity at (0,0) for ART-2 by goniophotometer type

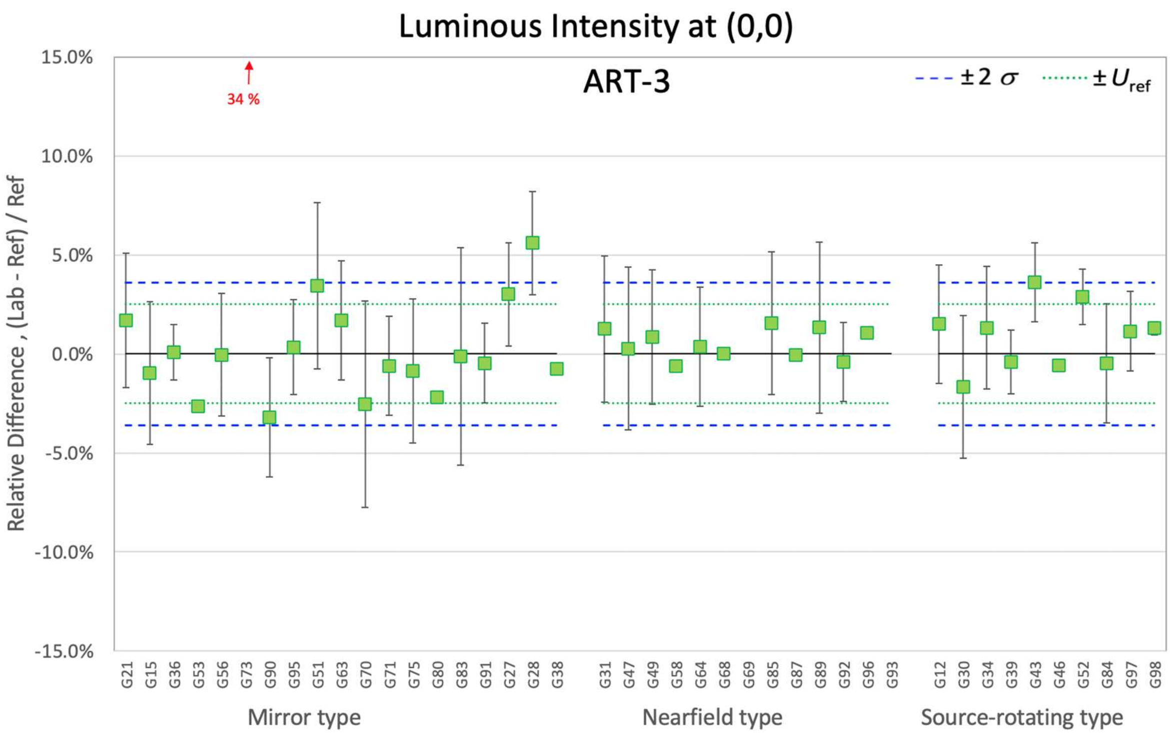

Figure 7-117. Relative differences of luminous intensity at (0,0) for ART-3 by goniophotometer type

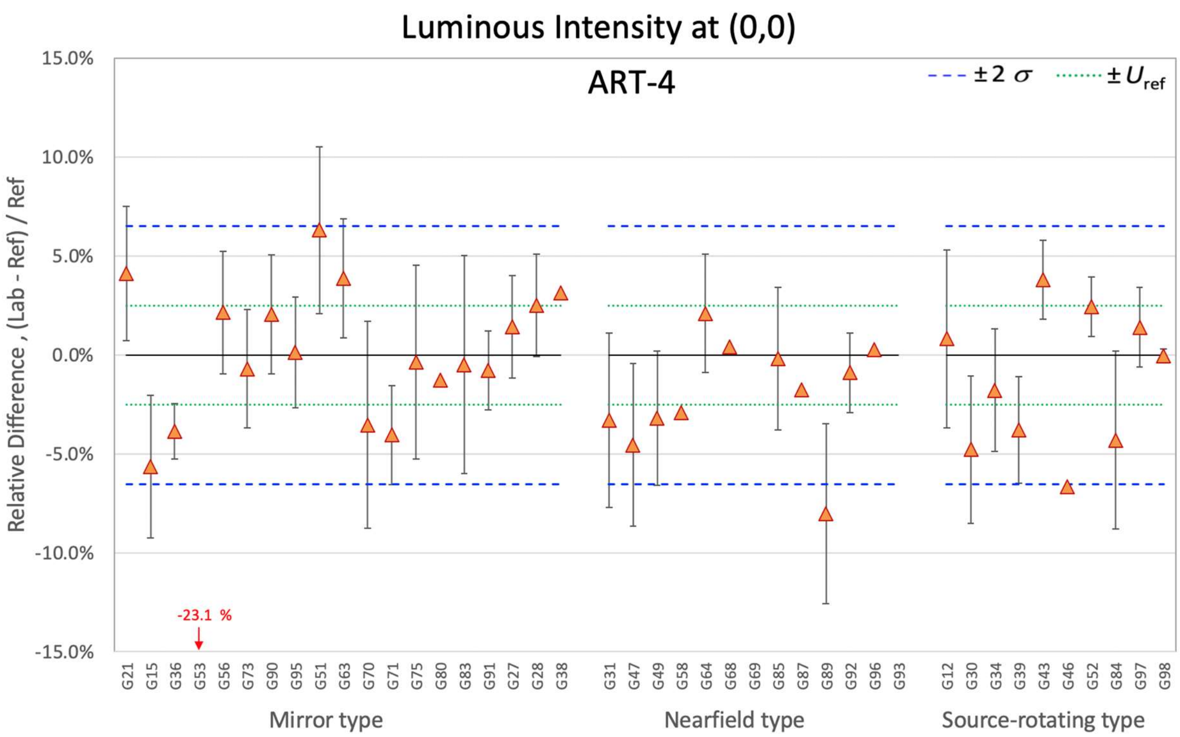

Figure 7-118. Relative differences of luminous intensity at (0,0) for ART-4 by goniophotometer type

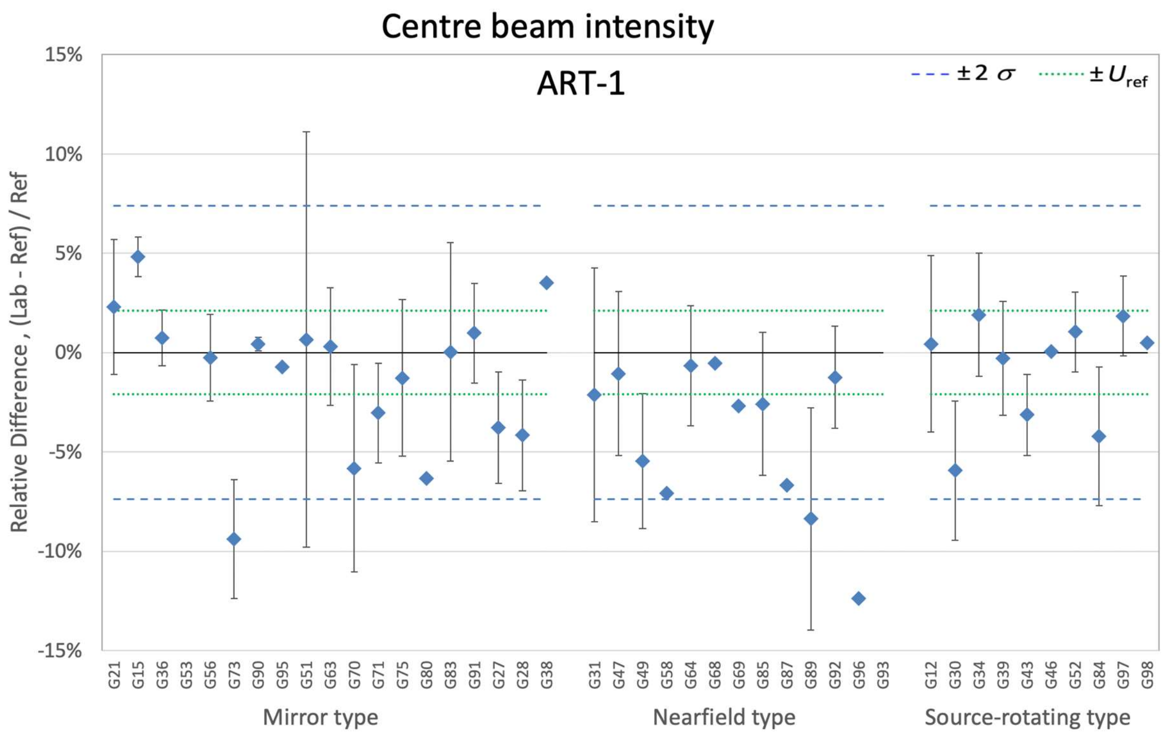

Figure 7-119. Relative differences of centre beam intensity for ART-1 by goniophotometer type

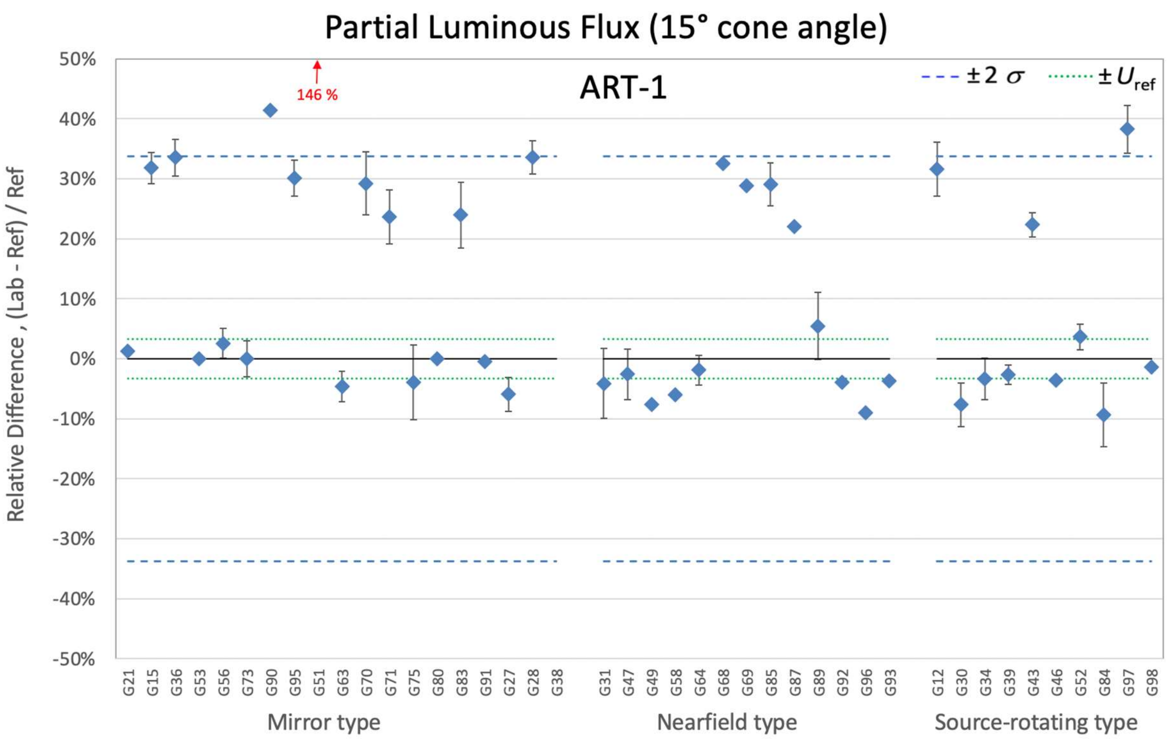

Figure 7-120. Relative differences of partial luminous flux for ART-1 by goniophotometer type

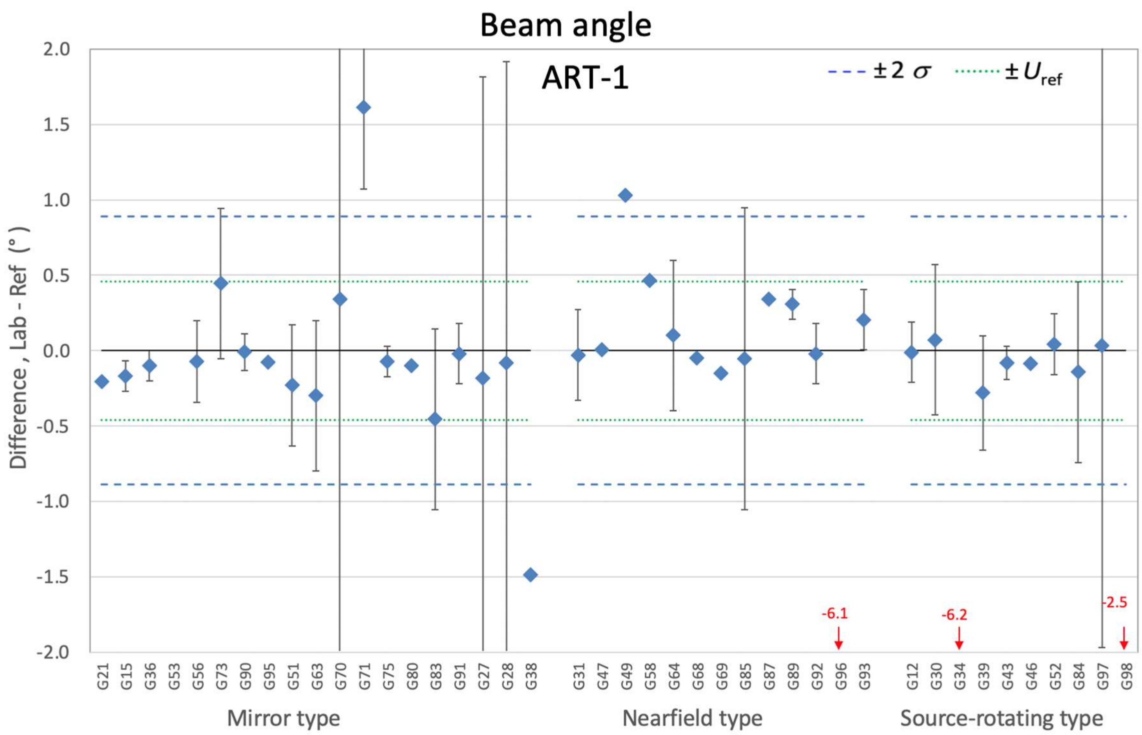

Figure 7-121. Differences of beam angle for ART-1 by goniophotometer type

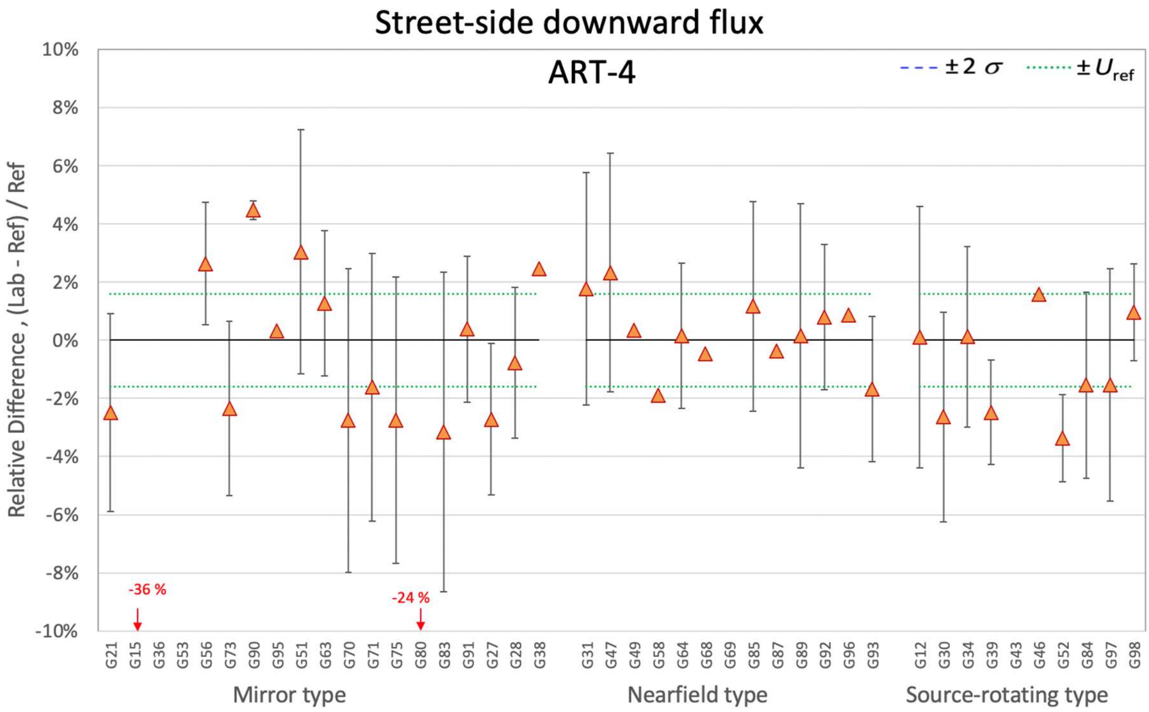

Figure 7-122. Relative differences of Street-side downward flux for ART-4 by goniophotometer type

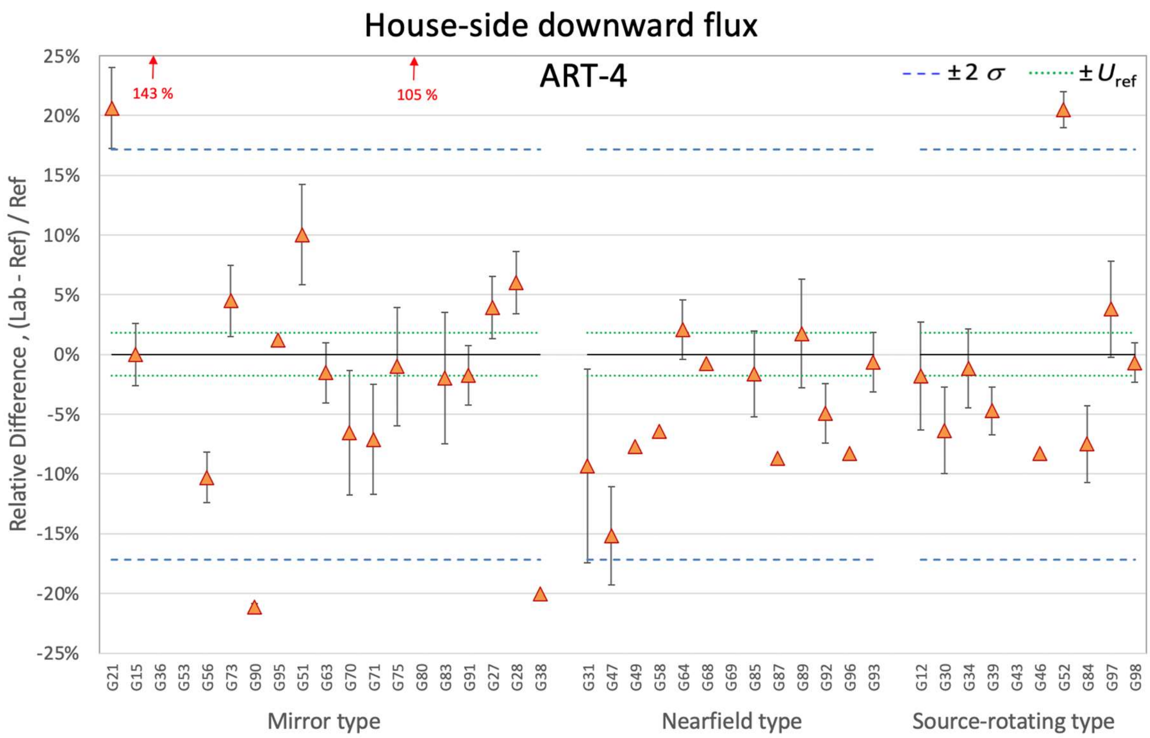

Figure 7-123. Relative differences of House-side downward flux for ART-4 by goniophotometer type

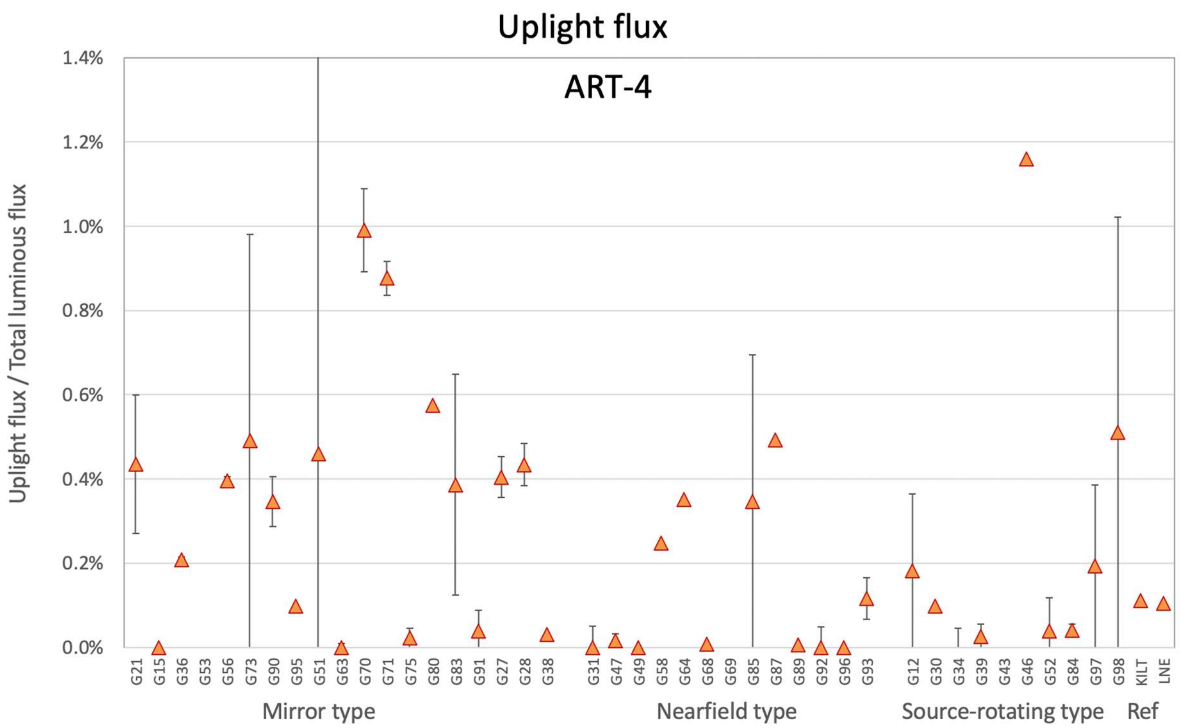

Figure 7-124. Uplight flux relative to total luminous flux for ART-4 by goniophotometer type

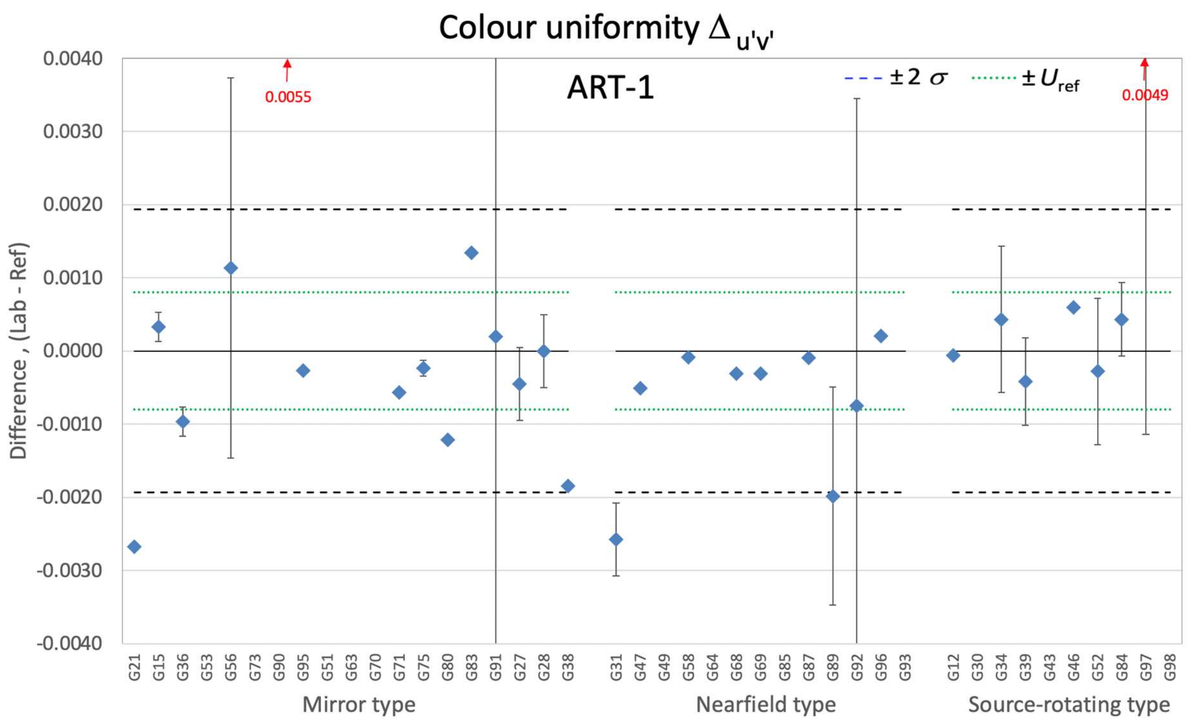

Figure 7-125. Differences of colour uniformity for ART-1 by goniophotometer type

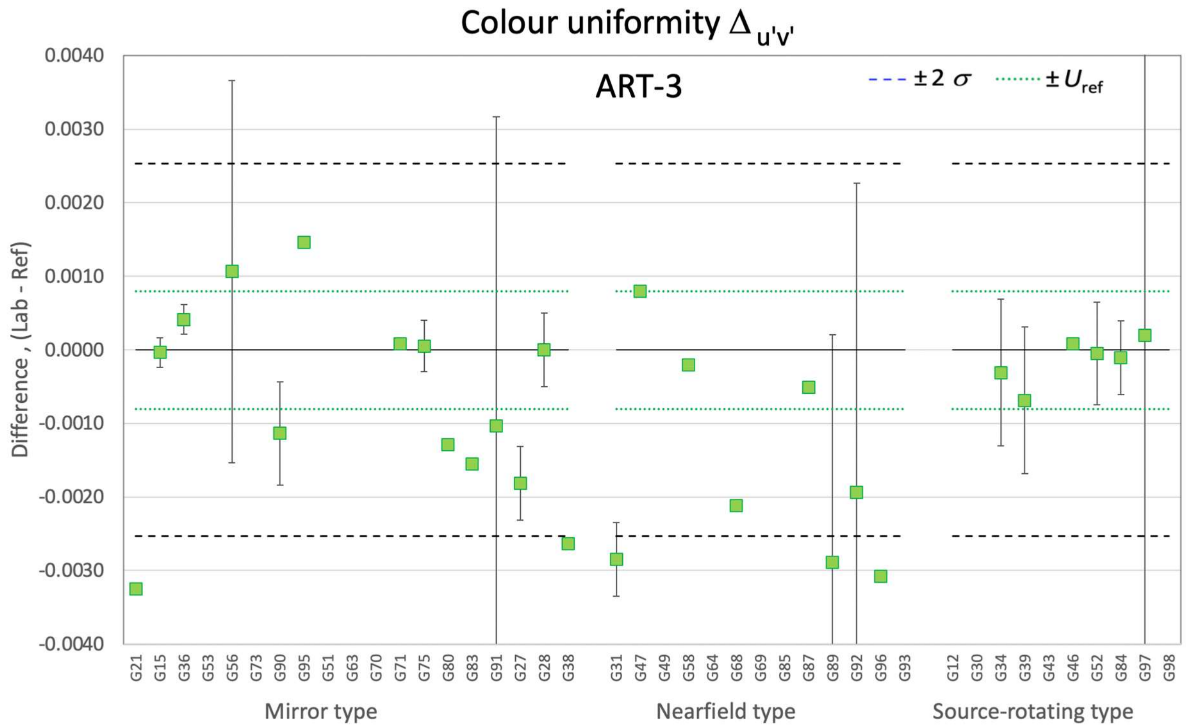

Figure 7-126. Differences of colour uniformity for ART-3 by goniophotometer types

7.4 Analysis of instrument type comparisons

The data presented in section 7.3 were analysed to evaluate equivalence between the instrument types. The graphs presented in this section show the average deviations from the reference value (bias) and standard deviations of the participants' results for each instrument type (excluding outliers marked in the graphs in section 7.3), for each artefact and for each measurement quantity.

Examples are shown in Figure 7-127 (a) and (b) below. The deviations from the reference value (biases) as shown in Figure 7-127 (a) may be caused by some systematic error components common among many participants in the group and/or some deviations in the measurements of the reference laboratory.

The green dotted lines in Figure 7-127 (a) show the uncertainty of the reference value (expanded uncertainty, k=2) (see Ref. [7] for the details). An average deviation (bias in the results) is considered significant if it is larger than the uncertainty of the reference value. The uncertainty may be different for each artefact. Generally, if a bias is within the uncertainty of reference value, it is considered not significant. The dashed line in Figure 7-127 (b) is the SDPA value. If the standard deviation is about this level or less, the measurement variation of the result is considered reasonable. These apply to all the graphs for other quantities presented in this subsection.

7.4.1 Total luminous flux and luminous efficacy

Figure 7-127 (a) presents the average deviations of total luminous flux for the different instrument types, which are shown as mostly insignificant. The total luminous flux results overall are considered equivalent among the three instrument types. ART-1 with near-field type, however, shows a larger deviation than other types, which indicates some larger uncertainty of near-field type for a source with a very narrow beam intensity distribution. Figure 7-127 (b) shows the standard deviations of these results, which, on the other hand, shows less variation for near-field type for ART-2, 3 and 4. This may be due to the fact that 10 out of the 12 near-field goniophotometers in this comparison are from the same manufacturer and the calibration traceability for these 10 instruments is probably the same, which may be contributing to the smaller variations in results. Note that, a cosine-corrected illuminance measuring head is used for total luminous flux measurement (illuminance integration) in these near field goniophotometers, and these results reflect the operation in this measurement mode.

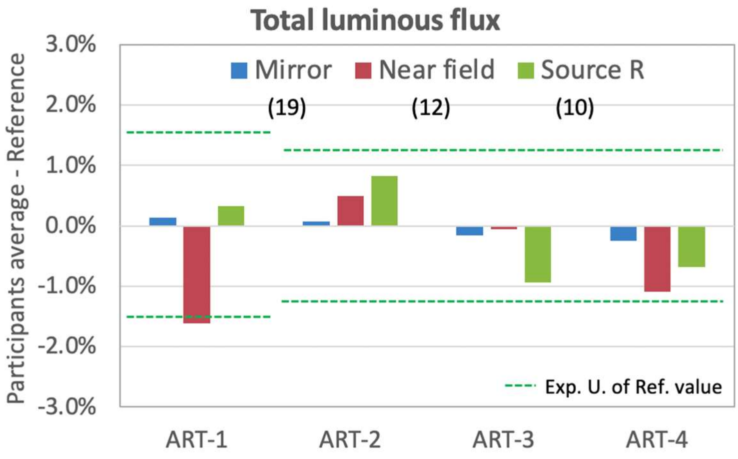

(a) Average deviations

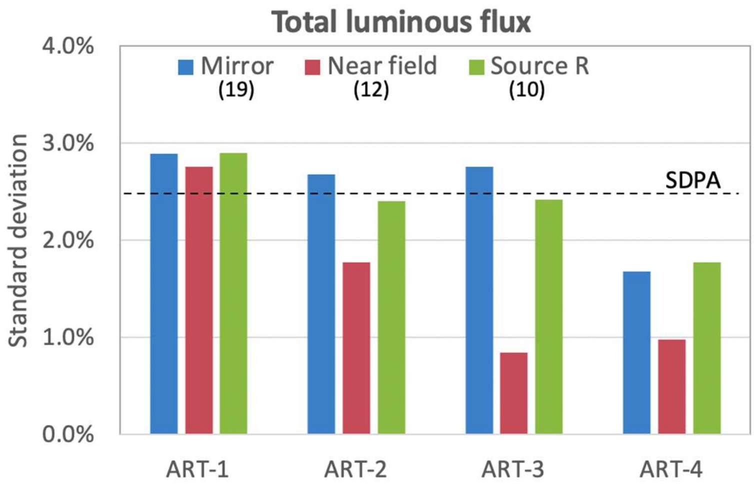

(b) Standard deviations

Figure 7-127. Average deviations from the reference value (a) and the standard deviations (b) of total luminous flux results for each instrument type

Figure 7-128 (a) and (b) show the average deviations and the standard deviations of luminous efficacy comparing each instrument type. This result reflects the results of total luminous flux and active power. The variations of ART-1 (Figure 7-128 (b)) are large for all instrument types, affected by large variations in measured power.

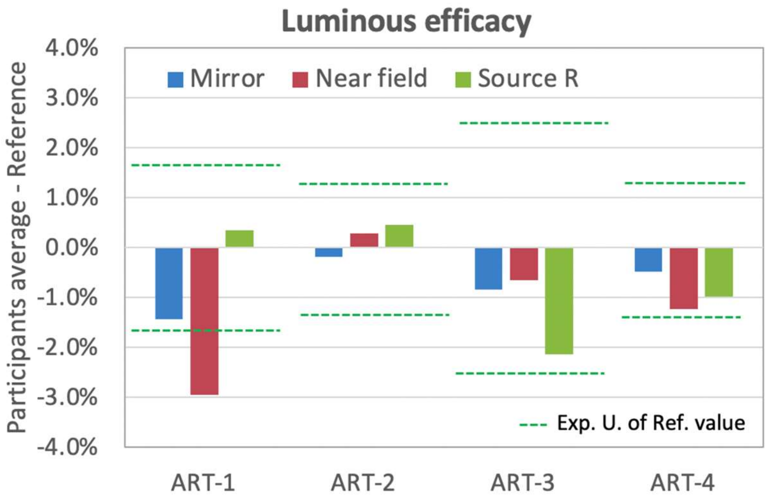

(a) Average deviations

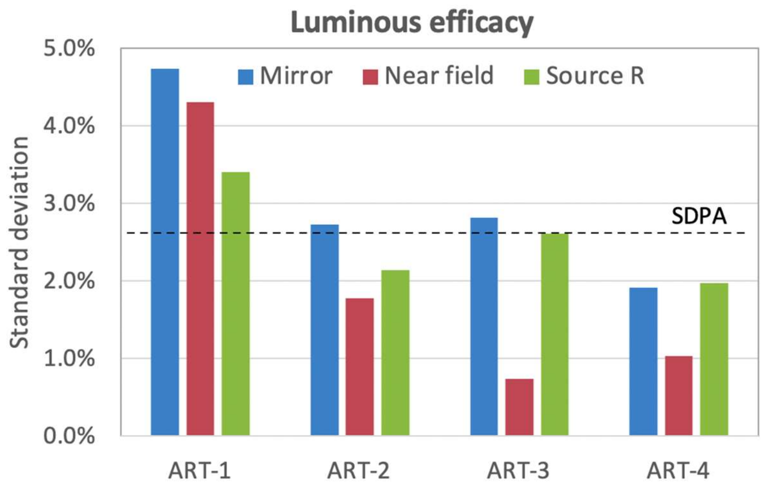

(b) Standard deviations

Figure 7-128. Average deviations from the reference value (a) and the standard deviations (b) of luminous efficacy for each instrument type

7.4.2 Electrical quantities

Figure 7-129, Figure 7-130, and Figure 7-131 show the average deviations and standard deviations of RMS current, active power, and power factor, respectively, comparing different goniophotometer types. Significant deviations and variations are shown for the results of ART-1 for both RMS current and active power, while ART-2 shows much smaller variations for all instrument types, the reasons for which are discussed in sections 7.2.2 and 7.2.3. The power factor for ART-3 shows significantly large variation, which is discussed in 7.2.5.

Some notable differences among different instrument types are observed on some artefacts. For example, RMS current variation with source-rotating type for ART-3 (Figure 7-129 (b)) is much higher than others, while this type shows the smallest deviation and variation for ART-1. Any effects that could contribute to electrical quantities by different goniophotometer types could be the operating orientation of the artefacts (source-rotating type) or differences in the cable length between power supply and the artefact on the goniophotometer. One participant using a source-rotating type goniophotometer reported that the effects of operating orientation were insignificant (+ 0.25 % for ART-1, + 0.2 % for ART-2, - 0.5 % for ART-3, and 0.0 % for ART-4 in total luminous flux).

Figure 7-132 shows the average lengths of the cables used in participants' goniophotometers. The average length for the source-rotating type is shorter than the other two types. However, this data does not explain the variations in these results. It is considered that the variations in these electrical measurements are much related to artefacts' specific electrical characteristics and the variations in participants' electrical instruments rather than goniophotometer types.

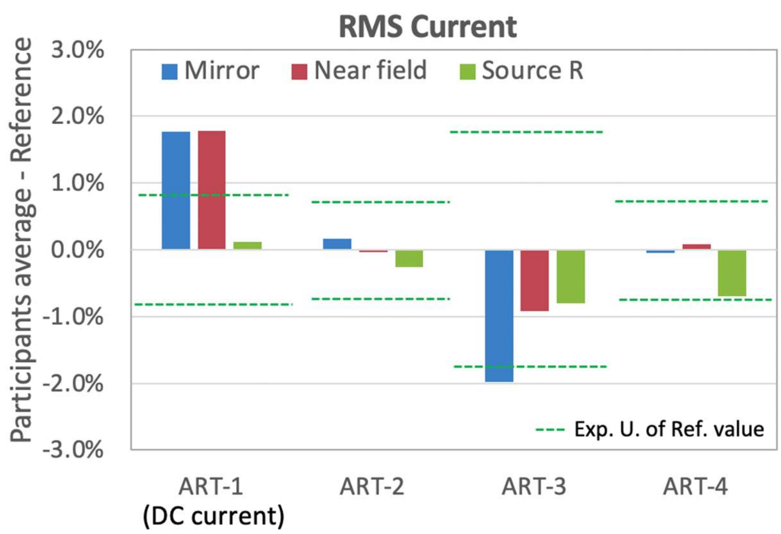

(a) Average deviations

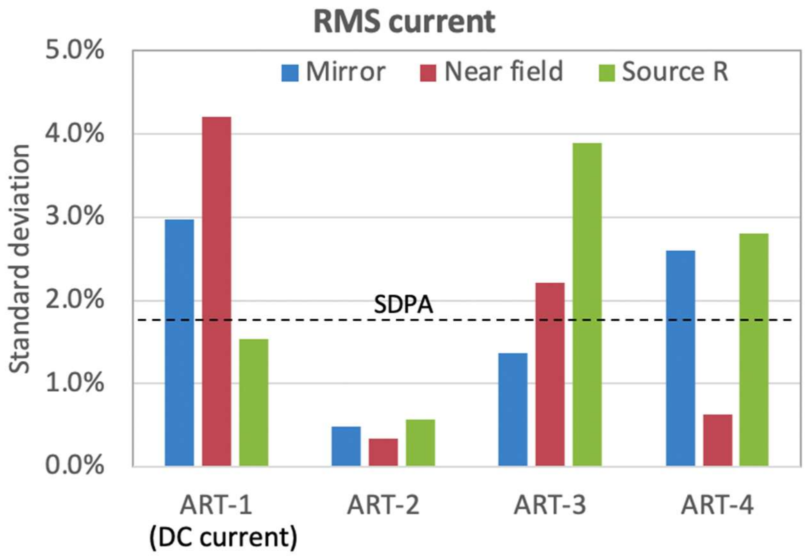

(b) Standard deviations

Figure 7-129. Average deviations from the reference value (a) and the standard deviations (b) of RMS current results for each instrument type

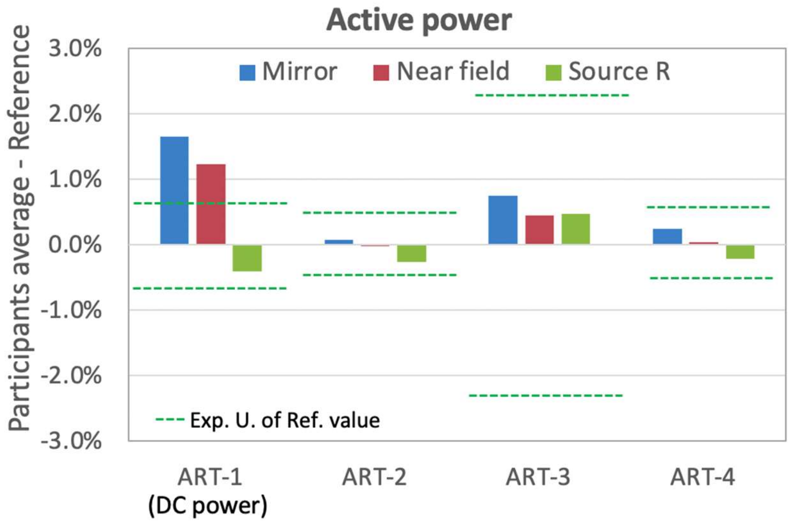

(a) Average deviations

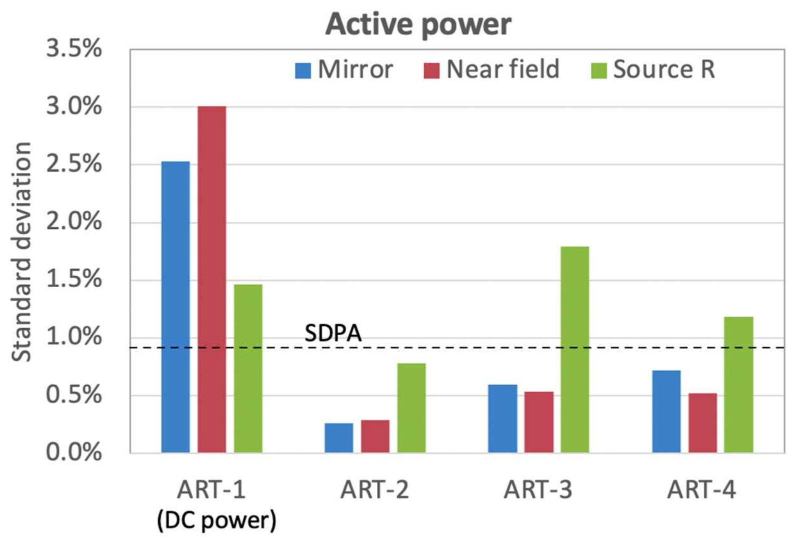

(b) Standard deviations

Figure 7-130 Average deviations from the reference value (a) and the standard deviations (b) of active power results for each instrument type

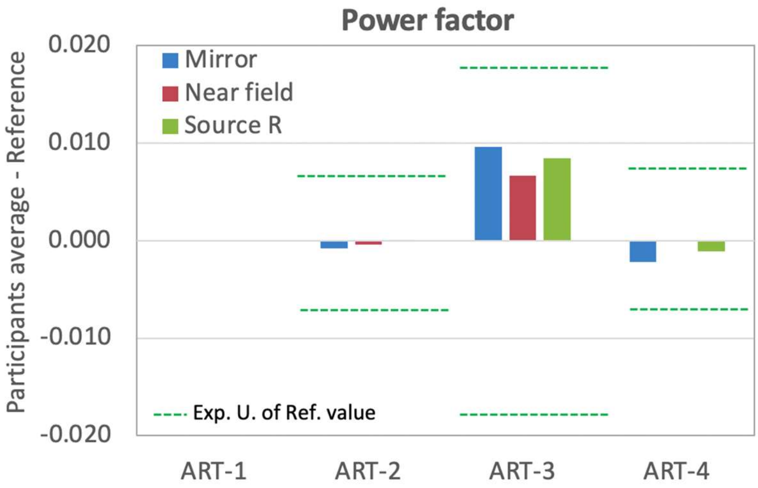

(a) Average deviations

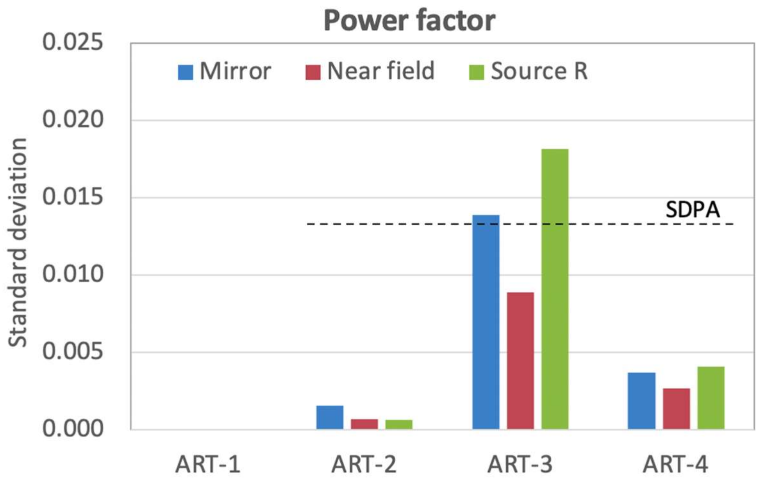

(b) Standard deviations

Figure 7-131 Average deviations from the reference value (a) and the standard deviations (b) of power factor for each instrument type

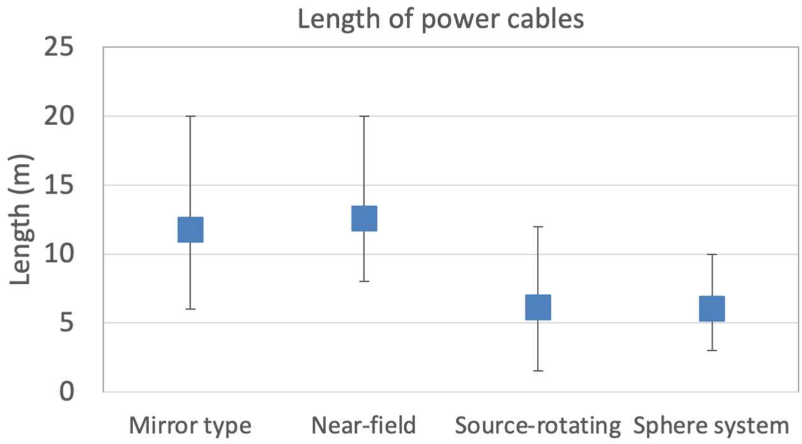

Figure 7-132. Average length of power cables between power supply and artefacts on the goniophotometer in all participants' labs

7.4.3 Chromaticity coordinates *u'*, *v'*

Figure 7-133 and Figure 7-134 show comparisons of instrument types for chromaticity *u*', *v*', including sphere systems. In this case, goniophotometers of all types operated as gonio-spectroradiometers and sphere systems operated as sphere-spectroradiometers. The numbers in parenthesis in the figure shows the number of instruments of each type.

The average deviation graphs show some biases, which vary with different instrument types and artefacts, but in most cases they are within or close to the uncertainties of the reference value, and not considered significant. In some cases the biases, though not significant, appear in one direction for all instrument types (e.g., ART-2 for both *u', v'*), which could be due to deviation of the reference laboratory's measurement, but the cause is unknown.

The standard deviations in these results are also mostly within or close to SDPA value and appear to be reasonable. Thus, no significant differences among different goniophotometer types are identified. However, Figure 7-133 (b) shows larger variations of sphere system for ART-4. Since ART-4 is a large-size luminaire with dark colour surfaces, there may be larger uncertainties due to significant self-absorption in the sphere that affected results spectrally and cannot be fully corrected even after self-absorption correction.

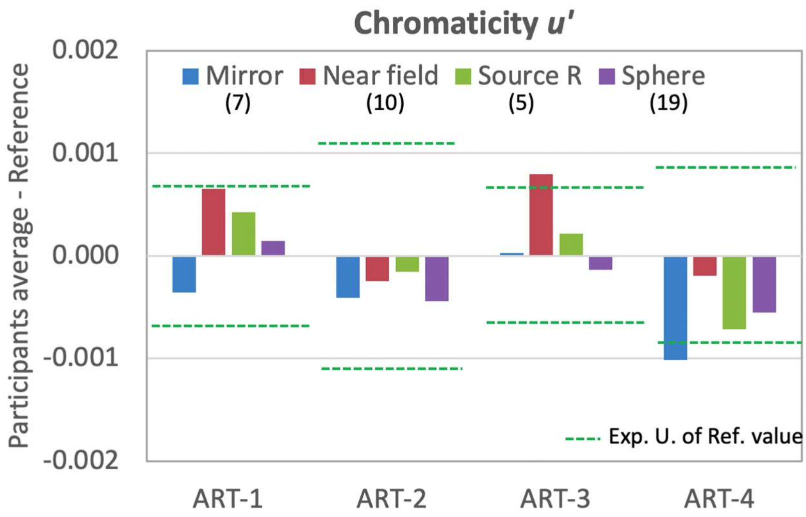

(a) Average deviations

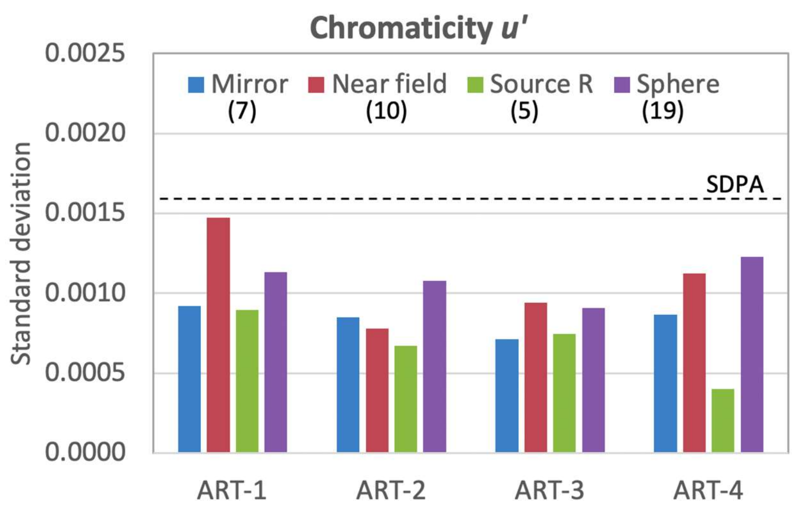

(b) Standard deviations

Figure 7-133. Average deviations from the reference value (a) and the standard deviations (b) of chromaticity u' results for each instrument type

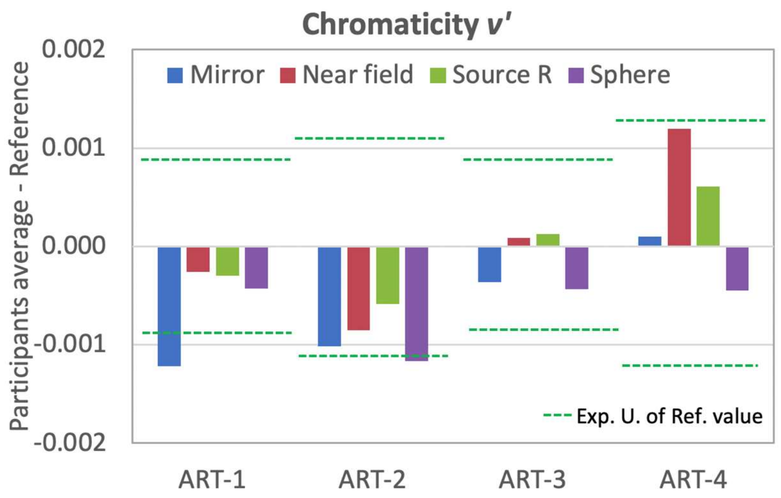

(a) Average deviations

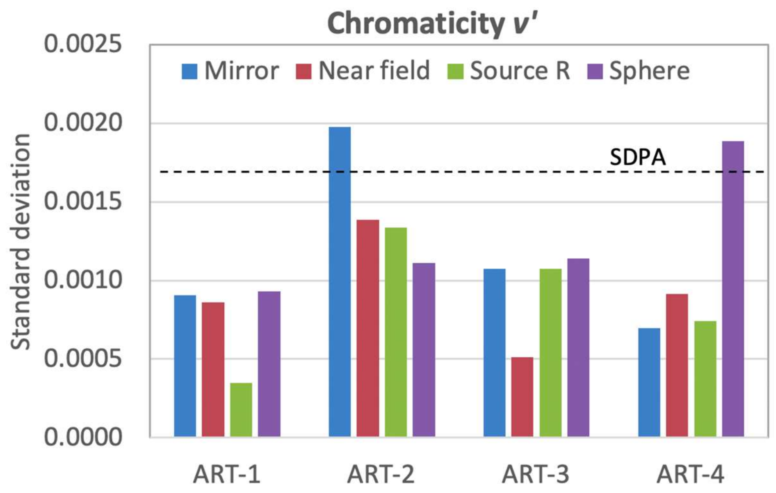

(b) Standard deviations

Figure 7-134. Average deviations from the reference value (a) and the standard deviations (b) of chromaticity v' results for each instrument type

To provide further comparisons between gonio systems and sphere systems, the average deviations and the standard deviations of the three gonio types were averaged (weighted by number of instruments) and presented in Figure 7-135 as comparisons between gonio systems and sphere systems. The differences are not significant, but the variations tend to be larger for sphere systems, especially for ART-4 as observed in Figure 7-135 (b).

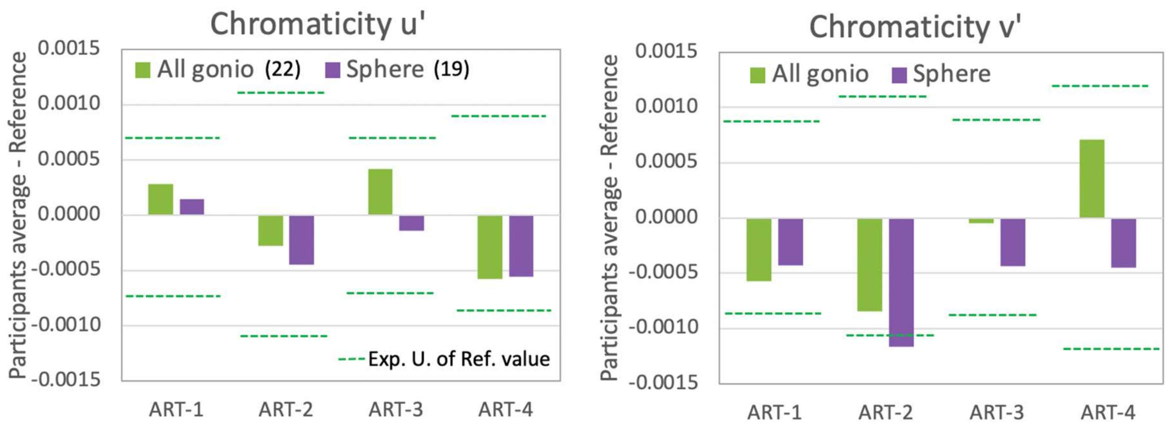

(a) Average deviations

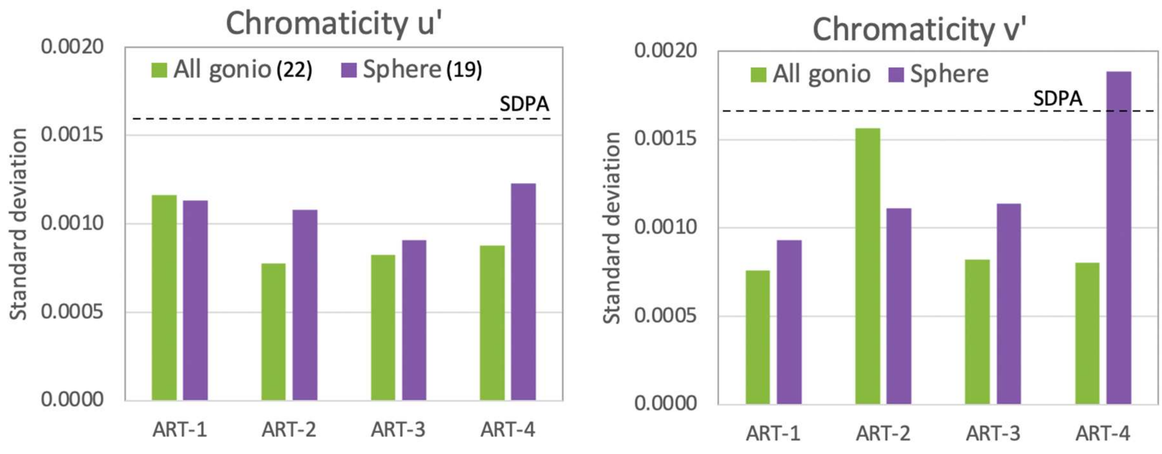

(b) Standard deviations

Figure 7-135. Average deviations from the reference value (a) and the standard deviations (b) of chromaticity results for sphere and all goniophotometers

7.4.4 CCT and CRI R_a

Figure 7-136 and Figure 7-137 show comparison of instrument types for CCT and CRI R_a. The results of CCT show that, in most cases, the average deviations appear within the uncertainty of the reference value and the standard deviations appear comparable to the SDPA values for all instrument types, and no notable differences among instrument types were observed.

It is noted that the variation of CCT of ART-4 for sphere systems (Figure 7-136 (b)) appear much larger than the other instrument types, similar to the results of chromaticity *v'*, (Figure 7-143 (b)), the reason for which was discussed in 7.4.3. The one-sided deviations for ART-2 are also consistent with that in *u'*, *v'* results. The results of CRI R_a show reasonable agreement and variations, and no significant differences for any particular instrument type or artefact type were observed.

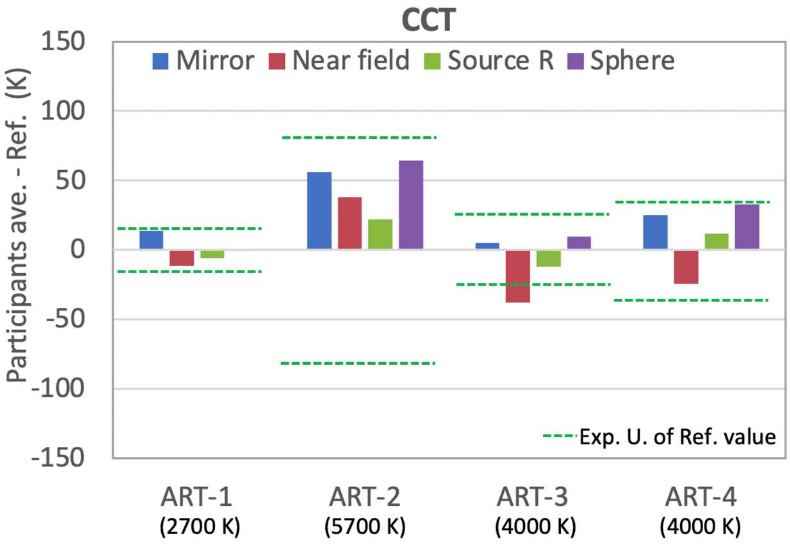

(a) Average deviations

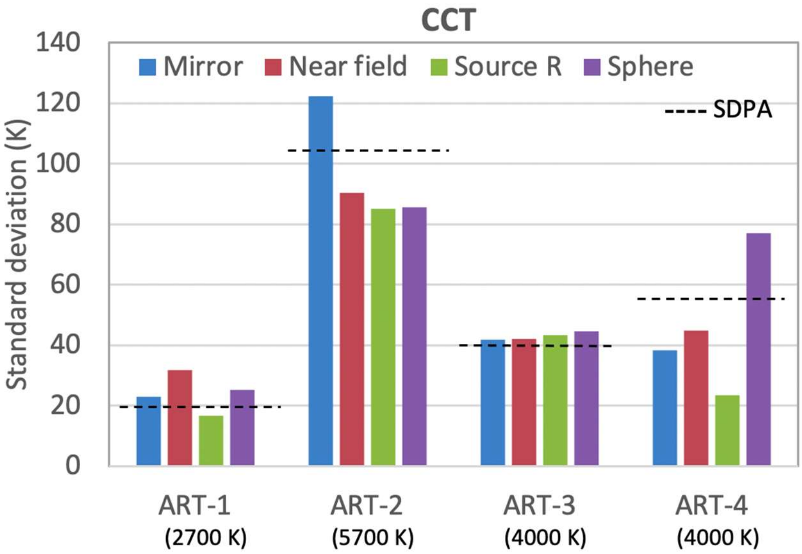

(b) Standard deviations

Figure 7-136. Average deviations from the reference value (a) and the standard deviations (b) of CCT results for sphere and gonio

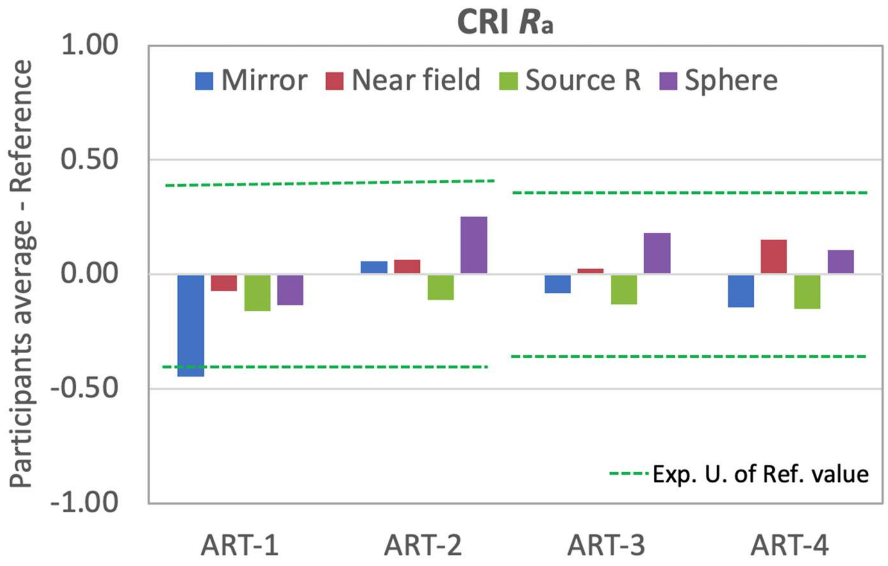

(a) Average deviations

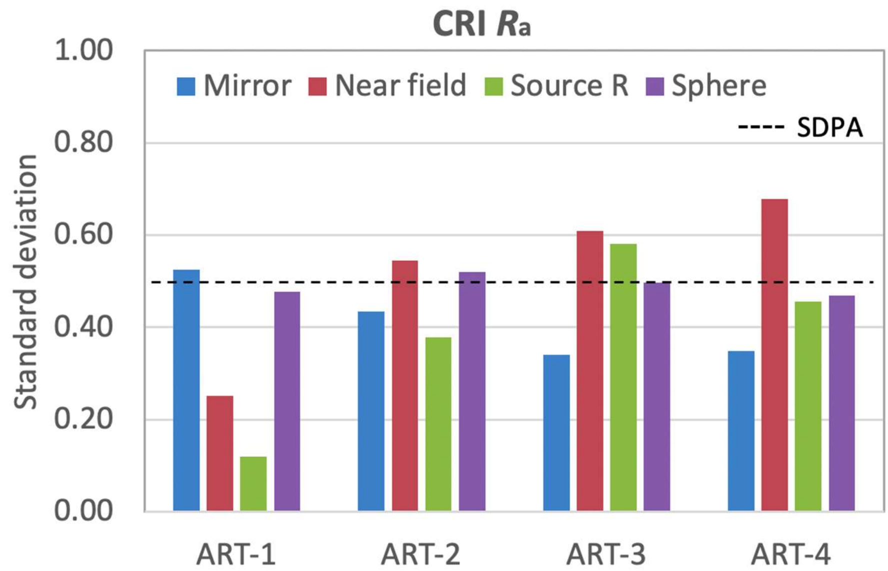

(b) Standard deviations

Figure 7-137. Average deviations from the reference value (a) and the standard deviations (b) of CRI R_a results for sphere and gonio

7.4.5 Luminous intensity at (0,0)

Figure 7-138 (a) and (b) shows the comparison of results for luminous intensity at (0,0). Figure 7-138 (a) shows that, overall, the average deviations are much smaller than the uncertainty of the reference value (except a case with near-field type), while the standard deviations are fairly high.

Figure 7-138 (a) shows a notable bias of near-field type for ART-1 (-3.5 %) and a smaller bias for ART-4 (-2 %), which indicates some negative errors of near-field type for narrow or structured intensity distributions, though this level of uncertainty may be acceptable. These biases follow a similar trend to those in total luminous flux (Figure 7-127 (a)) but the luminous intensity biases were much larger. Figure 7-138 (b), on the other hand, shows smaller variations in near-field type for all artefact types. This result is similar to that of luminous flux (Figure 7-127 (b)), indicating that these smaller variations may be due to the same reason (i.e., possibly related to the traceability of the scale of the instruments). The biases for ART-1 are negative for all instrument types, the reason for which was discussed in section 7.2.9.

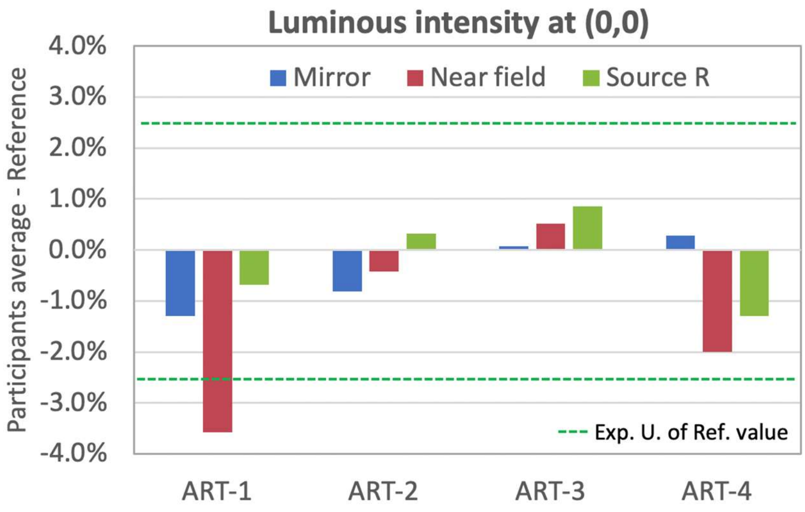

(a) Average deviations

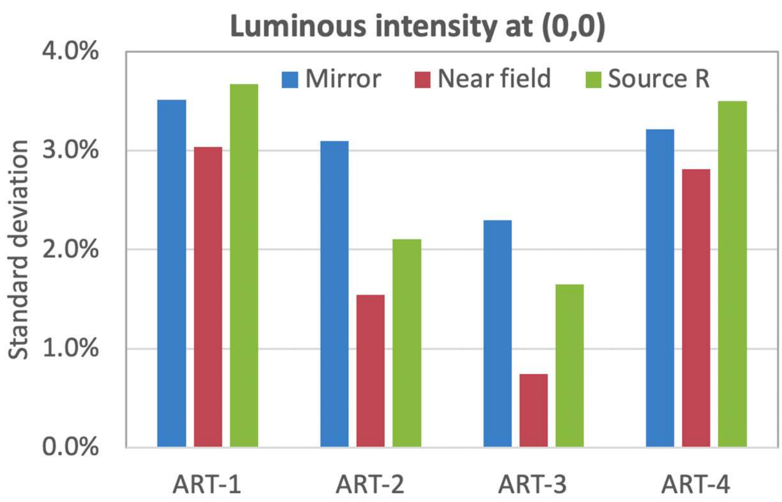

(b) Standard deviations

Figure 7-138. Average deviations from the reference value (a) and the standard deviations (b) of luminous intensity at (0,0) results for each instrument type

7.4.6 Centre beam intensity, partial luminous flux, and beam angle (ART-1)

Figure 7-139, Figure 7-140, and Figure 7-141 shows the comparison for centre beam intensity, partial luminous flux, and beam angle, all of which are measurement quantities for beam lamps.

Figure 7-139 (a) for centre beam intensity shows a large negative bias of near-field type, similar to the results of luminous intensity at (0,0) for ART-1. The standard deviations (Figure 7-139 (b)) are also similar to those of luminous intensity at (0,0).

Figure 7-140 (a) for partial luminous flux (15° cone angle) shows very large deviation (≈ 15 %) for mirror type but it is not related to instrument type. Figure 7-140 (b) shows extremely high level of standard deviations (≈17 %) for all instrument types. This is because many participants deviated from the reference value by about 30 % (see Figure 7-120) due to their mistake, the detail of which was discussed in section 7.2.10.

Figure 7-141 (a) for beam angle shows that the biases of all instruments are small and indicates no significant differences among instrument types. However, Figure 7-141 (b) shows large differences in standard deviations among different instrument types, with mirror type the largest. Beam angle is calculated at half the maximum intensity on both sides of a beam profile, where the slope of luminous intensity is sharply changing. Therefore, the calculated beam angle is very sensitive to the angle accuracy of goniophotometer movement, signal delays, and noise in the photometer signal. It is possible that large mirror-type goniophotometers with a heavy mirror mounted on a long rotating arm may have larger uncertainties in setting angles compared to source-rotating type goniophotometers, in which the artifact is mounted directly on a rotating platform with no arm. Note that there were three outliers excluded in the results of Figure 7-141, a mistake made by two participants is discussed in section 7.2.10.

Another consideration is that, if maximum intensity is measured as a lower value (as the case of near-field type in Figure 7-139 (a) below), the calculated beam angle will be larger. Figure 7-141 (a) shows small positive bias of near-field type, possibly for this reason, although the deviation is at an insignificant level.

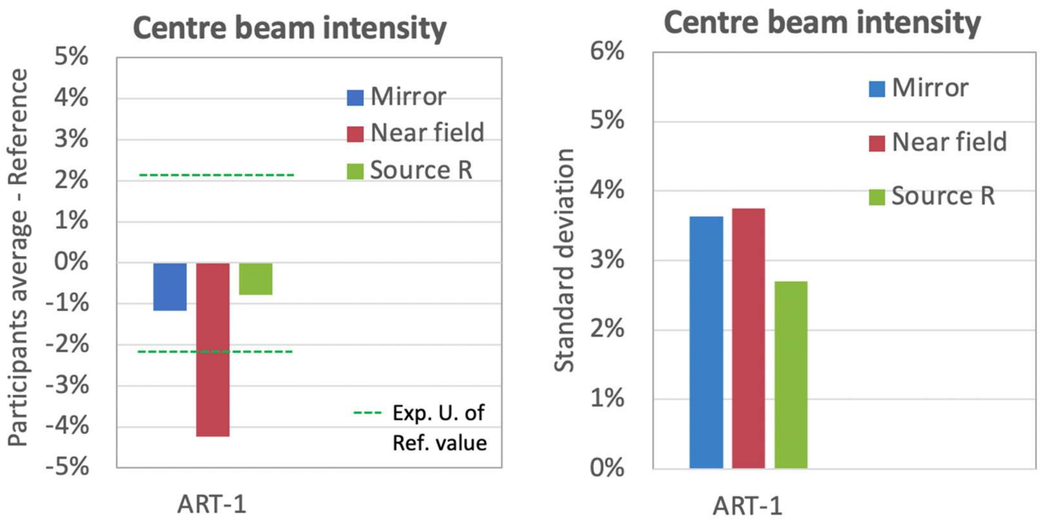

(a) Average deviations (b) Standard deviations

Figure 7-139. Average deviations from the reference value (a) and the standard deviations (b) deviations of centre beam intensity results for each instrument type

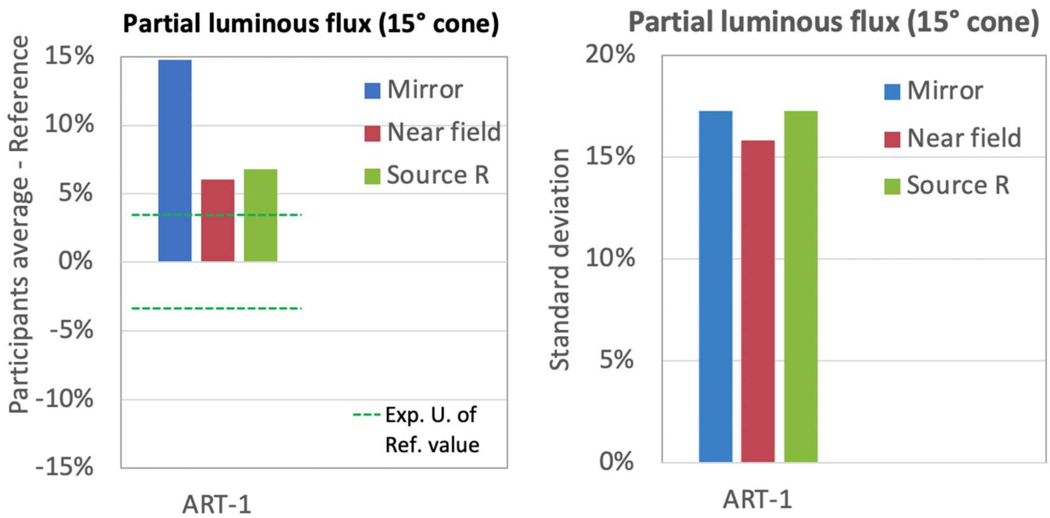

(a) Average deviations (b) Standard deviations

Figure 7-140. Average deviations from the reference value (a) and the standard deviations (b) of the results of partial luminous flux (15° cone) for each instrument type

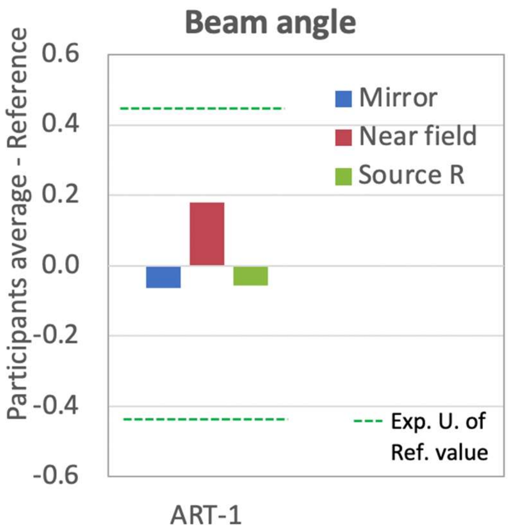

(a) Average deviations

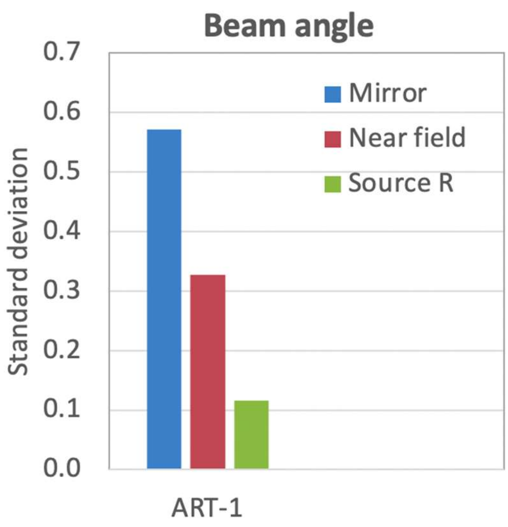

(b) Standard deviations

Figure 7-141. Average deviations from the reference value (a) and the standard deviations (b) of beam angle for each instrument type

7.4.7 Partial fluxes for street lighting luminaire

Figure 7-142, Figure 7-143, and Figure 7-144 show the comparisons for three partial fluxes for street-lighting luminaire; Street-side downward flux, House-side downward flux, and Uplight, measured for ART-4. Figure 7-143 (b) illustrates that the House-side downward flux showed large standard deviations which are four times larger than those in Street-side downward flux (Figure 7-142 (b)), the reason for which was discussed in section 7.2.10.

Figure 7-143 (a) shows a large negative deviation for near-field type (≈ - 5 %), which is significant. This may be also related to a very sharp slope of luminous intensity distribution for House-side downward flux (see 7.2.11 (b)).

Figure 7-144 presents the results for uplight flux (ratio to total luminous flux) in a different way. Figure 7-144 (a) shows the average results by participants for each instrument type and by Reference lab, and Figure 7-144 (b) shows their standard deviations. While the measured uplight flux levels are not significant, the results show lower values for near-field type and source-rotating type, which indicates that these types have an advantage for easier control of stray light compared to mirror-rotating type goniophotometers.

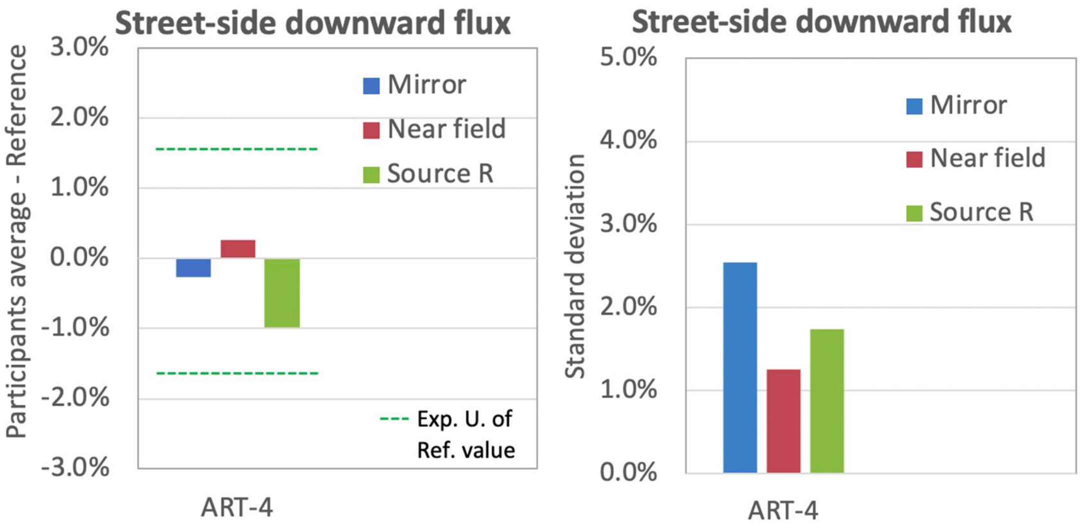

(a) Average deviations (b) Standard deviations

Figure 7-142. Average deviations from the reference value (a) and the standard deviations (b) of the results of Street-side downward flux for each instrument type

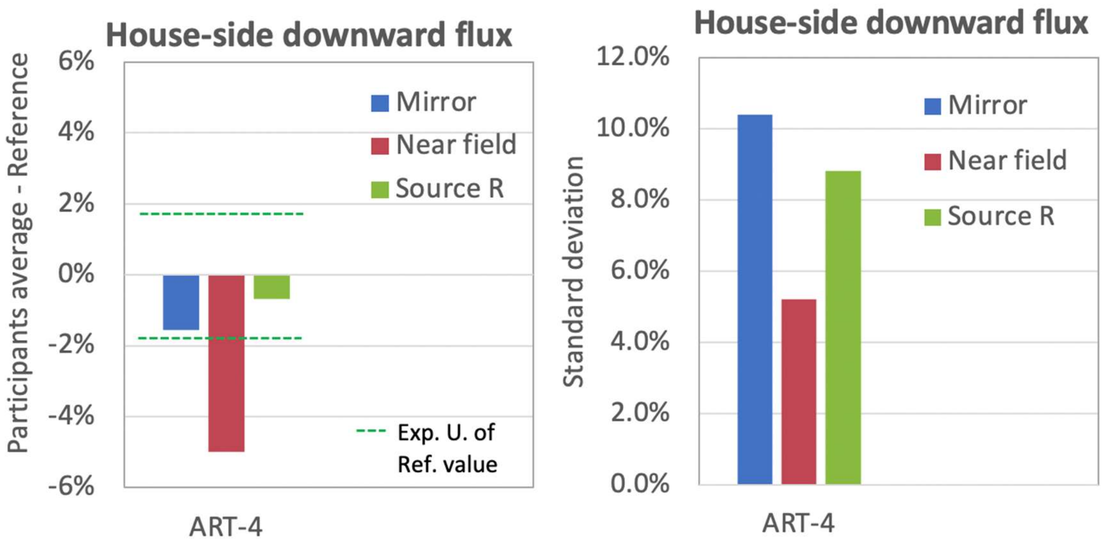

(a) Average deviations (b) Standard deviations

Figure 7-143. Average deviations from the reference value (a) and the standard deviations (b) of the results of House-side downward flux for each instrument type

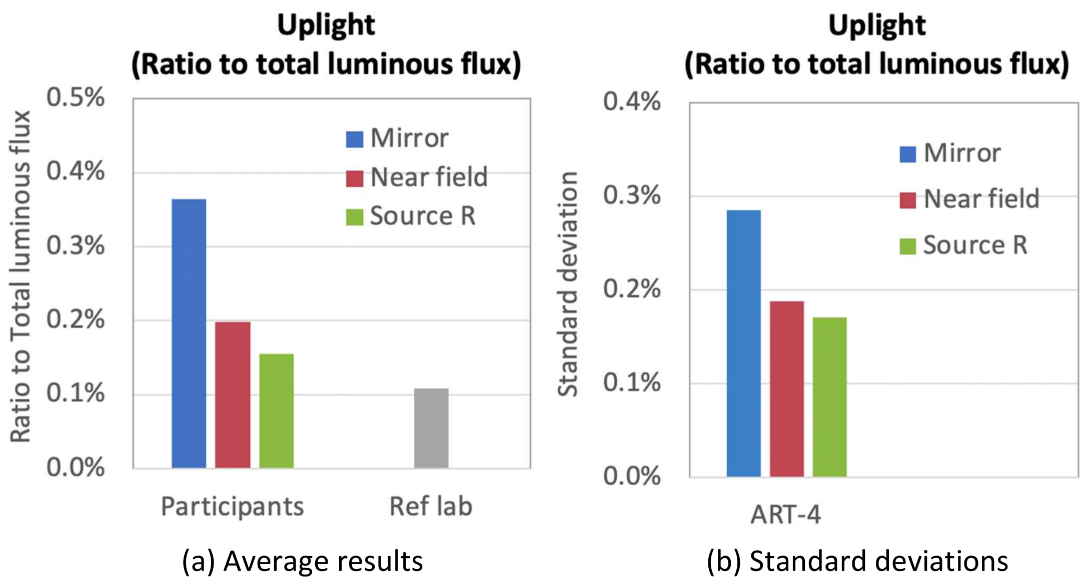

Figure 7-144. The results of Uplight (ratio to total luminous flux) (a) and their standard deviations (b) for each instrument type

7.4.8 Colour uniformity

Figure 7-145 shows the comparison for colour uniformity. Figure 7-145 (b) for standard deviations (two outlier points excluded) shows significantly large variations overall. In Figure 7-145 (a), the large deviation by near-field type for ART-3 is significant, the reason for which is unknown. Figure 7-146 shows the plots of the raw results of colour uniformity for ART-3, showing the problem more clearly that some participants reported unreasonably small values. The source-rotating type shows good results in all three figures. The reason might be that the spectroradiometer position (photometric distance) can be easily moved to shorter distances in the case of source-rotating type goniophotometers to increase signal level for the spectroradiometer, as colour uniformity is determined as the maximum deviation in chromaticity and the accurary at low intensity levels is critical. Some mirror-type goniophotometers with the mirror in the arm's rotation center (and the luminaire rotates around it) also allows changing the position of the detector easily, but only one participant and LNE (Nucleus Lab) used this type.

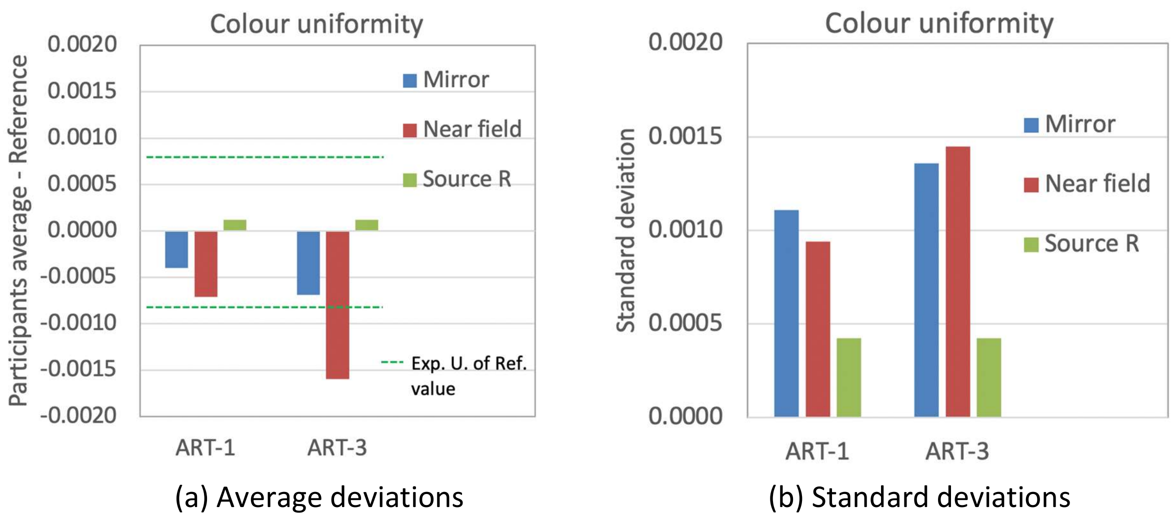

Figure 7-145. Average deviations from the reference value (a) and the standard deviations (b) of the results for colour uniformity for each instrument type

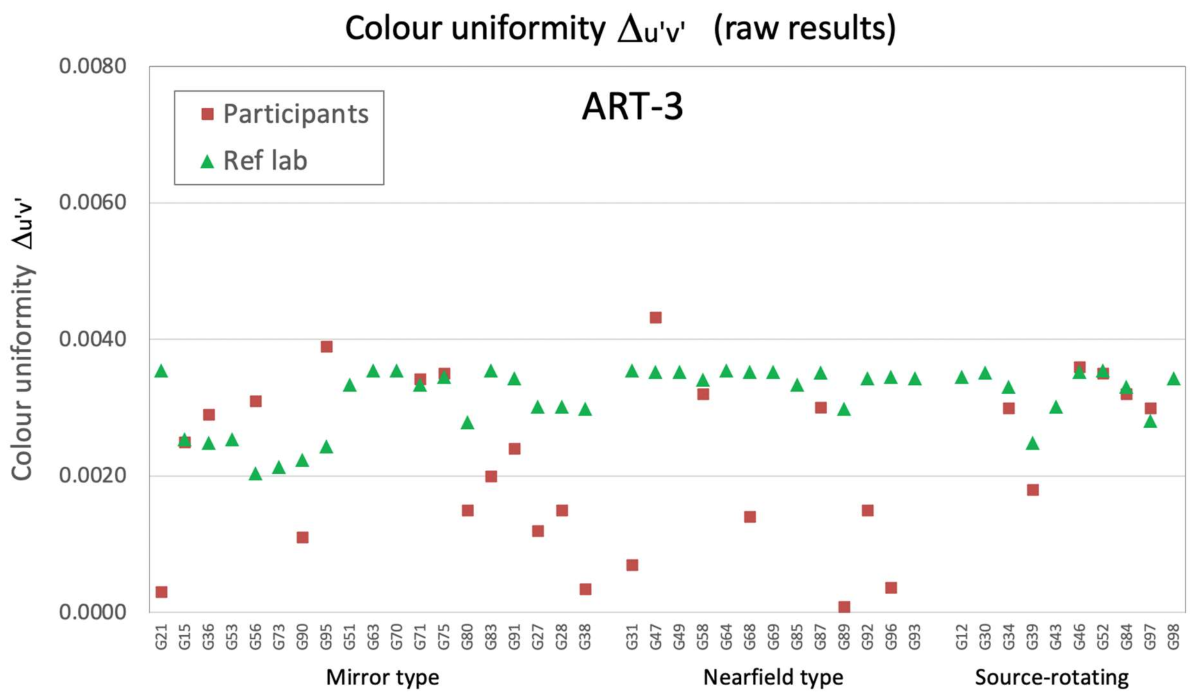

Figure 7-146. Raw results of colour uniformity measured by the participants and the reference lab grouped for each instrument type

7.5 Luminous intensity distributions

Luminous intensity distributions (LID) for four C-planes (0°, 90°, 180°, 270°) were reported by the participants. The γ angle steps varied for different artefacts. The submitted data in many cases did not match the C-planes of the reference lab. The C angle rotation was opposite in some cases (CIE coordinate system was not followed) and/or the origin was different (not following the IC 2017 protocol). The LID curves were compared after adjusting the C planes of these participants' reported data.

All data were converted to graphical representations as examples shown in Figure 7-147 to Figure 7-150 for each artefact. These are typical examples of results from the mirror type or source-rotating type goniophotometers with reasonable agreement to the curves of the reference lab.

Figure 7-151 and Figure 7-152 show typical example data of a near-field goniophotometer, for ART-1 and ART-4, respectively. Though these artefacts were considered challenging for near-field type goniophotometers (see Figure 3-1), the results showed reasonable agreement with the reference lab results similar to Figure 7-147 and Figure 7-150. Other data of near-field goniophotometers are similar to these examples and no notable problems were observed on visual comparison.

In Figure 7-153 to Figure 7-156, some problematic examples are shown. Figure 7-153 and Figure 7-154 show a poor alignment of ART-1 lamp and ART-4 luminaire to the goniophotometer. Figure 7-155 shows a case where the upper angle emission of ART-3 was not measured correctly. It is considered that this goniophotometer (source-rotating type) was designed to measure only forward ($2\boldsymbol{\pi}$) emissions. Figure 7-156 shows noisy curves from unknown reasons (no noise was evident for other artefacts for this lab).

There were a few cases where the participants reported the luminous intensity values in cd/1000 lm. This unit is not used for LED luminaires and not allowed in CIE S 025. We contacted the participants and allowed them to correct the data, although this fact was reported in their Individual Test Report. The corrected results are used for analyses in this Final Report.

Since the LID data of only four C planes were collected from participants, more rigorous LID comparisons could not be conducted, unfortunately. The comparisons of LID curves were done only visually, which was often difficult, as in many cases, there were differences in alignment of artefact (especially ART-1 and ART-4). If full LID data were available, alignment differences could be removed by computation to allow more detailed comparison of LID results. On the other hand, the LID results were also often used to investigate the reasons for problematic results or interpret the specific results in the photometric quantities and goniophotometric quantities as discussed in sections 7.2 to 7.4.

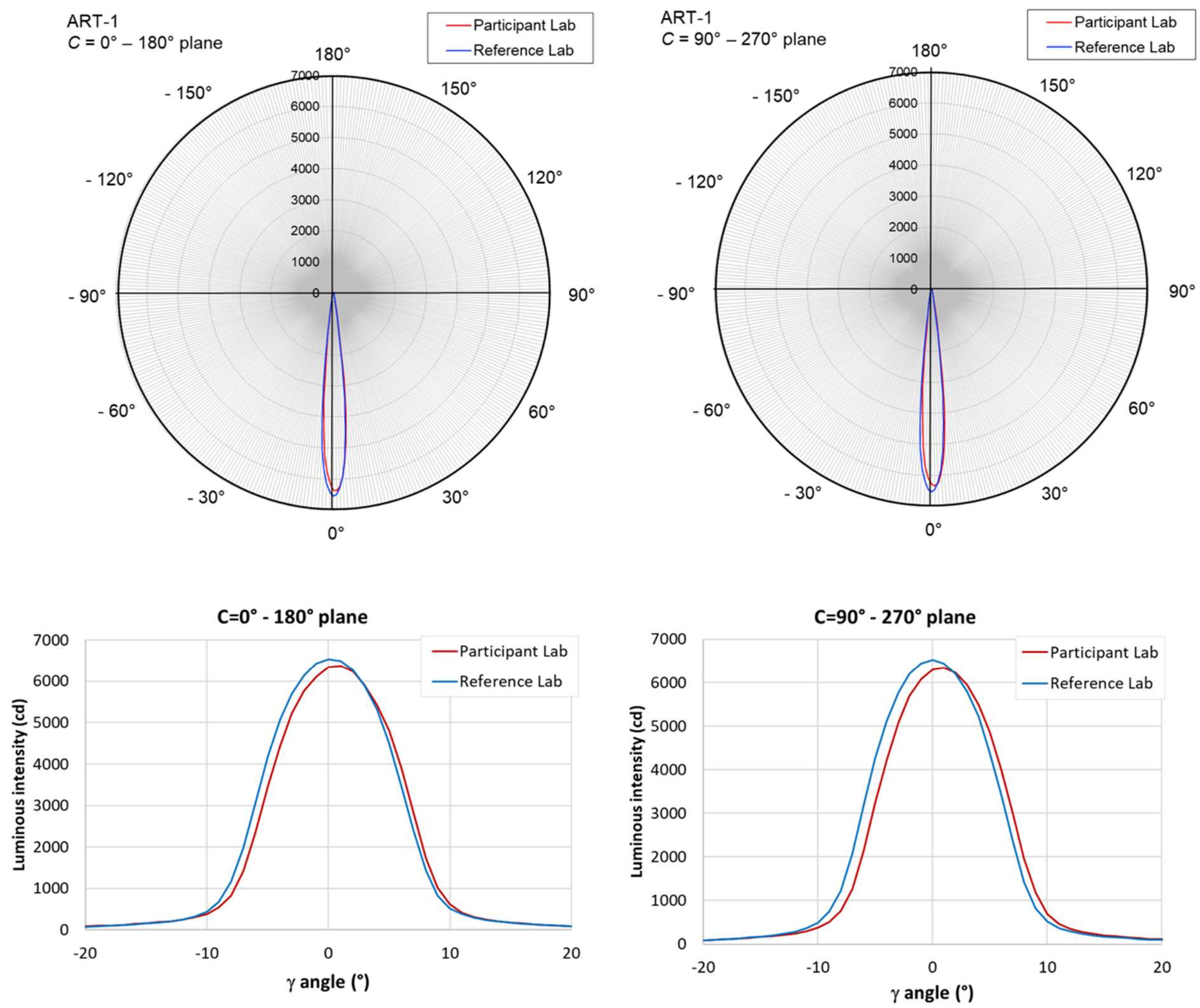

Figure 7-147. Example of luminous intensity distribution comparison of ART-1 (participant: source-rotating type goniophotometer)

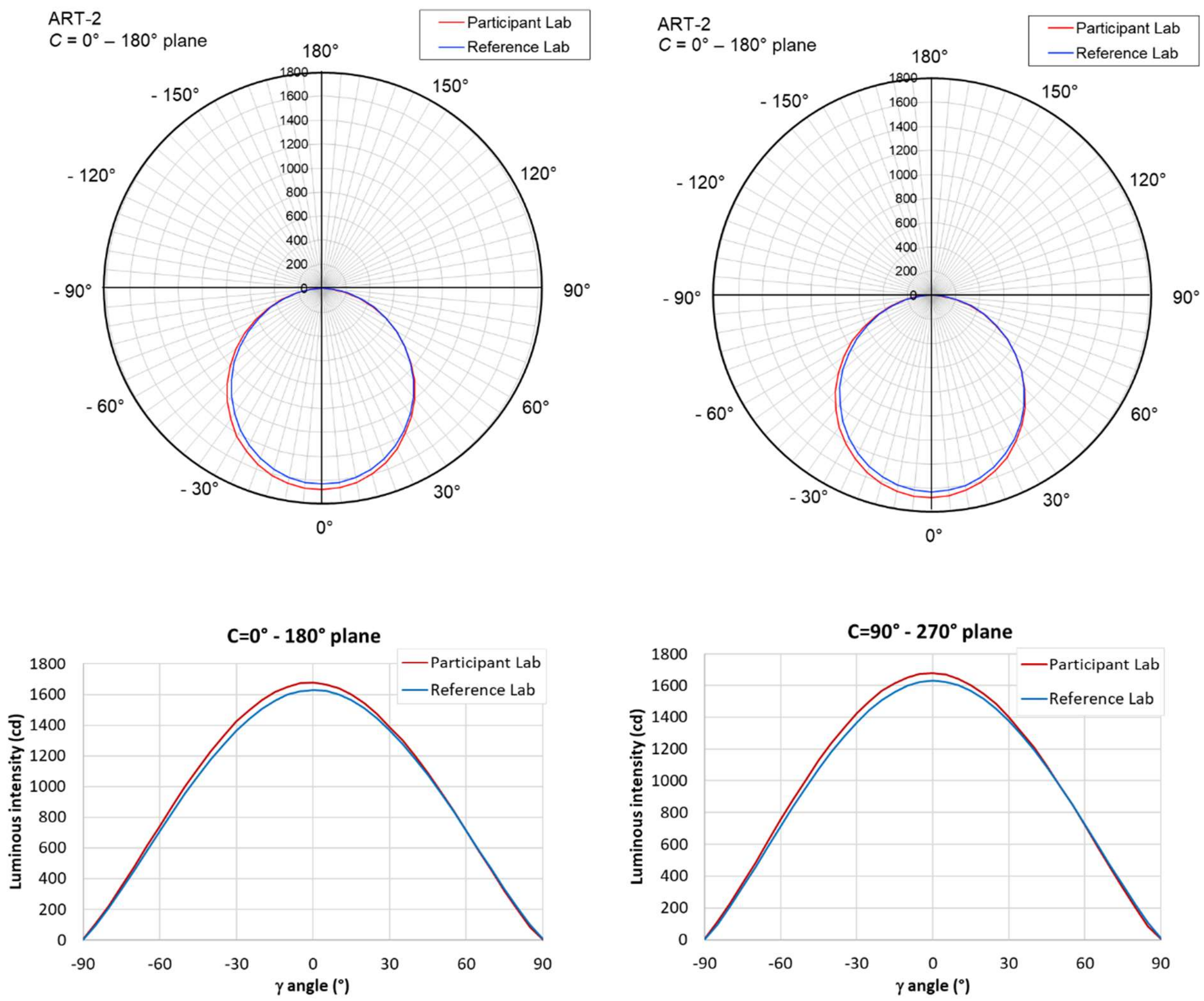

Figure 7-148. Example of luminous intensity distribution comparison of ART-2 (participant: mirror type goniophotometer)

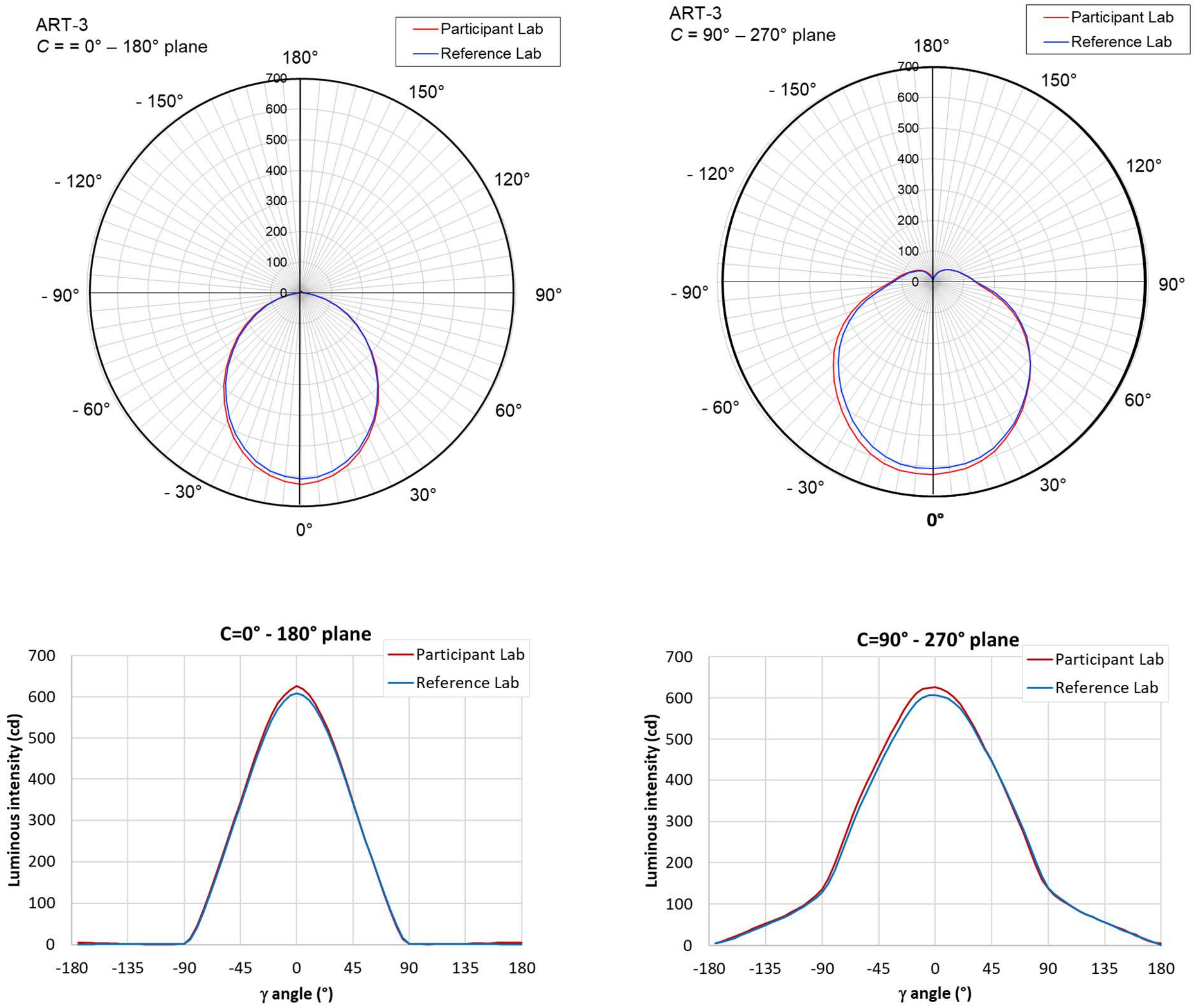

Figure 7-149. Example of luminous intensity distribution comparison of ART-3 (participant: mirror type goniophotometer)

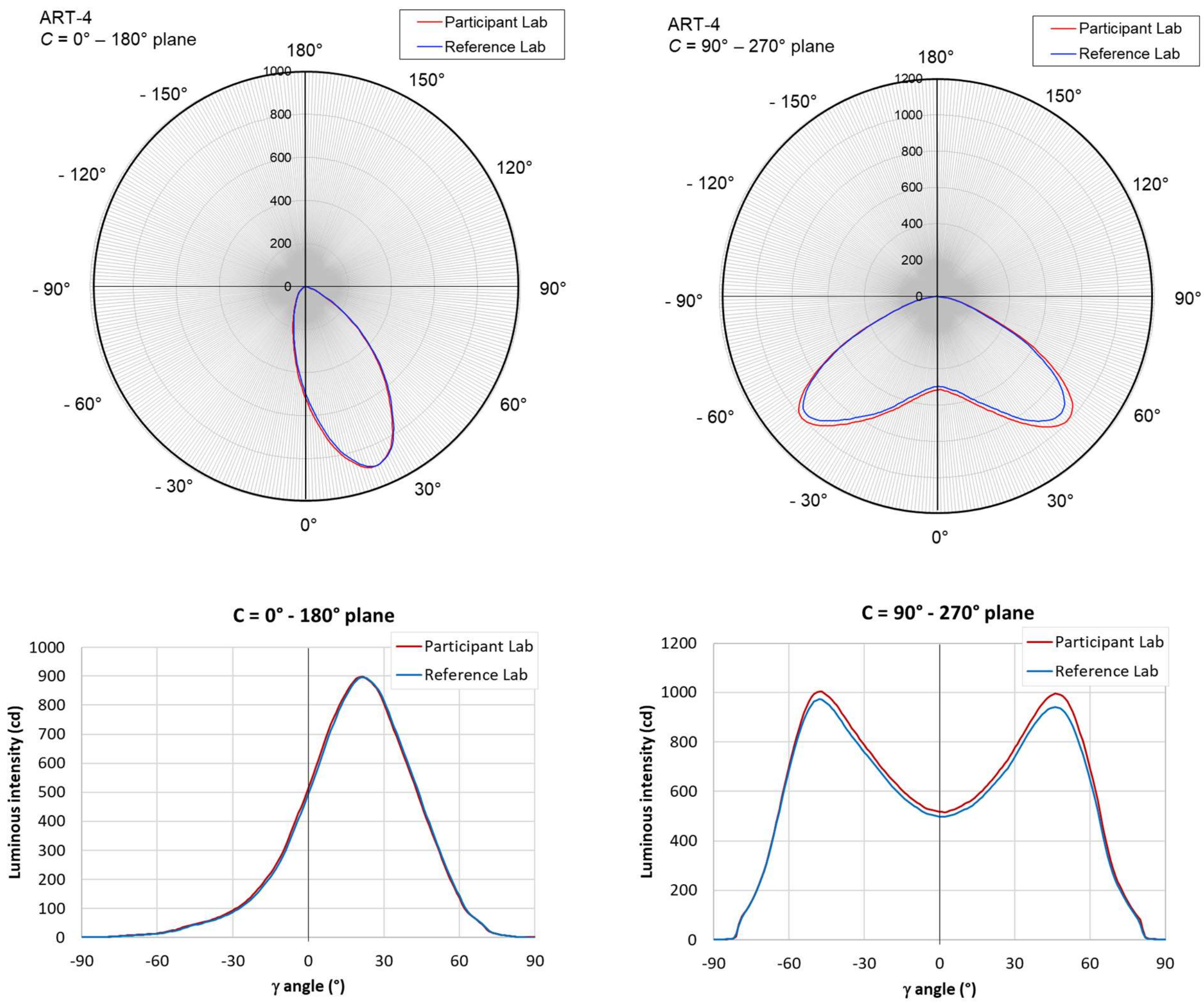

Figure 7-150. Example of luminous intensity distribution comparison of ART-4 (participant: source-rotating type goniophotometer)

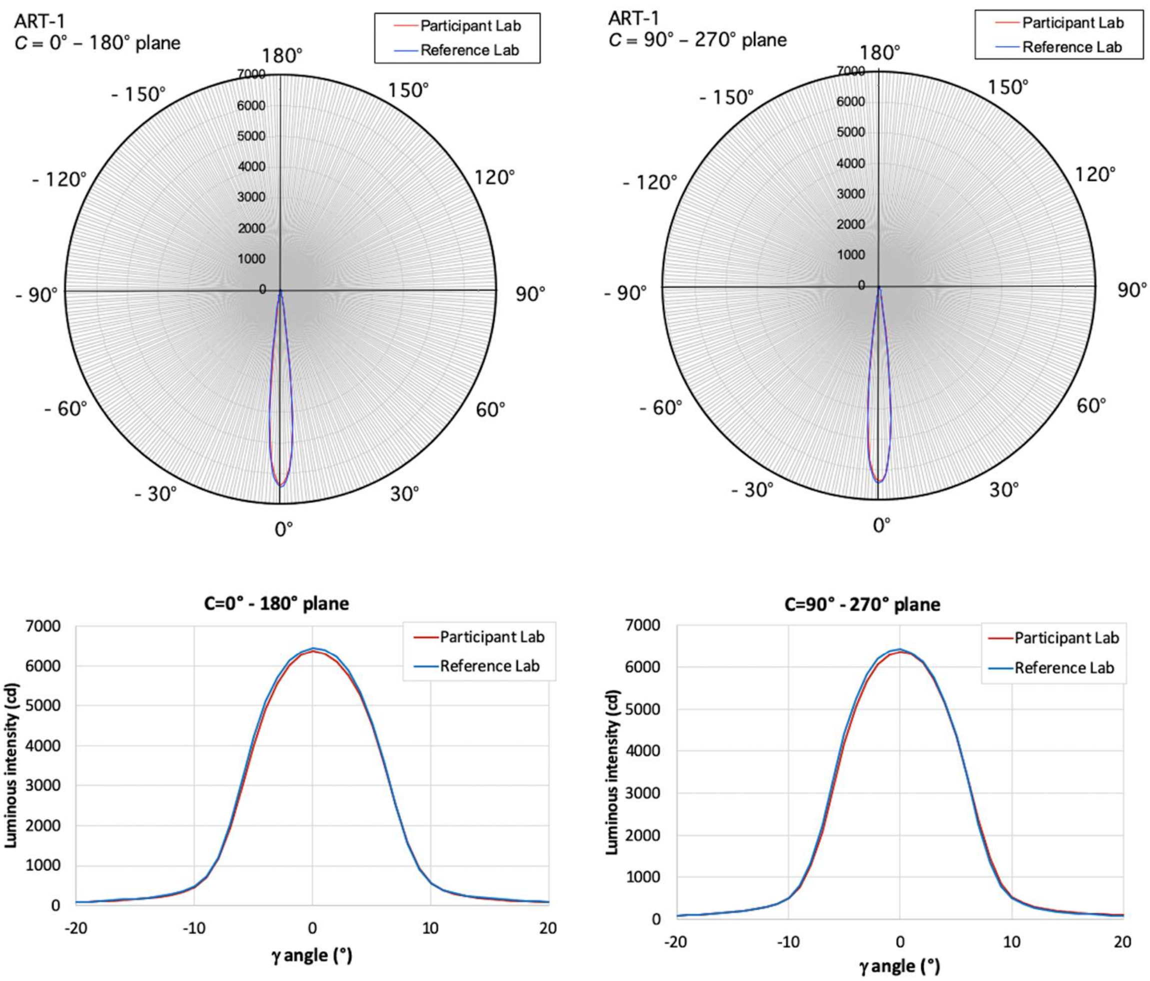

Figure 7-151. Example of luminous intensity distribution comparison of ART-1 (participant: near-field goniophotometer)

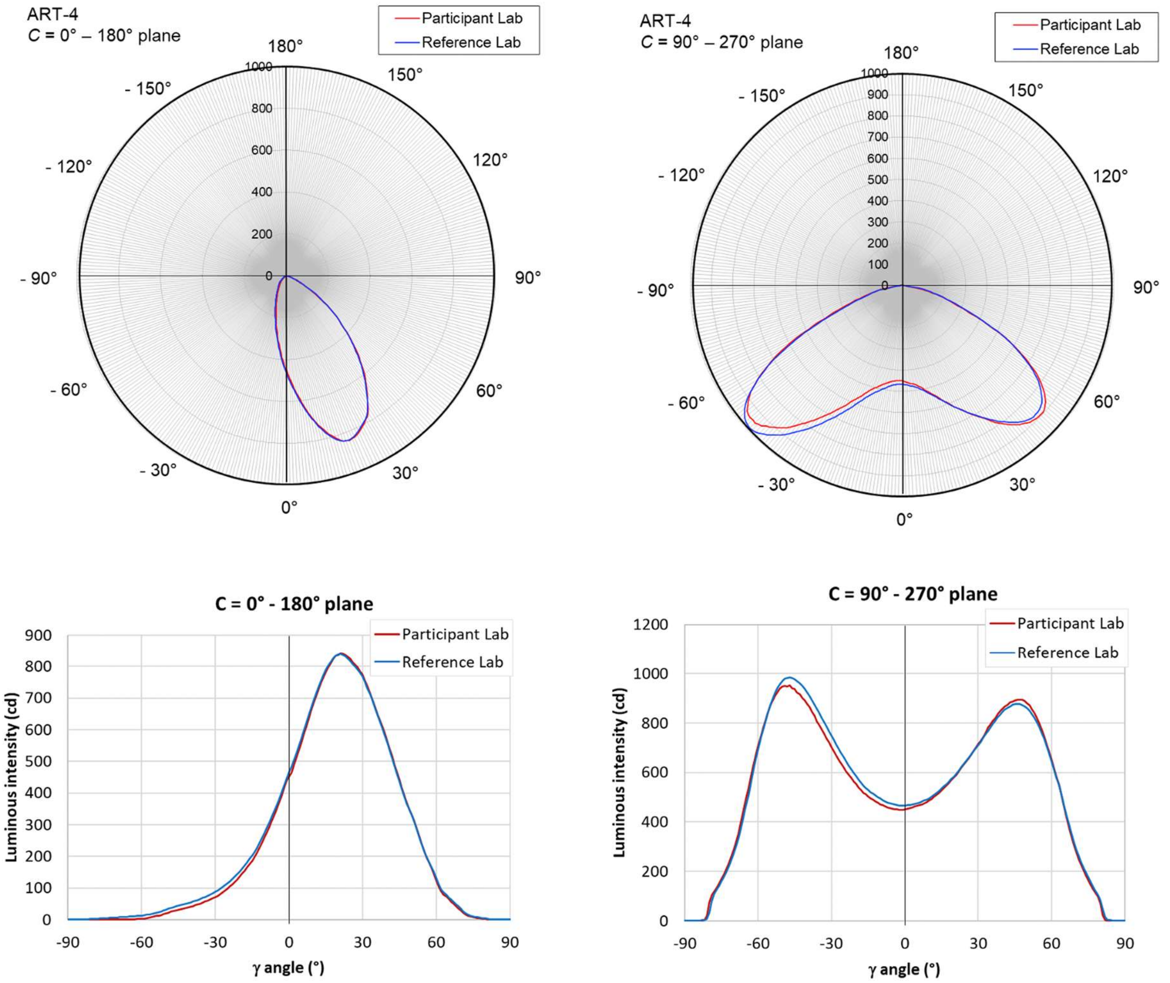

Figure 7-152. Example of luminous intensity distribution comparison of ART-4 (participant: near-field goniophotometer)

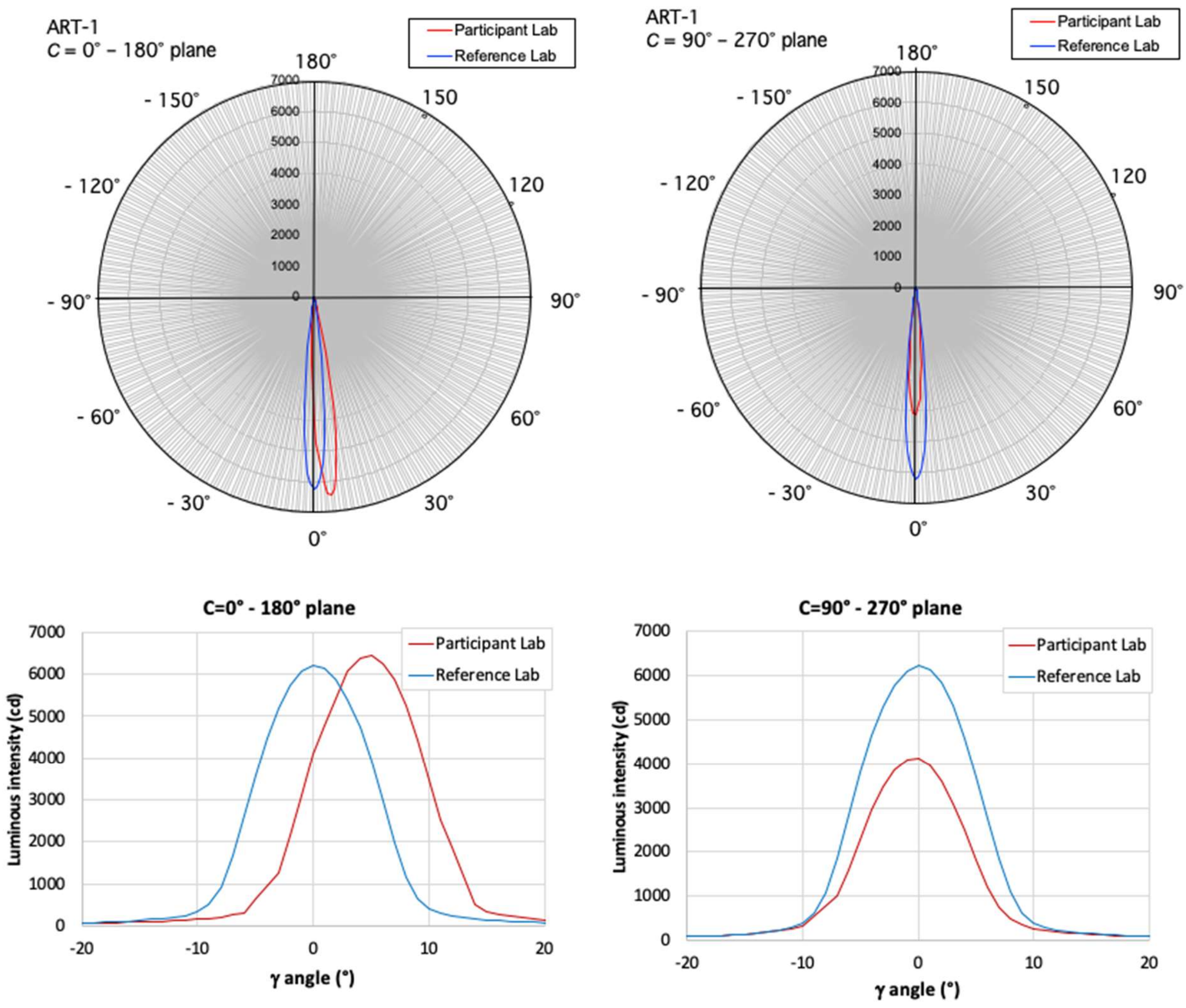

Figure 7-153. Example of a problem in poor alignment of the artefact (ART-1) (participant: mirror ype goniophotometer)

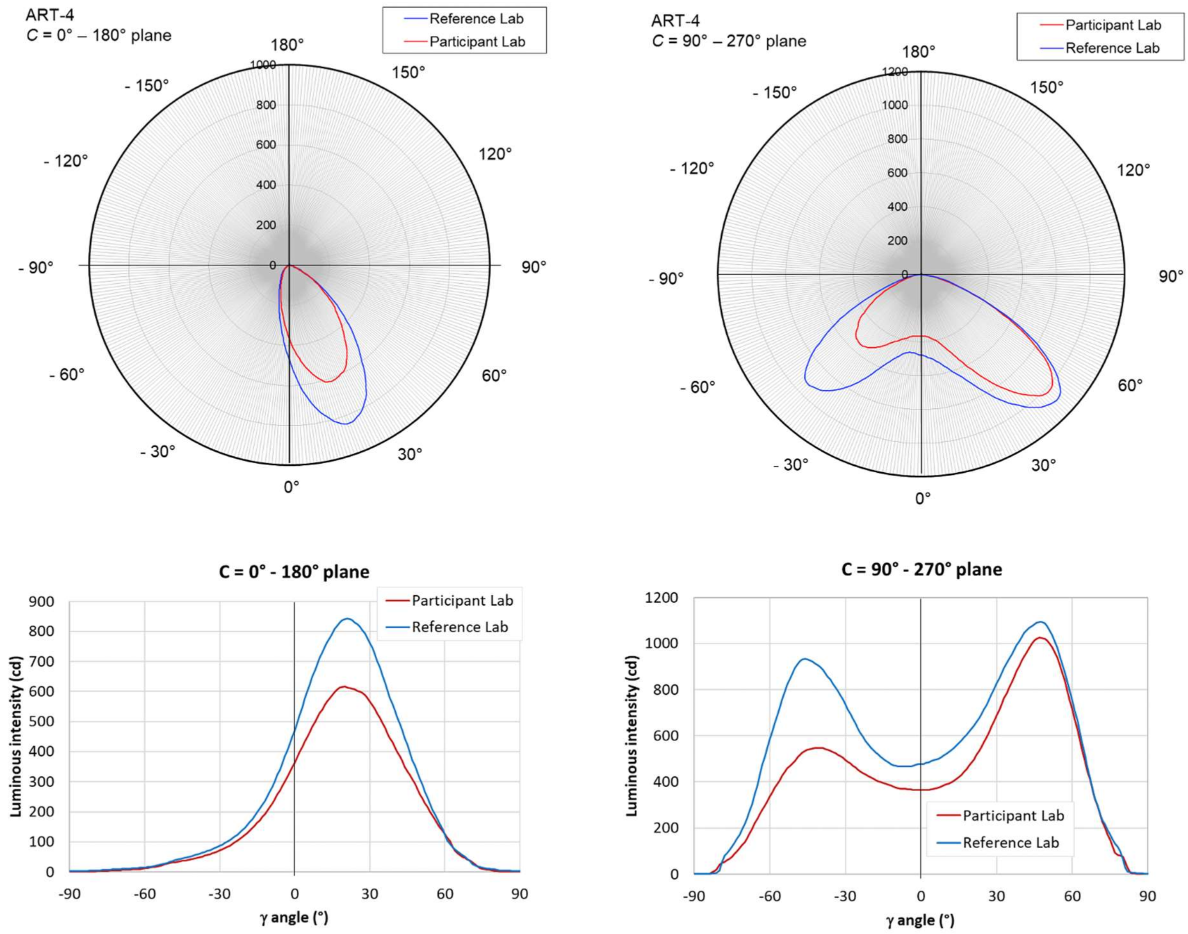

Figure 7-154. Example of a problem in poor alignment of the artefact (ART-4) (participant: mirror type goniophotometer)

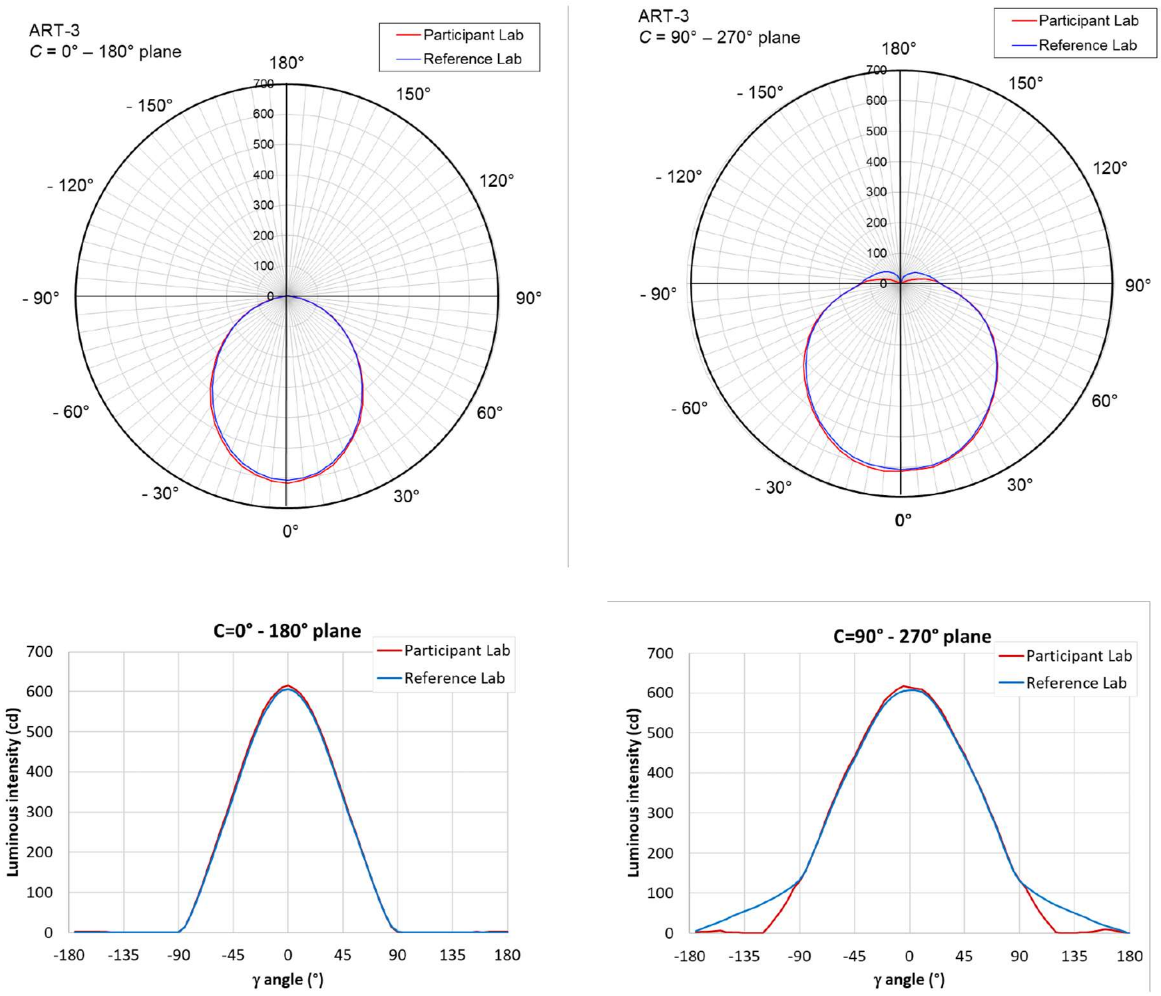

Figure 7-155. Example of a problem in dead angle of the goniophotometer for ART-3 (Participant's curve beyond γ = ± 150° is shadowed) (participant: source-rotating type goniophotometer)

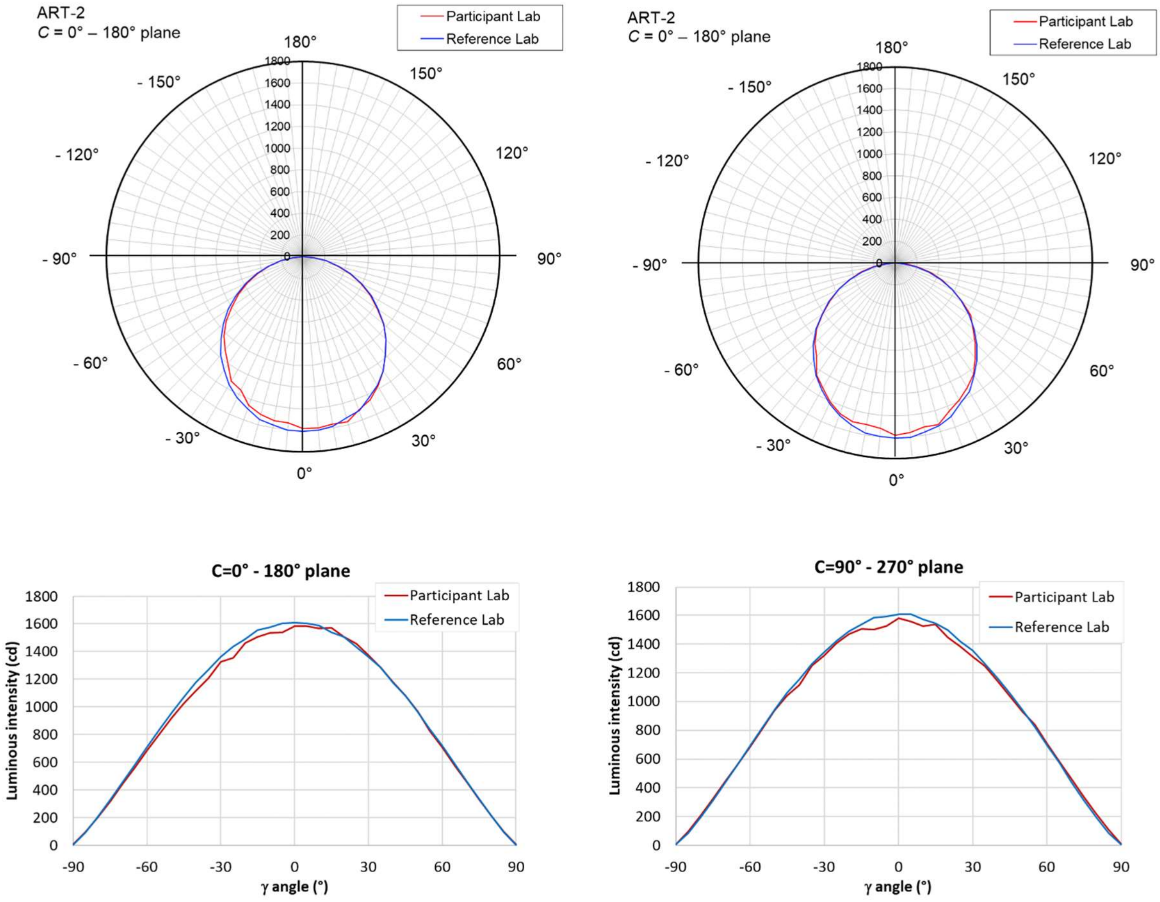

Figure 7-156. Example of noisy intensity distribution curves (ART-2) (participant: mirror type goniophotometer)

7.6 Results of *z'* scores and E_n numbers

The z' scores and E_n numbers were calculated for all applicable results of the participants and reported in the Individual Test Reports sent to each participant. This was for the purpose of providing data as needed in a proficiency test. In Figure 7-157 to Figure 7-160, some examples of the *z'* score results and E_n number results are shown. In the figures presenting the z' scores, dashed lines are $z' = \pm 2$, within which the results are generally considered satisfactory. In the figures presenting the E_n number results, dashed lines are $E_n = \pm 1$, within which the results are generally considered satisfactory in relation to the uncertainties reported.

Figure 7-161 shows the percentages of the labs that had $|z'|$ higher than 2, where the lab results are considered questionable or unsatisfactory, comparing among all quantities and artefacts. Figure 7-162 shows the percentages of the labs that had $|E_n|$ higher than 1, where the lab results are considered unsatisfactory in relation to the uncertainties reported. These results clearly show which artefacts and quantities had unexpectedly large variations of results and these may be considered when *z'* score or E_n number results are evaluated by accreditation programmes. Also, there were larger numbers of unsatisfactory points in E_n number results than z' score results indicating that the participants' reported uncertainties tended to be underestimated.

E_n number is widely used in proficiency testing for calibration laboratories to certify their claimed measurement uncertainties. However, in IC 2017, $|E_n|\leq 1$ does not guarantee that the reported uncertainty is valid, because the E_n number also depends on the uncertainty of the reference value (see Eq. 10), and in some cases in this comparison, the uncertainty of the reference value is fairly large due to some problems with the artefacts. In such cases, all the participants' results within the uncertainty range of the reference value, no matter how small the participant's reported uncertainty is, will get E_n value of less than 1. On the other hand, if $|E_n|>1$, it means the result is statistically inconsistent and certainly indicates a problem in the participant's result and uncertainty. In the case of proficiency testing for calibration laboratories, well-controlled reproducible standard artefacts are used and the uncertainty of reference value is sufficiently small. However this is not the case in testing of products. The E_n numbers like in this comparison can be useful to identify unsatisfactory results in relation to claimed uncertainty, however, the E_n number should not be used to certify the claimed measurement uncertainties by participants.

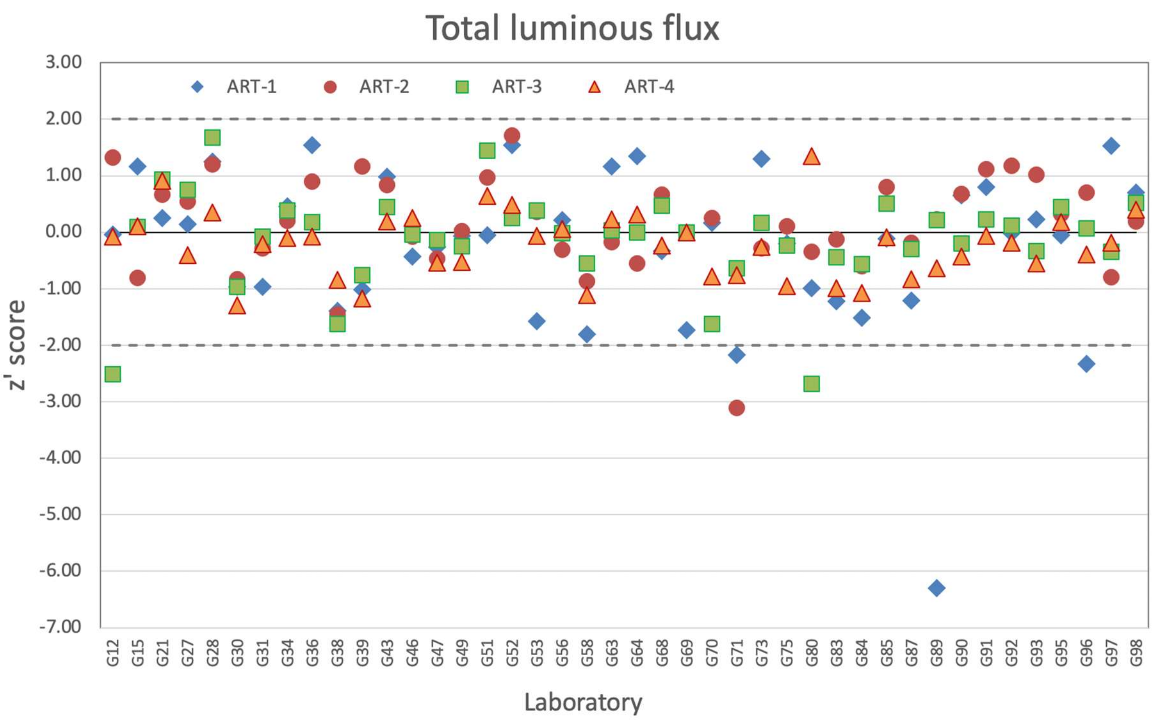

Figure 7-157. z' score results for total luminous flux for all artefacts

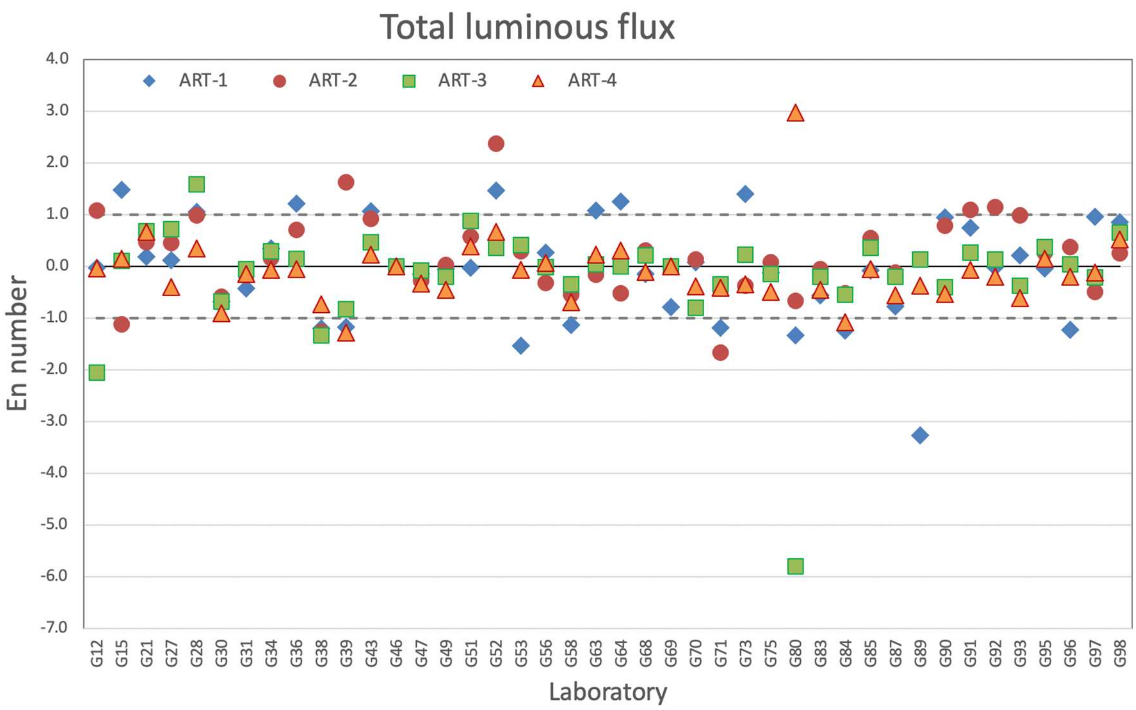

Figure 7-158. E_n number results for total luminous flux for all artefacts

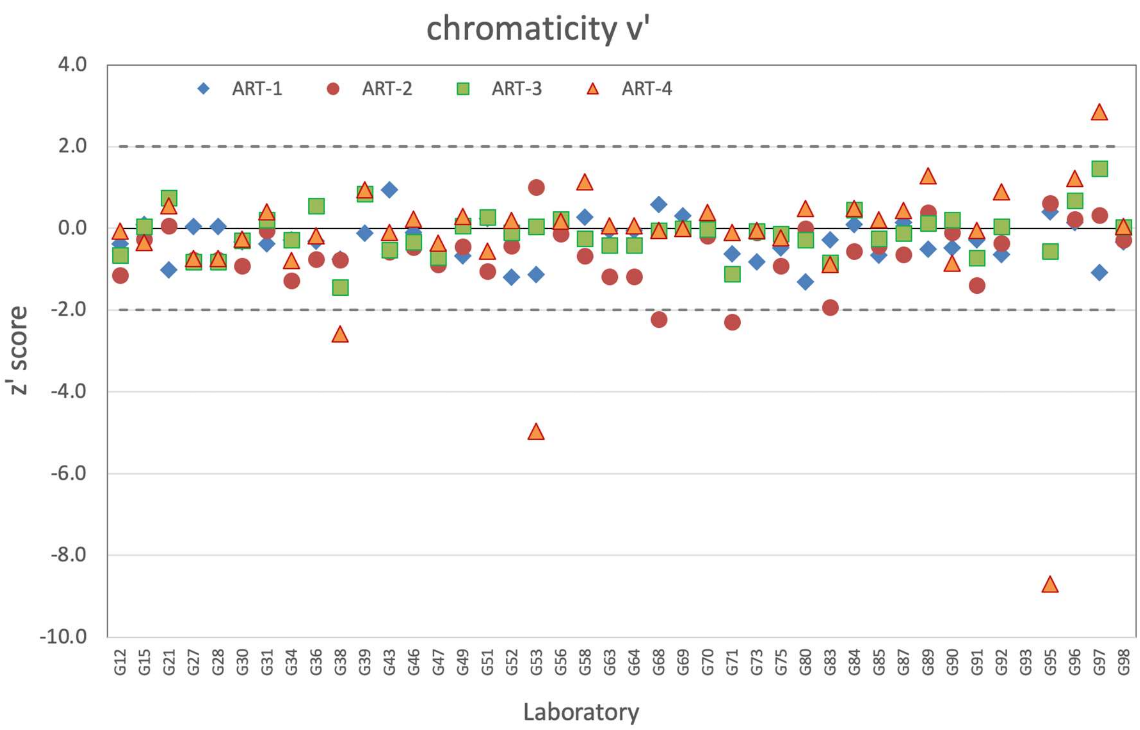

Figure 7-159. z' score results for chromaticity *v'* for all artefacts

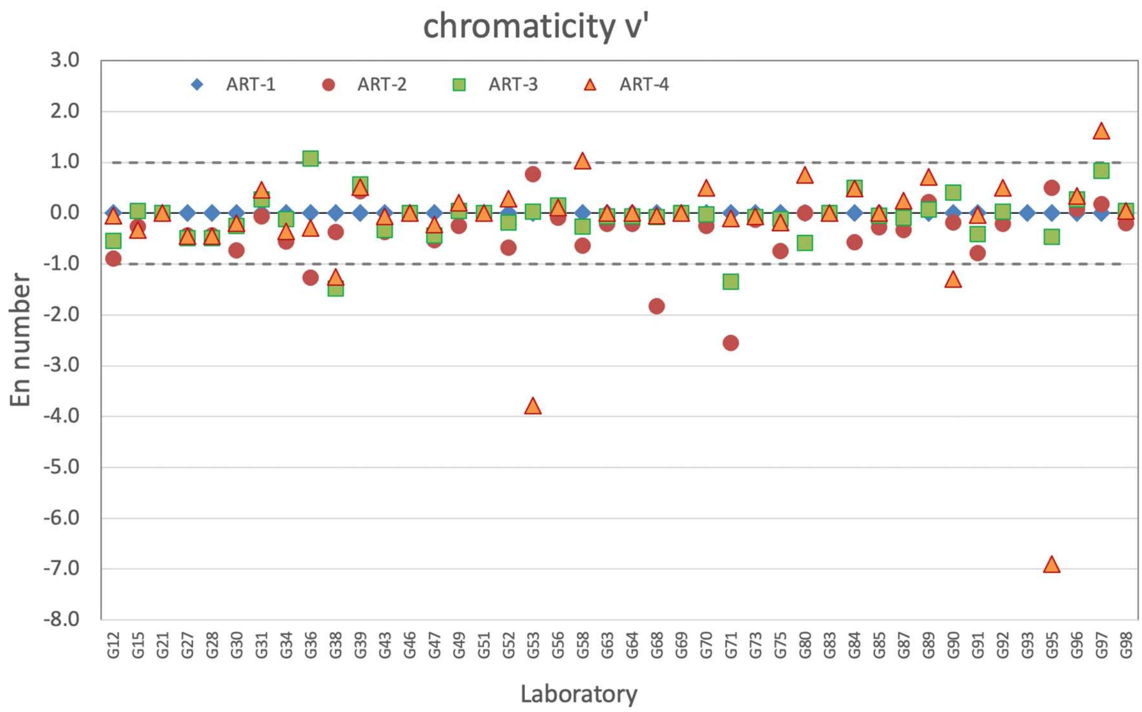

Figure 7-160. E_n number results for chromaticity *v'* for all artefacts

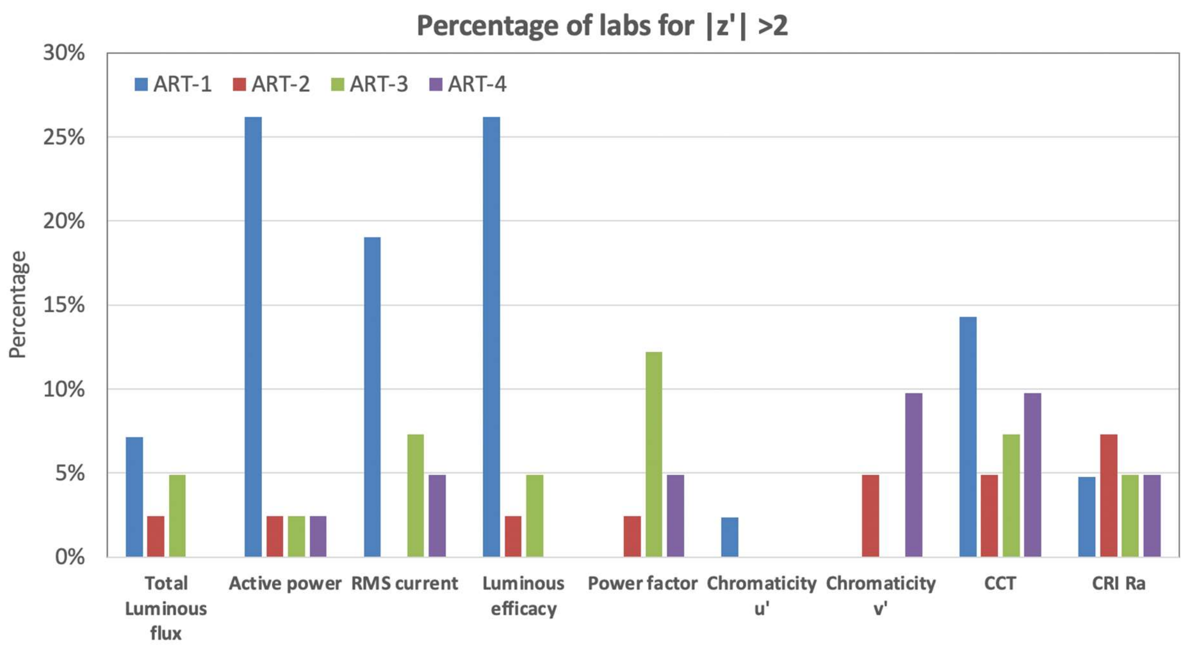

Figure 7-161. Percentage of labs that had z' scores outside -2 ≤ z' ≤ 2

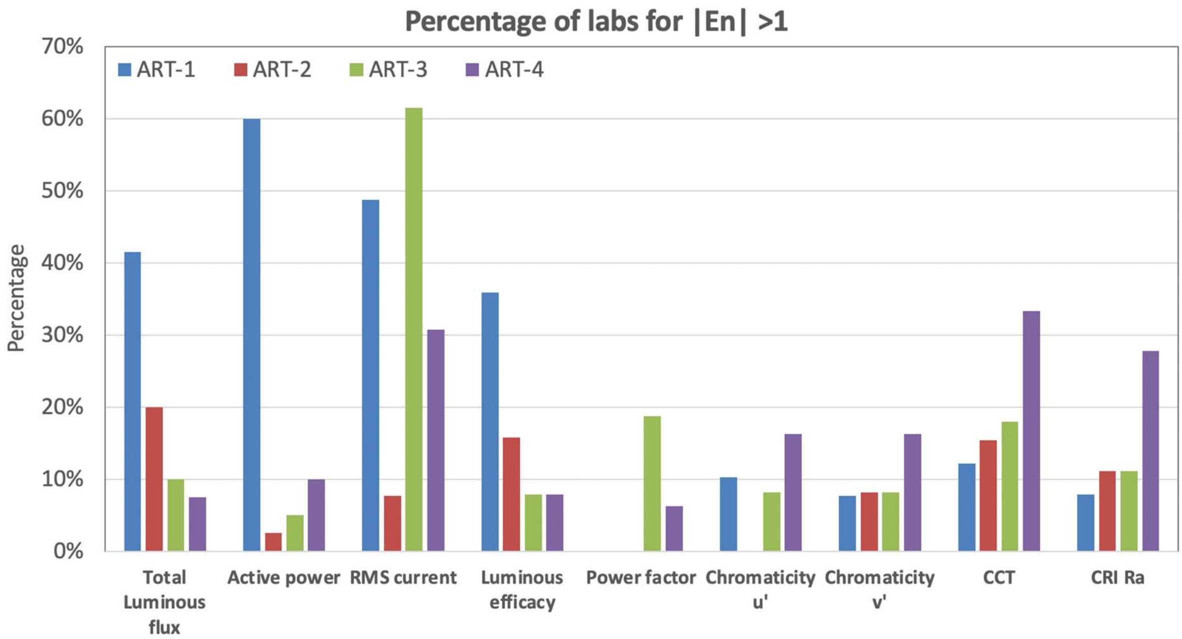

Figure 7-162. Percentage of labs that had E_n numbers outside $-1 \leq E_n \leq 1$

8 Summaries of Results

8.1 Comparisons of 42 instruments

Section 7.2 presents a comparison of the results across all 42 instruments that participated in IC 2017. The participants' total luminous flux results were mostly within ± 5 % (± 2 x SDPA) from the reference value, which is an expected level of variation. However, the electrical quantities showed some unexpected results. RMS (or DC) current showed much larger variations than were expected, with a standard deviation of about 3 % for ART-1, while the participants' reported uncertainties were mostly less than 1 % (k=2). The variations of the results depended very much on the artefact. The standard deviation of the RMS current for ART-2 was only ≈ 0.5 %. The standard deviation of the power factor measurements for ART-3 was calculated to be 0.016, whereas for ART-2 it was only ≈ 0.001, representing a very large difference between the artefacts.

The chromaticity coordinates u', v' were overall in good agreement, mostly within ± 0.002 from the reference value, with only a few outliers in v'. The results of CCT ranged from a standard deviation of 26 K for ART-1 (average CCT 2700 K) to 91 K for ART-2 (average CCT 5500 K), which are considered reasonable. The variations in CRI R_a results also showed good agreement overall with reasonable variations in the results. Note too that many participants opted to use a sphere-spectroradiometer for colour measurements.

For goniophotometric quantities (centre beam intensity, beam angle, partial fluxes, colour uniformity), there were larger variations than expected in many cases, and some specific problems were identified. In the 15° cone angle partial flux measurement, many participants were off by ≈ 30 %, which indicated that they mistakenly calculated flux for a 15° radius cone (twice the cone angle). For beam angle (≈ 12°), two participants reported half angle (≈ 6°), possibly mistaking the beam angle as the radius of the cone. While the definitions of these terms are clearly given in the terminology section of CIE S 025, a reminding note in the measurement sections could help to avoid such users' errors. The house-side downward flux of the street lighting luminaire showed large variations up to ± 20 %, with standard deviation of ≈ 8 % (four times larger than that of street-side downward flux), which is due to alignment sensitivity for this partial flux, while most participants reported the same uncertainty values for both. This is an example that further guidance on uncertainty budget is needed. The variations of colour uniformity (two times standard deviation) were 0.0020 for ART-1 and 0.0025 for ART-3, while the average measured colour uniformity values were ≈ 0.002 and ≈ 0.003 for ART-1 and ART-3, respectively, indicating that the measurement uncertainties for colour uniformity were unacceptably large.

In many of the graphs, there were often a few outliers with very large deviations, which indicate some mistakes made by the participants. These large deviations should be investigated by the participants to determine the causes.

The comparisons of luminous intensity distribution (LID) data were only made visually. In many cases the LID curves did not match initially because the C plane angles reported by participants were incorrect. The LID curves for ART-1 (also ART-4) showed large variations due to angle alignment variations of the artefact, which made it difficult to compare the LID results. A few cases showed that ART-3 upward emission was not fully measured due to the large dead angle of goniophotometers.

IC 2017 Individual Test Reports (ITRs) were issued to each participant reporting only that participant's results compared to those of the Nucleus Laboratory. In the ITRs, the participants were informed if some problems had been found in their results. The ITR was prepared so it could also be used as a proficiency test report.

8.2 Comparisons between different goniophotometer types

The results sorted by different goniophotometer types are presented in section 7.3 and extensive analyses are given in section 7.4 comparing the observed differences in results between different types of goniophotometers. In summary, the results of IC 2017 showed that the overall differences in results measured by the three types of goniophotometer were insignificant for all the quantities, and both near-field type and source-rotating type goniophotometers can be considered to have equivalent accuracies to those of the mirror-type goniophotometers within typical acceptable uncertainties, for the types of artefacts used in this comparison. The comparison of the LID curves presented in section 7.5 also showed that the agreement between the LID curves by near-field goniophotometers and those of the reference lab, on visual comparison, were similar to those of mirror type goniophotometers. Near-field goniophotometers other than the manufacturer/models used in this comparison need to be tested.

Note also that near-field type goniophotometers showed notable negative biases in the results of ART-1 (and ART-4) for luminous intensity at (0,0), centre beam intensity, and house-side downward flux. This indicates that the near-field type goniophotometers that participated in IC 2017 had slightly larger uncertainties for very narrow beam or structured intensity distributions, though the magnitude of the deviations is probably within acceptable levels of measurement uncertainties.

The source-rotating type goniophotometers did not show any issues in their results (except a few of them showed a problem of dead angle for the batten luminaire in the upward direction). In fact, on average, source-rotating type showed better results for beam angle, colour uniformity, and uplight flux (stray light) than mirror type goniophotometers. Note that source-rotating type goniophotometers require correction of results for operating position change of the artefacts per CIE S 025, however, this effect was reported to be very small, less than 0.5 % for total luminous flux for the artefacts used in this comparison. This level of deviation could be included in the uncertainty budget without actually applying the correction, though each different type/design of DUT should be tested for this effect. It is desired that the effects of operating orientation be investigated for more varieties of products**.** The testing of changes in operating position and correction may then not be needed for common products (with a certain general uncertainty contribution to be added for the possible effect).

The comparison of colour quantity results between gonio-spectroradiometers and sphere-spectroradiometers presented in Figure 7-133 to Figure 7-137 showed no notable differences overall between the two types. An exception is that, for ART-4, sphere system (sphere-spectroradiometers) showed larger variations for chromaticity *v'* and CCT, which indicates larger uncertainties of measurement with a sphere system for large luminaires like this street lighting luminaire (ART-4) with dark surface colour, possibly causing significant spectrally selective self-absorption.

8.3 Future improvements on test methods and guidance

While CIE S 025 [5] (or EN 13032-4 [6]) refers to CIE 121 for (C, γ) coordinate system, many participants in IC 2017 reported the C angle rotation in the LID results incorrectly. Giving more guidance will be useful.

Further guidance is needed on how to calculate centre beam intensity and beam angle of a directional lamp. The definition of beam angle is available in CIE S 025 [5] only for one plane. IC 2017 used an average of two C planes but it seemed insufficient. A further guidance or specification may be needed on how to determine the beam angle of a lamp product (from how many C planes) and how to deal with the case when the optical axis of the beam deviated from the mechanical axis (due to inaccurate alignment, etc.).

There were large variations in luminous intensity distributions of the ART-1 lamp and other artefacts for some participants. The main reason for the large variations was found to be variations in alignment angle of the artefact on the goniophotometer. Such information may be in CIE 121 but more specific guidance is needed in CIE S 025 [5] on how to mount and accurately align a narrow-beam lamp to the goniophotometer for the mechanical axis or optical axis of the lamp.

For the goniophotometric quantities, there were many cases where the participants did not report uncertainties. Out of 42 instruments tested, 15 to 20 did not report uncertainties for beam angle, centre beam intensity, and partial luminous flux, while only 2 did not report uncertainty for total luminous flux and 5 did not report uncertainty for colour quantities. Guidance for practical uncertainty evaluation for goniophotometric quantities is needed.

In CIE S 025 [5] (or EN 13032-4 [6]), near-field goniophotometers are accepted if equivalence to a far-field goniophotometer is demonstrated, but no details and no acceptance criteria are given. The criteria need to be developed and included in the test method.

Source-rotating type goniophotometers are allowed in CIE S 025 [5] if corrections are applied for the effect of operating position change, however, this type is not allowed in some other regional test methods (e.g., IES LM-79 [10]). Goniophotometers of this type, together with near-field goniophotometers, have a big advantage in that they do not require the large space needed by mirror-type goniophotometers. Since the source-rotating type goniophotometers that participated in IC 2017 demonstrated equivalent accuracies to mirror type goniophotometers, the use of goniophotometers of this type (with the required correction for operating position) may be more widely accepted.

Also, it is recommended that the effects of change of the operating orientation of luminaires or lamps be tested for varieties of products to clarify whether this correction for source-rotating type goniophotometers is required for all products or could be dealt with by adding some general uncertainty contributions for this effect.

9 Conclusions

IC 2017, with 36 participants and 42 instruments from around the world, is the largest interlaboratory comparison of goniophotometers ever undertaken. This comparison provided precious data comparing measurements of SSL products by different types of goniophotometers for 16 different quantities for four artefacts: three different LED luminaires and one narrow beam lamp.

This interlaboratory comparison verified reasonable agreement overall among the participants' measurements of the important quantities such as total luminous flux, luminous efficacy, and colour quantities. On the other hand, it showed unexpected large variations for some electrical quantities and goniophotometric quantities depending on artefact measured. It also revealed a number of specific measurement problems in goniophotometric quantities in participants' results, indicating that more guidance in CIE S 025 or other relevant standards is needed for measurements of these quantities for SSL products.

This IC also evaluated equivalence among different types of goniophotometers. The mirror type is the comparison reference, the type also used by both of the Nucleus Labs in IC 2017. The study verified that near-field goniophotometers and source-rotating type goniophotometers that participated in this comparison had overall equivalent accuracies to mirror type (far-field) goniophotometers within typical acceptable uncertainties, for the type of products used in this IC. This verification does not cover all types of products in the market, and verification will still be needed for products having extreme specifications or for the instruments of different designs than those used in this comparison. Note that near-field type showed slightly higher uncertainty for a very narrow beam intensity distribution, and that the source-rotating type requires corrections for operating position change of artefacts per CIE S 025.

Both near-field type and source-rotating type goniophotometers have the advantage that they do not require a large dark room space as required by mirror-type goniophotometers, thus these types of instruments, with appropriate verifications or corrections, may be more widely used.

We thank all the participants of this comparison for their valuable participation in this challenging global interlaboratory comparison of goniophotometers. We believe that the results of IC 2017 will be useful for future improvements in metrology, standards and best practice in the measurement and testing of SSL products.

10 References

1. IEA 4E SSL Annex, Solid State Lighting Annex: 2013 Interlaboratory Comparison, Final Report. Yoshi Ohno, Koichi Nara, Elena Revtova, Wei Zhang, Tatsuya Zama, Cameron Miller. Published: 10 September 2014. Link: https://www.iea-4e.org/wp-content/uploads/2020/10/IC2013_Final_Report_final_10.09.2014a.pdf

2. Solid State Lighting Annex: Interlaboratory Comparison 2017 (IC 2017), Technical Protocol version 1.0; Yoshi Ohno, Sangkyoo Jeon, Jimmy Dubard. Published: 30 June 2017. Link: https://www.iea-4e.org/wp-content/uploads/publications/2021/05/IC-2017-Technical-Protocol_v.1.0_final.pdf

3. IEA 4E Solid State Lighting Annex: Launch of IEA 4E SSL Annex 2017 Interlaboratory Comparison of Goniophotometer Measurements (IC 2017, Published 30 June 2017. Link: https://www.iea-4e.org/ssl/news/launch-of-iea-4e-ssl-annex-2017-interlaboratory-comparison-of-goniophotometer-measurements-ic-2017/

4. ISO/IEC 17043:2010, Conformity Assessment – General Requirements for Proficiency Testing.

5. CIE S 025/E:2015, Test Method for LED lamps, LED luminaires and LED modules.

6. EN 13032-4:2015, Light and lighting - Measurement and presentation of photometric data of lamps and luminaires - Part 4: LED lamps, modules and luminaires.

7. IEA 4E SSL Annex, IC 2017 Nucleus Laboratory Comparison Report. Published 28 May 2019. Link: https://www.iea-4e.org/wp-content/uploads/publications/2021/01/IC_2017_Nucleus_Lab_Comparison_Report_-Final_Revised_-_2019-09-30.pdf

8. IES TM-15-11, Luminaire Classification System for Outdoor Luminaire.

9. CIE 121:1996, Photometry and Goniophotometry of Luminaires

10. ANSI/IES LM-79-19, Approved Method: Optical and Electrical Measurements of Solid-State Lighting Products

Annex 1: Types of Goniophotometer

For measurement of light sources and lighting products (lamps and luminaires), there are three main types of goniophotometers used: mirror type, near-field type, and source-rotating type, as covered in IC 2017. These are illustrated in Figure A1-1. The mirror type and source-rotating type are far-field goniophotometers, where the “detector” is placed at a far-field distance from the light source (requirements for far-field distance are given in section 4.5.3 of CIE S 025). The “detector” can be either a photometer head or a spectroradiometer (see A1.4), or a combination of a photometer head and luminance camera which is typically used in the near-field type goniophotometer.

There are some variations of the design of mirror type. What is shown to the left in Figure A1-1 is the most common design of mirror-type goniophotometer. Futher descriptions of these three types of goniophotometer are given in the following sections.

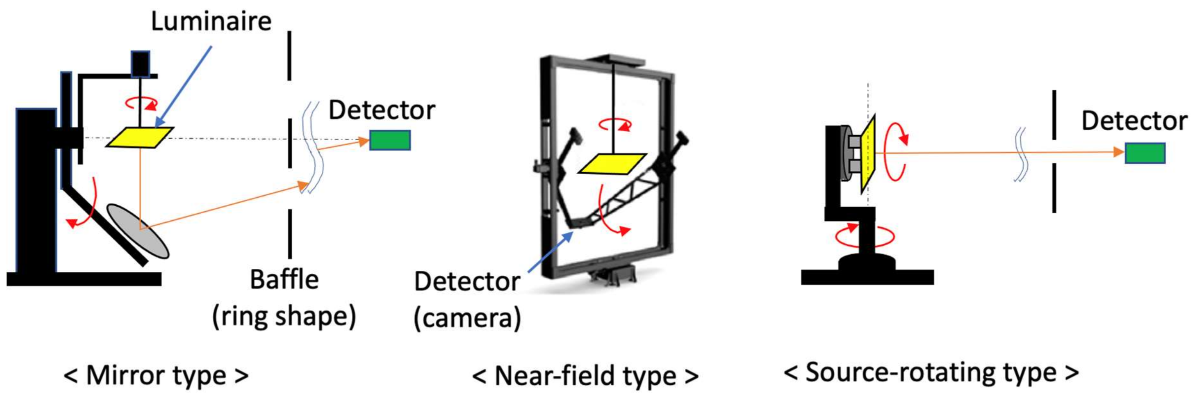

Figure A1-1. Schematics of three types of goniophotometers covered in IC 2017

A1.1 Mirror-type goniophotometers

The mirror type goniophotometer is most commonly used for testing of luminaires and is normally designed to accommodate large-size luminaires (as well as small ones). The diameter of the mirror can be as large as 2 m and the dark room space required for the mechanism and mirror movement can be several metres high. Also, for measurement of large luminaires, a long photometric distance (often more than 10 m) is used to ensure far-field distance for largest size of the luminaire tested, thus requiring a large dark room. An important feature of the mirror type is that the operating position (with respect to gravity) of the luminaire under test is kept constant during measurement, which is a requirement of CIE S 025[3] and other test methods for traditional luminaires using discharge lamps[4].

There are three basic variations of mirror type goniophotometers as shown in Figure A1-2. All three designs of the mirror-type goniophotometer illustrated were used in IC2017 by at least one participant. Design 1 is simplest and most common. The position of the detector (thus, photometric distance) is fixed (not variable), which is a disadvantage for spectroradiometer measurement, in which the signal level can be insufficient in the low intensity directions of the luminaire, with a fairly long photometric distance.

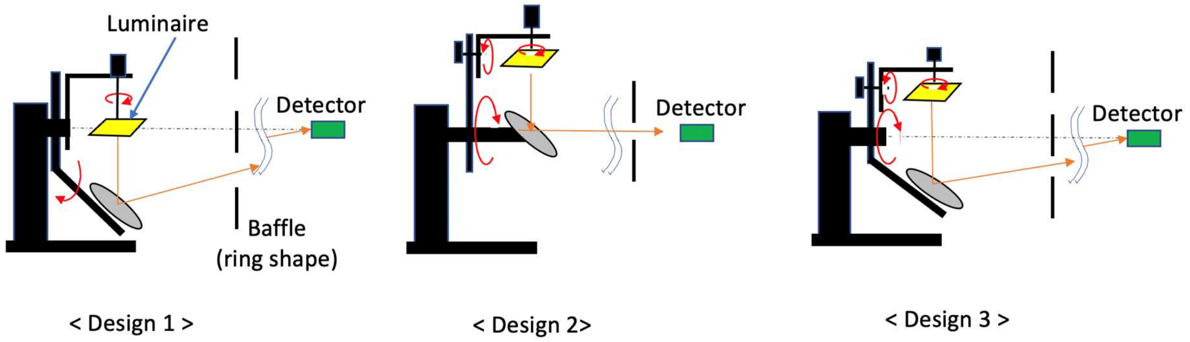

Figure A1-2. Three variations of the mirror type goniophotometer design

In Design 2, the mirror is at the rotation centre of the arm and rotates with the arm, so that the light to be measured is always on the optical axis of the detector, providing an advantage that the detector position (thus photometric distance) can be changed when needed (e.g., shorter distance at spectroradiometer measurement). With this design, it is also easier to control spatial stray light. However, another rotation stage is needed to keep the operating position of the luminaire constant while the arm is rotating.

Design 3 is a combination of Designs 1 and 2. Both mirror and luminaire rotate around the rotational centre of the arm, while the luminaire's operating position is kept constant. This is most complex, but this design has an advantage that it requires less height and is suitable for laboratories with limited ceiling height.

A1.2 Near-field type goniophotometers

Near-field type goniophotometers are designed to hold the light source fixed in position in the centre, and having detectors moving on a virtual sphere around it at a short distance (e.g.,

[3] While light output of an LED chip is not sensitive to its orientation, the operating position of an LED lamp or LED luminaire affects temperature profile throughout the lamp/luminaire which ultimately affects the in-situ temperature of the LED chips inside, thus affecting the total luminous flux output, as LED chip output varies with its temperature.

[4] Operating position of a discharge lamp affects luminous flux emitted due to changes in the thermal gradients and gas pressures within the bulb.

1 m). The detector is usually a combination of a luminance camera and a photometer head. The luminous intensity distribution in the far field is calculated from the luminance distribution of the light source in all directions measured by the luminance camera. The total luminous flux is obtained through integration of the illuminances measured by the photometer head (cosine-corrected), possibly more accurately than from luminous intensity distributions. The near-field type goniophotometer has a great advantage that it does not require a large dark room with a long distance to the detector. However, this type is still fairly new and the accuracies are still not well researched and quantified. CIE S 025, therefore, requires that this type of goniophotometer be demonstrated to have equivalent accuracies to a conventional mirror-type (far-field) goniophotometer for acceptance in SSL product testing.

A1.3 Source-rotating type goniophotometers

Source-rotating type goniophotometers are very common for measurement of directional sources (such as automotive headlights, displays, signal lights in transportation, etc.). The advantage of this type is that the mechanism is compact and can be installed in a low-ceiling lab, although a long photometric distance is still needed for testing large-size or narrow-beam sources. It is also advantageous that the detector (photometer or spectroradiometer) position can be changed when more signal level is needed since the detector axis is on the photometric axis. Control of spatial stray light is also easier to manage, as the detector is receiving the light, intended to be measured, from a fixed position and direction in space.

A disadvantage of this type, for measurement of lighting products, is that this type rotates the light source in two axes, and hence the operating position of the luminaire (with respect to gravity) changes, thus this type is generally not accepted in test methods for measurement of lighting products using discharge lamps or LED light sources (see footnotes 3 & 4). CIE S 025 accepts this type of goniophotometer if corrections are made for the changes to operating position of the source. An example is given in CIE S 025 (section 4.2.5) on how to measure such correction factors, but there are no details of the requirement of the correction. Also, many designs of this type of goniophotometer only cover forward (2 π) light emission and may not be suitable to measure products that have upward light emission (like ART-3 in IC 2017), though it is possible to design this type of goniophotometer to cover a larger solid angle (thereby reducing the "dead angle" in upward directions), as many of those used in IC 2017.

A1.4 Gonio-spectroradiometer

With any of the types of goniophotometer described above, when a spectroradiometer is used as the detector, the system is called a gonio-spectroradiometer. This system can measure spectral distributions of the source in each direction, thus measures colour quantities as well as luminous intensity distributions simultaneously. However, the measurement takes much longer time than when using a photometer head because measurement with a spectroradiometer normally requires the arm rotation to stop at each angle position (stop-and-go mode), whereas measurement with a photometer head can be done while the arm keeps rotating (on-the-fly mode). For this reason, photometer heads are still widely used in goniophotometers (though many goniophotometers are equipped with both a photometer head and a spectroradiometer), and many laboratories use sphere-spectroradiometers for colour measurement.